Molecular Regulation of Atrial-Selective Fibrotic Remodeling and its Role in Atrial Fibrillation

Yu Chen

Department of Pharmacology and Therapeutics

McGill University, Montréal

August, 2015

A thesis submitted to McGill University in partial fulfillment of the requirements of the degree of Doctor of Philosophy

© Yu Chen, 2015

This thesis is dedicated to:

My parents and grandparents, for their unwavering understanding, love, and encouragement. Without their endless support, this thesis would have never been completed.

In my heart you never left, dearest grandma.

I love you grandpa, I love you mum and dad.

Abstract

Atrial fibrillation (AF) is the most common sustained clinical arrhythmia leading to heart failure (HF). Atrial fibrosis, the main component of structural remodeling, features extracellular matrix (ECM) deposition within the myocardium and provides a key substrate for AF maintenance. Multiple cytokines, growth factors, signal transducers, and microRNAs (miRNA) are known to regulate the fibrotic response; however, the detailed mechanism of atrial fibrosis is not fully understood. Reversing fibrotic remodeling would be beneficial for AF prevention. The aim of this thesis was to identify novel mediators of atrial fibrotic remodeling with the ultimate goal of providing insights for new therapeutic approaches for AF. The principal animal model used in this thesis was ventricular tachypacing (VTP) in dogs. This model produced congestive heart failure (CHF)-related AF, and progressive atrial-selective fibrosis.

The platelet-derived growth factor (PDGF)-Janus kinase (JAK)–signal transducers and activators of transcription (STAT) pathways are important pro-fibrotic regulators. I observed increased expression of multiple PDGF-JAK-STAT components in CHF atria and set out to evaluate their possible functional role. Following PDGF stimulation, JAK-STAT enhancement and increased ECM secretion occurred in atrial fibroblasts, while smaller changes were observed in ventricular fibroblasts. The STAT3-selective inhibitor S3I-201 reduced STAT3 phosphorylation and abolished the pro-fibrotic effects of PDGF stimulation on fibroblasts. In vivo S3I-201 administration attenuated left atrial structural remodeling and fibrosis in a mouse myocardial infarction model.

While attempting to identify potential mediators of the differential response of atria and ventricles to stimuli, I found greater miRNA expression changes in CHF atria versus ventricles, implicating miRNAs in the atrial-selective fibrotic response. I therefore performed the first

detailed characterization of time, chamber, and cell-type selective miRNA changes in CHF. The time, tissue, and cell-type selective pattern of change in multiple miRNAs suggested their potential role in the atrial-selective fibrotic response. My findings also emphasized the importance of considering cell specificity of miRNA expression in studying mechanisms of cardiac remodeling paradigms, an important point ignored in most prior studies.

Based on my findings regarding the role of miRNAs in atrial remodeling, I considered its possible importance in the cardiac JAK-STAT system that I had studied. Opposite changes in JAK2 and miR-30a/133a in CHF suggested that miR-30a and miR-133a contribute to atrial fibrotic responses by targeting JAK2. PDGF reduced the expression of miR-30a and miR-133a and induced JAK2 expression in atrial fibroblasts. Luciferase assays confirmed that miR-30a and miR-133a target JAK2, and miR-133a overexpression reduced the expression of JAK2 in fibroblasts. The upregulation of JAK2 and collagen type I expression induced by PDGF-AB stimulation was reversed by miR-133a overexpression in atrial fibroblasts, directly implicating miR-133a in the changes I saw.

In conclusion, 1) the PDGF-JAK-STAT system is a novel contributor to atrial-selective fibrosis in HF; 2) a complex chamber and cell-type specific response of miRNAs contributes to the atrial-selective fibrotic response in CHF; 3) miR-30a and miR-133a may participate in AF-associated fibrotic responses by mediating PDGF effects targeting JAK2. My work suggests that a variety of miRNAs, together with the JAK-STAT system, are involved in atrial fibrosis and might represent novel therapeutic targets for AF prevention.

Keywords: atrial fibrillation, heart failure, atrial fibrosis, JAK-STAT, miRNA

Résumé

La fibrillation auriculaire (FA) est l'arythmie clinique la plus fréquente menant à l'insuffisance cardiaque (IC). Fibrose auriculaire, le composant principal du remodelage structurel, comporte une matrice extracellulaire (MEC) déposé à l'intérieur du myocarde et fournit un substrat clé pour la maintenance de la FA. De multiples cytokines, des facteurs de croissance, des transducteurs de signaux et les microARN (miARN) sont connues pour réguler la réponse fibrotique toutefois les mécanismes détaillé de la fibrose auriculaire n'est pas totalement comprise. Inverser le remodelage fibrotique serait bénéfique pour la prévention de la FA. L'objectif de cette thèse était d'identifier de nouveaux médiateurs impliqué dans le remodelage auriculaire dans le but de fournir de meilleurs outils pour la prévention de FA. Le modèle animal principal utilisé dans cette thèse était les chiens en tachystimulation ventriculaire (VTP). Ce modèle produit de l'insuffisance cardiaque congestive (ICC)-relié à FA, et la fibrose progressive au niveau auriculaire.

Le facteur de croissance dérivé des plaquettes (PDGF)-Janus Kinase (JAK)-transducteurs et activateurs du signal de la transcription (STAT) est un régulateur pro-fibrotique importante. Je observé une expression accrue des composants de PDGF-JAK-STAT au niveau des oreillettes en ICC et à commencer à évaluer leur rôle fonctionnel possible. Suite à la stimulation de PDGF, la voie de JAK-STAT s'est activé et a causé la sécrétion des MEC dans les fibroblastes auriculaires. Nous avons aussi observé de plus petits changements dans les fibroblastes ventriculaires. L'inhibiteur de STAT3-sélective S3I-201 a réduit l'expression de STAT3 phosphorylée et a abolit les effets profibrotiques de stimulation par PDGF sur les fibroblastes. In vivo l'administration de S3I-201 a atténué le remodelage structurel auriculaire et la fibrose dans un modèle d'infarctus du myocarde de la souris.

Tout en essayant d'identifier des médiateurs potentiels de la réponse différentielle des oreillettes et des ventricules à des stimuli, je remarqué de plus grands changements dans l'expression des miARN de ICC auriculaires par rapport aux ventricules, impliquant les miARN sélectif dans la réponse fibrotique auriculaire. Donc je réalisé la première caractérisation détaillée des miARN en ICC basé sur le temps, la localisation structurelle, et le type cellulaire. En fonction du temps, des changements auriculaires et des fibroblastes sélectifs de plusieurs miARN ont établi leur rôle potentiel dans une réponse fibrotique auriculaire sélective. Il a également souligné l'importance de considérer la spécificité cellulaire de l'expression des miARN dans les paradigmes de remodelage cardiaque, un point important ignoré de la plupart des études antérieures.

Basé sur mes conclusions concernant le rôle des miARN dans le remodelage auriculaire, je considérais son importance possible dans le système JAK-STAT cardiaque que j'avais étudié. Les changements opposés de JAK2 et de miR-30a/133a en ICC suggère que miR-30a et miR-133a peuvent contribuer à la réponse auriculaire-fibrotique en ciblant JAK2. Le PDGF réduit l'expression de miR-30a et miR-133a et induit l'expression de JAK2 dans les fibroblastes auriculaires. Les miR-30a et miR-133a, ont été confirmées pour cibler JAK2 par dosage de la luciférase et la surexpression de miR-133a réduit l'expression de JAK2 dans les fibroblastes. La régulation à la hausse de JAK2 et du collagène de type 1 induit l'expression par la stimulation de–PDGF-AB qui a été infirmée par la surexpression de miR-133a dans fibroblastes auriculaires, impliquant directement miR-133a dans les changements que je voyais.

En conclusion, 1) le système de PDGF-JAK-STAT est un nouvel contributeur à la fibrose auriculaire dans IC; 2) réponse complexe de miARN basé sur la localisation et le type de cellule spécifique contribue à la réponse fibrotique auriculaire sélectif en ICC; 3) miR-30a et miR-133a

peuvent participer à des réponses fibrotiques associés à FA via le PDGF en ciblant directement JAK2. Mon travail suggère qu'une variété de miARN, avec le système JAK -STAT, sont impliqués dans la fibrose auriculaire et pourrait représenter de nouvelles cibles thérapeutiques pour la prévention AF.

Mots-clés: fibrillation auriculaire, l'insuffisance cardiaque, la fibrose auriculaire, JAK-STAT, miARN

Table of Contents

List of Figures and Tables

Chapter 1-Introduction

Chapter 2-The role of JAK-STAT system in atrial fibrotic response

Chapter 3 The characterization of microRNA changes in congestive heart failure

Chapter 4 The role of microRNAs in mediating PDGF effects in heart failure-associated fibrotic response

Chapter 5 General Discussion

Acknowledgements

I would like to express my deepest gratitude to my supervisor, Dr. Stanley Nattel, for his continuous inspiration, guidance, and encouragement during the journey of pursuing my PhD. Thank you for your patience on every detailed explanation; thank you for every question, reminder, advice, critique and praise; thank you for the careful proof-reading and corrections for every abstract, manuscript, and thesis draft; thank you for every inspiring talk and each discussion we engaged in. From a well-known scientific pioneer to a friend that sits beside me at daily lunch, Dr. Nattel has been the most inspiring mentor during all the years of my studies. His strong passion and great intelligence for science, diligence and dedication toward work, and his attitude towards life will have a great influence upon my future career and life.

I would like to thank Dr. Dobromir Dobrev and Dr. Zhiguo Wang for their constructive suggestions and encouragement during my PhD studies. I give my deepest thanks also to my thesis advisory committee: Dr. Anne McKinney, Dr. Éric Thorin, and Dr. Bruce Allen, their valuable time and patience, constructive feedback and comments, expert critique and advice are truly appreciated. I would also like to thank our department chair Dr. Gerhard Multhaup and graduate program director Dr. Barbara Hales for their help and support.

All the work in this thesis would not have been accomplished without the help from all my colleagues, past and present. Deep gratitude to Drs. Ling Xiao and Xiao-Yan Qi who helped me combat my fears and lack of confidence, Drs. Mona Aflaki and Kristin Dawson who helped me through numerous frustrations. Great thanks to Drs. Xiaobin Luo, Reza Wakili and Jiening Xiao who provided enormous guidance and help for my research projects. Special thanks to my work sister Dr. Sirirat Surinkaew for providing accompaniment, encouragement, and joyfulness. I would like to thank present lab friends; Drs. Patrice Naud and Feng Xiong, Mr. Patrick

Vigneault and Eric Duong, and previous lab-mates; Drs. Artak Tadevosyan, Chia-Tung Wu, Hai Huang, Yiguo Sun, Takeshi Kato, Yuki Iwasaki, Masahide Harada, Ange Maguy, Begoña Benito, Balázs Ördög, Georghia Michael, and Sebastian Clauss for sharing their scientific knowledge, experience, and helping me with experiments, as well as numerous trainees/students who worked in Dr. Nattel's lab. Their continuous hospitality and friendship are important spiritual supports for me during the past years. Thanks to Maya Mamarbachi, Marc-Antoine Gillis, Francine Duval, Dr. Yanfen Shi, Natacha Duquette, and Marie-Élaine Clavet-Lanthier for their help with my experiments. I sincerely thank Chantal St-Cyr, Nathalie L'Heureux, and Audrey Bernard for efficient technical assistance, Roxanne Gallery, Jennifer Bacchi, Tina Tremblay, and Hélène Duplessis for excellent secretarial help, as well as France Thériault and Antoinette Paolitto for professional abstract/manuscript preparation.

Finally, I would like to thank my dearest parents for being the strongest supports and motivators throughout my life. I can never thank you enough. Thanks to my fiancé Lei Zou for his continuous support, enabling me to achieve my accomplishments. Thanks to all my friends at the Montreal Heart Institute (especially from Dr. Thorin's lab!) and the Department of Pharmacology. The moments we spent together will never be forgotten.

In the end, I would like to extend my sincere gratitude to Dr. Simon Rousseau and Dr. Jonathan Kalman for evaluating this thesis and providing insightful suggestions and comments. I am very grateful to every member of my defense committee. Your time and support are truly appreciated.

Statement of the Contribution of Authors

The McGill Faculty of Graduate and Postdoctoral Studies guidelines state that, "In the case of collaborative work presented in either a standard format or manuscript-based thesis, there must be an explicit statement of the contributions of all parties, including the student, in the Preface of the thesis."

This is a manuscript-based thesis and contains three manuscripts, one of which is published in a scientific journal; one is submitted and a third one that is in preparation. The contribution of each author is described in detail below:

Paper 1 (Chapter 2)

Yu Chen, Sirirat Surinkaew, Chia-Tung Wu, Patrice Naud, Xiao-Yan Qi, Hai Huang, Marc-Antoine Gillis, Francine Duval, Yan-Fen Shi, Jean-Claude Tardif, Dobromir Dobrev, Stanley Nattel. JAK-STAT signaling and the atrial fibrillation-promoting fibrotic substrate: Pathogenic role and possible therapeutic target. *Submitted to Journal of the American College of Cardiology.*

Yu Chen - I proposed the initial research idea. I collected cell and tissue samples from VTP-dogs and MI mice, cultured fibroblasts and stimulated with PDGF and/or S3I-201, performed qPCR and western blot experiments. I performed ECG recordings and analysis, helped to perform echocardiographic recordings, and assisted in surgical procedures for mice (myocardial infarction). I performed all the surgeries of installing the osmotic pumps and sacrificed all of the mice. I took all the images of dog and mouse tissue sections and quantified fibrosis area. I generated all of the figures, performed the statistical analysis, and wrote the manuscript.

Dr. Surinkaew – Assisted in fibroblast collection, performed PDGF-stimulation experiments, and provided additional fibroblast samples for qPCR quantification in Figure 3; **Dr. Wu -** Performed the surgical procedures for VTP-dogs and performed cell isolations to obtain cardiac fibroblasts and cardiomyocytes; **Dr. Naud –** Helped to write the *in vivo* mouse experiments protocol in order to obtain approval from the Research Ethics Committee; Provided tissue samples for fibrosis quantification in Supplemental Figure 1; **Dr. Qi and Dr. Huang –** Performed cell isolations to obtain cardiac fibroblasts and cardiomyocytes; **Mr. Gillis –** Performed the surgical procedures for mice; **Mrs. Duval –** Performed echocardiographic recordings for mice; **Dr. Shi and Dr. Tardif –** Analyzed echocardiographic recordings and provided data for Figure 7 and Supplemental Figure 3; **Dr. Dobrev –** Provided intellectual input; **Dr. Nattel –** Helped develop the project idea, supervised the project, provided intellectual input and edited the final manuscript.

Paper 2 (Chapter 3)

Yu Chen, Reza Wakili, Jiening Xiao, Chia-Tung Wu, Xiaobin Luo, Sebastian Clauss, Kristin Dawson, Xiaoyan Qi, Patrice Naud, Yan-Fen Shi, Jean-Claude Tardif, Steven Kääb, Dobromir Dobrev, Stanley Nattel. Detailed characterization of microRNA changes in a canine heart failure model: Relationship to arrhythmogenic structural remodeling. *Journal of molecular and cellular cardiology*. 2014;77:113-24.

Yu Chen – I collected all cardiomyocyte and fibroblast samples, performed all of the RNA isolations and qPCR experiments, produced Figure 1 E-F, Figure 2-8 and Supplemental Figure 5-6. I took all of the images of tissue fibrosis, performed transfection experiments on fibroblasts

and produced Supplemental Figure 1, 3, and 4. I performed the statistical analysis for all figures, I generated and wrote the manuscript.

Dr. Wakili – Helped to develop the initial research idea, performed the surgical procedures for the first set of VTP-dogs and produced Figure 1 A-D, provided dog tissue samples for Figure 2 and Figure 3, proofread the manuscript; **Dr. Xiao –** Constructed all of the plasmids, cultured HEK 293 cells and performed luciferase activity assays; **Dr. Wu –** Performed the surgical procedures for the second set of VTP-dogs, performed cell isolations to obtain cardiomyocytes and fibroblasts; **Dr. Luo –** Helped to perform the RNA isolation of dog tissue samples for Figure 2 and Figure 3, helped to analyze the results of microRNA array; **Dr. Clauss –** Quantified amount of fibrosis and produced Figure 1E and performed statistical analysis; **Dr. Dawson –** Provided intellectual input and proofread the manuscript; **Dr. Qi –** Performed cell isolations to obtain cardiomyocytes and fibroblasts; **Dr. Naud –** Helped to analyze microRNA array results and produced Supplemental Figure 2; **Dr. Shi and Dr. Tardif –** Performed all echocardiographic measurements and provided data for Figure 1 A-D ; **Dr. Kääb and Dr. Dobrev -** Helped to develop the initial research idea, provided intellectual input, and proofread the manuscript; **Dr. Nattel –** Proposed the initial research idea, supervised the whole project, provided intellectual input and edited the final manuscript.

Paper 3 (Chapter 4)

Yu Chen, Sirirat Surinkaew, Jiening Xiao, Chia-Tung Wu, Hai Huang, Yiguo Sun, Dobromir Dobrev, Stanley Nattel. MicroRNAs mediate PDGF effects by targeting JAK-STAT in heart failure-associated fibrotic response. *In preparation.*

Yu Chen: I proposed the initial research idea. I collected fibroblast samples and stimulated with PDGF, and performed all qPCR measurements. I conducted the sequence alignments and searched all putative miRNA targets. I conducted the transfection experiments on fibroblasts and performed all qPCR and Western Blot. I generated all of the figures, performed the statistical analysis, and wrote the manuscript.

Dr. Surinkaew – Performed PDGF-stimulation experiments and provided additional fibroblast samples for figure 1; **Dr. Xiao –** Constructed all of the plasmids and performed luciferase activity assays, provided data for Figure 3; **Dr. Wu, Dr. Huang, and Dr. Sun –** Performed cell isolations to obtain cardiac fibroblasts; **Dr. Dobrev–**Provided intellectual input; **Dr. Nattel –** Helped to develop the project idea, supervised the project, provided intellectual input and edited the final manuscript.

I have not included the other manuscripts that I have co-authored in this thesis. These manuscripts include three peer-reviewed original research articles as a co-author, in which I generated data that contributed to their acceptance for publication.

1. Fibroblast inward-rectifier potassium current upregulation in profibrillatory atrial remodeling. Qi XY, Huang H, Ordog B, Luo X, Naud P, Sun Y, Wu CT, Dawson K, Tadevosyan A, **Chen Y**, Harada M, Dobrev D, Nattel S.*Circ Res.* 2015 Feb 27;116(5):836-45.

   Chen Y. –I provided intellectual input for the miRNA study. I collected fibroblast samples, performed RNA extraction and qPCR quantification in order to provide data for Figure 8.

2. Guasch E, Benito B, Qi X, Cifelli C, Naud P, Shi Y, Mighiu A, Tardif JC, Tadevosyan A, **Chen Y**, Gillis MA, Iwasaki YK, Dobrev D, Mont L, Heximer S, Nattel S. Atrial fibrillation promotion by endurance exercise: demonstration and mechanistic exploration in an animal model. *J Am Coll Cardiol*. 2013 Jul 2;62(1):68-77.

   Chen Y. - I assisted in the treadmill training experiments for rats and recording original data. I also collected tissue samples, performed RNA isolation, and quality control in order to provide data for Figures 6 and 7.

3. Dawson K, Wakili R, Ordög B, Clauss S, **Chen Y**, Iwasaki Y, Voigt N, Qi XY, Sinner MF, Dobrev D, Kääb S, Nattel S.MicroRNA29: a mechanistic contributor and potential biomarker in atrial fibrillation. *Circulation.* 2013 Apr9;127(14):1466-75.

   Chen Y. - I collected fibroblast samples, performed RNA extraction and qPCR measurements in order to provide data for Figures 2 and 3.

Statement of Originality

The McGill Faculty of Graduate and Postdoctoral Studies guidelines state that: "The Preface of a Doctoral thesis must also include a statement clearly indicating those elements of the thesis that are considered original scholarship and distinct contributions to knowledge."

Chapter 2

Atrial-fibrillation-associated atrial selective fibrotic remodeling has been identified in previous studies but the mechanism is unknown. PDGF is a potential regulator but its downstream signaling in cardiac fibrosis has not been elucidated. Specific treatment for reversing atrial fibrotic remodeling is not available. More fibrotic signaling pathways need to be identified and characterized for the development of anti-fibrotic therapy.

The novel findings addressing the above concerns in this chapter are as follows:

- The activation of PDGF-JAK-STAT components were enhanced in a canine experimental heart failure model. Fibroblasts stimulated with PDGF, revealed JAK-STAT as an active downstream effector.
- Elevation of the PDGF-JAK-STAT system in heart failure and in cultured fibroblasts (with PDGF-stimulation) was atrial-selective, corresponding to the predominant atrial fibrotic response seen in congestive heart failure or atrial fibrillation.
- It is the first study that provided a signaling mechanism for atrial selective remodeling and explained how PDGF contributed to an atrial selective fibrotic response.
- STAT3 blockade was effective in preventing atrial fibrotic remodeling *in vitro* and *in vivo.* STAT3 inhibition may serve as a novel therapy for the prevention of atrial selective fibrosis and atrial fibrillation.

Chapter 3

Individual quantification of miRNA expression with related functions has been shown in the literature. However, a detailed system response of miRNAs in cardiac remodeling has never been studied. Fibroblasts and cardiomyocytes have distinct roles in cardiac remodeling but cell-type specific miRNA changes have not been demonstrated. Again, the molecular mechanism of atrial-selective fibrosis is not fully understood and miRNAs are a potential regulator that warrants further study.

The novel contributions in this chapter are as follows:

- A detailed characterization was provided of miRNA changes overtime, both cell-specific and chamber-specific in a heart failure model.
- MiRNAs are potential novel contributors to atrial-selective fibrotic remodeling, given by the following evidence:
    1) MiRNA changes matched the time course of atrial fibrosis development;
    2) Atrial changes were larger than ventricular;
    3) Fibroblasts were particularly affected;
    4) ECM protein changes correlated with those of regulatory miRNAs in fibroblasts.
- Two novel notions are raised in this study:
    1) The system response of multiple miRNAs may be more functionally relevant to a disease condition than a single miRNA change. MiRNAs may work in concert by targeting common signaling pathways and fibrotic genes.
    2) Cellular changes could not be predicted from tissue data. Cell-type specific miRNA changes must be considered in analyzing miRNA function.

Chapter 4

In this chapter, we continued to explore the regulatory role of miRNAs in atrial fibrotic remodeling, specifically regulating the JAK-STAT system, of which the significance has been shown in Chapter 2. The novel contributions to knowledge of this study are as follows:

- MiR-1, miR-30a, miR-133a were responsive to PDGF-stimulation in cardiac fibroblasts. MiRNA changes were inversely correlated to JAK-STAT alterations.
- JAK2 was validated as a direct target of miR-30a and miR-133a.
- JAK2 expression, collagen type I secretion, and fibroblast response to PDGF-stimulation can be modulated by miR-133a manipulation. Interfering with miR-133a expression may serve as a novel method of reversing fibrotic remodeling.
- JAK-STAT system and regulatory miRNAs are novel contributors to atrial fibrosis development and are potential targets for atrial fibrillation prevention.

List of Abbreviations

α-MHC	Alpha-myosin heavy chain
α-SMA	Alpha-smooth muscle actin
ACE(Is)	Angiotensin-converting enzyme inhibitors
AF	Atrial fibrillation
AMO	Antagomir oligonucleotide
Ang-II	Angiotensin II
AP	Action potential
AP-1	Activating protein-1
APD	Action potential duration
ARBs	Angiotensin-receptor blockers
AT1/AT2	Angiotensin II type 1 or type 2 receptor
ATP	Atrial tachypacing
ATR	Atrial tachycardia remodeling
AV node	Atrioventricular node
CaMKII	Calcium/calmodulin-dependent protein kinase II
CHF	Congestive heart failure
CO	Cardiac output
CSCs	Cardiac stem cells
CT-1	Cardiotrophin-1
CTGF	Connective tissue growth factor
CVD	Cardiovascular diseases
Cx	Connexins

DADs	Delayed afterdepolarizations
EADs	Early afterdepolarizations
ECG	Electrocardiogram
ECM	Extracellular matrix
EGF	Epidermal growth factor
EMT	Epithelial-mesenchymal transition
EndoMT	Endothelial-mesenchymal transition
ERK	Extracellular signal-regulated kinase
ERP	Effective refractory period
ET-1	Endothelin-1
FGF	Fibroblast growth factor
FSP-1	Fibroblast-specific protein 1
HDAC	Histone deacetylase
HF	Heart failure
I_{CaL}	L-type calcium current
IFN-α/β/γ	Interferon-alpha/beta/gamma
I_{K1}	Background K^+ current
I_{KACh}	Constitutive acetylcholine-regulated K^+ current
I_{Kr}	Rapidly activated delayed rectifier potassium current
I_{Ks}	Slowly activated delayed rectifier potassium current
IL-1/6	Interleukin-1 or 6
I_{to}	Transient outward K^+ current

JAK	Janus kinase
JNK	c-Jun N-terminal kinase
LA	Left atrium orleft atrial
LEF	Lymphoid enhancer-binding factor
LOX	Lysyl oxidase
LV	Left ventricle or left ventricular
MAPKs	Mitogen-activated protein kinase(s)
MI	Myocardial infarction
miR/miRNA	MicroRNA
MMPs	Matrix metalloproteinase(s)
NADPH	Nicotinamide adenine dinucleotide phosphate
NCX	Na^{+}/Ca^{2+} exchanger
NFAT	Nuclear factor of activated T cells
NF-κB	Nuclear factor-kappa B
NSR	Normal sinus rhythm
PDGF(R)	Platelet derived growth factor (receptor)
PIAS3	Protein inhibitor of activated STAT3
Pitx2	Paired-like homeodomain transcription factor 2
PKA/C	Protein kinase A/C
PTPN1	Protein tyrosine phosphatase non-receptor type 1
RA	Right atrium
RAAS	Rennin angiotensin aldosterone system
RISC	RNA-induced silencing complex

ROS	Reactive oxygen species
RV	Right ventricle
RyR2	Ryanodine receptor type 2
SA node	Sinoatrial node
SMAD	Contraction of Sma and Mad (Mothers against decapentaplegic)
SR	Sinus rhythm
STAT	Signal transducers and activators of transcription
SOCS	Suppressor of cytokine signaling
TAK1	TGF-β1-activated kinase 1
TGF-β	Transforming growth factor-beta
TGFβR1/2	Transforming growth factor-beta receptor 1 or 2
TIMP	Tissue inhibitor of metalloproteinase
TNF-α	Tumor necrosis factor alpha
TRPC	Transient receptor potential canonical
TRPM	Transient receptor potential melastatin
UTRs	Untranslated regions
VEGF	Vascular endothelial growth factor
Vs.	Versus
VTP	Ventricular tachypacing
ZFHX	Zinc finger homeobox 3

Index and calculation formula used to evaluate cardiac functions

End-systolic/diastolic volume index:

LVDs - Left ventricular dimension at end cardiac systole

LVDd - Left ventricular dimension at end cardiac diastole

LVVs - left ventricular volume at end cardiac systole

LVVd - left ventricular volume at end cardiac diastole

Cardiac output (CO) = Heart rate X stroke volume /1000

Left Ventricular Stroke volume = LVVd - LVVs

LV-EF% (left ventricular ejection fraction) = (LVVd - LVVs) / LVVd X 100%

LV-FS% (left ventricular fractional shortening) = (LVDd - LVDs) / LVDd X 100%

LV-FAC% (Left ventricular fractional area change) = (LVArea d – LVArea s) / LVArea d X 100%

Chapter 1

Introduction

1.1 Overview

Cardiovascular diseases (CVDs) are the leading cause of natural death globally; more people die annually from CVDs than from any other cause. Cardiac arrhythmias are common and lethal manifestation affecting the cardiovascular system [1]. The focus of this thesis is to determine the mechanisms underlining atrial fibrillation (AF), which is the most common cardiac arrhythmia observed in clinical practice. A schematic outline of Introduction and the relationships among sections is provided in Figure 1.

1.2 Cardiac structure and function

1.2.1 Cardiac structure

The heart is a powerful muscular organ that works as a pump to send oxygen-rich blood through the circulatory system to all parts of the body, and assists in the removal of metabolic waste from tissues [2]. On average, a human heart beats 100,000 times per day and pumps more than 16,000 L of blood throughout the body. The heart is composed of four chambers, two upper chambers known as the atria, and two lower chambers known as the ventricles (Figure 2). The interatrial septum separates the atria, while the interventricular septum separates the ventricles. In a healthy heart, heart valves ensure unidirectional blood flow through the heart and prevent backflow (Figure 2). In addition, the heart is enclosed in a protective double-membraned sac known as the pericardium, and has its own blood supply—the coronary circulation.

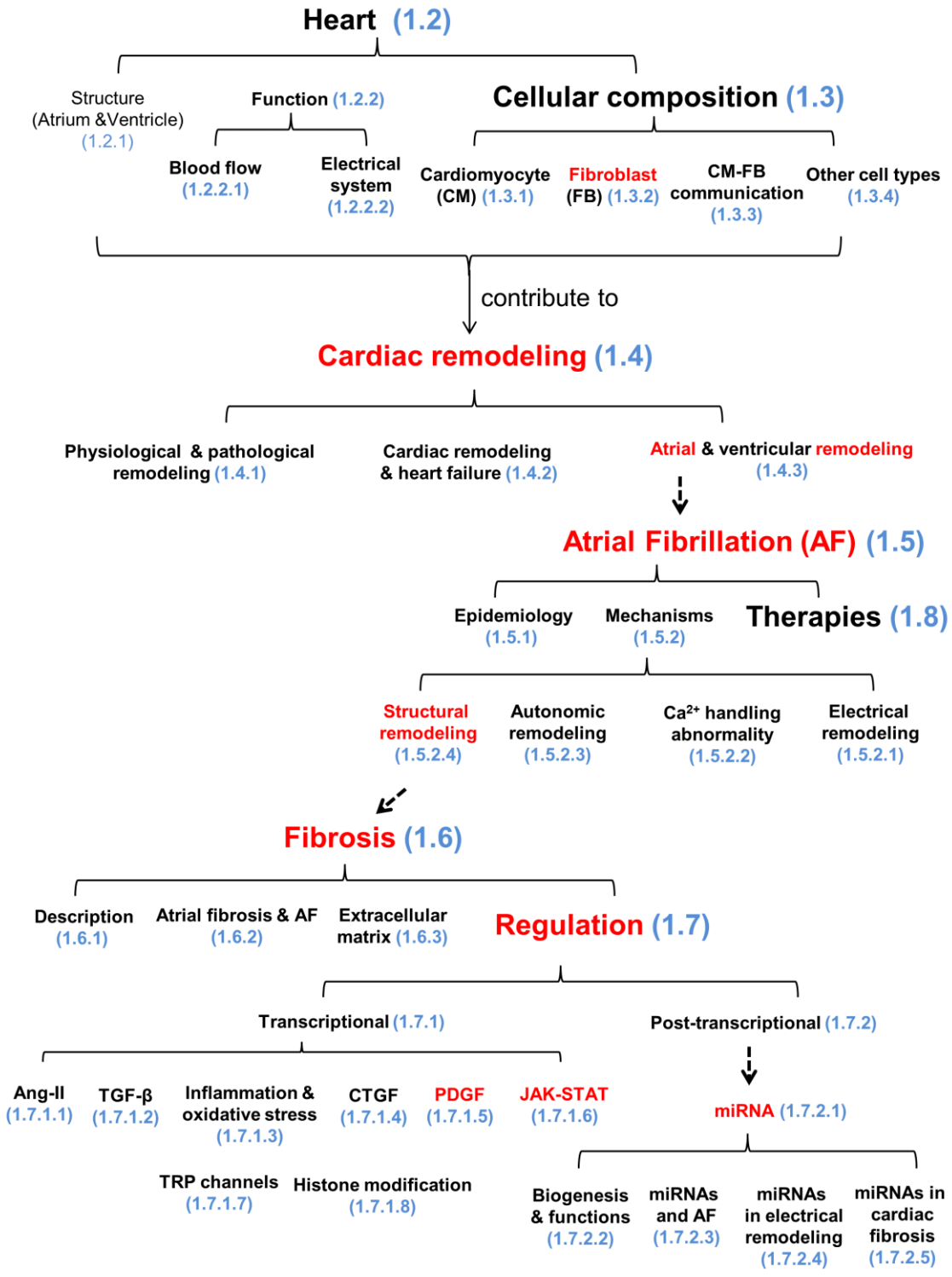

Figure 1. Schematic outline of the Introduction.

Title names in larger font indicate the sections numbering with the highest level. Red color indicates the key words of the introduction and the main sections. Blue color indicates the numbering of corresponding sections.

1.2.2 Cardiac function

1.2.2.1 Blood flow

The heart circulatory system includes the systemic circulation maintained by the left side of the heart, the left atrium (LA) and left ventricle (LV), and the pulmonary circulation maintained by the right side of the heart, the right atrium (RA) and right ventricle (RV). Blood in the pulmonary circulation collects oxygen from the lungs and delivers carbon dioxide for exhalation. Blood in the systemic circuit transports oxygen to the body and returns relatively deoxygenated blood and carbon dioxide to the lungs. The ventricles are stronger and have thicker muscular walls than the atria because ventricles pump blood further away from the heart. The chambers of the heart may be found in one of two states—systole (contraction) and diastole (relaxation). The coordination between atria and ventricles ensures blood is pumped efficiently to the body. Cardiac output (CO) is the volume of blood pumped by the heart in one minute, and is determined by the heart rate and the stroke volume. On average, a heart can eject approximately 5-5.5 L of blood per minute at rest [2-5].

1.2.2.2 Cardiac electrical system

Sinus rhythm (SR) is the normal rhythm of the heart and produces correct activation of the entire heart in an appropriate sequence. Any variation from SR is termed an arrhythmia. The sinoatrial node (SA node) is the heart's pacemaker, which is located in the upper and back wall of the RA. The SA node spontaneously fires periodically to begin each activation, and proceeds to activate both atria before reaching the atrioventricular node (AV node). At the AV node, activation proceeds more slowly to allow for optimal ventricular filling. The activation then enters the His-Purkinje system, which allows rapid propagation throughout the ventricles to induce a strong and

synchronized contraction. The heart beats and produces a single coordinated electrical wave that can be seen as a normal electrocardiogram (EKG or ECG). Variations in the waveform and distance between the peaks of the ECG can be used clinically to diagnose arrhythmias, myocardial infarction (MI), congenital heart conditions, and electrolyte imbalances [3, 4, 6]. The Electrical system of the heart and its correlation to the ECG is illustrated in Figure 3.

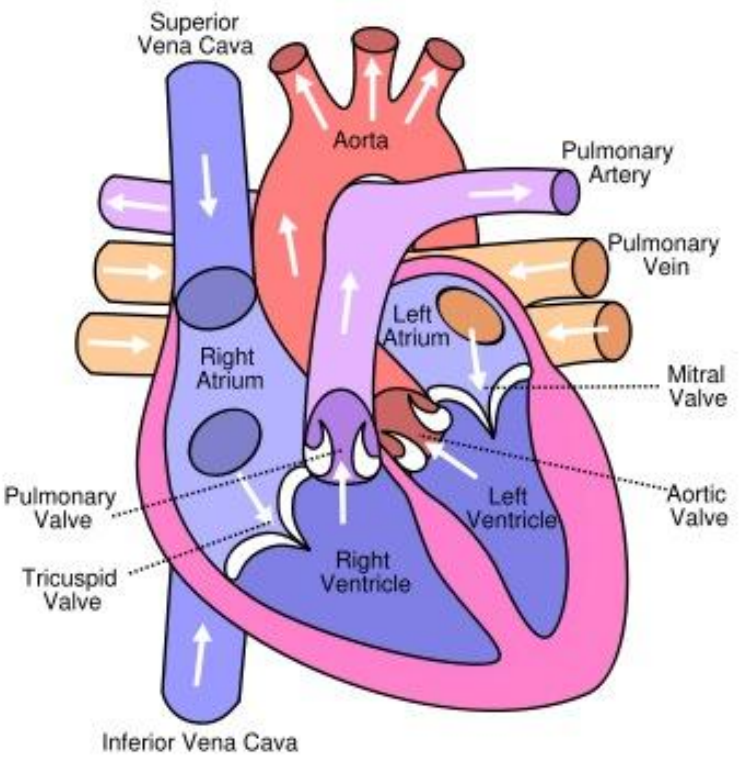

Figure 2. Simplified structure of the human heart.

This illustration depicts the chambers, valves, arteries, and veins. The white arrows indicate the normal direction of blood flow. The left atrium (LA) receives blood from the pulmonary veins. The right atrium (RA) receives blood from the superior vena cava (carrying deoxygenated blood from the head and upper body) and the inferior vena cava (carrying deoxygenated blood from the legs and lower torso). The right ventricle (RV) pumps oxygen-poor blood through the pulmonary artery and to the lungs. The left ventricle (LV) pumps oxygen-rich blood through the aorta and to the rest of the body. The four main cardiac valves are the two atrioventricular valves known as the mitral and tricuspid valves, and the two semilunar valves known as the aortic and pulmonary valves.

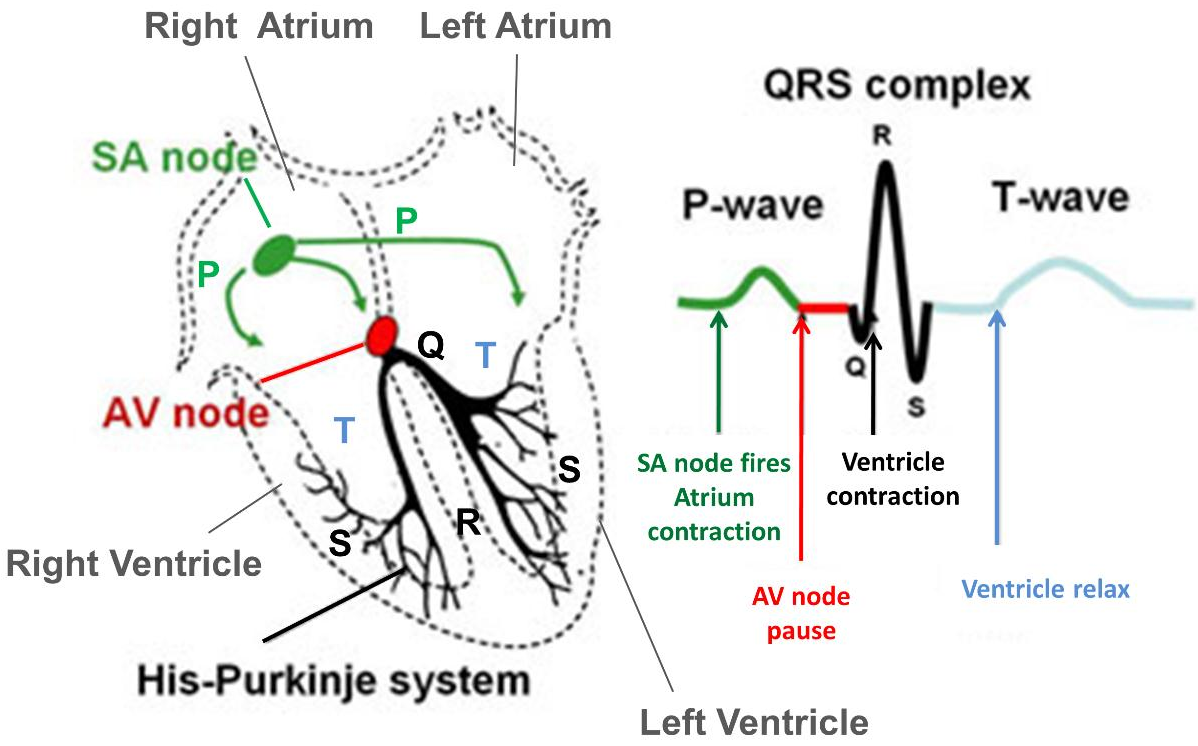

Figure 3. Electrical system of the heart and its correlation to the ECG.

The SA node spontaneously beats to begin each activation, and proceeds to activate both atria and reach the AV node. At the AV node, the activation then enters the His-Purkinje system, which allows rapid propagation throughout the ventricles to induce a strong and synchronized contraction. P-wave (green color) represents the spread of electrical impulse through the atrial musculature (activation or depolarization); QRS complex (black color) represents the spread of electrical impulse through the ventricular muscle (depolarization); T-wave (blue color) represents the period of recovery for the ventricles (repolarization). AV node, atrioventricular node; ECG, electrocardiogram; SA node, sinoatrial node.

1.3 Cellular composition

The wall of the heart is made up of three layers: the epicardium, myocardium, and endocardium [3]. The myocardium is the middle muscular layer predominantly comprising cardiomyocytes, fibroblasts, endothelial cells, and vascular smooth muscle cells. Together, these cells maintain the electric, chemical, and biomechanical function of the organ. Different cell types communicate with each other via autocrine and paracrine actions of secreted factors, as well as direct cell–cell interactions. Alterations in these biomechanical inputs can cause adaptive or deleterious remodeling in the heart.

1.3.1 Cardiomyocytes

The cardiomyocyte is the most important cell component and makes up approximately 75% of cardiac tissue volume [7]. The properties and functions of cardiomyocytes provide the unique ability of cardiac contractility, automaticity and rhythmicity. Cardiomyocytes are tightly bound and connected by gap junctions, through which ions can move. Action potentials (AP) originating from pacemaker cells excite cardiomyocytes and then spread to adjacent cardiomyocytes to allow succinct coordinated contraction of the atria and ventricles [8].

1.3.2 Fibroblasts

The major non-myocyte cells in the heart are predominantly fibroblasts, which are widely distributed and constitute 60%–70% of all cells in cardiac tissue [9]. Cardiac fibroblasts are mesenchymal in origin; the cells are flat and spindle-shaped with multiple processes sprouting from the main body [10, 11]. Fibroblasts derive from cardiac resident fibroblasts, endothelial cells via endothelial-mesenchymal transition (EndMT), epicardium-derived (epithelial) cells

through epithelial-mesenchymal transition (EMT), as well as perivascular cells, bone marrow-derived progenitor cells, and circulating fibrocytes; however, the functional relevance or contribution of each of these sources to fibrosis is unclear [12-15].

Cardiac fibroblasts play a central role in the maintenance of myocardial tissue structure and function. Unlike cardiomyocytes, fibroblast content increases with normal development and aging [9]. Fibroblasts are usually resting or quiescent. In response to external stressors, fibroblasts are activated and differentiate into myofibroblasts, which are more mobile, express alpha-smooth muscle actin (α-SMA), and acquire a contractile phenotype (Figure 4) [16, 17]. Activated fibroblasts display extensive rough endoplasmic reticulum, which is utilized to secrete extracellular matrix (ECM) [18]. The global functions of fibroblasts also include proliferation, migration, and the synthesis/secretion of ECM-regulating molecules such as cytokines, growth factors, and matrix metalloproteinases (MMPs) (Figure 4) [10]. Fibroblasts respond to a wide range of mechanical, chemical, and electrical signals, as well as stimuli such as hypoxia [9, 18]. It has been shown to sense mechanical stress via integrins, stretch-activated ion channels, and second messengers. Mechanical stimulation can induce signal transduction pathways, cell proliferation, and the upregulation of ECM, MMP, cytokines, and growth factors [9]. Chemical signals include hormones (e.g. adrenergic stimulation), circulating pro- or anti-inflammatory cytokines (e.g.interleukin-1 beta [IL-1β], interleukin-6 [IL-6], tumor necrosis factor alpha [TNF-α]), pro-fibrotic factors (e.g. angiotensin II [Ang-II], transforming growth factor-beta [TGF-β], and platelet-derived growth factor [PDGF]).

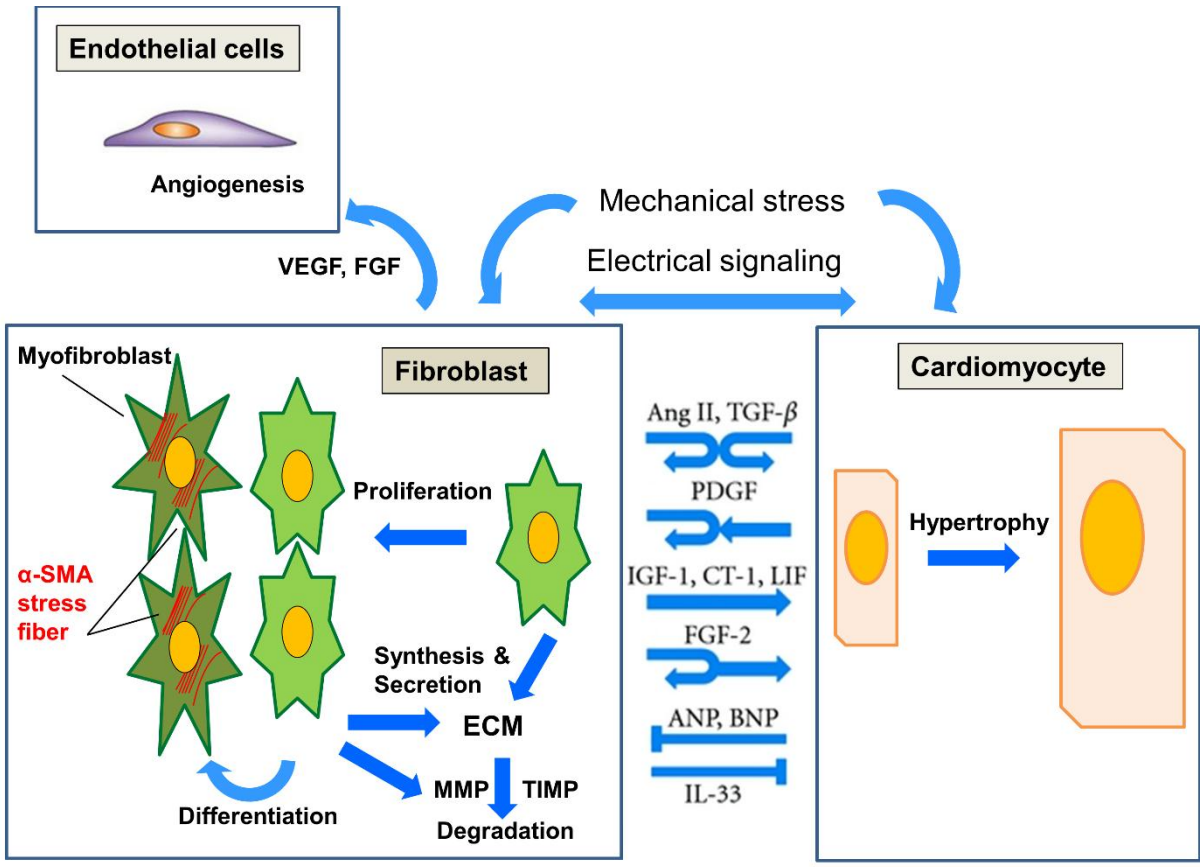

Figure 4. Reciprocal interactions between fibroblasts, cardiomyocytes, and endothelial cells.

Fibroblasts and cardiomyocytes are responsive to external mechanical stress, and communicate through chemical and electrical coupling. Many growth factors and cytokines act in an autocrine and/or paracrine fashion to induce proliferative responses of fibroblasts, hypertrophic responses of cardiomyocytes and angiogenesis of endothelial cells. Fibroblasts are activated and differentiate to myofibroblasts which is featured by α-SMA stress fiber. Fibroblasts and myofibroblasts synthesize and secrete ECM. ECM degradation is controlled by the balance between functional MMPs and TIMPs. This scheme only depicts some of the factors identified. α-SMA, alpha-smooth muscle actin; Ang-II, angiotensin II; ANP, atrial natriuretic peptide; BNP, brain natriuretic peptide; CT-1, cardiotrophin-1; ECM, extracellular matrix; FGF-2, fibroblast growth factor 2; IGF-1,insulin-like growth factor-1; IL-33, interleukin-33; LIF, leukemia inhibitory factor; MMP, matrix metalloproteinase; PDGF, platelet-derived growth factors; TGF-β, transforming growth factor-β; TIMP, tissue inhibitor of matrix metalloproteinase.

1.3.3 Cardiomyocyte–fibroblast communication

Fibroblasts and cardiomyocytes have an extensive, reciprocal communication via several means, including paracrine signaling molecules and direct contact via gap junctions (Figure 4). Cardiac fibroblasts induce proliferation of cardiomyocytes through fibroblast growth factor (FGF), ECM, periostin, and heparin-binding epidermal growth factor (EGF)-like growth factor in a paracrine fashion [19-21]. IL-6 is also important for maintaining the survival of adult cardiomyocytes [22, 23]. Signaling molecules like Ang-II, TNF-α and TGF-β are involved in cardiomyocyte hypertrophy during adaptive and maladaptive cardiac remodeling [24-26]. In turn, most of these mediators (e.g. Ang-II, TGF-β, and PDGF) are secreted by cardiomyocytes and trigger fibroblast proliferation, differentiation, and ECM deposition or turnover [26], with the exception of atrial natriuretic peptide and brain natriuretic peptide, which suppress the fibrogenic activity of fibroblasts [27, 28].

The electrical coupling between cardiomyocytes and fibroblasts has been well-established *in vitro*. The coupling of cardiomyocyte and fibroblast via gap junctions in culture system provides the possibility for electrical transmission and contribute to arrhythmogenesis [29]. Changes in expression of connexin (Cx) 43 in fibroblasts modulate intercellular coupling of cardiomyocytes [30-33]. However, whether, and how much, of such coupling exists *in vivo* is under strong debate. Immunohistochemical studies suggested the localization of Cx and functional coupling between cardiomyocytes and fibroblasts in native tissues [34-36]. Some other reports such as one study on rabbit SA node did not support the regular presence of heterocellular gap junctions in the heart [37]. Recently, potassium (K^+) channels have been identified in fibroblasts and connect with cardiomyocytes *in vitro* [38, 39].

1.3.4 Other cell types

The remaining cell types in cardiac tissue are endothelial cells, vascular smooth muscle cells, resident stem cells, immune cells and neural elements. Endothelial cells are capable of producing various chemical mediators that contribute to cardiac hypertrophy and fibrosis, such as endothelin-1 (ET-1). Communication between fibroblasts and endothelial cells affects angiogenesis during wound healing through FGF and vascular endothelial growth factor (VEGF) secreted by fibroblasts (Figure 4) [10, 40]. Resident stem cells, or cardiac progenitor cells, have the potential to differentiate into specific cardiac cells [41-43]. Stem cell therapy reduces myocardial scar formation and improves overall cardiac function experimentally and clinically [44-47]. Immune cells, such as macrophages are recruited and infiltrate the myocardium during cardiac injury and can promote cardiac remodeling by releasing cytokines and MMPs [48, 49]. Neural elements are part of autonomic nervous system which controls the heart rate and is involved in cardiac arrhythmogenesis [50].

1.4 Cardiac remodeling

Cardiac remodeling is defined as molecular, cellular, and interstitial changes that manifest clinically as alterations in structure (e.g. dimensions, mass, size, and shape) and function of the heart [51]. Cardiac remodeling can be classified as physiological (adaptive) or pathological (maladaptive) [52].

1.4.1 Physiological and pathological remodeling

Physiological remodeling describes the compensatory changes in the dimensions and function of the heart in response to physiologic stimuli such as endurance exercise and pregnancy. In order

to maintain or improve LV function and CO, the heart must either increase heart rate (as observed during transient exercise) or stroke volume (as observed with long-term exercise). The increase in stroke volume usually appears as increased heart mass, wall thickness, and chamber size. Physiological remodeling is a reversible and benign adaptation, associated with normal or enhanced cardiac function. Pathological remodeling, which occurs in cardiovascular diseases, is irreversible and associated with reduced cardiac function, accumulation of collagen (fibrosis) and increased mortality [53]. Pressure (or hemodynamic) overload, volume overload, and cardiac injury are the most observed causes of pathological remodeling. Cardiac injury is typically seen in MI. It is characterized by cell death and compensatory scar formation in the infarcted cardiac region, and a combination of volume and pressure load in non-infarcted zones. The different subtypes of cardiac remodeling share common molecular, biochemical, mechanical, and electrical alterations. Cellular changes that occur during cardiac remodeling include hypertrophy, apoptosis or necrosis of cardiomyocytes, and proliferation or differentiation of fibroblasts [54-56]. These alterations further deteriorate cardiac performance and contribute to the genesis of cardiac arrhythmias.

1.4.2 Cardiac remodeling and heart failure

Adverse remodeling causes loss or failure of cardiac functions which is heart failure (HF) [51]. Neurohormonal activation including norepinephrine of the sympathetic nervous system, angiotensin II (Ang II), and aldosterone in the renin angiotensin aldosterone system (RAAS), and endothelin 1 (ET-1), is increased by positive feedback as pathological remodeling progresses and further deteriorates cardiac performance. This is accompanied by an elevated end-systolic volume index and reduction in LV ejection fraction. Changes in cardiac function index are

important predictors of mortality [57]. The transition from pathological remodeling to HF and its time course vary greatly under different conditions [51].

1.4.3 Atrial and ventricular remodeling

Atrial remodeling has not been investigated as extensively as ventricular remodeling. Atrial remodeling is often due to LV diastolic dysfunction whereby the atria are adaptively changed to meet the requirement of pumping more blood into the ventricles. Similar cellular and molecular changes occur during atrial and ventricular remodeling [58, 59]. Qualitative- and quantitative-differential remodeling between the two chambers was first reported in dogs with ventricular tachypacing-induced HF [60, 61]. A clinical analysis found that cardiac remodeling occurred in a chamber-specific manner and that ECM content was greater in the atrial myocardium compared to the ventricle myocardium [62]. Various substrates including HF, hypertension, valve disease and sinus node disease cause atrial remodeling [63-69] and predispose to AF [70]. Atrial remodeling has emerged as a key pathophysiological mechanism underlying AF [70]. This thesis focuses on the molecular basis of atrial remodeling and how it provides substrates for AF.

1.5 AF

AF is a cardiac dysrhythmia (an irregular heart rhythm) in which there is chaotic electrical activity (at 350–600 beats per minute) in the atria. This causes the atria to quiver instead of contracting in an organized way. With rapid and irregular impulses traveling to the ventricles, the ventricles contract at a rapid rate and in an irregular rhythm (Figure 5).

1.5.1 Epidemiology of AF

AF is the most common sustained clinical arrhythmia associated with high risk for stroke, HF, thromboembolic events, and mortality [71, 72]. AF can occur at any age and its prevalence increases markedly with increasing age. The prevalence of AF is close to 2% in people older than 65 years and 10% in those aged above 80 years. AF is also more prevalent in men than in women [73]. AF can occur in patients without evident heart disease (so-called lone AF); however, clinical conditions such as congestive heart failure (CHF), hypertension, cardiomyopathy, valvular and coronary artery diseases are usually associated with the occurrence and persistence of AF and contribute to the development of AF substrate [70, 74, 75].

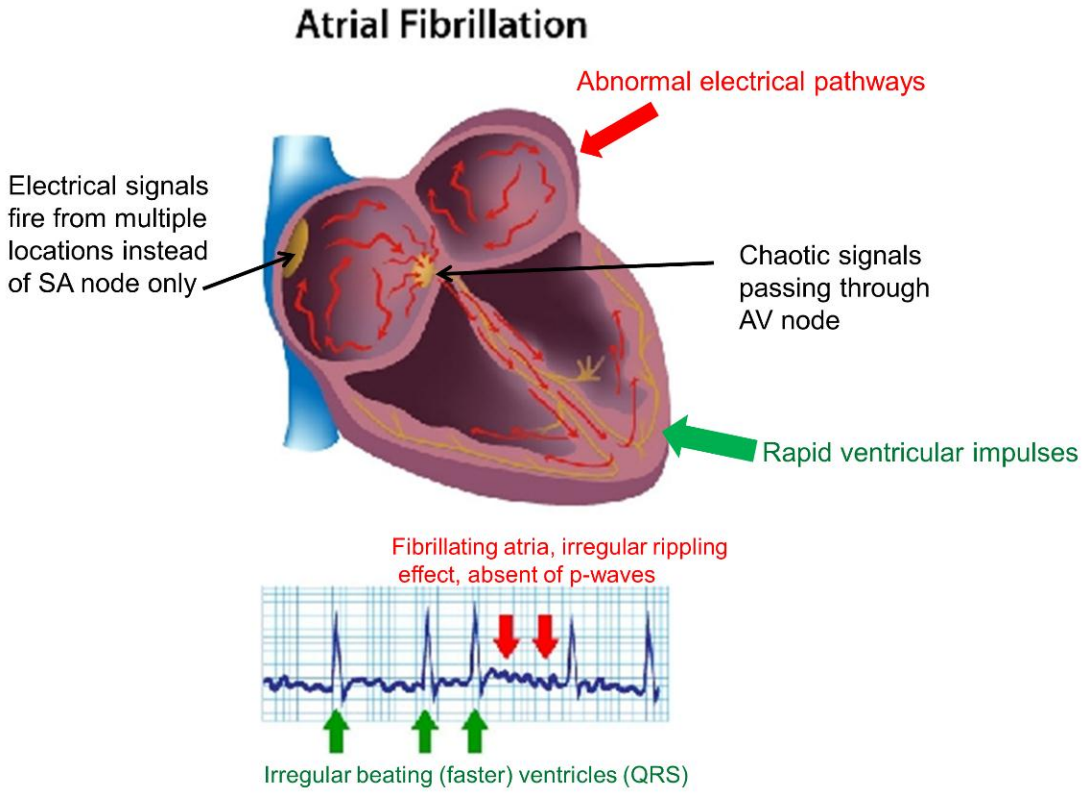

Figure 5. An illustration of atrial fibrillation (AF).

The top panel shows the pattern of abnormal electrical pathways in the atria and ventricles. The bottom panel shows the typical ECG recording of a patient with AF. AV, atrioventricular; ECG, electrocardiogram; SA, sinoatrial.

1.5.2 Mechanisms of AF

AF is often initiated by rapid firing (or triggers) from the pulmonary veins. In the early course of AF, SR can be spontaneously restored. As the substrate remodels further over time, AF becomes persistent or permanent [75]. Atrial remodeling promotes the occurrence or maintenance of AF by influencing the fundamental arrhythmia mechanisms, which are ectopic firing (or triggered automaticity) and reentry [69].

A normal cardiac action potential (AP) is illustrated in Figure 6A. The AP is governed by a sequence of actions involving the influx and efflux of sodium (Na^+), K^+, and calcium (Ca^{2+}) ions. Contractile cells have an AP with a much more stable resting phase and an extended plateau phase. This property results in an extended refractory period to allow complete contraction for the heart to pump blood effectively before cells are capable of firing for a second time. Triggered automaticity is generated in three ways: enhanced automaticity, early afterdepolarizations (EADs), or delayed afterdepolarizations (DADs) (Figure 6B and 6C). Ectopic firing provides triggers for the induction of reentry. When an ectopic beat encounters refractory tissue in one direction during propagation, it may be able to conduct in faster-recovering tissue in the other direction. If the impulse traverses the entire circuit slowly enough for all points to regain excitability, or the conduction time is greater than the longest refractory period in the circuit, reentry is maintained. The wavelength, which is the distance traveled by an impulse in one refractory period, or the shortest path length for reentry, determines the size of functional reentry circuits. Shortened AP refractory periods, slowed conduction velocity, and increased size/number of waves promote reentry [69].

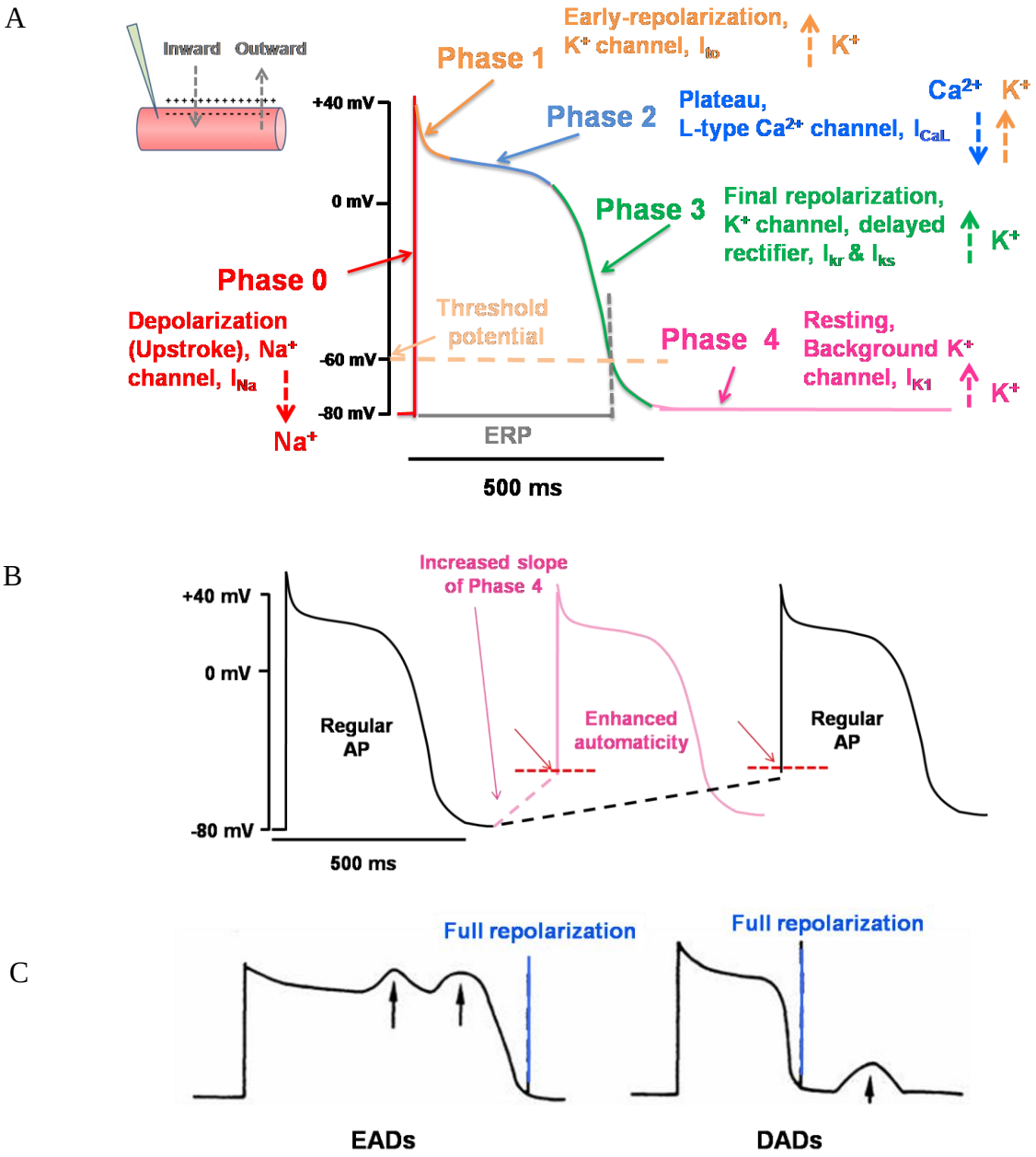

Figure 6. (A) A normal cardiac action potential (AP). Phases 0 to 4 occur in sequence and are shown in different colors with corresponding cellular changes, the responsible ion channels and currents. The dashed arrows indicate the influx (downward arrow) or efflux (upward arrow) of ions from the cell. During the effective refractory period (ERP) another AP cannot be generated. Threshold potential is the voltage at which the cell fires an AP. **(B)** Enhanced automaticity. Increased slope of the Phase 4 leads to spontaneous depolarization and next AP occur before one would normally arise. **(C)** Early afterdepolarizations (EADs) and delayed afterdepolarizations (DADs). EADs are caused by excessive AP prolongation, which allows Ca^{2+} channels (Phase 2) to recover and depolarize the cell leading to the generation of a premature AP. DADs are caused by spontaneous diastolic Ca^{2+} release leading to more positive membrane potentials and the firing of a premature AP.

AF itself causes AF-promoting abnormalities and induces atrial remodeling that makes spontaneous SR more difficult to recover, then promote the perpetuation of AF [77]. These findings have led to the theory that "AF begets AF" [76, 77]. There are four principal cellular or molecular mechanisms contributing to AF: electrical remodeling, Ca^{2+} handling abnormalities (sometimes included in electrical remodeling), autonomic nervous system changes, and structural remodeling (Figure 7A) [69, 78]. These mechanisms can create or facilitate electrical re-entrant circuits or triggers that lead to AF. Each mechanism will be described in detail in the following sections.

1.5.2.1 Electrical remodeling

AF alters atrial electrophysiological properties, promoting AF induction and maintenance [77]. Electrical remodeling denotes the alterations in atrial electrical properties, including rapid functional changes and slower alterations in ion channel gene expression. Electrical remodeling predominantly shortens the atrial refractory period by decreasing action potential duration (APD). The principle components of electrical remodeling have been identified as decreased L-type Ca^{2+} current (I_{CaL}) carried by L-type Ca^{2+} channels (the mechanism of Ca^{2+} entry into the cell), increased inward-rectifier K^+ currents such as background current I_{K1} and the constitutive acetylcholine-regulated K^+ current (I_{KACh}), decreased transient outward K^+ current (I_{to}), and abnormal expression/distribution of the gap junction Cx channels [78-82].

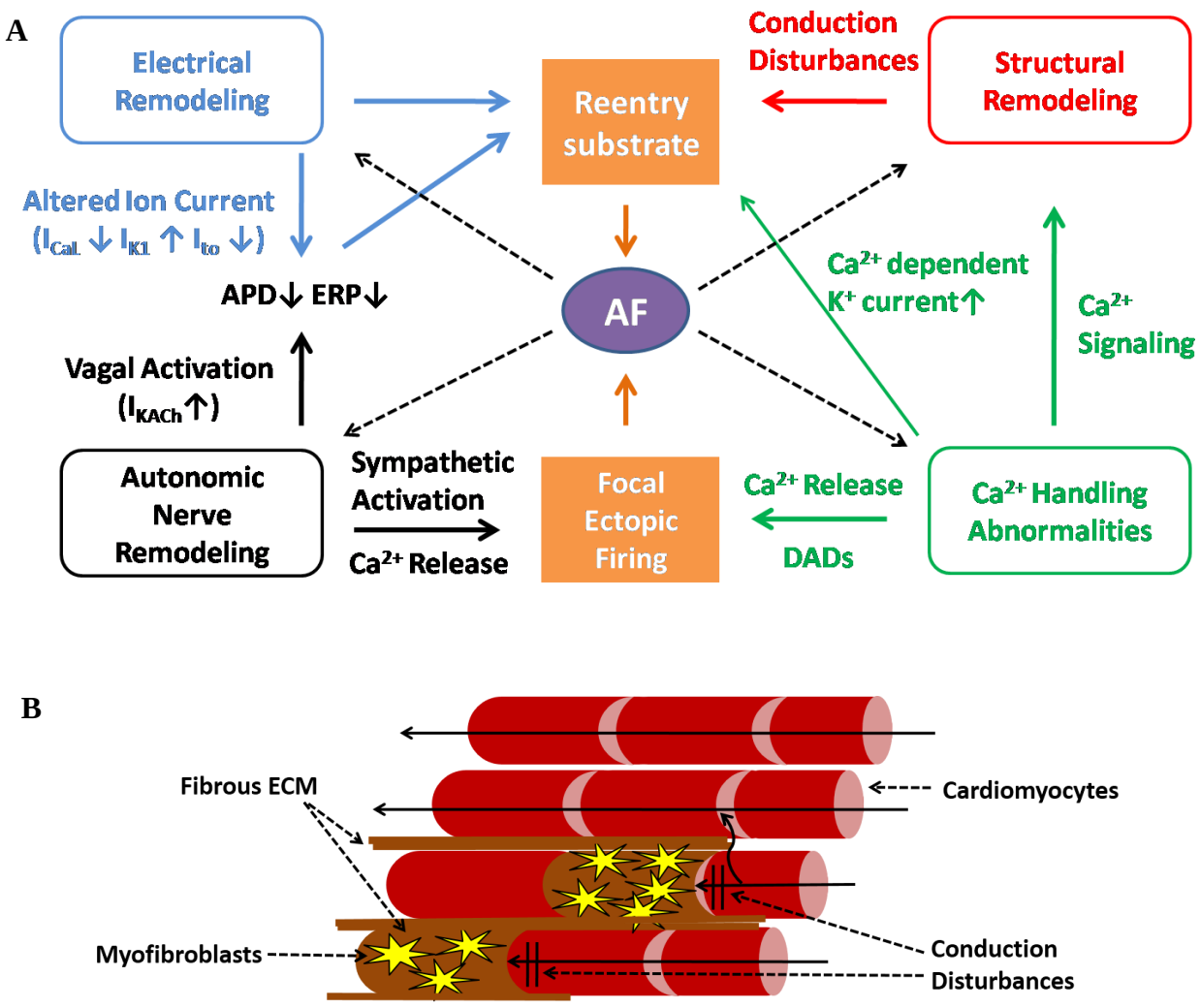

Figure 7. Principal mechanisms contributing to AF.

(A) The contributions of electrical remodeling, Ca^{2+} handling abnormalities, autonomic nerve remodeling, and structural remodeling. Ion channel expression or functional changes cause current alternation and abbreviate APD and ERP, providing reentry substrates (Electrical Remodeling). Atrial structural alterations induce conduction disturbances, facilitating re-entrant mechanisms (Structural Remodeling). Ca^{2+} release causes DADs and induces focal ectopic firing (Ca^{2+} handling abnormalities); Sympathetic activation increases spontaneous Ca^{2+} release leading to atrial ectopic beats. Increased vagal activation increases I_{KACh} and shortens APD (Autonomic Nervous Remodeling), thereby promoting AF. AF causes positive-feedback enhancement of these pathophysiological changes, allowing AF to become more stable with time**. (B)** Fibrotic remodeling contributes to AF. Cardiomyocyte death, fibroblasts proliferation and excess ECM deposition cause conduction disturbances between cardiomyocytes and impede electric propagation, favoring reentry. AF, atrial fibrillation; APD, action potential duration; DADs, delayed afterdepolarizations; ECM, extracellular matrix; ERP, Effective refractory period; $I_{CaL,}$ L-type calcium current; I_{KACh}, acetylcholine-dependent potassium currents; $I_{K1,}$ background K^+ current; $I_{to,}$ transient outward K^+ current.

Atrial cardiomyocytes respond by reducing Ca^{2+} influx via I_{CaL} to prevent potentially cytotoxic Ca^{2+} overload. Reduced I_{CaL} decreases the influx of positive ions (Ca^{2+}) into the cell (Figure 6A, Phase 2), favoring APD shortening and AF perpetuation [78]. Sustained AF causes more persistent I_{CaL} decreases, predominantly via downregulation of L-type Ca^{2+} channel subunit mRNA or via posttranscriptional mechanisms [78]. Oxidative stress, zinc homeostasis related protein ZnT-1 and tyrosine kinases are found to play an important role in I_{CaL} changes [83-85]. I_{K1}, which controls the cardiomyocyte resting potential, (Figure 6A, Phase 4) is formed by Kir2-family subunits, especially Kir2.1 [69]. AF increases expression of Kir2.1 mRNA and protein, enlarging I_{K1} and abbreviating APD [81, 86]. The inward-rectifier K^+ current I_{KACh} is activated by acetylcholine which is released from vagal nerve endings mediating cardiac parasympathetic effects. Increased I_{KACh} causes cell-membrane hyperpolarization and promotes AF by stabilizing atrial reentry [69]. Different from I_{K1}, I_{KACh} enhancement in AF is not due to increased expression of the underlying ion channel subunits but increased protein kinase C-mediated phosphorylation [82, 87]. I_{to} produces an outward-current component that oppose inward Na^+ current during the AP upstroke (Figure 6A, Phase 0). So the reduced I_{to} may facilitate wave propagation by indirectly increasing AP amplitude rather than shortening APD [78]. Reduction of mRNA and protein level of its pore-forming subunit Kv4.3 was seen in dog model of AF [88]. Increased proteolysis via calpain, and protein phosphatase calcineurin are suggested to suppress Kv4.3 expression in AF [89, 90]. Comparatively, less is certain about gap junction remodeling in AF [91]. Time-course changes in the distribution and content of Cx40 were observed in a goat AF model [92]. Clinical evidence was also provided on the link of Cx40 genetic variance and AF vulnerability [93, 94].

1.5.2.2 Ca^{2+} handling abnormalities

Abnormalities in Ca^{2+} handling can cause EADs and DADs. EADs generate abnormal depolarizations at plateau potentials. DADs cause cell firing either as a single ectopic beat or as a sustained tachycardia (Figure 6B and 6C). Any change that enhances diastolic Ca^{2+} loading will favor Ca^{2+} extrusion from the cell through the Na^{+}/Ca^{2+} exchanger (NCX) which produces a depolarizing current causing arrhythmogenic DADs and producing triggered activity. Cytosolic changes that favors DADs include enhanced phospholamban phosphorylation, protein kinase A (PKA) and Ca^{2+}/calmodulin-dependent protein kinase II (CaMKII) activity, calsequestrin deficiency and increased open probability of the ryanodine receptor type 2 (RyR2) through which Ca^{2+} leaves the sarcoplasmic reticulum (the principal Ca^{2+} storage organelle) to produce Ca^{2+}-induced Ca^{2+} release, and these changes were important contributor to AF-related ectopic activity [69, 78]. In addition, Ca^{2+}-activated K^{+} channels (SK channel) activated by increased levels of intracellular Ca^{2+} can abbreviate the APD [95]. These abnormalities may be due to underlying heart disease or genetic pre-disposition.

1.5.2.3 Autonomic nerve remodeling

Autonomic nervous system activation can induce significant changes in atrial electrophysiology and induce AF [96]. Heterogeneously increased atrial sympathetic innervations was documented in dogs with pacing-induced AF or ventricular myocardial infarction [97, 98]. Increased sympathetic nerve densities were also found in AF dogs and patients [99, 100]. The sympathetic and parasympathetic nervous subsystems have been implicated in regulating atrial electrophysiology, and both play a critical roles in the initiation of AF [70, 101, 102]. Sympathetic activation via adrenergic activation through beta-adrenoceptors (primarily β1-

receptors) increases spontaneous Ca^{2+} release by altering I_{CaL}, RyR2 open probability, and phospholamban phosphorylation (governing sarcoplasmic reticulum Ca^{2+} load), and promote arrhythmogenesis. Adrenergic drive is required to manifest Ca^{2+} release and ectopic activity in a canine model of atrial ischemia [103]. In addition, slow delayed rectifier K^+ current (I_{Ks}, Figure 6A, Phase 3) and I_{K1} are regulated by adrenergic activity. $I_{CaL,}$ I_{Ks} and I_{K1} are closely related to the occurrence of enhanced automaticity and EAD. The parasympathetic or vagal stimulation via cholinergic activation causes increased constitutive I_{KACh} and APD shortening [96].

1.5.2.4 Structural remodeling

Atrial structural remodeling includes atrial hypertrophy, dilation, necrotic and apoptotic cell loss, and fibrosis. Atrial dilation increases the amount of atrial tissue and promotes AF by increasing circuit path space so that larger reentry circuits can be supported and/or a larger number of circuits can be accommodated. Atrial dimensions are an important determinant of the occurrence of multiple-circuit reentry, and a clinical predictor of AF maintenance [104]. In contrast, fibrosis mainly interferes with local atrial conduction by disturbing the continuous cable-like arrangement and impairing the mechano-electric coupling of cardiomyocytes (Figure 7B) [63, 105]. A study using a pacing sheep model concluded that electrical remodeling is sufficient to induce spontaneous AF maintenance, while structural changes are necessary for longer-lasting persistent AF [106]. After full hemodynamic recovery from CHF, atrial dilation resolves but fibrosis remains, which probably underlies the AF inducibility [105].

1.6 Fibrosis

1.6.1 Description

In general, tissue fibrosis is a scarring process characterized by fibroblast accumulation and excess deposition of ECM proteins. Fibrosis leads to distorted organ architecture and function [107]. Cardiac fibrosis is similar to fibrosis in other organs such as the liver, lungs, and kidney; there is excessive ECM deposition, as well as the accumulation of activated fibroblasts and mononuclear infiltrate [108, 109]. Fibrosis manifests in two forms: reparative and reactive fibrosis. Reparative (or replacement) fibrosis often refers to scarring or wound healing and usually accompanies cardiomyocyte death. This is typically seen after acute cardiac injury such as MI. Reactive fibrosis appears as interstitial or perivascular deposits and is not directly associated with cardiomyocyte death. Cardiac fibrosis is initially an adaptive response aimed to preserve the capacity or function of the heart [110, 111].

1.6.2 Atrial fibrosis and AF

Atrial fibrosis is an important factor in the progression from paroxysmal to persistent and permanent AF [105]. Fibrotic replacement between cardiomyocytes causes conduction delays and allows for alternate pathways of conduction [69]. Atrial fibrosis is sufficient, but it is not necessary, for the induction of AF. Canine models of HF have demonstrated a progressive increase in AF inducibility with increasing fibrosis [63, 112]. Chronic fibrosis induced by chronic rapid ventricular pacing or overexpression of TGFβ-1 significantly increased AF susceptibility [113, 114]. However, atrial biopsy samples from patients with lone AF revealed that 25% of these patients exhibited no hallmarks of atrial fibrosis; subsequently, a goat model of AF was developed without significant evidence of atrial fibrosis [115, 116]. AF is also capable of enhancing atrial fibrosis. It has been shown that AF patients with normal sized atria upon diagnosis showed structural remodeling of the atria over a subsequent period of 20 months [117].

1.6.3 ECM

Imbalance between ECM deposition and degradation is the main cause of cardiac fibrosis. The ECM includes a variety of proteins such as collagens, proteoglycans, glycoproteins, and proteases. The ECM serves several purposes under physiological conditions including providing scaffolding for all cardiac cells, transducing mechanical signals to individual cells, and electrically separating the atria and the ventricles [108]. However, excessive ECM deposition throughout the myocardium results in pathological remodeling: (1) it increases mechanical stiffness and diastolic dysfunction; (2) it disrupts electrical coupling between cardiomyocytes, leading to impaired cardiac conduction (Figure 7B); and (3) it can lead to perivascular fibrosis which may decrease the flow of oxygen and nutrients [118-120]. Fibroblasts are responsible for ECM homeostasis due to their ability to secrete and breakdown proteins that form the ECM. ECM accumulation is a secondary effect influenced by signaling pathways induced by cytokines, growth factors, hormones, cellular transformation, and physical stress [121].

1.6.3.1 Collagen and fibronectin

Increased production or accumulation of collagens is the hallmark of tissue fibrosis. There are more than 30 types of collagen and collagen-related proteins but the most abundant type is collagen I [122]. Collagen type I and type III comprise approximately 90% of all collagen in the heart, responsible for maintaining the structural integrity of myocardial tissue [122]. Collagen type I is characterized by thick fibers that confer stiffness and resistance to stretch and deformation; it contributes to systolic and diastolic dysfunction in cardiomyopathy [123]. Procollagen is secreted to the extracellular space where it undergoes further processing, including cleavage, aggregation, and crosslinking to fibrils and fibers. The deposited mature

collagens with decreased digestibility in the myocardium contribute to myocardial fibrosis and dysfunction [124]. Synthesis and deposition of collagens are highly coordinated processes, and are regulated by autocrine and paracrine factors such as Ang-II, TGF-β, and aldosterone [125]. In addition to secretion, changes in the degree of collagen crosslinking is also associated with cardiac function [126].

Less abundant ECM molecules in the myocardium include collagen types IV, V, and VI, fibronectin, fibrillin, elastin, and laminin [127]. Different cardiac pathologies have different ECM characteristics. Fibronectin is a dimeric glycoprotein that connects cardiomyocytes to collagen fibers, and influences diverse cellular properties including adhesion, growth, and wound repair [128]. Fibronectin has been shown to interact with collagen type I and is critical for collagen fibril formation *in vivo* [122]. It also plays an essential role in the assembly of fibrillin-1 into a structural network [129]. In HF and AF, fibronectin-1 and fibrillin-1 are upregulated and correlate with increases in collagens [130, 131].

1.6.3.2 MMP and Tissue inhibitors of MMP (TIMP)

Fibroblasts modulate the degradation of ECM by altering the expression of MMPs and their natural inhibitors, TIMPs. MMPs are a family of zinc-dependent endopeptidases and in most cases are secreted to the extracellular space as inactive pro-MMPs. Twenty-six human MMPs have been identified, and all are extracellular including the membrane-bound ones like membrane-type I MMP (MT1-MMP) [132, 133]. In contrast, there are only 4 types of TIMPs, TIMP-1 to -4. TIMPs can directly inhibit the proteolytic activity of activated MMPs [134].

It was reported that MMP-9 expression or activity was increased in an atrial-paced canine model with HF and AF patients [62, 135, 136]. Upregulation of MMP-2 and downregulation of

TIMP-1, TIMP-2, and TIMP-4 were also observed in AF atria [136-138]. However, in a rapid-pacing sheep and porcine model, MMP-2 expression was decreased and TIMP-1/2/3 expression was increased [106, 139]. A delicate balance between MMPs and TIMPs in ECM degradation is seen in AF [62, 130, 135]. Expression of MMPs and TIMPs can be regulated by neurohormonal peptides, Ang-II, growth factors (e.g. TGF-β), inflammatory cytokines (e.g. IL-1α and TNF-α), and reactive oxygen species (ROS) [140-142]. The detailed fibrogenetic signaling pathways related to ECM turnover will be explained in the following sections.

1.7 Molecular regulation of atrial fibrosis

The molecular mechanisms that lead to the development of atrial fibrosis are highly complex (Figure 8).Yet the precise mechanisms and signaling pathways involved remain to be clarified. Expression of pro-fibrotic or anti-fibrotic proteins can be regulated by transcriptional and post-transcriptional modification, which will be detailed in the following sections.

1.7.1 Transcriptional regulation

1.7.1.1 Ang-II

Ang-II is part of the renin-angiotensin system that helps regulate blood pressure. Ang-II is converted from Ang-I and binds to Ang-II receptors type I (AT-1) and type II (AT-2), which induce opposing responses. The activation of AT-1 by Ang-II activates mitogen-activated protein kinases (MAPKs), which stimulate proliferation of fibroblasts [143, 144]. The phosphorylation cascade includes orderly activations of Src family, small GTPase Ras, and serial activation of extracellular signal-regulated kinases (ERK)-related kinases [142]. Transcription factors activated by the Ang-II pathway include activating protein-1 (AP-1), nuclear factor-kappa B

(NF-κB), and signal transducers and activators of transcription (STAT) [145]. In vascular smooth muscle cells and cardiomyocytes, Ang-II signaling cascade induces Ca^{2+} release from intracellular stores by activating protein kinase C (PKC), cellular hypertrophy, and apoptosis [146-148]. In contrast, activation of AT-2 inhibits MAPK resulting in anti-proliferative effects, which supports cell survival [149, 150].

Many studies support the role of Ang-II in AF. Overexpression of cardiac-specific angiotensin-converting enzyme (ACE) causes atrial fibrosis and cardiac arrhythmia in mice [151]. In clinical studies, Ang-II concentrations are elevated and ERK activation is increased in patients with atrial fibrosis and AF development [143]. Furthermore, several studies in patients with CHF and animal models of AF have shown that ACE inhibitors and angiotensin-receptor blockers (ARBs) reduce atrial fibrosis and the occurrence of or vulnerability to AF [152-155].

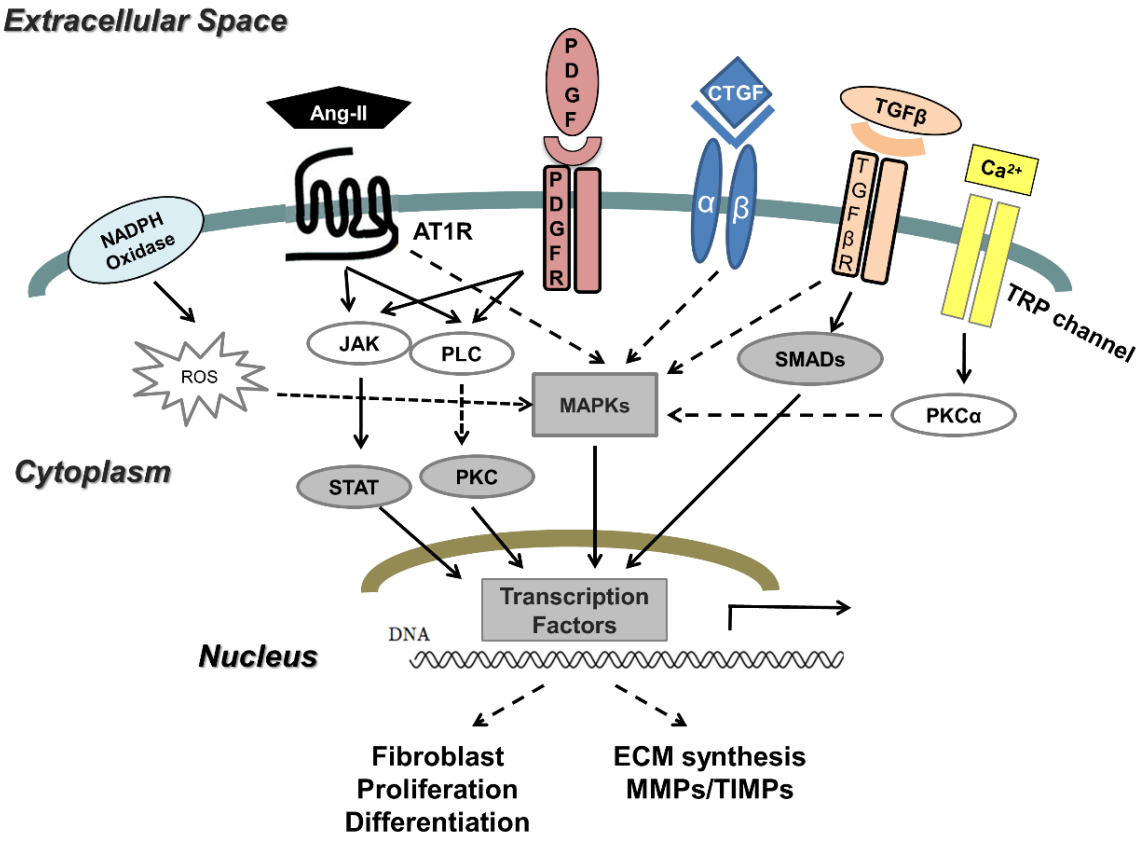

Figure 8. Known pro-fibrotic signaling pathways in the heart.

Signaling pathways induced by Ang-II, TGF-β, oxidative stress, CTGF, PDGF, and TRP channels are depicted. MAPK is a central downstream mediator of oxidative stress, Ang-II (AT1R), TGF-β, CTGF, and TRP channels. Multiple transcription factors participate in the activation of gene transcription responsible for proliferation and differentiation of fibroblasts, or ECM synthesis including collagens, MMPs and TIMPs. Bold arrows indicate direct activation and dash arrows indicated indirect activation. Ang-II, angiotensin II; AT1R, angiotensin II type I receptor; CTGF, connective tissue growth factor; ECM, extracellular matrix; JAK, Janus kinase; MAPKs, mitogen-activated protein kinases; MMPs, matrix metalloproteinases; NADPH, nicotinamide adenine dinucleotide phosphate; PDGF, platelet-derived growth factor; PDGFR, platelet-derived growth factor receptor; PLC, phospholipase C; PKC, protein kinase C; ROS, reactive oxygen species; SMADs, contraction of Sma and Mad (Mothers against decapentaplegic); STAT, signal transducers and activators of transcription; TGF-β, transforming growth factor-beta; TIMPs, tissue inhibitor of matrix metalloproteinases; TRP, transient receptor potential.

1.7.1.2 TGF-β

There is accumulating evidence to suggest a critical role for TGF-β1 in atrial fibrosis and AF pathogenesis. TGF-β1 is a growth factor belonging to the TGF-β family involved in many cellular process including cell growth and cell differentiation. It can be upregulated by Ang-II and norepinephrine [156, 157]. TGF-β1 induces signaling cascades through binding to serine/threonine kinase receptors and phosphorylating the SMAD family of intracellular signal transducers. The most important responsive gene of TGF-β1 related to fibrosis is collagen type I [140]. TGF-β1 can also upregulate MMP-2 and membrane-type MMPs in fibroblasts [156, 158]. In addition to the SMADs, transcription factors that participate in TGF-β1 signaling include c-Jun, AP-1, activated transcription factor-2, and Elk-1 [145]. Other than pro-fibrotic effects, TGF-β1 is involved in immunosuppression and tumor suppression as it is anti-proliferative in epithelial cells [159]. TGF-β1 signaling is upregulated in porcine fibrillating atria, canine CHF atria, and in clinical patients with AF [61, 160, 161]. Transgenic mouse models overexpressing TGF-β1 exhibit atrial-selective fibrosis [114]. TGF-β1 monoclonal antibodies are shown to reduce ECM expression and prevent fibrosis and diastolic dysfunction [162, 163]. The use of TGF-β production inhibitor pirfenidone reduced arrhythmogenic atrial remodeling and AF vulnerability canine model of HF [164-166].

1.7.1.3 Inflammation and oxidative stress

As previously mentioned, inflammatory mediators such as IL-1β, TNF-α, and IL-6 modulate fibroblast behavior by activating transcription factors like NF-κB and AP-1 through ERKs, JNK, p38, or ROS. By activating MMP activity, inflammatory cytokines are important regulators of ECM protein turnover [167-169]. Inflammatory infiltrates have been found with fibrosis in atrial

tissue of patients with AF and in a canine model [115, 170, 171]. Atrial fibrosis and susceptibility to AF increase by overexpressing TNF-α in a transgenic mouse model [172]. ROS arises from oxidative stress through the activation of nicotinamide adenine dinucleotide phosphate (NADPH) oxidase. It activates similar pathways to the inflammatory pathways which are activated in both cardiomyocytes and fibroblasts. The recognized functions of ROS include increasing fibroblast proliferation and collagen expression, as well as maintaining balance between MMP and TIMP activities [173, 174]. Treatment with anti-inflammatory and anti-oxidant agents appear to reduce atrial structural remodeling and the recurrence of AF [155, 175, 176].

1.7.1.4 CTGF

CTGF is a cysteine-rich mitogenic protein secreted in connective cells, e.g. fibroblasts. The specific receptor for CTGF has yet to be identified but binding to integrins and heparin is essential for CTGF activity [177]. CTGF can trigger many of the cellular processes that contribute to fibrogenesis, such as cell proliferation, adhesion, migration and ECM synthesis [178]. There are TGF-β1 responsive elements localized in the CTGF promoter site and CTGF is coordinately expressed with TGF-β1 [178-180]. In addition to TGF-β1, a number of regulators of CTGF expression have been identified, including Ang-II, VEGF, TNF-α, shear stress, cell stretch, and ROS. CTGF can directly bind matrix components such as fibronectin, and it functions as a molecular bridge aiding in the integration between extracellular and intracellular signaling networks [181, 182]. CTGF acts through Rac1 to activate the mixed-lineage protein kinase 3 (MLK3)/JNK pathway and trigger collagen I expression [183]. Adam et al. showed that the left-atrial fibrosis in patients with AF was associated with elevated expression of CTGF,

which contributed to the Ang-II-induced signal transduction during the atrial fibrogenesis [184-186]. CTGF is upregulated in the atrial tissue of AF dogs, and patients with chronic AF, and higher baseline level of serum CTGF is associated with the AF recurrence in patients with non-paroxysmal AF following catheter ablation [187-189]. All these suggest the important role of CTGF in AF pathogenesis.

1.7.1.5 PDGF

PDGF is a member of the VEGF family and is known to stimulate proliferation, migration, and differentiation in multiple types of cardiac cells. PDGF precursors including A-, B-, C-, and D-chains are synthesized and undergo processing and intracellular assembly before secretion. PDGF-A and -B are induced by early growth response factor-1 (Egr-1) and Krüppel-Like Factor-5 (KLF5) activated by Ang-II [190]. PDGF homo- or hetero-dimers, including PDGF-AA, -AB, -BB, -CC, and -DD bind to PDGF receptor dimmers (PDGF receptor αα, αβ, or ββ). The expression level and mitogen effects of PDGF isoforms differ in different cardiac cell types. After PDGF binds to its receptor, PDGF receptors dimerize and activate a tyrosine kinase (e.g. Janus kinases, JAKs) that initiates the RAS/ERK1, phosphoinositide 3-kinase (PI3K)/AKT, JAK/STAT, or phospholipase C (PLC)/PKC signaling pathways. PDGFs elevate the transcription of mitogenic genes such as c-Myc and Fos [69, 191]. However, the detailed signaling pathways triggered by PDGF in fibrogenesis remain poorly understood.

Transgenic mice with cardiac-specific overexpression of PDGF-A/-C/-D show cardiac fibrosis followed by HF or early lethality [192, 193]. PDGF-D promotes fibrogenesis through activation of the TGF-β1 pathway, which exerts positive feedback on PDGF-D synthesis [194]. PDGF receptor blockade significantly suppresses fibrogenesis in non-infarcted myocardium

post-MI [195]. Thus, PDGF is a crucial molecule that mediates cardiac fibrosis. In addition, PDGF is associated with atrial-selective fibroblast hyper-responsiveness observed in experimental HF model [196, 197]. In addition, administration of PDGF-AA promoted atrial fibrosis and enhanced AF susceptibility in normal hearts; Injection of neutralizing PDGF receptor α-specific antibody attenuated atrial fibrosis and AF inducibility in pressure-overloaded hearts [197]. Furthermore, PDGF released by myofibroblasts contributes to electrical remodeling by shortening the APD and reducing the density of I_{CaL} in cardiomyocytes [198]. All this evidence suggests the important role of PDGF in atrial fibrosis and AF.

1.7.1.6 JAK-STAT pathway

JAK belongs to a family of non-receptor protein tyrosine kinases comprising JAK1, JAK2, JAK3, and Tyk2. Each JAK is associated with particular cytokine receptors. STATs are latent transcription factors that reside in the cytoplasm until activated. Seven mammalian STATs have been identified: STAT1, 2, 3, 4, 5A, 5B, and 6. More than 30 cytokines and hormones can activate the JAK-STAT pathway, including Ang-II, PDGF, IL-6, interferons alpha/beta/gamma (IFN-α/β/γ), cardiotrophin-1 (CT-1), and leukemia inhibitor factor (LIF) [199]. When ligands bind to the receptor, two JAKs are brought into close proximity allowing cross-phosphorylation of tyrosine residues on each JAK. Activated JAKs subsequently phosphorylate the receptor and STATs on the tyrosine sites. Phosphorylation permits dimerization and translation of STATs into the nucleus. STAT dimers bind to DNA and other gene regulatory proteins and stimulate the transcription of target genes [200]. JAKs also phosphorylate other signaling proteins, linking JAK signaling to pathways such as MAPK [201]. The responsive genes of the JAK-STAT pathway include cell-cycle progression genes such as Fos, cyclin-D, c-Myc, and

angiotensinogens [190, 202]. Therefore, the JAK-STAT pathway plays a key role in cytokine-mediated signal transduction leading to cell growth, differentiation, and death. The JAK-STAT signaling pathway is illustrated in Figure 9.

The JAK-STAT pathway participates in CTGF-induced proliferation and differentiation of human hypertrophic scar fibroblasts [203]. STAT3 mediates IL-6–induced cardiac collagen upregulation during hypertrophy in rats [204]. Ang-II is found to activate STAT3 via Rac1 in atrial fibroblasts and cardiomyocytes *in vitro*, as well as in the atrial tissue of patients with permanent AF [205, 206]. STAT1 and STAT3 are activated and nuclear translocation of STAT3 is increased in a pacing-induced sustained AF model [207]. In addition, the JAK-STAT pathway is involved in cardiomyocyte hypertrophy, ventricular remodeling, and decreased expression of L-type Ca^{2+} channel [202, 207].

Thus far, evidence linking PDGF stimulation and the JAK-STAT pathway is limited. PDGF is known to induce phosphorylation of the JAK family (JAK1, JAK2, and Tyk2) and STAT proteins (STAT1, STAT3 and STAT5), accompanied by specific DNA binding activities [208, 209]. STAT6 and JAK1 are common elements in PDGF and IL-4 signaling in fibroblasts [210]. One recent study found that STAT3-mediated Myc expression is required for PDGF-induced mitogenesis [211]. JAK1 and JAK2 inhibitors, such as INCB16562 and Ruxolitinib (INCB018424) have been used clinically for the treatment of myelofibrosis [212, 213]. The STAT3 selective inhibitor cryptotanshinone relieves cardiac fibrosis in acute myocardial infarction by downregulating Ang-II–induced ERK1/2 phosphorylation and upregulating the expression of MMP-2 [214, 215]. Another STAT3 selective inhibitor S3I-201 decreases collagen synthesis in hypertrophied hearts [216]. In addition, S3I-201 can protect against Ang-II–induced oxidative stress, endothelial dysfunction and hypertension [217].

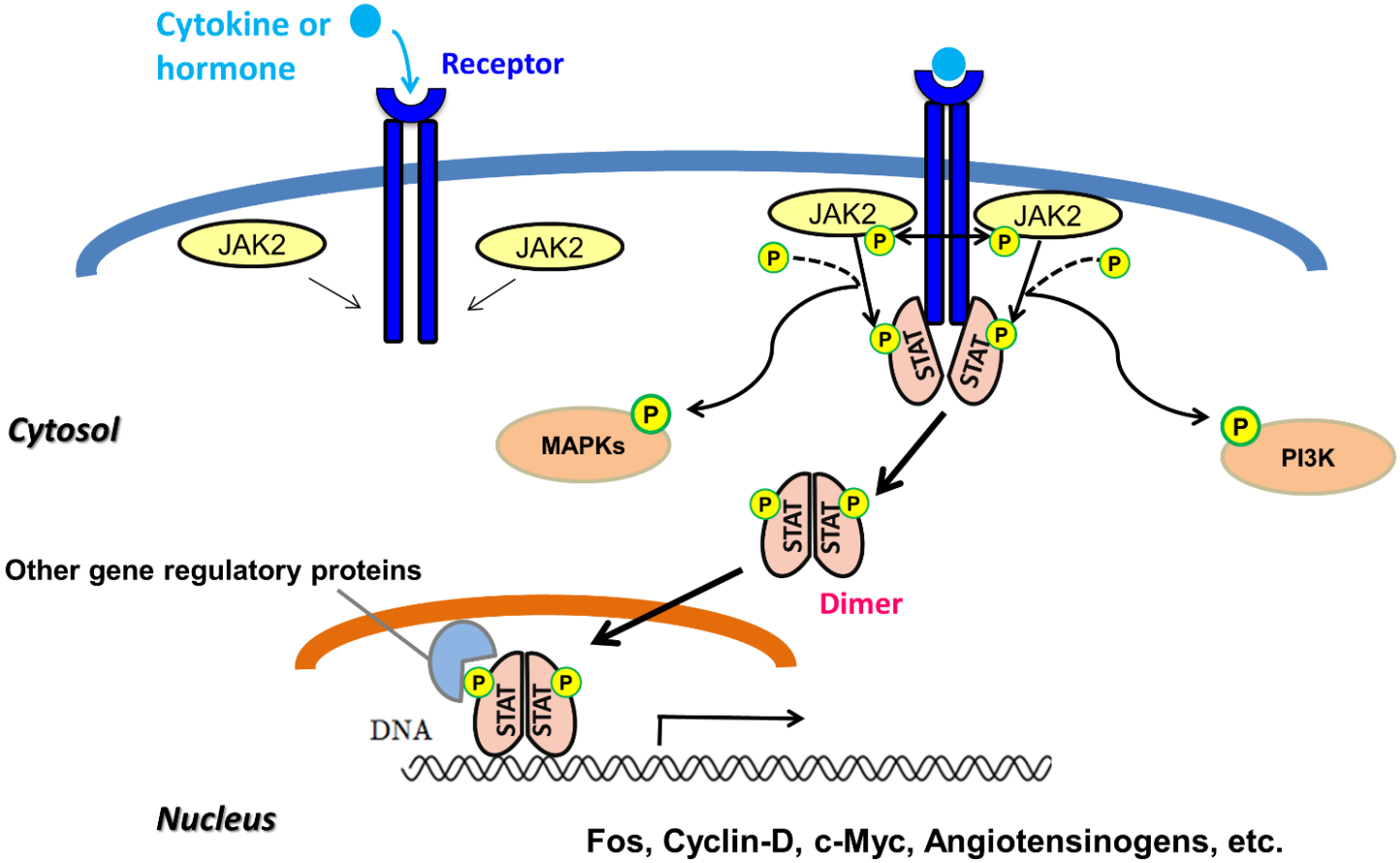

Figure 9. Schematic representation of JAK-STAT signaling.

Binding of cytokines or hormones cross-links adjacent receptors, leading to cross-phosphorylation of JAKs and phosphorylation on the receptors. The STATs that dock on the receptor are phosphorylated by JAKs. After dissociation from the receptor, the STATs dimerize and migrate into the nucleus where they bind to DNA and other gene regulatory proteins to activate gene transcription. JAKs also phosphorylate other signaling proteins such as MAPKs and PI3K. MAPK, mitogen-activated protein kinase; JAK, Janus kinase; P, phosphorylation; PI3K, phosphoinositide 3-kinase; STAT, signal transducers and activators of transcription.

1.7.1.7 Transient receptor potential (TRP) channels

Recently, TRP channels were found to be Ca^{2+} permeable channels in fibroblasts and are associated with fibroblast proliferation and differentiation [218, 219]. TRP channels are sensitive to mechanical stretch, chemical stimuli, oxidative stress and intracellular Ca^{2+} concentration [220, 221]. TRP canonical 3 (TRPC3) is a non-selective cation channel implicated in cellular Ca^{2+} entry, particularly in the response of fibroblasts [222]. TRPC3 enhances fibroblast proliferation and differentiation via Ca^{2+} dependent ERK1/2 signaling [219]. Atrial fibroblast TRPC3 current is increased in canine models of AF and protein expression is upregulated in clinical AF [219].

Taken together, there is a highly coordinated network of pro-fibrotic signaling pathways with many reactive regulators involved. Cytoplasmic effectors including signaling transducers and transcription factors overlap among the different pathways. There is cross-regulation among the secreted regulators as well. The regulatory network is summarized in Figure 10. Note that in addition to MAPKs (shown in Figure 8), JAK-STAT is a potential signal transducer of multiple pro-fibrotic cytokines and growth factors (Figures 9 and 10).

1.7.1.8 Histone modification

Histone deacetylase (HDAC) reverses the action of histone acetyl transferases by removing acetyl groups from lysine residues on histones and non-histone regulators of transcription, leading to chromatin condensation and transcriptional repression [223]. Cardiac-specific knockout of HDAC3 (class I HDAC) or Sirtuin 3/6 (class III HDAC) in mice revealed severe ventricular hypertrophy and fibrosis [224-227]. On the other hand, HDAC inhibition appears to reverse atrial fibrosis, Cx40 remodeling, and atrial arrhythmia vulnerability dependent or

independent of Ang-II stimulation [228]. Thus, histone modification also participates in the atrial-fibrotic response. Histone modification, together with chromatin remodeling, DNA methylation and non-coding RNA are epigenetic alterations that occur in HF [229]. Among these, only microRNA (miRNA, miR), a class of small non-coding RNAs, has been intensively studied in atrial fibrogenesis. The post-transcriptional regulation achieved by miRNAs will be discussed in the following section.

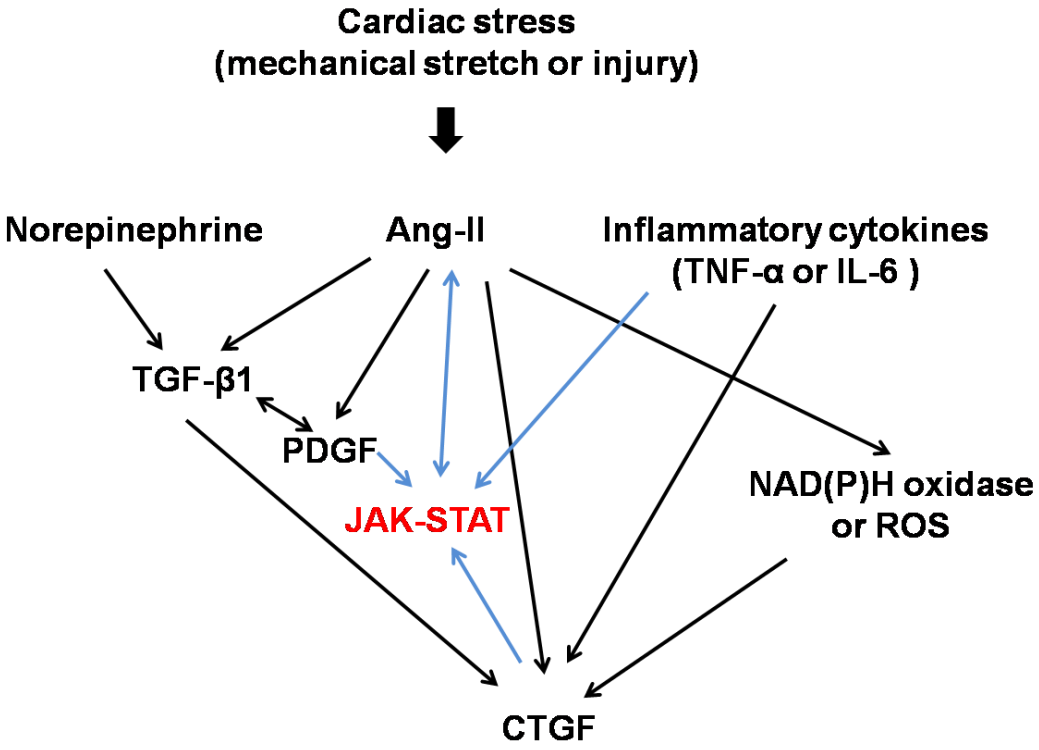

Figure 10. Regulatory network of the fibrotic factors secreted in the heart.

Under cardiac stress, such as mechanical stretch or cardiac injury, multiple cytokines and growth factors are released and active the downstream signaling pathways and cross-regulate other pro-fibrotic regulators. For example, Ang-II increases TGF-β1, CTGF, and PDGF expression, while TGF-β1 activates CTGF and PDGF. JAK-STAT is a common downstream signal transducer of Ang-II, IL-6, PDGF, and CTGF. JAK-STAT can induce Ang-II expression. Ang-II, angiotensin II; CTGF, connective tissue growth factor; IL-6, interleukin 6; JAK-STAT, Janus kinase–signal transducers and activators of transcription; PDGF, platelet-derived growth factor; ROS, reactive oxygen species; TGF-β1, transforming growth factor-beta type 1; TNF-α, tumor necrosis factor alpha.

1.7.2 Post-transcriptional regulation

1.7.2.1 MiRNAs

MiRNAs are short naturally-occurring interfering RNAs, which are evolutionarily conserved. Mature miRNAs are single-stranded with 18–24 nucleotides. To date, more than 1400 miRNAs have been identified in the human genome, and appear to regulate the expression of more than 60% of protein-coding genes [230]. Each tissue or disease condition has its own miRNA expression profile. In most cases, altered expression of miRNAs leads to a modest 1.5- to 4-fold change in protein expression of their target genes. However, if a miRNA is sufficiently abundant it can behave as a "switch" to turn some genes on or off [231].

1.7.2.2 MiRNA biogenesis and functions

Most miRNA genes are located in introns, exons and untranslated regions (UTRs) of protein-coding genes. MiRNAs can be independent transcription units, or co-expressed with host genes [232]. MiRNAs are transcribed as pri-miRNAs, which contain one or more mature miRNA sequences. Pri-miRNAs are cleaved by endonuclease Drosha, creating pre-miRNAs that are 60–100 nucleotide hairpin structures. Pre-miRNAs are then transported to the cytoplasm and further processed by Dicer, another endonuclease that releases a functionally active, mature miRNA duplex with a length of ~22 nucleotides. The mature single-stranded short nucleotide sequence, which is called the "seed strand" is incorporated into the RNA-induced silencing complex (RISC), allowing the recognition of target mRNA and the formation of a miRNA:mRNA duplex (Figure 11) [232].

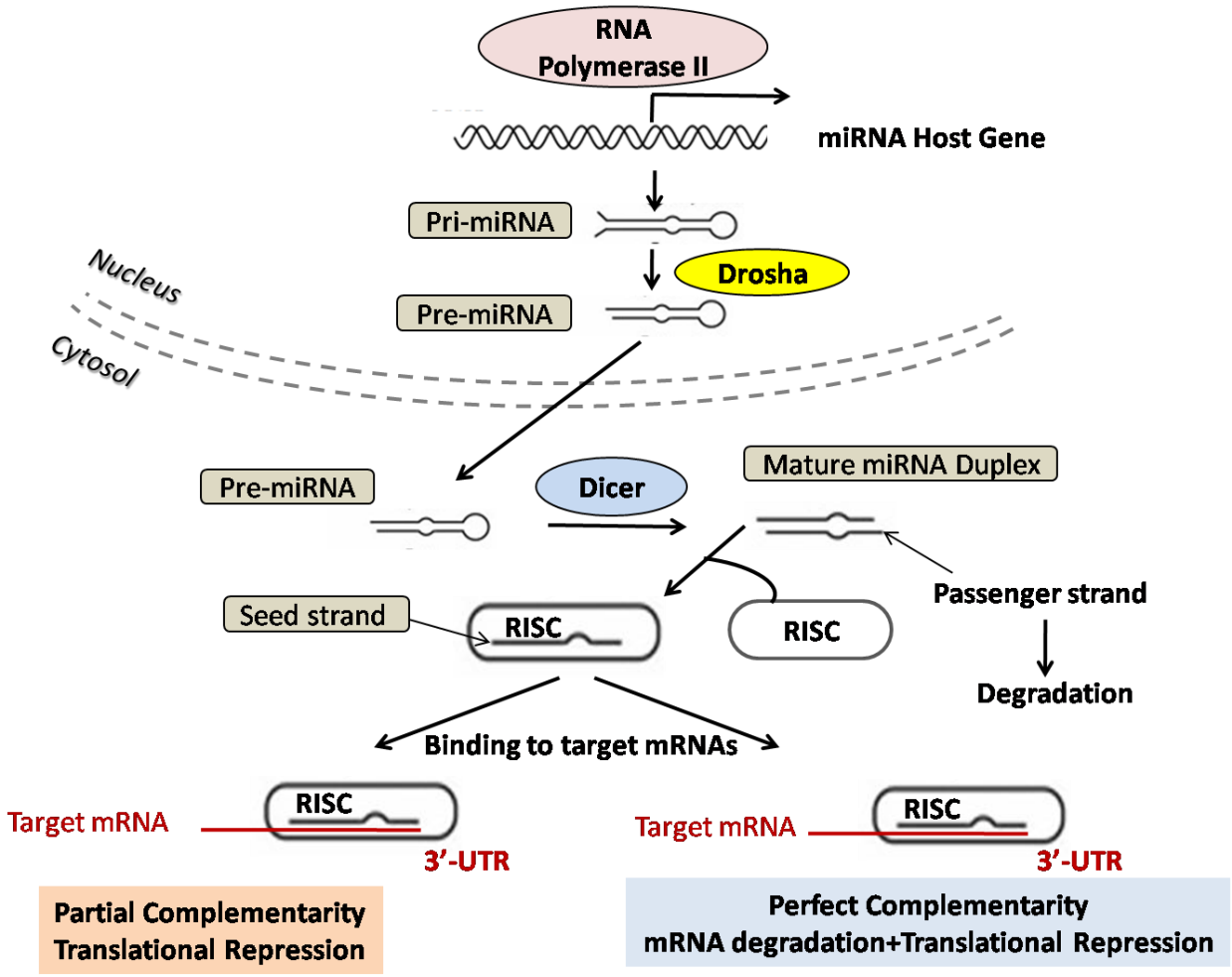

Figure 11. Schematic representation of miRNA biogenesis and functions.

MiRNAs are transcribed as pri-miRNAs by RNA Polymerase II, and cleaved to pre-miRNAs by Drosha. Pre-miRNAs are then transported to the cytoplasm and further processed by Dicer, producing mature miRNA duplexes. The "seed strands" of miRNAs are then released and incorporated into the RISC that binds with high affinity via "seed sequences" to the complementary sequences of mRNAs. This partial complementary binding interferes with protein translation from the target mRNA, reducing its protein expression. Perfect complementary binding destabilizes target mRNA, reducing mRNA and protein expression. miRNA, microRNA; mRNAs, messenger RNAs; Pri-miRNA, primary miRNA; Pre-miRNA, precursor miRNA; RISC, RNA-induced silencing complex; 3'-UTR, 3'-untranslated region.

The complementary binding sites reside at the seed region at nucleotides 2–8 of the miRNA, and 3’-UTR of the binding mRNA. The gene-repression function of miRNA occurs either through translational silencing of mRNA through partially complementary or “imperfect” binding, or degradation of mRNA when miRNA:mRNA binding is perfectly complementary (Figure 11). Translational repression predominates in humans; however, in rare cases miRNAs can switch their negative regulatory function towards gene activation [233]. The nature of partial complementarity of miRNA:mRNA binding allows for high flexibility — one miRNA can target hundreds of genes, and one gene can be regulated by multiple miRNAs [234, 235]. The miRNA:mRNA interaction is influenced by other variables, such as miRNA binding site accessibility, RNA secondary structure, position of the binding site in the 3’-UTR, and reciprocal interference between different miRNAs sharing the same target [232, 236]. Although the regulation of miRNA expression has not been fully uncovered, miRNAs are able to control their own expression by positive or negative regulatory loops [237]. Also, DNA and histone modifications also modulate miRNA transcription [238].

1.7.2.3 MiRNAs and AF

MiRNAs play important pathophysiological roles in development and in various cardiac conditions. Studies have revealed altered miRNA expression in the atrial tissue and blood of animal models and patients with AF [239]. MiRNAs are relatively stable molecules and easily detectable in plasma and serum. Several circulating miRNAs have been suggested as potential biomarkers for AF [239]. For example, miR-150 level was decreased in the plasma of patients with paroxysmal and persistent AF [240]. MiR-29b was reduced in the plasma of patients with CHF or AF, and was further decreased in patient with CHF and AF [241]. And miR-328 was

associated with prevalent AF [242]. However, none are currently used as biomarkers or as treatment options for AF.

1.7.2.4 MiRNAs in AF-associated electrical remodeling

MiRNAs are known to exert their functions in the AF paradigm by targeting electrical remodeling, Ca^{2+} handling abnormalities and structural remodeling. Several miRNAs have been implicated in altering ion channel expression and current, such as I_{K1} and I_{CaL}. Levels of miR-1 were found to be reduced in patients with persistent AF, with an increase in Kir2.1 expression; a reduction of miR-1 expression may enhance I_{K1} [243]. In contrast, another study on rabbit with atrial tachypacing suggested that miR-1 upregulation abbreviates atrial ERP by targeting K^+ channel subunit voltage-gated potassium channel subfamily E member 1 (minK) and voltage-gated potassium channel subfamily B member 2 (Kv2.2) [244]. Luo et al. found that miR-26 isoform expression was reduced in atria from dogs and patients with AF, and miR-26 had a protective role in AF by targeting Kir2.1 and governing I_{K1} [245]. MiR-208a-knock out mice developed frequent spontaneous AF with unknown mechanism [246]. MiR-21 and miR-328 are pro-arrhythmic miRNAs that upregulated AF dogs or patients — they both decrease I_{CaL} by reducing expression of L-type calcium channel α and β subunits [247, 248]. MiR-499 was also found to be upregulated in AF patients and it targets and downregulates small conductance calcium-activated potassium channel protein 3 (SK3) [249]. The uncovered miRNA functions contributing to AF-associated electrical remodeling are summarized in Table 1.

Table 1. MiRNAs related to AF-associated electrical remodeling

MiRNA (change in AF)	Model	Target(s)	Target validation	Potential role in AF	Ref.#
miR-1(↓/↑)	AF patients	KCNJ2	N.A.	↑I_{K1}via↑ Kir2.1	[243]
	ATP rabbits	KCNE1,KCNB2	*In vivo* functional assay	↑I_{Ks}, ↓AERP via ↓minK and Kv2.2	[244]
miR-21(↑)	Chronic AF patients	CACNA1C CACNB2	Reporter gene assay; target protein changes in mimic/silencing miRNA transfection	↓I_{CaL} via ↓APD ↓Cav1.2 and Cavβ1	[247]
miR-26(↓)	AF patients; ATP dogs; mice subjected to atrial-programmed stimulation	KCNJ2	Reporter gene assay; *in vivo* functional assay	↑I_{K1} via ↑Kir2.1	[245]
miR-208a(↓)	miR-208a-Tg mice	Unknown	N.A.	Maintain expressions of Cx40, Hop and GATA4	[246]
miR-328(↑)	AF patients; ATP dogs; miR-328-Tg mice; miR-328-knockdown-Tg mice	CACNA1C CACNB1	Reporter gene assay; target protein changes in mimic/silencing miRNA transfection; *in vivo* functional assay	↓I_{CaL} ↓atrial APD via ↓ Cav1.2 and Cavβ1	[248]
miR-499(↑)	AF patients	KCNN3	Reporter gene assay; target protein changes in mimic/silencing miRNA transfection	↓I_{Ks} via ↓ SK3	[249]

AERP, atrial effective refractory period; AF, atrial fibrillation; APD Action potential duration; ATP, atrial-tachypacing;CACNA1C, L-type calcium channel α subunit (Cav1.2); CACNB1; L-type calcium channel β subunit (Cavβ1); Cx40, connexin 40; GATA4, GATA binding protein; I_{CaL} L-type calcium current; I_{K1} background K^+ current; I_{Ks}, slowly activated delayed rectifier potassium current; KCNB2, voltage-gated potassium channel subfamily B member 2, (K_v2.2); KCNE1, voltage-gated potassium channel subfamily E member 1(minK); KCNJ 2, inward-rectifier potassium channel 2 (Kir2.1); KCNN3, small conductance calcium-activated potassium channel protein 3 (SK3); N.A., not applicable; Tg, transgenic.

1.7.2.5 MiRNAs involved in cardiac fibrosis

According to the literature, more than 10 miRNAs have been associated with cardiac fibrosis by targeting pro- or anti-fibrotic genes, ranging from regulatory cytokines, growth factors, signal transducers, and ECM proteins. The role of miRNAs in cardiac fibrogenesis and target genes of these miRNAs are summarized in Table 2. Within these miRNAs, some have been shown to have direct pro- or anti-fibrotic effects *in vivo* (e.g. miR-21, miR-29b, and miR-133); some modulate fibroblast proliferation and differentiation *in vitro* (e.g. miR-26); while some regulate ECM production (e.g. miR-17, miR-18, miR-19), though direct links to cardiac fibrosis have yet to be revealed. Some miRNAs are involved in ventricular fibrosis (e.g. miR-208, miR-22 and miR-24), some are directly associated with AF-induced atrial remodeling (e.g. miR-21, miR-26, miR-29b, miR-133, and miR-590). Here we focus on the pro- or anti-fibrotic miRNAs that have been implicated to play a role in AF-associated atrial fibrosis.

MiR-21

MiR-21 has been intensively studied in models of hypertrophy and MI (mouse and rat) [250-252]. MiR-21 is confirmed to target and suppress expression of sprout homologue 1 (Spry-1), a negative regulator of a pro-fibrotic factor extracellular signal-regulated kinase (ERK) [250]. MiR-21 expression was enhanced in atria from MI rats with increased susceptibility to AF; miR-21 knockdown reduced atrial fibrosis and prevented AF substrate development in MI rats [252]. In addition, miR-21 responses to ischemia-reperfusion in the mouse heart and regulates fibroblast MMP-2 expression by targeting phosphatase and tensin homologue (PTEN) [253]. Patients with AF also showed increased miR-21 expression in the atria [254]. To date, miR-21 is probably the most well-known player in AF-inducing fibrotic remodeling.

Table 2. MiRNAs related to cardiac fibrosis

MiRNA	Model (chamber)	Target(s)	Target validation	Proposed roles in fibrosis	Ref.#
Pro-fibrotic miRNAs					
miR-17	MI mice; miR-17-Tg mice (LV)	TIMP1 TIMP2	Reporter gene assay; *in vivo* functional assay	Regulate matrix remodeling	[255]
miR-21	MI rats/mice (LA); TAC mice (LV); AF (LA)/HF (LV) patients; Rac1/miR-21-Tg mice (LV); MI mice (LV)	Spry1 PTEN	Reporter gene assay; target protein changes in mimic/silencing miRNA transfection; *in vivo* functional assay	De-repression of ERK/MAPK via Spry1 ↑MMP via PTEN	[250, 252-254]
miR-22	Aging mice (LV)	Mimecan	Reporter gene assay; target protein functional changes in mimic/silencing miRNA transfection	↓Mimecan ↑Fibroblasts senescence and migratory activity	[256]
miR-208	miR-208-mutant mice (LV)	THRAP1	Reporter gene assay; *in vivo* functional assay	↓Myocardial contractility, ↑Fibrosis by↓ negative regulators of stress response genes	[257]
Anti-fibrotic miRNAs					
miR-18a, 19a/b	Aging-associated HF mice (LV)	CTGF TSP-1	Target protein changes in mimic/silencing miRNA transfection	↓CTGF ↓TSP-1	[258]
mR-24	MI mice (LV)	Furin	Target protein changes in mimic/silencing miRNA transfection; *in vivo* functional assay	↓TGF-β signaling via Furin	[259]

MiRNA	Model (chamber)	Target(s)	Target validation	Proposed roles in fibrosis	Ref.#
miR-26	AF patients (RAA); AF canine model with CHF (LA)	TRPC3	Reporter gene assays	↓FB activation via Ca^{2+}dependent ERK signaling	[219]
miR-29b	MI mice (LV); AF patients (RAA); AF canine model with CHF (LA)	COL1A1 COL1A2 COL3A1 FBN1 ELN1	Reporter gene assays; target protein changes in mimic/silencing miRNA transfection; *in vivo* functional assay	Directly ↓collagen and other ECM synthesis	[241, 260]
miR-30c	Pathological hypertrophy rodents/patients (LV)	CTGF	Reporter gene assay; target protein changes in mimic/silencing miRNA transfection	↓CTGF signaling	[261]
miR-133	Pathological hypertrophy rodents/patients (LV); diabetic mice (LA); nicotine-induced AF canine model/patients (LA & RA); Ang-II-dependent hypertension rats	CTGF TGF-β1 COL1A1	Reporter gene assay; target mRNA changes in mimic/silencing miRNA; *in vivo* functional assay transfection	↓TGF-β signaling, ↓CTGFsignaling,↓COL1A1	[261-263]
miR-590	Nicotine-induced AF canine model/patients (LA & RA)	TGFβR2	Reporter gene assay; target mRNA changes in mimic/silencing miRNA transfection	↓TGF-β signaling	[262]

MiRNAs in **fold** have been implicated in AF-associated atrial fibrosis. AF, atrial fibrillation; COL, collagen; ECM, extracellular matrix; ELN, elastin 1; CTGF, connective tissue growth factor; ERK, extracellular signal-regulated kinase; FBN1, fibrillin 1; HF, heart failure; LA, left atria; LV, left ventricle; ; MAPK, mitogen-activated protein kinase; MI, myocardial infarction; MMP, matrix metalloproteinase; PTEN, phosphatase and tensin homolog; RAA, right-atrial appendage; Spry1, protein sprouty homolog 1; TAC, transverse aortic constriction; Tg, transgenic; TGF-β(R), transforming growth factor-beta (receptor); THRAP1, thyroid hormone receptor associated protein 1; TIMP1/2, tissue inhibitor of metalloproteinase 1 or 2; TRPC3, transient receptor potential canonical 3; TSP-1, thrombospondin-1.

MiR-26

In addition to its role in electrical remodeling, miR-26 has been recently revealed to be involved in atrial fibrotic remodeling contributing to AF-inducing substrate. MiR-26 directly targets and represses the expression of TRPC3, a channel that mediates fibroblast proliferation and differentiation (Section 1.7.1.7) through ERK signaling [219]. MiR-26 is downregulated in atrial fibroblasts from a canine model with AF, and atrial tissue from AF patients [220]. Experimental knock-down of miR-26 activates fibroblast proliferation [220]. Therefore, miR-26 is an important regulator of atrial-fibrosis in AF development by modulating TRPC3 in fibroblasts.

MiR-29

The role of miR-29 in cardiac fibrosis was first revealed in a mouse model with MI [261]. It is downregulated in the region of the ventricular tissue adjacent to the infarct [261]. MiR-29 family targets multiple ECM genes including collagens, fibrillins, and elastin [260]. Later on, miR-29b was found reduced in the atrial tissue and fibroblasts from dogs with AF [242]. *In vivo* knockdown of miR-29 in mice increases atrial collagen production [242]. And miR-29b expression level is reduced in plasma and atria of patients with CHF or AF [241].

MiR-30, miR-133 and miR-159

MiR-30 and miR-133 regulate ventricular fibrosis by depressing the expression of CTGF, an important pro-fibrotic protein (Section 1.7.1.4) [261]. Atrial expression of miR-30 and miR-133 (decreased) were inversely related to the change of CTGF expression (increased) in human pathological left ventricular hypertrophy [262]. The downregulation of miR-133a contributes to Ang-II-induced ventricular fibrosis via directly targeting collagen 1α1 [263]. Furthermore, miR-

133 and miR-590 are reduced in a dog model of a nicotine-induced AF, which accounts for the increase of their target TGFβ-1 and TGFβ receptor II [262]. However, none of miR-30, miR-133 and miR-159 expression has been measured in tissue or blood samples from AF patients.

1.8 Clinical therapies for AF

The clinical treatments for AF patients depend on the severity of symptoms, the length of the AF condition, and other underlying medical issues. Medication options include blood thinners or anti-clotting drugs, rate controllers and rhythm controllers. The anti-clotting drugs such as Aspirin and Warfarin are prescribed to decrease the risk of thromboembolism. The pharmacological rate controllers are predominantly beta blockers and Ca^{2+}channel blockers. The rhythm controllers (or anti-arrhythmic drugs) are mainly Na^{+} and K^{+} channel blockers, which act to prolong atrial refractoriness and thereby prevent AF [264]. Certain classes of drugs are only effective for certain types of arrhythmias [264]. Long-lasting AF alters atrial electrophysiological properties, making drug-induced termination more difficult [265]. Although there is improvement in quality of life, the limitation of the present pharmacological therapy includes limited range of available choices, incomplete efficacy and significant adverse effects, such as pro-arrhythmic complications (in the ventricle) of anti-arrhythmic agents, and bleeding with anti-coagulants [266, 267]. Non-pharmacologic therapies including left atrial ablation and AV node ablation and pacemaker implantation which are only effective in strictly selected cases, or patients in whom pharmacologic drug is ineffective [267]. Therefore, the development of new drugs that target AF-substrates is needed to meet the precise needs of individual patients with greater efficacy and safety.

1.8.1 Pharmacological therapies targeting structural remodeling

Therapeutic development for AF aiming at reversing structural remodeling has triggered more and more attention. “Upstream therapy” is a term that describes the targeting of remodeling-induced substrate development, which refers to the use of non-antiarrhythmic drugs that modulate the target-specific mechanisms of AF [268]. The key targets of upstream therapy are structural changes in the atria, such as fibrosis, hypertrophy, inflammation and oxidative stress. At the same time, they have direct or indirect effects on atrial electrophysiology by modulating ion channels, gap junction and Ca^{2+} handling. As AF is a progressive disease secondary to aging and deterioration of underlying heart diseases, the current therapy aims at preventing the occurrence of AF (primary prevention) and its consequences (secondary prevention) [269, 270]. Accumulated clinical evidence suggests that upstream therapy may have different effects on primary prevention and secondary prevention [268, 269].

1.8.1.1 Inhibitors of rennin-angiotensin-aldosterone system (RAAS)

Inhibitors of RAAS include angiotensin-converting enzyme inhibitors (ACEIs) and angiotensin receptor blockers (ARBs). Retrospective analyses and reports show in the studies in which AF was a secondary endpoint, new-onset AF was sustainably reduced by ACEIs and ARBs in patients with left ventricular dysfunction, hypertrophy and heart failure [154, 270]. Treatment with the ACEI trandolapril reduces the incidence of AF in patients with LV dysfunction after acute MI (Trandolapril Cardiac Evaluation, TRACE study) [271]. The ARB valsartan can reduce the risk of newly detected AF in patients with heart failure (Valsartan Heart Failure Trial, Val-HeFT) [272]. Thus, ACEIs and ARBs may be effective in the primary prevention of AF. The effect of RAAs inhibition on primary prevention of AF was less evident in hypertension than in

CHF, and less clear in other risk factors including diabetes mellitus, coronary artery disease, etc. [268]. For secondary prevention, no strong recommendation can be made regarding the use of ACEIs and ARBs for reduction of AF recurrences [269]. The anti-fibrotic effects of these agents may be associated with the effects on hypertrophy and electrical remodeling [152]. The direct roles of ACEIs and ARBs in patients with atrial fibrotic remodeling remain to be elucidated.

1.8.1.2 Statins

Statins are 3-hydroxy-3-methylglutaryl-coenzyme reductase inhibitors. The effects of statins in preventing AF are derived from its properties of anti-inflammatory, anti-oxidant actions, MMP regulation and improvement of lipid metabolism (preventing atherosclerosis) [268]. However, the key mechanism of its antiarrhythmic effects on atrial myocardium have not been established. To date, the beneficial effects of statins for primary prevention for AF has only been clearly demonstrated in patients undergoing cardiac surgery, and is recommended for post-operative AF or AF-CHF by European Society of Cardiology guidelines on AF management [273]. However, controversial evidence and lack of data from randomized controlled studies preclude definite recommendations for the use of statins for secondary prevention of AF [269].

.

1.8.1.3 Polyunsatuarted fatty acids (PUFA) and corticosteroids

The possible anti-fibrillatory mechanisms of PUFAs include regulating membrane fluidity and multiple ion channels (such as I_{Na}, I_{KAch}, I_{CaL}), anti-inflammatory, anti-oxidant actions and regulation of MAPK activity [268]. In experimental AF model induced by ventricular tachypacing, vagal stimulation and cardiac surgery, n-3 (ω-3) PUFA attenuated structural modeling in the atria and reduce AF susceptibility [274-276]. However, proof of its efficacy on

AF in large-scale clinical trials is lacking, and its anti-arrhythmic effect on AF after cardiac surgery remains controversial [268]. Corticosteroids are steroidal anti-inflammatory agents. The effect of corticosteroids on AF prevention is limited in post-operative AF [277-279]. And corticosteroids therapy is associated with incidence of hypertension, diabetes and CHF; high-dose corticosteroids may cause ventricular pro-arrhythmic and promote AF [268, 280]. At present there is not robust evidence to make any recommendation for the use of PUFAs or corticosteroids for secondary prevention of AF [269].

In summary, upstream therapy with RAAS inhibitors, statins, and possibly n-3 PUFA may be valuable for primary prevention of AF in selected patient categories. These effects may be due to the possibly reversal of atrial structural remodeling, and treatment of the underling cardiovascular disease that promotes the development of AF. Clear clinical indications remain to be defined and confirmed. A safe and effective preventive measures or therapy for AF is still far way to go, but identifying or understanding of the key molecular mechanisms should help us in defining targets for therapeutic interventions.

1.9 Rationale for thesis

AF becomes more frequent and less reversible when the atria undergo structural remodeling due to progressive fibrosis associated with hemodynamic stress or injury [281]. It will be important to develop early-diagnosis or upstream prevention strategies that target AF substrates before they become fixed and irreversible. Therefore, reversal of atrial fibrosis is important for AF prevention. However, specific treatments that reverse cardiac fibrosis are still lacking and the clinical potential and mechanisms of this approach are still under investigation. The identification of novel regulators of atrial fibrogenesis and corresponding upstream/downstream

signaling, is essential before we can develop more specific therapies for fibrotic remodeling in AF. The main goal of this thesis was to identify novel aspects of the molecular control of atrial fibrosis in atrial-selective AF-associated remodeling, with the ultimate aim of aiding in the development of new pharmacological strategies to prevent atrial fibrosis and AF.

Project #1 (Chapter 2) — Does PDGF-activated JAK-STAT signaling cascade contribute to AF-substrates?

Ventricular tachypacing (VTP)–induced experimental CHF models display marked differences in remodeling between the atria and ventricles [60, 61, 63]. A previous study published by the laboratory of Dr. Nattel highlights a potential role for PDGF in atrial–ventricular remodeling differences in HF [196]. However, the underling mechanism and downstream molecules mediating the effects of PDGF are still unknown. When investigating the transcriptional regulators of fibrotic signaling, we found that the JAK-STAT system is involved in controlling fibroblast behavior, which is similar to MAPKs; however, its function in cardiac fibrosis has not been clearly identified. Therefore, we aimed to evaluate the involvement of the JAK-STAT system in atrial fibrotic responses associated with AF. We first studied the JAK-STAT system in atria versus ventricles in a canine HF model that has atrial-selective fibrosis and high AF inducibility. We also attempted to mimic the fibrotic response *in vitro* by PDGF stimulation, and compared the behavior of atrial and ventricular fibroblasts with changes in the JAK-STAT system. Finally, we used a STAT3 selective inhibitor to confirm the pro-fibrotic involvement of the JAK-STAT system *in vitro* and *in vivo*.

Project #2 (Chapter 3) — What is the system-response of miRNAs in HF? How might it contribute to arrhythmogenic structural remodeling?

Intensive studies have indicated the role of miRNAs in structural remodeling and the functions of individual miRNA in AF have been revealed. However, no study has analyzed the overall expression profile of miRNA responses in the atria and ventricles in AF conditions. This led us to characterize and detail the miRNA changes that occur in an experimental HF-associated AF model, with specific interest in comparing time, chamber, and cell-type selectivity, and the relationship to ECM remodeling.

Project #3 (Chapter 4) — What is the role of miRNAs in the regulation of the JAK-STAT system in the AF-related fibrotic response?

Multiple miRNAs have been shown to contribute to fibrosis by targeting ECM proteins or upstream mediators, such as CTGF, TGF-β and TGFβR (Table 2). However, no studies have investigated whether miRNA targets JAK-STAT components that contribute to cardiac fibrosis. Based on the findings of Projects 1 and 2, we hypothesized that miRNAs may contribute to the AF-promoting fibrotic response by directly targeting JAK-STAT genes. We first correlated the changes in miRNA expression and JAK-STAT in an HF model and in cultured fibroblasts stimulated with PDGF, with a focus on atrial alterations. We then validated the predicted targets within the JAK-STAT system of the altered miRNAs. Finally, we manipulated miRNAs in fibroblasts to measure effects on target proteins and downstream effectors (ECM proteins).

References-Introduction

1. Delisle, B.P., et al., *Biology of cardiac arrhythmias: ion channel protein trafficking.* Circ Res, 2004. **94**(11): p. 1418-28.
2. *Ganong's review of medical physiology*. 2010, McGraw-Hill Medical: New York.
3. Wilhelm, P.B., R.W. Rhees, and K.M. Van De Graaff, *Human anatomy and physiology : based on Schaum's outline of theory and problems of human anatomy and physiology by Kent M. Van De Graaff and R. Ward Rhees*. Schaum's easy outlines. 2001, New York: McGraw-Hill. v, 186 p.
4. Hall, J.E. and A.C. Guyton, *Guyton and Hall textbook of medical physiology*. 12th ed. 2011, Philadelphia, Pa.: Saunders/Elsevier. xix, 1091 p.
5. Longo, D.L., *Harrison's principles of internal medicine*. 18th ed. 2012, New York: McGraw-Hill.
6. Costanzo, L.S., *Physiology*. 5th ed. Board review series. 2011, Philadelphia: Wolters Kluwer Health/Lippincott Williams & Wilkins. xiii, 314 p.
7. Vliegen, H.W., et al., *Myocardial changes in pressure overload-induced left ventricular hypertrophy. A study on tissue composition, polyploidization and multinucleation.* Eur Heart J, 1991. **12**(4): p. 488-94.
8. Severs, N.J., *The cardiac muscle cell.* Bioessays, 2000. **22**(2): p. 188-99.
9. Camelliti, P., T.K. Borg, and P. Kohl, *Structural and functional characterisation of cardiac fibroblasts.* Cardiovasc Res, 2005. **65**(1): p. 40-51.
10. Souders, C.A., S.L. Bowers, and T.A. Baudino, *Cardiac fibroblast: the renaissance cell.* Circ Res, 2009. **105**(12): p. 1164-76.
11. Baudino, T.A., et al., *Cardiac fibroblasts: friend or foe?* Am J Physiol Heart Circ Physiol, 2006. **291**(3): p. H1015-26.
12. Zeisberg, E.M., et al., *Endothelial-to-mesenchymal transition contributes to cardiac fibrosis.* Nat Med, 2007. **13**(8): p. 952-61.
13. van Tuyn, J., et al., *Epicardial cells of human adults can undergo an epithelial-to-mesenchymal transition and obtain characteristics of smooth muscle cells in vitro.* Stem Cells, 2007. **25**(2): p. 271-8.
14. Zhou, B., et al., *Genetic fate mapping demonstrates contribution of epicardium-derived cells to the annulus fibrosis of the mammalian heart.* Dev Biol, 2010. **338**(2): p. 251-61.
15. van Amerongen, M.J., et al., *Bone marrow-derived myofibroblasts contribute functionally to scar formation after myocardial infarction.* J Pathol, 2008. **214**(3): p. 377-86.
16. Tomasek, J.J., et al., *Myofibroblasts and mechano-regulation of connective tissue remodelling.* Nat Rev Mol Cell Biol, 2002. **3**(5): p. 349-63.
17. Sun, Y. and K.T. Weber, *RAS and connective tissue in the heart.* Int J Biochem Cell Biol, 2003. **35**(6): p. 919-31.
18. Lajiness, J.D. and S.J. Conway, *Origin, development, and differentiation of cardiac fibroblasts.* J Mol Cell Cardiol, 2014. **70**: p. 2-8.
19. Ieda, M., et al., *Cardiac fibroblasts regulate myocardial proliferation through beta1 integrin signaling.* Dev Cell, 2009. **16**(2): p. 233-44.
20. Engel, F.B., et al., *p38 MAP kinase inhibition enables proliferation of adult mammalian cardiomyocytes.* Genes Dev, 2005. **19**(10): p. 1175-87.
21. Kuhn, B., et al., *Periostin induces proliferation of differentiated cardiomyocytes and promotes cardiac repair.* Nat Med, 2007. **13**(8): p. 962-9.
22. Hirota, H., et al., *Continuous activation of gp130, a signal-transducing receptor component for interleukin 6-related cytokines, causes myocardial hypertrophy in mice.* Proc Natl Acad Sci U S A, 1995. **92**(11): p. 4862-6.

23. Kamimura, D., K. Ishihara, and T. Hirano, *IL-6 signal transduction and its physiological roles: the signal orchestration model.* Rev Physiol Biochem Pharmacol, 2003. **149**: p. 1-38.
24. Vasquez, C., N. Benamer, and G.E. Morley, *The cardiac fibroblast: functional and electrophysiological considerations in healthy and diseased hearts.* J Cardiovasc Pharmacol, 2011. **57**(4): p. 380-8.
25. Porter, K.E. and N.A. Turner, *Cardiac fibroblasts: at the heart of myocardial remodeling.* Pharmacol Ther, 2009. **123**(2): p. 255-78.
26. Takeda, N. and I. Manabe, *Cellular Interplay between Cardiomyocytes and Nonmyocytes in Cardiac Remodeling.* Int J Inflam, 2011. **2011**: p. 535241.
27. Kapoun, A.M., et al., *B-type natriuretic peptide exerts broad functional opposition to transforming growth factor-beta in primary human cardiac fibroblasts: fibrosis, myofibroblast conversion, proliferation, and inflammation.* Circ Res, 2004. **94**(4): p. 453-61.
28. Glenn, D.J., et al., *Atrial natriuretic peptide suppresses endothelin gene expression and proliferation in cardiac fibroblasts through a GATA4-dependent mechanism.* Cardiovasc Res, 2009. **84**(2): p. 209-17.
29. Miragoli, M., G. Gaudesius, and S. Rohr, *Electrotonic modulation of cardiac impulse conduction by myofibroblasts.* Circ Res, 2006. **98**(6): p. 801-10.
30. Zhang, Y., et al., *Connexin43 expression levels influence intercellular coupling and cell proliferation of native murine cardiac fibroblasts.* Cell Commun Adhes, 2008. **15**(3): p. 289-303.
31. Roell, W., et al., *Engraftment of connexin 43-expressing cells prevents post-infarct arrhythmia.* Nature, 2007. **450**(7171): p. 819-24.
32. Kizana, E., et al., *Gene transfer of connexin43 mutants attenuates coupling in cardiomyocytes: novel basis for modulation of cardiac conduction by gene therapy.* Circ Res, 2007. **100**(11): p. 1597-604.
33. Kizana, E., et al., *Fibroblasts can be genetically modified to produce excitable cells capable of electrical coupling.* Circulation, 2005. **111**(4): p. 394-8.
34. Camelliti, P., et al., *Fibroblast network in rabbit sinoatrial node: structural and functional identification of homogeneous and heterogeneous cell coupling.* Circ Res, 2004. **94**(6): p. 828-35.
35. Kohl, P. and P. Camelliti, *Fibroblast-myocyte connections in the heart.* Heart Rhythm, 2012. **9**(3): p. 461-4.
36. Camelliti, P., et al., *Spatially and temporally distinct expression of fibroblast connexins after sheep ventricular infarction.* Cardiovasc Res, 2004. **62**(2): p. 415-25.
37. De Maziere, A.M., et al., *Spatial and functional relationship between myocytes and fibroblasts in the rabbit sinoatrial node.* J Mol Cell Cardiol, 1992. **24**(6): p. 567-78.
38. Chilton, L., et al., *K+ currents regulate the resting membrane potential, proliferation, and contractile responses in ventricular fibroblasts and myofibroblasts.* Am J Physiol Heart Circ Physiol, 2005. **288**(6): p. H2931-9.
39. Walsh, K.B. and J. Zhang, *Neonatal rat cardiac fibroblasts express three types of voltage-gated K+ channels: regulation of a transient outward current by protein kinase C.* Am J Physiol Heart Circ Physiol, 2008. **294**(2): p. H1010-7.
40. Murakami, M. and M. Simons, *Fibroblast growth factor regulation of neovascularization.* Curr Opin Hematol, 2008. **15**(3): p. 215-20.
41. Sturzu, A.C. and S.M. Wu, *Developmental and regenerative biology of multipotent cardiovascular progenitor cells.* Circ Res, 2011. **108**(3): p. 353-64.
42. Urbanek, K., et al., *Stem cell niches in the adult mouse heart.* Proc Natl Acad Sci U S A, 2006. **103**(24): p. 9226-31.
43. Bearzi, C., et al., *Human cardiac stem cells.* Proc Natl Acad Sci U S A, 2007. **104**(35): p. 14068-73.

44. Penn, M.S., et al., *Autologous cell transplantation for the treatment of damaged myocardium.* Prog Cardiovasc Dis, 2002. **45**(1): p. 21-32.
45. Elnakish, M.T., P. Kuppusamy, and M. Khan, *Stem cell transplantation as a therapy for cardiac fibrosis.* J Pathol, 2013. **229**(2): p. 347-54.
46. Suncion, V.Y., I.H. Schulman, and J.M. Hare, *Concise review: the role of clinical trials in deciphering mechanisms of action of cardiac cell-based therapy.* Stem Cells Transl Med, 2012. **1**(1): p. 29-35.
47. Sanganalmath, S.K. and R. Bolli, *Cell therapy for heart failure: a comprehensive overview of experimental and clinical studies, current challenges, and future directions.* Circ Res, 2013. **113**(6): p. 810-34.
48. Epelman, S., P.P. Liu, and D.L. Mann, *Role of innate and adaptive immune mechanisms in cardiac injury and repair.* Nat Rev Immunol, 2015. **15**(2): p. 117-29.
49. Mortensen, R.M., *Immune cell modulation of cardiac remodeling.* Circulation, 2012. **125**(13): p. 1597-600.
50. Shen, M.J. and D.P. Zipes, *Role of the autonomic nervous system in modulating cardiac arrhythmias.* Circ Res, 2014. **114**(6): p. 1004-21.
51. Cohn, J.N., R. Ferrari, and N. Sharpe, *Cardiac remodeling--concepts and clinical implications: a consensus paper from an international forum on cardiac remodeling. Behalf of an International Forum on Cardiac Remodeling.* J Am Coll Cardiol, 2000. **35**(3): p. 569-82.
52. Dorn, G.W., 2nd, J. Robbins, and P.H. Sugden, *Phenotyping hypertrophy: eschew obfuscation.* Circ Res, 2003. **92**(11): p. 1171-5.
53. Weeks, K.L. and J.R. McMullen, *The athlete's heart vs. the failing heart: can signaling explain the two distinct outcomes?* Physiology (Bethesda), 2011. **26**(2): p. 97-105.
54. Sharov, V.G., et al., *Evidence of cardiocyte apoptosis in myocardium of dogs with chronic heart failure.* Am J Pathol, 1996. **148**(1): p. 141-9.
55. Teiger, E., et al., *Apoptosis in pressure overload-induced heart hypertrophy in the rat.* J Clin Invest, 1996. **97**(12): p. 2891-7.
56. Olivetti, G., et al., *Apoptosis in the failing human heart.* N Engl J Med, 1997. **336**(16): p. 1131-41.
57. White, H.D., et al., *Left ventricular end-systolic volume as the major determinant of survival after recovery from myocardial infarction.* Circulation, 1987. **76**(1): p. 44-51.
58. Casaclang-Verzosa, G., B.J. Gersh, and T.S. Tsang, *Structural and functional remodeling of the left atrium: clinical and therapeutic implications for atrial fibrillation.* J Am Coll Cardiol, 2008. **51**(1): p. 1-11.
59. De Jong, A.M., et al., *Atrial remodeling is directly related to end-diastolic left ventricular pressure in a mouse model of ventricular pressure overload.* PLoS One, 2013. **8**(9): p. e72651.
60. Cardin, S., et al., *Marked differences between atrial and ventricular gene-expression remodeling in dogs with experimental heart failure.* J Mol Cell Cardiol, 2008. **45**(6): p. 821-31.
61. Hanna, N., et al., *Differences in atrial versus ventricular remodeling in dogs with ventricular tachypacing-induced congestive heart failure.* Cardiovasc Res, 2004. **63**(2): p. 236-44.
62. Mukherjee, R., et al., *Selective induction of matrix metalloproteinases and tissue inhibitor of metalloproteinases in atrial and ventricular myocardium in patients with atrial fibrillation.* Am J Cardiol, 2006. **97**(4): p. 532-7.
63. Li, D., et al., *Promotion of atrial fibrillation by heart failure in dogs: atrial remodeling of a different sort.* Circulation, 1999. **100**(1): p. 87-95.
64. Boixel, C., et al., *Fibrosis of the left atria during progression of heart failure is associated with increased matrix metalloproteinases in the rat.* J Am Coll Cardiol, 2003. **42**(2): p. 336-44.

65. Kistler, P.M., et al., *Atrial electrical and structural abnormalities in an ovine model of chronic blood pressure elevation after prenatal corticosteroid exposure: implications for development of atrial fibrillation.* Eur Heart J, 2006. **27**(24): p. 3045-56.
66. Lau, D.H., et al., *Hypertension and atrial fibrillation: evidence of progressive atrial remodeling with electrostructural correlate in a conscious chronically instrumented ovine model.* Heart Rhythm, 2010. **7**(9): p. 1282-90.
67. Anne, W., et al., *Matrix metalloproteinases and atrial remodeling in patients with mitral valve disease and atrial fibrillation.* Cardiovasc Res, 2005. **67**(4): p. 655-66.
68. Corradi, D., et al., *Differential structural remodeling of the left-atrial posterior wall in patients affected by mitral regurgitation with or without persistent atrial fibrillation: a morphological and molecular study.* J Cardiovasc Electrophysiol, 2012. **23**(3): p. 271-9.
69. Nattel, S., B. Burstein, and D. Dobrev, *Atrial remodeling and atrial fibrillation: mechanisms and implications.* Circ Arrhythm Electrophysiol, 2008. **1**(1): p. 62-73.
70. Kumar, S., et al., *Atrial remodeling in varying clinical substrates within beating human hearts: relevance to atrial fibrillation.* Prog Biophys Mol Biol, 2012. **110**(2-3): p. 278-94.
71. Heeringa, J., et al., *Prevalence, incidence and lifetime risk of atrial fibrillation: the Rotterdam study.* Eur Heart J, 2006. **27**(8): p. 949-53.
72. Chugh, S.S., et al., *Epidemiology and natural history of atrial fibrillation: clinical implications.* J Am Coll Cardiol, 2001. **37**(2): p. 371-8.
73. Go, A.S., et al., *Prevalence of diagnosed atrial fibrillation in adults: national implications for rhythm management and stroke prevention: the AnTicoagulation and Risk Factors in Atrial Fibrillation (ATRIA) Study.* JAMA, 2001. **285**(18): p. 2370-5.
74. Schotten, U., et al., *Pathophysiological mechanisms of atrial fibrillation: a translational appraisal.* Physiol Rev, 2011. **91**(1): p. 265-325.
75. Allessie, M.A., et al., *Pathophysiology and prevention of atrial fibrillation.* Circulation, 2001. **103**(5): p. 769-77.
76. Wijffels, M.C., et al., *Atrial fibrillation begets atrial fibrillation. A study in awake chronically instrumented goats.* Circulation, 1995. **92**(7): p. 1954-68.
77. Nattel, S., *New ideas about atrial fibrillation 50 years on.* Nature, 2002. **415**(6868): p. 219-26.
78. Nattel, S. and M. Harada, *Atrial remodeling and atrial fibrillation: recent advances and translational perspectives.* J Am Coll Cardiol, 2014. **63**(22): p. 2335-45.
79. Yue, L., et al., *Ionic remodeling underlying action potential changes in a canine model of atrial fibrillation.* Circ Res, 1997. **81**(4): p. 512-25.
80. Cha, T.J., et al., *Kir3-based inward rectifier potassium current: potential role in atrial tachycardia remodeling effects on atrial repolarization and arrhythmias.* Circulation, 2006. **113**(14): p. 1730-7.
81. Dobrev, D., et al., *Molecular basis of downregulation of G-protein-coupled inward rectifying K(+) current (I(K,ACh) in chronic human atrial fibrillation: decrease in GIRK4 mRNA correlates with reduced I(K,ACh) and muscarinic receptor-mediated shortening of action potentials.* Circulation, 2001. **104**(21): p. 2551-7.
82. Dobrev, D., et al., *The G protein-gated potassium current I(K,ACh) is constitutively active in patients with chronic atrial fibrillation.* Circulation, 2005. **112**(24): p. 3697-706.
83. Carnes, C.A., et al., *Atrial glutathione content, calcium current, and contractility.* J Biol Chem, 2007. **282**(38): p. 28063-73.
84. Etzion, Y., et al., *Correlation between atrial ZnT-1 expression and atrial fibrillation in humans: a pilot study.* J Cardiovasc Electrophysiol, 2008. **19**(2): p. 157-64.

85. Greiser, M., et al., *Pharmacological evidence for altered src kinase regulation of I (Ca,L) in patients with chronic atrial fibrillation.* Naunyn Schmiedebergs Arch Pharmacol, 2007. **375**(6): p. 383-92.
86. Gaborit, N., et al., *Human atrial ion channel and transporter subunit gene-expression remodeling associated with valvular heart disease and atrial fibrillation.* Circulation, 2005. **112**(4): p. 471-81.
87. Voigt, N., et al., *Differential phosphorylation-dependent regulation of constitutively active and muscarinic receptor-activated IK,ACh channels in patients with chronic atrial fibrillation.* Cardiovasc Res, 2007. **74**(3): p. 426-37.
88. Yue, L., et al., *Molecular mechanisms underlying ionic remodeling in a dog model of atrial fibrillation.* Circ Res, 1999. **84**(7): p. 776-84.
89. Brundel, B.J., et al., *Activation of proteolysis by calpains and structural changes in human paroxysmal and persistent atrial fibrillation.* Cardiovasc Res, 2002. **54**(2): p. 380-9.
90. Bukowska, A., et al., *Activation of the calcineurin signaling pathway induces atrial hypertrophy during atrial fibrillation.* Cell Mol Life Sci, 2006. **63**(3): p. 333-42.
91. Nattel, S., et al., *Arrhythmogenic ion-channel remodeling in the heart: heart failure, myocardial infarction, and atrial fibrillation.* Physiol Rev, 2007. **87**(2): p. 425-56.
92. van der Velden, H.M., et al., *Gap junctional remodeling in relation to stabilization of atrial fibrillation in the goat.* Cardiovasc Res, 2000. **46**(3): p. 476-86.
93. Firouzi, M., et al., *Association of human connexin40 gene polymorphisms with atrial vulnerability as a risk factor for idiopathic atrial fibrillation.* Circ Res, 2004. **95**(4): p. e29-33.
94. Gollob, M.H., et al., *Somatic mutations in the connexin 40 gene (GJA5) in atrial fibrillation.* N Engl J Med, 2006. **354**(25): p. 2677-88.
95. Qi, X.Y., et al., *Role of small-conductance calcium-activated potassium channels in atrial electrophysiology and fibrillation in the dog.* Circulation, 2014. **129**(4): p. 430-40.
96. Chen, P.S., et al., *Role of the autonomic nervous system in atrial fibrillation: pathophysiology and therapy.* Circ Res, 2014. **114**(9): p. 1500-15.
97. Miyauchi, Y., et al., *Altered atrial electrical restitution and heterogeneous sympathetic hyperinnervation in hearts with chronic left ventricular myocardial infarction: implications for atrial fibrillation.* Circulation, 2003. **108**(3): p. 360-6.
98. Jayachandran, J.V., et al., *Atrial fibrillation produced by prolonged rapid atrial pacing is associated with heterogeneous changes in atrial sympathetic innervation.* Circulation, 2000. **101**(10): p. 1185-91.
99. Chang, C.M., et al., *Nerve sprouting and sympathetic hyperinnervation in a canine model of atrial fibrillation produced by prolonged right atrial pacing.* Circulation, 2001. **103**(1): p. 22-5.
100. Nguyen, B.L., et al., *Histopathological substrate for chronic atrial fibrillation in humans.* Heart Rhythm, 2009. **6**(4): p. 454-60.
101. Chou, C.C. and P.S. Chen, *New concepts in atrial fibrillation: neural mechanisms and calcium dynamics.* Cardiol Clin, 2009. **27**(1): p. 35-43, viii.
102. Shen, M.J., et al., *Neural mechanisms of atrial arrhythmias.* Nat Rev Cardiol, 2012. **9**(1): p. 30-9.
103. Nishida, K., et al., *Mechanisms of atrial tachyarrhythmias associated with coronary artery occlusion in a chronic canine model.* Circulation, 2011. **123**(2): p. 137-46.
104. Zou, R., et al., *Substrate size as a determinant of fibrillatory activity maintenance in a mathematical model of canine atrium.* Am J Physiol Heart Circ Physiol, 2005. **289**(3): p. H1002-12.
105. Shinagawa, K., et al., *Dynamic nature of atrial fibrillation substrate during development and reversal of heart failure in dogs.* Circulation, 2002. **105**(22): p. 2672-8.

106. Anne, W., et al., *Self-terminating AF depends on electrical remodeling while persistent AF depends on additional structural changes in a rapid atrially paced sheep model.* J Mol Cell Cardiol, 2007. **43**(2): p. 148-58.
107. Weber, K.T., *Fibrosis and hypertensive heart disease.* Curr Opin Cardiol, 2000. **15**(4): p. 264-72.
108. Krenning, G., E.M. Zeisberg, and R. Kalluri, *The origin of fibroblasts and mechanism of cardiac fibrosis.* J Cell Physiol, 2010. **225**(3): p. 631-7.
109. Zeisberg, M. and R. Kalluri, *Cellular mechanisms of tissue fibrosis. 1. Common and organ-specific mechanisms associated with tissue fibrosis.* Am J Physiol Cell Physiol, 2013. **304**(3): p. C216-25.
110. Anderson, K.R., M.G. Sutton, and J.T. Lie, *Histopathological types of cardiac fibrosis in myocardial disease.* J Pathol, 1979. **128**(2): p. 79-85.
111. Weber, K.T., et al., *Patterns of myocardial fibrosis.* J Mol Cell Cardiol, 1989. **21 Suppl 5**: p. 121-31.
112. Knackstedt, C., et al., *Association of echocardiographic atrial size and atrial fibrosis in a sequential model of congestive heart failure and atrial fibrillation.* Cardiovasc Pathol, 2008. **17**(5): p. 318-24.
113. Yang, S.S., et al., *Effects of spironolactone on electrical and structural remodeling of atrium in congestive heart failure dogs.* Chin Med J (Engl), 2008. **121**(1): p. 38-42.
114. Verheule, S., et al., *Increased vulnerability to atrial fibrillation in transgenic mice with selective atrial fibrosis caused by overexpression of TGF-beta1.* Circ Res, 2004. **94**(11): p. 1458-65.
115. Frustaci, A., et al., *Histological substrate of atrial biopsies in patients with lone atrial fibrillation.* Circulation, 1997. **96**(4): p. 1180-4.
116. Remes, J., et al., *Persistent atrial fibrillation in a goat model of chronic left atrial overload.* J Thorac Cardiovasc Surg, 2008. **136**(4): p. 1005-11.
117. Sanfilippo, A.J., et al., *Atrial enlargement as a consequence of atrial fibrillation. A prospective echocardiographic study.* Circulation, 1990. **82**(3): p. 792-7.
118. Chaturvedi, R.R., et al., *Passive stiffness of myocardium from congenital heart disease and implications for diastole.* Circulation, 2010. **121**(8): p. 979-88.
119. Spach, M.S. and J.P. Boineau, *Microfibrosis produces electrical load variations due to loss of side-to-side cell connections: a major mechanism of structural heart disease arrhythmias.* Pacing Clin Electrophysiol, 1997. **20**(2 Pt 2): p. 397-413.
120. Kai, H., et al., *Pressure overload-induced transient oxidative stress mediates perivascular inflammation and cardiac fibrosis through angiotensin II.* Hypertens Res, 2006. **29**(9): p. 711-8.
121. Goette, A., et al., *Determinants and consequences of atrial fibrosis in patients undergoing open heart surgery.* Cardiovasc Res, 2002. **54**(2): p. 390-6.
122. Kadler, K.E., A. Hill, and E.G. Canty-Laird, *Collagen fibrillogenesis: fibronectin, integrins, and minor collagens as organizers and nucleators.* Curr Opin Cell Biol, 2008. **20**(5): p. 495-501.
123. Tayebjee, M.H., R.J. MacFadyen, and G.Y. Lip, *Extracellular matrix biology: a new frontier in linking the pathology and therapy of hypertension?* J Hypertens, 2003. **21**(12): p. 2211-8.
124. Bradshaw, A.D., et al., *Pressure overload-induced alterations in fibrillar collagen content and myocardial diastolic function: role of secreted protein acidic and rich in cysteine (SPARC) in post-synthetic procollagen processing.* Circulation, 2009. **119**(2): p. 269-80.
125. Weber, K.T., *From inflammation to fibrosis: a stiff stretch of highway.* Hypertension, 2004. **43**(4): p. 716-9.
126. Graham, H.K., M. Horn, and A.W. Trafford, *Extracellular matrix profiles in the progression to heart failure. European Young Physiologists Symposium Keynote Lecture-Bratislava 2007.* Acta Physiol (Oxf), 2008. **194**(1): p. 3-21.
127. Bosman, F.T. and I. Stamenkovic, *Functional structure and composition of the extracellular matrix.* J Pathol, 2003. **200**(4): p. 423-8.

128. Ahumada, G.G. and J.E. Saffitz, *Fibronectin in rat heart: a link between cardiac myocytes and collagen.* J Histochem Cytochem, 1984. **32**(4): p. 383-8.
129. Halper, J. and M. Kjaer, *Basic components of connective tissues and extracellular matrix: elastin, fibrillin, fibulins, fibrinogen, fibronectin, laminin, tenascins and thrombospondins.* Adv Exp Med Biol, 2014. **802**: p. 31-47.
130. Cardin, S., et al., *Contrasting gene expression profiles in two canine models of atrial fibrillation.* Circ Res, 2007. **100**(3): p. 425-33.
131. Lin, C.S., et al., *Increased expression of extracellular matrix proteins in rapid atrial pacing-induced atrial fibrillation.* Heart Rhythm, 2007. **4**(7): p. 938-49.
132. Chakraborti, S., et al., *Regulation of matrix metalloproteinases: an overview.* Mol Cell Biochem, 2003. **253**(1-2): p. 269-85.
133. Visse, R. and H. Nagase, *Matrix metalloproteinases and tissue inhibitors of metalloproteinases: structure, function, and biochemistry.* Circ Res, 2003. **92**(8): p. 827-39.
134. Nagase, H., R. Visse, and G. Murphy, *Structure and function of matrix metalloproteinases and TIMPs.* Cardiovasc Res, 2006. **69**(3): p. 562-73.
135. Nakano, Y., et al., *Matrix metalloproteinase-9 contributes to human atrial remodeling during atrial fibrillation.* J Am Coll Cardiol, 2004. **43**(5): p. 818-25.
136. Hoit, B.D., et al., *Remodeling of the left atrium in pacing-induced atrial cardiomyopathy.* Mol Cell Biochem, 2002. **238**(1-2): p. 145-50.
137. Xu, J., et al., *Atrial extracellular matrix remodeling and the maintenance of atrial fibrillation.* Circulation, 2004. **109**(3): p. 363-8.
138. Zhang, W., et al., *Matrix metalloproteinase-9/tissue inhibitors of metalloproteinase-1 expression and atrial structural remodeling in a dog model of atrial fibrillation: inhibition with angiotensin-converting enzyme.* Cardiovasc Pathol, 2008. **17**(6): p. 399-409.
139. Chen, C.L., et al., *Upregulation of matrix metalloproteinase-9 and tissue inhibitors of metalloproteinases in rapid atrial pacing-induced atrial fibrillation.* J Mol Cell Cardiol, 2008. **45**(6): p. 742-53.
140. Tsuchida, K., et al., *Role of Smad4 on TGF-beta-induced extracellular matrix stimulation in mesangial cells.* Kidney Int, 2003. **63**(6): p. 2000-9.
141. Deschamps, A.M. and F.G. Spinale, *Pathways of matrix metalloproteinase induction in heart failure: bioactive molecules and transcriptional regulation.* Cardiovasc Res, 2006. **69**(3): p. 666-76.
142. Creemers, E.E., et al., *Matrix metalloproteinase inhibition after myocardial infarction: a new approach to prevent heart failure?* Circ Res, 2001. **89**(3): p. 201-10.
143. Goette, A., et al., *Increased expression of extracellular signal-regulated kinase and angiotensin-converting enzyme in human atria during atrial fibrillation.* J Am Coll Cardiol, 2000. **35**(6): p. 1669-77.
144. Sugden, P.H. and A. Clerk, *Regulation of the ERK subgroup of MAP kinase cascades through G protein-coupled receptors.* Cell Signal, 1997. **9**(5): p. 337-51.
145. Lin, C.S. and C.H. Pan, *Regulatory mechanisms of atrial fibrotic remodeling in atrial fibrillation.* Cell Mol Life Sci, 2008. **65**(10): p. 1489-508.
146. Dostal, D.E., et al., *Molecular mechanisms of angiotensin II in modulating cardiac function: intracardiac effects and signal transduction pathways.* J Mol Cell Cardiol, 1997. **29**(11): p. 2893-902.
147. Ushio-Fukai, M., et al., *p38 Mitogen-activated protein kinase is a critical component of the redox-sensitive signaling pathways activated by angiotensin II. Role in vascular smooth muscle cell hypertrophy.* J Biol Chem, 1998. **273**(24): p. 15022-9.

148. Schluter, K.D. and S. Wenzel, *Angiotensin II: a hormone involved in and contributing to pro-hypertrophic cardiac networks and target of anti-hypertrophic cross-talks.* Pharmacol Ther, 2008. **119**(3): p. 311-25.
149. Matsubara, H., *Pathophysiological role of angiotensin II type 2 receptor in cardiovascular and renal diseases.* Circ Res, 1998. **83**(12): p. 1182-91.
150. Padia, S.H. and R.M. Carey, *AT2 receptors: beneficial counter-regulatory role in cardiovascular and renal function.* Pflugers Arch, 2013. **465**(1): p. 99-110.
151. Xiao, H.D., et al., *Mice with cardiac-restricted angiotensin-converting enzyme (ACE) have atrial enlargement, cardiac arrhythmia, and sudden death.* Am J Pathol, 2004. **165**(3): p. 1019-32.
152. Ehrlich, J.R., S.H. Hohnloser, and S. Nattel, *Role of angiotensin system and effects of its inhibition in atrial fibrillation: clinical and experimental evidence.* Eur Heart J, 2006. **27**(5): p. 512-8.
153. Lozano, H.F., et al., *Treatment and prevention of atrial fibrillation with non-antiarrhythmic pharmacologic therapy.* Heart Rhythm, 2005. **2**(9): p. 1000-7.
154. Healey, J.S., et al., *Prevention of atrial fibrillation with angiotensin-converting enzyme inhibitors and angiotensin receptor blockers: a meta-analysis.* J Am Coll Cardiol, 2005. **45**(11): p. 1832-9.
155. Madrid, A.H., et al., *The role of angiotensin receptor blockers and/or angiotensin converting enzyme inhibitors in the prevention of atrial fibrillation in patients with cardiovascular diseases: meta-analysis of randomized controlled clinical trials.* Pacing Clin Electrophysiol, 2004. **27**(10): p. 1405-10.
156. Briest, W., et al., *Norepinephrine-induced changes in cardiac transforming growth factor-beta isoform expression pattern of female and male rats.* Hypertension, 2004. **44**(4): p. 410-8.
157. Campbell, S.E. and L.C. Katwa, *Angiotensin II stimulated expression of transforming growth factor-beta1 in cardiac fibroblasts and myofibroblasts.* J Mol Cell Cardiol, 1997. **29**(7): p. 1947-58.
158. Zigrino, P., C. Drescher, and C. Mauch, *Collagen-induced proMMP-2 activation by MT1-MMP in human dermal fibroblasts and the possible role of alpha2beta1 integrins.* Eur J Cell Biol, 2001. **80**(1): p. 68-77.
159. Blom, I.E., R. Goldschmeding, and A. Leask, *Gene regulation of connective tissue growth factor: new targets for antifibrotic therapy?* Matrix Biol, 2002. **21**(6): p. 473-82.
160. Barth, A.S., et al., *Reprogramming of the human atrial transcriptome in permanent atrial fibrillation: expression of a ventricular-like genomic signature.* Circ Res, 2005. **96**(9): p. 1022-9.
161. Chen, C.L., et al., *Altered expression of FHL1, CARP, TSC-22 and P311 provide insights into complex transcriptional regulation in pacing-induced atrial fibrillation.* Biochim Biophys Acta, 2007. **1772**(3): p. 317-29.
162. Kuwahara, F., et al., *Transforming growth factor-beta function blocking prevents myocardial fibrosis and diastolic dysfunction in pressure-overloaded rats.* Circulation, 2002. **106**(1): p. 130-5.
163. Tomita, H., et al., *Early induction of transforming growth factor-beta via angiotensin II type 1 receptors contributes to cardiac fibrosis induced by long-term blockade of nitric oxide synthesis in rats.* Hypertension, 1998. **32**(2): p. 273-9.
164. Hocher, B., et al., *Inhibition of left ventricular fibrosis by tranilast in rats with renovascular hypertension.* J Hypertens, 2002. **20**(4): p. 745-51.
165. Martin, J., et al., *Tranilast attenuates cardiac matrix deposition in experimental diabetes: role of transforming growth factor-beta.* Cardiovasc Res, 2005. **65**(3): p. 694-701.
166. Lee, K.W., et al., *Pirfenidone prevents the development of a vulnerable substrate for atrial fibrillation in a canine model of heart failure.* Circulation, 2006. **114**(16): p. 1703-12.
167. Siwik, D.A., D.L. Chang, and W.S. Colucci, *Interleukin-1beta and tumor necrosis factor-alpha decrease collagen synthesis and increase matrix metalloproteinase activity in cardiac fibroblasts in vitro.* Circ Res, 2000. **86**(12): p. 1259-65.

168. Sarkar, S., et al., *Influence of cytokines and growth factors in ANG II-mediated collagen upregulation by fibroblasts in rats: role of myocytes.* Am J Physiol Heart Circ Physiol, 2004. **287**(1): p. H107-17.
169. Li, Y.Y., C.F. McTiernan, and A.M. Feldman, *Proinflammatory cytokines regulate tissue inhibitors of metalloproteinases and disintegrin metalloproteinase in cardiac cells.* Cardiovasc Res, 1999. **42**(1): p. 162-72.
170. Pan, M., et al., *Inflammation: a possible pathogenic link to atrial fibrillation.* Med Hypotheses, 2006. **67**(6): p. 1305-7.
171. Verheule, S., et al., *Alterations in atrial electrophysiology and tissue structure in a canine model of chronic atrial dilatation due to mitral regurgitation.* Circulation, 2003. **107**(20): p. 2615-22.
172. Saba, S., et al., *Atrial contractile dysfunction, fibrosis, and arrhythmias in a mouse model of cardiomyopathy secondary to cardiac-specific overexpression of tumor necrosis factor-{alpha}.* Am J Physiol Heart Circ Physiol, 2005. **289**(4): p. H1456-67.
173. Murdoch, C.E., et al., *NADPH oxidase-dependent redox signalling in cardiac hypertrophy, remodelling and failure.* Cardiovasc Res, 2006. **71**(2): p. 208-15.
174. Siwik, D.A. and W.S. Colucci, *Regulation of matrix metalloproteinases by cytokines and reactive oxygen/nitrogen species in the myocardium.* Heart Fail Rev, 2004. **9**(1): p. 43-51.
175. Yared, J.P., et al., *Effects of single dose, postinduction dexamethasone on recovery after cardiac surgery.* Ann Thorac Surg, 2000. **69**(5): p. 1420-4.
176. Shiroshita-Takeshita, A., et al., *Effects of simvastatin on the development of the atrial fibrillation substrate in dogs with congestive heart failure.* Cardiovasc Res, 2007. **74**(1): p. 75-84.
177. Shi-Wen, X., A. Leask, and D. Abraham, *Regulation and function of connective tissue growth factor/CCN2 in tissue repair, scarring and fibrosis.* Cytokine Growth Factor Rev, 2008. **19**(2): p. 133-44.
178. Chen, M.M., et al., *CTGF expression is induced by TGF- beta in cardiac fibroblasts and cardiac myocytes: a potential role in heart fibrosis.* J Mol Cell Cardiol, 2000. **32**(10): p. 1805-19.
179. Moussad, E.E. and D.R. Brigstock, *Connective tissue growth factor: what's in a name?* Mol Genet Metab, 2000. **71**(1-2): p. 276-92.
180. Grotendorst, G.R., *Connective tissue growth factor: a mediator of TGF-beta action on fibroblasts.* Cytokine Growth Factor Rev, 1997. **8**(3): p. 171-9.
181. Leask, A. and D.J. Abraham, *The role of connective tissue growth factor, a multifunctional matricellular protein, in fibroblast biology.* Biochem Cell Biol, 2003. **81**(6): p. 355-63.
182. Chen, Y., et al., *CCN2 (connective tissue growth factor) promotes fibroblast adhesion to fibronectin.* Mol Biol Cell, 2004. **15**(12): p. 5635-46.
183. Lin, C.H., et al., *Connective tissue growth factor induces collagen I expression in human lung fibroblasts through the Rac1/MLK3/JNK/AP-1 pathway.* Biochim Biophys Acta, 2013. **1833**(12): p. 2823-33.
184. Adam, O., et al., *Rac1-induced connective tissue growth factor regulates connexin 43 and N-cadherin expression in atrial fibrillation.* J Am Coll Cardiol, 2010. **55**(5): p. 469-80.
185. Adam, O., et al., *Role of Rac1 GTPase activation in atrial fibrillation.* J Am Coll Cardiol, 2007. **50**(4): p. 359-67.
186. Adam, O., et al., *Increased lysyl oxidase expression and collagen cross-linking during atrial fibrillation.* J Mol Cell Cardiol, 2011. **50**(4): p. 678-85.
187. Kiryu, M., et al., *Angiotensin II-mediated upregulation of connective tissue growth factor promotes atrial tissue fibrosis in the canine atrial fibrillation model.* Europace, 2012. **14**(8): p. 1206-14.

188. Li, Y., et al., *Increased expression of connective tissue growth factor and transforming growth factor-beta-1 in atrial myocardium of patients with chronic atrial fibrillation.* Cardiology, 2013. **124**(4): p. 233-40.
189. Song, Z.P., X. Liu, and D.D. Zhang, *Connective tissue growth factor: a predictor of recurrence after catheter ablation in patients with nonparoxysmal atrial fibrillation.* Pacing Clin Electrophysiol, 2014. **37**(5): p. 630-7.
190. Manabe, I., T. Shindo, and R. Nagai, *Gene expression in fibroblasts and fibrosis: involvement in cardiac hypertrophy.* Circ Res, 2002. **91**(12): p. 1103-13.
191. Simm, A., M. Nestler, and V. Hoppe, *Mitogenic effect of PDGF-AA on cardiac fibroblasts.* Basic Res Cardiol, 1998. **93 Suppl 3**: p. 40-3.
192. Ponten, A., et al., *Transgenic overexpression of platelet-derived growth factor-C in the mouse heart induces cardiac fibrosis, hypertrophy, and dilated cardiomyopathy.* Am J Pathol, 2003. **163**(2): p. 673-82.
193. Ponten, A., et al., *Platelet-derived growth factor D induces cardiac fibrosis and proliferation of vascular smooth muscle cells in heart-specific transgenic mice.* Circ Res, 2005. **97**(10): p. 1036-45.
194. Zhao, T., et al., *Platelet-derived growth factor-D promotes fibrogenesis of cardiac fibroblasts.* Am J Physiol Heart Circ Physiol, 2013. **304**(12): p. H1719-26.
195. Liu, C., et al., *Platelet-derived growth factor blockade on cardiac remodeling following infarction.* Mol Cell Biochem, 2014. **397**(1-2): p. 295-304.
196. Burstein, B., et al., *Differential behaviors of atrial versus ventricular fibroblasts: a potential role for platelet-derived growth factor in atrial-ventricular remodeling differences.* Circulation, 2008. **117**(13): p. 1630-41.
197. Liao, C.H., et al., *Cardiac mast cells cause atrial fibrillation through PDGF-A-mediated fibrosis in pressure-overloaded mouse hearts.* J Clin Invest, 2010. **120**(1): p. 242-53.
198. Musa, H., et al., *Inhibition of platelet-derived growth factor-AB signaling prevents electromechanical remodeling of adult atrial myocytes that contact myofibroblasts.* Heart Rhythm, 2013. **10**(7): p. 1044-51.
199. Freed, D.H., et al., *Cardiotrophin-1: expression in experimental myocardial infarction and potential role in post-MI wound healing.* Mol Cell Biochem, 2003. **254**(1-2): p. 247-56.
200. Shuai, K. and B. Liu, *Regulation of JAK-STAT signalling in the immune system.* Nat Rev Immunol, 2003. **3**(11): p. 900-11.
201. Rawlings, J.S., K.M. Rosler, and D.A. Harrison, *The JAK/STAT signaling pathway.* J Cell Sci, 2004. **117**(Pt 8): p. 1281-3.
202. Mascareno, E., M. Dhar, and M.A. Siddiqui, *Signal transduction and activator of transcription (STAT) protein-dependent activation of angiotensinogen promoter: a cellular signal for hypertrophy in cardiac muscle.* Proc Natl Acad Sci U S A, 1998. **95**(10): p. 5590-4.
203. Tao, L., et al., *Role of the JAK-STAT pathway in proliferation and differentiation of human hypertrophic scar fibroblasts induced by connective tissue growth factor.* Mol Med Rep, 2010. **3**(6): p. 941-5.
204. Fan, B., et al., *Role of PDGFs/PDGFRs signaling pathway in myocardial fibrosis of DOCA/salt hypertensive rats.* Int J Clin Exp Pathol, 2014. **7**(1): p. 16-27.
205. Xue, X.D., J.H. Huang, and H.S. Wang, *Angiotensin II activates signal transducers and activators of transcription 3 via Rac1 in the atrial tissue in permanent atrial fibrillation patients with rheumatic heart disease.* Cell Biochem Biophys, 2015. **71**(1): p. 205-13.
206. Tsai, C.T., et al., *Angiotensin II activates signal transducer and activators of transcription 3 via Rac1 in atrial myocytes and fibroblasts: implication for the therapeutic effect of statin in atrial structural remodeling.* Circulation, 2008. **117**(3): p. 344-55.

207. Tsai, C.T., et al., *Membrane translocation of small GTPase Rac1 and activation of STAT1 and STAT3 in pacing-induced sustained atrial fibrillation.* Heart Rhythm, 2008. **5**(9): p. 1285-93.
208. Vignais, M.L., et al., *Platelet-derived growth factor induces phosphorylation of multiple JAK family kinases and STAT proteins.* Mol Cell Biol, 1996. **16**(4): p. 1759-69.
209. Valgeirsdottir, S., et al., *Activation of Stat5 by platelet-derived growth factor (PDGF) is dependent on phosphorylation sites in PDGF beta-receptor juxtamembrane and kinase insert domains.* Oncogene, 1998. **16**(4): p. 505-15.
210. Patel, B.K., et al., *Stat6 and Jak1 are common elements in platelet-derived growth factor and interleukin-4 signal transduction pathways in NIH 3T3 fibroblasts.* J Biol Chem, 1996. **271**(36): p. 22175-82.
211. Bowman, T., et al., *Stat3-mediated Myc expression is required for Src transformation and PDGF-induced mitogenesis.* Proc Natl Acad Sci U S A, 2001. **98**(13): p. 7319-24.
212. Mascarenhas, J.O., N.C. Cross, and R.A. Mesa, *The future of JAK inhibition in myelofibrosis and beyond.* Blood Rev, 2014. **28**(5): p. 189-96.
213. Koppikar, P., et al., *Efficacy of the JAK2 inhibitor INCB16562 in a murine model of MPLW515L-induced thrombocytosis and myelofibrosis.* Blood, 2010. **115**(14): p. 2919-27.
214. Ma, S., et al., *Cryptotanshinone attenuates isoprenaline-induced cardiac fibrosis in mice associated with upregulation and activation of matrix metalloproteinase-2.* Mol Med Rep, 2012. **6**(1): p. 145-50.
215. Ma, Y., et al., *Cryptotanshinone attenuates cardiac fibrosis via downregulation of COX-2, NOX-2, and NOX-4.* J Cardiovasc Pharmacol, 2014. **64**(1): p. 28-37.
216. Mir, S.A., et al., *Inhibition of signal transducer and activator of transcription 3 (STAT3) attenuates interleukin-6 (IL-6)-induced collagen synthesis and resultant hypertrophy in rat heart.* J Biol Chem, 2012. **287**(4): p. 2666-77.
217. Johnson, A.W., et al., *Small-molecule inhibitors of signal transducer and activator of transcription 3 protect against angiotensin II-induced vascular dysfunction and hypertension.* Hypertension, 2013. **61**(2): p. 437-42.
218. Du, J., et al., *TRPM7-mediated Ca2+ signals confer fibrogenesis in human atrial fibrillation.* Circ Res, 2010. **106**(5): p. 992-1003.
219. Harada, M., et al., *Transient receptor potential canonical-3 channel-dependent fibroblast regulation in atrial fibrillation.* Circulation, 2012. **126**(17): p. 2051-64.
220. Clapham, D.E., *TRP channels as cellular sensors.* Nature, 2003. **426**(6966): p. 517-24.
221. Yue, Z., et al., *Role of TRP channels in the cardiovascular system.* Am J Physiol Heart Circ Physiol, 2015. **308**(3): p. H157-82.
222. Harada, M., et al., *MicroRNA regulation and cardiac calcium signaling: role in cardiac disease and therapeutic potential.* Circ Res, 2014. **114**(4): p. 689-705.
223. Marin-Garcia, J. and A.T. Akhmedov, *Epigenetics of the failing heart.* Heart Fail Rev, 2015.
224. Montgomery, R.L., et al., *Maintenance of cardiac energy metabolism by histone deacetylase 3 in mice.* J Clin Invest, 2008. **118**(11): p. 3588-97.
225. Lombard, D.B., et al., *Mammalian Sir2 homolog SIRT3 regulates global mitochondrial lysine acetylation.* Mol Cell Biol, 2007. **27**(24): p. 8807-14.
226. Sundaresan, N.R., et al., *Sirt3 blocks the cardiac hypertrophic response by augmenting Foxo3a-dependent antioxidant defense mechanisms in mice.* J Clin Invest, 2009. **119**(9): p. 2758-71.
227. Sundaresan, N.R., et al., *The sirtuin SIRT6 blocks IGF-Akt signaling and development of cardiac hypertrophy by targeting c-Jun.* Nat Med, 2012. **18**(11): p. 1643-50.
228. Liu, F., et al., *Histone-deacetylase inhibition reverses atrial arrhythmia inducibility and fibrosis in cardiac hypertrophy independent of angiotensin.* J Mol Cell Cardiol, 2008. **45**(6): p. 715-23.

229. Duygu, B., E.M. Poels, and P.A. da Costa Martins, *Genetics and epigenetics of arrhythmia and heart failure.* Front Genet, 2013. **4**: p. 219.
230. Friedman, R.C., et al., *Most mammalian mRNAs are conserved targets of microRNAs.* Genome Res, 2009. **19**(1): p. 92-105.
231. Farazi, T.A., et al., *miRNAs in human cancer.* J Pathol, 2011. **223**(2): p. 102-15.
232. Bartel, D.P., *MicroRNAs: genomics, biogenesis, mechanism, and function.* Cell, 2004. **116**(2): p. 281-97.
233. Vasudevan, S., Y. Tong, and J.A. Steitz, *Switching from repression to activation: microRNAs can upregulate translation.* Science, 2007. **318**(5858): p. 1931-4.
234. Lim, L.P., et al., *Microarray analysis shows that some microRNAs downregulate large numbers of target mRNAs.* Nature, 2005. **433**(7027): p. 769-73.
235. Ambros, V., *The functions of animal microRNAs.* Nature, 2004. **431**(7006): p. 350-5.
236. Bartel, D.P., *MicroRNAs: target recognition and regulatory functions.* Cell, 2009. **136**(2): p. 215-33.
237. Chen, C.Y., et al., *Coregulation of transcription factors and microRNAs in human transcriptional regulatory network.* BMC Bioinformatics, 2011. **12 Suppl 1**: p. S41.
238. Vettori, S., S. Gay, and O. Distler, *Role of MicroRNAs in Fibrosis.* Open Rheumatol J, 2012. **6**: p. 130-9.
239. Luo, X., B. Yang, and S. Nattel, *MicroRNAs and atrial fibrillation: mechanisms and translational potential.* Nat Rev Cardiol, 2015. **12**(2): p. 80-90.
240. Liu, Z., et al., *The expression levels of plasma micoRNAs in atrial fibrillation patients.* PLoS One, 2012. **7**(9): p. e44906.
241. Dawson, K., et al., *MicroRNA29: a mechanistic contributor and potential biomarker in atrial fibrillation.* Circulation, 2013. **127**(14): p. 1466-75, 1475e1-28.
242. McManus, D.D., et al., *Relations between circulating microRNAs and atrial fibrillation: data from the Framingham Offspring Study.* Heart Rhythm, 2014. **11**(4): p. 663-9.
243. Girmatsion, Z., et al., *Changes in microRNA-1 expression and IK1 upregulation in human atrial fibrillation.* Heart Rhythm, 2009. **6**(12): p. 1802-9.
244. Jia, X., et al., *MicroRNA-1 accelerates the shortening of atrial effective refractory period by regulating KCNE1 and KCNB2 expression: an atrial tachypacing rabbit model.* PLoS One, 2013. **8**(12): p. e85639.
245. Luo, X., et al., *MicroRNA-26 governs profibrillatory inward-rectifier potassium current changes in atrial fibrillation.* J Clin Invest, 2013. **123**(5): p. 1939-51.
246. Callis, T.E., et al., *MicroRNA-208a is a regulator of cardiac hypertrophy and conduction in mice.* J Clin Invest, 2009. **119**(9): p. 2772-86.
247. Barana, A., et al., *Chronic atrial fibrillation increases microRNA-21 in human atrial myocytes decreasing L-type calcium current.* Circ Arrhythm Electrophysiol, 2014. **7**(5): p. 861-8.
248. Lu, Y., et al., *MicroRNA-328 contributes to adverse electrical remodeling in atrial fibrillation.* Circulation, 2010. **122**(23): p. 2378-87.
249. Ling, T.Y., et al., *Regulation of the SK3 channel by microRNA-499--potential role in atrial fibrillation.* Heart Rhythm, 2013. **10**(7): p. 1001-9.
250. Thum, T., et al., *MicroRNA-21 contributes to myocardial disease by stimulating MAP kinase signalling in fibroblasts.* Nature, 2008. **456**(7224): p. 980-4.
251. Patrick, D.M., et al., *Stress-dependent cardiac remodeling occurs in the absence of microRNA-21 in mice.* J Clin Invest, 2010. **120**(11): p. 3912-6.
252. Cardin, S., et al., *Role for MicroRNA-21 in atrial profibrillatory fibrotic remodeling associated with experimental postinfarction heart failure.* Circ Arrhythm Electrophysiol, 2012. **5**(5): p. 1027-35.

253. Roy, S., et al., *MicroRNA expression in response to murine myocardial infarction: miR-21 regulates fibroblast metalloprotease-2 via phosphatase and tensin homologue.* Cardiovasc Res, 2009. **82**(1): p. 21-9.
254. Adam, O., et al., *Role of miR-21 in the pathogenesis of atrial fibrosis.* Basic Res Cardiol, 2012. **107**(5): p. 278.
255. Li, S.H., et al., *miR-17 targets tissue inhibitor of metalloproteinase 1 and 2 to modulate cardiac matrix remodeling.* FASEB J, 2013. **27**(10): p. 4254-65.
256. Jazbutyte, V., et al., *MicroRNA-22 increases senescence and activates cardiac fibroblasts in the aging heart.* Age (Dordr), 2013. **35**(3): p. 747-62.
257. van Rooij, E., et al., *Control of stress-dependent cardiac growth and gene expression by a microRNA.* Science, 2007. **316**(5824): p. 575-9.
258. van Almen, G.C., et al., *MicroRNA-18 and microRNA-19 regulate CTGF and TSP-1 expression in age-related heart failure.* Aging Cell, 2011. **10**(5): p. 769-79.
259. Wang, J., et al., *MicroRNA-24 regulates cardiac fibrosis after myocardial infarction.* J Cell Mol Med, 2012. **16**(9): p. 2150-60.
260. van Rooij, E., et al., *Dysregulation of microRNAs after myocardial infarction reveals a role of miR-29 in cardiac fibrosis.* Proc Natl Acad Sci U S A, 2008. **105**(35): p. 13027-32.
261. Duisters, R.F., et al., *miR-133 and miR-30 regulate connective tissue growth factor: implications for a role of microRNAs in myocardial matrix remodeling.* Circ Res, 2009. **104**(2): p. 170-8, 6p following 178.
262. Shan, H., et al., *Downregulation of miR-133 and miR-590 contributes to nicotine-induced atrial remodelling in canines.* Cardiovasc Res, 2009. **83**(3): p. 465-72.
263. Castoldi, G., et al., *MiR-133a regulates collagen 1A1: potential role of miR-133a in myocardial fibrosis in angiotensin II-dependent hypertension.* J Cell Physiol, 2012. **227**(2): p. 850-6.
264. Goldstein, R.N. and B.S. Stambler, *New antiarrhythmic drugs for prevention of atrial fibrillation.* Prog Cardiovasc Dis, 2005. **48**(3): p. 193-208.
265. Nattel, S., *From guidelines to bench: implications of unresolved clinical issues for basic investigations of atrial fibrillation mechanisms.* Can J Cardiol, 2011. **27**(1): p. 19-26.
266. Echt, D.S., et al., *Mortality and morbidity in patients receiving encainide, flecainide, or placebo. The Cardiac Arrhythmia Suppression Trial.* N Engl J Med, 1991. **324**(12): p. 781-8.
267. Nattel, S., et al., *New directions in cardiac arrhythmia management: present challenges and future solutions.* Can J Cardiol, 2014. **30**(12 Suppl): p. S420-30.
268. Savelieva, I., et al., *Upstream therapies for management of atrial fibrillation: review of clinical evidence and implications for European Society of Cardiology guidelines. Part I: primary prevention.* Europace, 2011. **13**(3): p. 308-28.
269. Savelieva, I., et al., *Upstream therapies for management of atrial fibrillation: review of clinical evidence and implications for European Society of Cardiology guidelines. Part II: secondary prevention.* Europace, 2011. **13**(5): p. 610-25.
270. Schneider, M.P., et al., *Prevention of atrial fibrillation by Renin-Angiotensin system inhibition a meta-analysis.* J Am Coll Cardiol, 2010. **55**(21): p. 2299-307.
271. Pedersen, O.D., et al., *Trandolapril reduces the incidence of atrial fibrillation after acute myocardial infarction in patients with left ventricular dysfunction.* Circulation, 1999. **100**(4): p. 376-80.
272. Maggioni, A.P., et al., *Valsartan reduces the incidence of atrial fibrillation in patients with heart failure: results from the Valsartan Heart Failure Trial (Val-HeFT).* Am Heart J, 2005. **149**(3): p. 548-57.

273. European Heart Rhythm, A., et al., *Guidelines for the management of atrial fibrillation: the Task Force for the Management of Atrial Fibrillation of the European Society of Cardiology (ESC).* Europace, 2010. **12**(10): p. 1360-420.
274. Sakabe, M., et al., *Omega-3 polyunsaturated fatty acids prevent atrial fibrillation associated with heart failure but not atrial tachycardia remodeling.* Circulation, 2007. **116**(19): p. 2101-9.
275. Sarrazin, J.F., et al., *Reduced incidence of vagally induced atrial fibrillation and expression levels of connexins by n-3 polyunsaturated fatty acids in dogs.* J Am Coll Cardiol, 2007. **50**(15): p. 1505-12.
276. Mayyas, F., et al., *Dietary omega3 fatty acids modulate the substrate for post-operative atrial fibrillation in a canine cardiac surgery model.* Cardiovasc Res, 2011. **89**(4): p. 852-61.
277. Marik, P.E. and R. Fromm, *The efficacy and dosage effect of corticosteroids for the prevention of atrial fibrillation after cardiac surgery: a systematic review.* J Crit Care, 2009. **24**(3): p. 458-63.
278. Ho, K.M. and J.A. Tan, *Benefits and risks of corticosteroid prophylaxis in adult cardiac surgery: a dose-response meta-analysis.* Circulation, 2009. **119**(14): p. 1853-66.
279. Baker, W.L., et al., *Effect of perioperative corticosteroid use on the incidence of postcardiothoracic surgery atrial fibrillation and length of stay.* Heart Rhythm, 2007. **4**(4): p. 461-8.
280. Chiappini, B. and G. El Khoury, *Risk of atrial fibrillation with high-dose corticosteroids.* Expert Opin Drug Saf, 2006. **5**(6): p. 811-4.
281. Wakili, R., et al., *Recent advances in the molecular pathophysiology of atrial fibrillation.* J Clin Invest, 2011. **121**(8): p. 2955-68.

Chapter 2

The role of JAK-STAT system in atrial fibrotic response

Linking statement

As discussed in the Introduction, no specific treatment has been shown to control cardiac fibrotic remodeling in clinical AF. Although some regulatory factors have been identified (Section 1.7), the underlying mechanism of atrial fibrogenesis is still poorly understood. In this thesis I sought to identify novel signaling pathways involved in AF-associated atrial fibrosis. Previous studies from our laboratory have indicated the potential role of PDGF in regulating differential behaviour of atrial versus ventricular fibroblasts, which makes the atria particularly vulnerable to fibrosis and may potentially underlie AF substrate development. The JAK-STAT system, a downstream signaling pathway of PDGF, has been implicated in fibrotic remodeling in other systems but its role in AF-associated atrial fibrosis is poorly understood. In this Chapter, I hypothesized that PDGF, together with its downstream JAK-STAT system, participates in the atrial fibrotic response, in AF-inducing contexts. I used both ventricular tachypacing (VTP) to create a heart failure (HF) model in dogs and a myocardial infarction (MI) model to induce cardiac dysfunction in mice and examine the determinants of AF-associated atrial fibrosis. My aim was to investigate the role of the PDGF/JAK-STAT system in HF-related atrial fibrotic responses. Because I obtained evidence supporting a significant role for this system, I studied the effects of STAT3 inhibition on fibroblast behaviour and atrial fibrosis, obtaining both mechanistic support for my hypothesis and evidence for a potential therapeutic application.

JAK-STAT signaling and the atrial fibrillation-promoting fibrotic substrate: Pathogenic role and possible therapeutic target

Yu Chen, MSc[a,b,]; Sirirat Surinkaew, PhD[a]; Chia-Tung Wu, MD[a,d]; Patrice Naud, PhD[a]; Xiao-Yan Qi, PhD[a]; Hai Huang, PhD[a]; Marc-Antoine Gillis, MSc[a]; Francine Duval, MSc[a]; Yan-Fen Shi, MD[a]; Jean-Claude Tardif, MD[a]; Dobromir Dobrev, MD[c]; Stanley Nattel, MD [a,b,c*]

[a]Department of Medicine and Research Center Montreal Heart Institute and Université de Montréal, Montreal, Quebec, Canada;

[b]Department of Pharmacology and Therapeutics McGill University, Montreal, Quebec, Canada;

[c]Institute of Pharmacology, Faculty of Medicine, University Duisburg-Essen, Essen, Germany;

[d]Chang Gung Memorial Hospital and Chang Gung University Tao-Yuan, Taiwan;

Short title: JAK-STAT in AF-associated atrial fibrosis

*Corresponding author. 5000 Belanger Street East, Montreal, Quebec, Canada, H1T 1C8. Tel.: (514)-376-3330 ext. 3990. Fax: (514)-376-1355.E-mail: stanley.nattel@icm-mhi.org

Abstract

Introduction: Left atrial (LA) fibrosis is an important feature of many atrial fibrillation (AF) substrates. The JAK-STAT system, activated by platelet-derived growth factor (PDGF), contributes to cardiac remodeling but its role in AF is unknown. Here we investigated how JAK-STAT pathway components are altered in an AF-substrate and contribute to LA fibrotic responses.

Methods: LA-remodeling was studied in dogs with heart failure (HF) induced by ventricular tachypacing (VTP, 240 bpm), and in mice with left-ventricular (LV) dysfunction due to myocardial infarction (MI). Fibroblasts (FBs) were freshly isolated from LA and LV. The selective STAT-3 inhibitor S3I-201 was administered to FBs in vitro or mice *in vivo* (10 mg/kg/day, osmotic mini-pump).

Results: HF-dogs developed LA-selective fibrosis and AF-susceptibility at 1-wk VTP. PDGF isoforms A/C/D and JAK2 mRNA expression increased in LA FBs from 1-wk VTP. HF upregulated protein-expression of PDGF-receptor β and phosphorylated (activated) STAT3 in LA. PDGF-AB stimulation of LA fibroblasts increased PDGFR-α, STAT3 and phosphorylated-STAT3 expression, as well as collagen-1 and fibronectin-1 protein secretion (by 1.6-20-fold), with smaller changes in LV fibroblasts. Phosphorylated-STAT3 and collagen-1/3 upregulation were suppressed by the STAT3-inhibitor SI3-201. *In vivo* S3I-201 treatment of MI-mice attenuated LA fibrosis, LA dilation and P-wave duration changes versus vehicle-control.

Conclusions: HF activates the LA JAK-STAT system via enhanced PDGF-signaling. JAK-STAT inhibition reduces the profibrotic effects of PDGF stimulation on canine fibroblasts in vitro and attenuates *in vivo* LA fibrosis and remodeling post-MI in mice, suggesting that the

JAK/STAT pathway contributes to LA-fibrogenesis and is a potential target for LA-fibrosis prevention.

Keep words: Heart failure, PDGF, JAK-STAT, Atrial fibrosis

Introduction

Atrial fibrillation (AF) promoting atrial remodeling is induced by multiple stresses, including mechanical stretch and cytokine stimulation [1, 2]. Atrial fibrosis, a major component of atrial structural remodeling, can be induced by AF per se [3]. In the fibrotic response, fibroblasts are activated and produce excessive extracellular matrix (ECM) remodeling that negatively influences cardiac electrical, structural and contractile properties [3, 4].

A range of profibrotic signaling pathways has been implicated in myocardial fibrotic remodeling. Angiotensin II (Ang-II), transforming growth factor beta (TGF-β), and connective tissue growth factor (CTGF) are the best-known secreted factors [3, 5-7]. Mitogen-activated protein kinases (MAPKs) are important downstream effectors that control fibroblast survival and fibrosis [3, 8]. Platelet-derived growth factor (PDGF) stimulates fibroblast proliferation and differentiation to myofibroblasts [9]. PDGF blockade reduces interstitial fibrosis of infarcted hearts in rats [10] and a PDGF inhibitor suppresses atrial-selective canine fibroblast activation, eliminating the characteristic atrial-ventricular fibroblast activation differences [11]. Limited information is available about PDGF signaling and its downstream effectors in cardiac fibrosis and congestive heart failure (CHF) paradigms. PDGF activates RAS-ERK1/2 or PI3K-Akt/mTOR pathways, triggering the expression of proto-oncogenes such as c-*fos* and c-*myc* and promoting proliferation and protein synthesis in vascular smooth muscle cells [12, 13]. Signal

transducer and activator of transcription 3 (STAT3) is a latent transcription factor that plays a critical role in cell survival and proliferation [14, 15]. PDGF directly activates the Janus kinase (JAK)-STAT pathway and induces mitogens is in fibroblasts [16-18]. JAK-STAT is activated in a pig model of electrically-maintained AF [19]. However, the contribution of the PDGF-activated JAK-STAT system to atrial fibrosis and clinically-relevant AF-substrates is unknown. The objective of this study was to assess the potential role of the PDGF-JAK-STAT system in regulating atrial fibroblast behaviour and atrial-selective fibrosis in CHF.

Materials and Methods

Animals

Animal-care procedures followed the guidelines of the Canadian Council on Animal Care and were approved by the Animals Research Ethics Committee of the Montreal Heart Institute. CHF was induced by ventricular tachypacing (VTP, 240 bpm). Forty-seven adult mongrel dogs weighing 18.4-35.0 kg were divided into five groups: non-paced controls (*n*=17), 12-hour VTP (*n*=5), 24-hour VTP (*n*=5), 1-week VTP (*n*=5) and 2-week VTP (*n*=15). In a first series of dogs, we examined tissue protein expression, with 5 control dogs and 5 dogs euthanized after 2 week VTP. In a second series, we analyzed gene expression in fibroblasts from 12 control dogs, and 5 each at 12 hours, 24 hours, and 1 week VTP, and 10 dogs at 2 weeks of VTP. Surgical details of dog preparation and handling for the VTP-model are detailed in the online-only Data Supplement.

Twenty five male C57BL/6 mice (8-10 weeks) weighing 20 to 25 g (Charles River, Saint-Constant, Quebec) were divided into three groups: sham controls (*n*=8), myocardial infarction (MI) +vehicle (*n*=9), MI+S3I-201 (*n*=8). MI was induced by left anterior descending coronary

artery ligation (LAD), which was maintained for 2 weeks (methods detailed in the online-only Data Supplement). Vehicle (Sham and MI groups) or S3I-201 (10 mg/kg/day, MI+S3I group) were delivered via osmotic mini-pumps (Alzet 2001; Cupertino, CA) implanted subcutaneously one day before surgery.

Echocardiography

Transthoracic echocardiographic studies under 2%-isoflurane were obtained before and 14 days after sham or MI surgery with a phased-array 10S probe (4.5–11.5 MHz) in a Vivid 7 Dimension System (GE Healthcare Ultrasound, Horten, Norway). Echocardiographic methods and measures are detailed in the online-only Data Supplement.

Tissue and cell harvesting

On study-days, dogs were anaesthetized with morphine (2 mg/kg s.c.) and alpha-chloralose (120 mg/kg i.v.) and mechanically ventilated. Dogs were then euthanized by cardiac excision. Their hearts were removed via median thoracotomy and immediately immersed in oxygenated Tyrode's solution. LA appendage, LA free wall and left ventricular (LV) free wall samples were fast-frozen in liquid-N_2 for molecular biology and/or stored in formalin for histology. LA and LV were perfused for cell isolation and collagenase digestion (see detailed description in Online Supplement). Freshly-isolated fibroblasts and cardiomyocytes were snap-frozen in liquid-N_2 and stored at -80 ℃.

Mice were anesthetized with 2%-isoflurane and the hearts were excised, briefly washed in cold 0.9% saline solution and weighed. Left atria were fixed in 10% formalin at room temperature.

Cell culture and treatment

Paired LA and LV cell-samples isolated from each control dog were plated in 6-well plastic plates (Corning Inc., Corning, NY) in parallel at equal density and cultured in DMEM containing 5%-FBS and 1%-penicillin/streptomycin. Fibroblasts were allowed to adhere for 2 days, rendered quiescent in serum-free medium for 16 hours, and then stimulated with PDGF-AB (Sigma-Aldrich, St. Louis, MO) at different concentrations (1-50 ng/ml) for 24 hours (mRNA quantification) or 48 hours (protein quantification) with or without the STAT3 inhibitor S3I-201 (Selleckchem, Houston, TX, 20, 50 or 100μM). DMSO-treated fibroblasts served as vehicle controls. Fibroblast number was counted by hemocytometer before plating and after the treatment. After treatment, supernatants of culture medium were collected and fibroblasts were pelleted by centrifugation followed by immediate freezing in liquid-N_2 for RNA extraction.

RNA extraction and Quantitative Real-Time Polymerase Chain Reaction (PCR) Analysis

RNA was isolated with mirVana kits (Ambion/Life Technology, Carlsbad, CA). Real-time quantitative polymerase chain reaction (qPCR) was performed with carboxy-fluorescein (FAM)-labeled fluorogenic TaqMan assay primers (Applied Biosystems, Foster City, CA) and TaqMan Universal Master Mix (Applied Biosystems). qPCR for PDGF isoforms A, B, C and D, JAK1, JAK2, PDGF receptor A (PDGFRA) and B (PDGFRB), STAT3, and collagen isoforms 1-alpha-1 (COL1A1) and 3 (COL3A1) was performed with dog-specific TaqMan primers (Applied Biosystems) and relative quantities ($2^{-\Delta Ct}$) calculated with the geometric mean of two reference genes (hypoxanthine phosphoribosyl transferase 1 [*HPRT-1*] and β2-microglobulin [B2M]) as internal standards.

Protein Extraction and Immunoblots

Protein extracts (30μg) of snap-frozen LA and LV tissue from dogs or cultured fibroblasts were separated by electrophoresis on 12% SDS-PAGE (Bio-Rad) and transferred to PVDF membranes (EMD Millipore, Billerica, MA). For secreted collagen type I, the supernatants of the medium (30 μl) from cultured fibroblasts were separated by electrophoresis on 8% SDS-PAGE and transferred to nitrocellulose membranes (Bio-Rad). Membranes were blocked and incubated overnight with the primary antibodies and then with secondary antibodies. All of the details regarding antibodies are provided in the Online Data Supplement.

Histology

LA appendage and left ventricular free wall tissues from dogs, and entire LAs from mice were preserved in 10% buffered formalin for paraffin embedment. Transverse sections of tissue (12-μm thickness, 500-μm spacing) were stained with Masson Trichrome. Analysis of 400×images (5-8 images from each animal) was performed with Image-Pro 7.0 software. Perivascular areas were avoided. Fibrous-tissue content was expressed as a percentage of field area and averaged across fields for each dog or mouse.

Statistical Analysis

Data are mean±SEM. For non-repeated measurements, one-way ANOVA was used for multiple-group comparisons, with post-hoc Bonferroni-corrected *t*-tests (between two selected groups) or Dunnett's test (for comparisons between each intervention group and a single control group). For repeated measurements, two-way ANOVA with Bonferroni post-tests were used. When a significant interaction or main effect was found, pairwise comparisons were performed with

Bonferroni-corrected *t*-tests. Statistical analyses were performed with GraphPad v5.0 (La Jolla, CA). A two-tailed $P<0.05$ was considered statistically significant.

Results

PDGF-JAK-STAT3 pathway activation in experimental CHF

CHF dogs developed progressive AF susceptibility and atrial fibrosis. AF duration increased significantly from 1-week VTP on and atrial-predominant fibrosis was noted (Supplemental Figure 1), consistent with previous work [3, 11]. The baseline expression levels of PDGFC and PDGFD in atrial fibroblasts were greater than those in ventricular (Supplemental Figure 2A). Fibroblast-selective expression (versus cardiomyocytes) was observed for PDGFB, PDGFC (in LA), and PDGFD. In particular, PDGFD expression was 10-fold higher in LA fibroblasts compared to LA cardiomyocytes (Supplemental Figure 2A). mRNA expression of PDGFA, PDGFC, and PDGFD was up-regulated in atrial fibroblasts from CHF dogs, whereas PDGFB did not change significantly (Figure 1A-D). No significant alterations were seen in ventricular fibroblasts, other than an isolated increase in PDGFC at 12-hour VTP (Figure 1A-D). In summary, PDGF isoforms showed fibroblast-selective expression at baseline and atrial-selective increases in CHF fibroblasts at time-points corresponding to *in vivo* AF-promotion and fibrosis development.

PDGF receptors α and β were predominantly expressed in fibroblasts compared to cardiomyocytes in both LA and LV (Supplemental Figure 2B). Protein expression of PDGF receptor α (PDGFRα) in LA tissue was higher than in LV tissues (Figure 1E-F). However, no significant differences were seen between control and 2-week VTP. PDGF receptor β (PDGFRβ) showed similar expression levels in LA versus LV (Figures 1E and 1G) but was increased in CHF

LA (but not LV) versus control (Figure 1G). These observations indicate that the expression of PDGF receptors may be related to atrial-selective fibrogenesis in the development of CHF.

The expression levels of the downstream effectors of PDGF signaling, JAK1/2 and STAT3, in control and CHF fibroblasts are shown in Figure 2. The mRNA expression of JAK1 did not change significantly with CHF (Figure 2A). JAK2 expression, however, was up-regulated with significant changes beginning at 1-week VTP, and similar changes in LA and LV fibroblasts (Figure 2B). Protein expression of phosphorylated and total STAT3 were increased by CHF in both LA and LV (Figure 2C-E). The ratio of phosphorylated-STAT3 to total-STAT3 was significantly upregulated, indicating STAT3 activation, in LA but not LV tissue (Figure 2F). A 2-fold greater expression of JAK2 was seen in fibroblasts versus cardiomyocytes (Supplemental Figure 2C), but the baseline expression of STAT3 was similar in fibroblasts and cardiomyocytes. In all, our results demonstrated that PDGFA/C/D, PDGFRβ, JAK2 and phosphorylated-STAT3 were upregulated in CHF dogs, and that the changes were atrial-selective.

PDGF-JAK-STAT3 pathway activation in fibroblasts after PDGF-stimulation

Our results indicate LA-selective enhancement of the expression of PDGF and its β-receptor isoform in CHF. It is tempting to speculate that the PDGF changes are responsible for the JAK-STAT activation that we noted. In order to study the effects of the PDGF-system enhancement observed in CHF dogs, freshly isolated fibroblasts from control dogs were cultured and exposed to recombinant PDGF-AB. PDGF-AB caused an augmentation of mRNA expression of PDGFRα and PDGFRβ (Figures 3A and B). Changes in the protein expression of PDGFRα were consistent with the mRNA changes (Figures 3C and D), and showed clear preferential response in LA versus LV at very low (5 ng/ml) concentrations.

The mRNA expression of JAK2 increased significantly, to a similar level in LA and LV fibroblasts at both 10 ng/ml and 50 ng/ml of PDGF (Figure 4A), consistent with the increases in JAK2 expression in both LA and LV fibroblasts with CHF (Figure 2B). In contrast, mRNA expression of STAT3 increased significantly in LA fibroblasts with 10 ng/ml (but not the higher concentration) of PDGF, without significant changes in LV fibroblasts at either PDGF concentration (Figure 4B). Phosphorylated-STAT3 to total-STAT3 ratio was increased significantly in LA fibroblasts by 4.2-fold at 5 ng/ml and 5-fold at 10 ng/ml PDGF versus vehicle (Figure 4D). There were no significant changes in LV fibroblasts at any concentration. Overall, the in vitro changes produced by PDGF were qualitatively similar to the expression changes seen for samples from CHF dogs, suggesting that PDGF activation is responsible for many of the alterations observed.

ECM production changes in fibroblasts after PDGF-stimulation

PDGF-stimulation (50 ng/ml) increased the cell number by 2.2-fold in LA fibroblasts, and by 1.9-fold in LV fibroblasts (Figure 5A). Fibroblast secretion of collagen type I (Collagen-1) into the culture supernatant was significantly increased by PDGF-stimulation (50 ng/ml) in LA fibroblasts; however, no changes were seen in LV fibroblasts (Figure 5B and C). Fibronectin-1 secretion was increased in a dose-dependent manner with PDGF-stimulation, and greater changes were seen in LA fibroblasts compared to LV fibroblasts (Figures 5B and D).

Effects of PDGF-stimulation on fibroblasts were attenuated by the STAT3 inhibitor S3I-201.

The mRNA expression of STAT3, collagen-1α1, and collagen 3α1 were all reduced by S3I-201 treatment in a dose-dependent manner (Figure 6A-C). The protein level of phosphorylated-STAT3

was increased by PDGF-stimulation and the change was reversed by S3I-201-treatment, while S3I-201 did not affect the expression level of total-STAT3 (Figure 6D), so that the ratio of phosphorylated-STAT3 to total-STAT3 was upregulated by PDGF and reversed by treatment with S3I-201 (Figure 6E). Furthermore, S3I-201 reversed the augmentation in collagen-1 secretion caused by PDGF-stimulation of LA fibroblasts (Figures 6 F and G). PDGF-exposure and S3I-201 had smaller and statistically nonsignificant effects on LV fibroblasts (Figures 6F and G), consistent to with atrial selective actions. Taken together, our results indicate that the *in vitro* pro-fibrotic effect induced by PDGF could be attenuated by the STAT3 phosphorylation inhibitor S3I-201, and implicate the JAK-STAT system in mediating profibrotic effects of PDGF.

To examine further possible downstream signaling, we studied the changes in the transforming growth factor beta (TGFβ) system, known to be important in atrial fibrosis [2, 3], caused by PDGF. PDGF increased the expression of both TGFβ and its type-2 receptor (TGFβR2) in LA fibroblasts (Supplemental Figure 3). These actions were blocked by the STAT3 inhibitor S3I-201, indicating that PDGF activation of the JAK-STAT system can activate the profibrotic TGFβ system.

Effects of S3I-201 in mice with post-MI LV dysfunction

Mice studied 2 weeks post-MI showed LV hypertrophy manifested as increased heart weight and increased LV mass/body-weight ratio (black bars in Supplemental Figures 4A and B). Their LVs were dilated (Supplemental Figures 4C and D) and showed significant functional impairment (Supplemental Figures 4E-H). Considerable LA fibrosis was noted (Figures 7A and B) and electrocardiographic P-wave durations were prolonged (Figure 7C), indicating LA conduction abnormalities. The LA was dilated in both systole and diastole (Figures 7D and E). These results

indicate significant LA-disease due to the LV dysfunction post-MI. The effects of the STAT3 blocker S3I-201 are illustrated in Figure 7 and Supplemental Figure 4 by the gray bars. S3I-201 did not significantly alter post-MI LV remodeling and dysfunction (Supplemental Figure 4). However, adverse LA remodeling post-MI was significantly attenuated, with nearly complete reversal of changes in LA fibrous tissue composition and P-wave duration (Figures 7A-C). LA dilation was modestly but significantly attenuated when measured at LV end-systole (Figure 7D), but not significantly altered at end-diastole (Figure 7E). Overall, the results indicate an important role of the JAK-STAT system in LA structural remodeling due to LV dysfunction in a clinically relevant *in vivo* model.

Discussion

In this study, we obtained novel insights into the role of PDGF/JAK-STAT signaling in the fibrotic process leading to the AF-substrate in CHF. We found that the PDGF/JAK-STAT pathway is activated in CHF-related atrial fibrotic remodeling (Figure 8 red arrows). We then tested the effects of PDGF-stimulation on atrial fibroblasts, noting that it induced up-regulation of JAK-STAT expression and activity, along with enhanced ECM-protein production (Figure 8 blue arrows). The profibrotic cellular effects of PDGF were attenuated by the STAT3 inhibitor S3I-201 (Figure 8 green symbols). Finally we showed that *in vivo* administration of S3I-201 reduces atrial structural, electrical and fibrotic remodeling in mice with LV-dysfunction after MI (Figure 8 green signs of blockade). Our findings suggest that the JAK-STAT pathway plays an important role in atrial fibrogenesis, and that its inhibition could be a novel therapeutic option for the prevention of atrial fibrosis and AF.

JAK-STAT in cardiac remodeling

Mechanical stretch, pressure overload [22, 23], myocardial infarction [24] and Ang-II treatment [25] have been shown to activate cardiac JAK-STAT signaling. In cardiomyocytes, JAK-STAT activation enhances cell survival and reduces apoptosis by regulating the expression of multiple cardioprotective, anti-inflammatory, or growth related genes [14]. The activation of STAT3 during the early stage of heart failure might be a protective response [14]. Myocyte-specific STAT3 KO mice are significantly more susceptible to cardiac injury [26]. IL-10 and IL-11 attenuate cardiac dysfunction, preventing apoptotic cell death and reducing inflammation, by activating STAT3 [24, 27]. On the other hand, JAK-STAT signaling activated by IL-1β and Ang-II leads to cardiomyocyte hypertrophy *in vitro* and in the mouse heart with pressure-overload [28, 29]. S3I-201 protects against Ang-II induced oxidative stress, endothelial dysfunction and hypertension in rats [30]. In the present study, S3I-210 attenuated atrial enlargement in mice with LV-dysfunction 2 weeks post-MI, but did not significantly affect ventricular remodeling.

Most studies analyzing the effects of JAK-STAT signaling at the cellular level have been performed in cardiomyocytes, with much less known about JAK-STAT actions in cardiac fibroblasts. JAK-STAT activation was found to correlate with early cell trans-differentiation, proliferation, and differentiation of fibroblasts in human hepatic and cutaneous scar tissue [31, 32]. Bowman et al. delineated the PDGF-Src-Stat3–Myc signaling pathway and pointed out its importance in normal PDGF-induced mitogenesis in NIH 3T3 fibroblasts [18]. Tsai et al. found that Ang-II activates STAT3 via Rac1 in both atrial cardiomyocytes and fibroblasts [33]. In the present study, we noted PDGF/JAK-STAT activation in CHF-induced atrial remodeling and demonstrated that the fibroblast-activating effects of PDGF, manifested as enhanced

proliferation and ECM-protein production) is mediated, at least in partial through JAK-STAT activation. JAK-STAT activation was atrial-selective, consistent with the greater degree of fibrosis in LA versus LV (Supplemental Figure 1), and was also selective for fibroblasts over cardiomyocytes, which did not show important JAK-STAT activation (Supplemental Figure 5). Our findings suggest that the JAK-STAT system plays an important role in regulating atrial fibroblast behaviour, likely contributing to atrial fibrotic remodeling.

JAK-STAT in atrial fibrosis associated with AF

Tsai et al. showed that STAT1 and STAT3 were both activated in pigs with pacing-inducing sustained AF [19]. Xue et al. showed that STAT3 protein expression was increased in atrial tissue from permanent AF patients with rheumatic heart disease compared to those in sinus rhythm, paralleling changes in atrial fibrous tissue content [36]. Our finding of reduced atrial fibrosis with STAT3 inhibition is consistent with observations that STAT3 inhibition has anti-fibrotic effects in other systems. For example, Pang et al. showed that inhibition of STAT3 attenuates renal interstitial fibroblast activation and interstitial fibrosis in obstructive nephropathy [34]. Mir et al. noted that inhibition of STAT3 attenuates collagen synthesis and hypertrophy in a rat cardiac hypertrophy model [35].

Novelty and potential significance

To the best of our knowledge, this is the first study to elucidate the role of the JAK-STAT system in AF-promoting atrial fibrotic remodeling. While the JAK-STAT system is indicated in schemas of potential profibrotic pathways in AF [37], the pathway has not previously been directly addressed in studies of atrial profibrillatory remodeling. JAK-STAT signaling can be activated

downstream to either Ang-II or PDGF receptors; the present study points to PDGF as an important component of the atrial profibrotic JAK-STAT axis.

This is also the first study to demonstrate atrial-selective activation of the PDGF/JAK-STAT system in cardiac remodeling. Our observations suggested that the JAK-STAT plays a significant role in atrial-selective fibrosis, which is an important component of the substrate for AF. In our study, the expression of TGFβ1 and TGFβR2 were increased by PDGF-stimulation in fibroblasts, effects attenuated by the STAT3 inhibitor S3I-201 (Supplemental Figure 3). Our results implicate activation of TGF-β1 signaling as a possible pathway for the pro-fibrotic effects of JAK-STAT stimulation. Other known profibrotic pathways, such as those mediated via Ang-II, IL-6 and CTGF, can involve the participation of JAK-STAT [32, 33]. Ang-II activates JAK-STAT through Rac1 in rat fibroblasts [33], and CTGF induces JAK-STAT activation in human hypertrophic scar fibroblasts [32]. JAK2 activation also leads to the phosphorylation of other proteins such as mitogen-activated protein kinases (MAPKs) [37]. In addition, JAK-STAT signaling represents one limb of an autocrine loop for Ang-II generation, which serves to amplify the action of Ang-II in cardiac remodeling [22]. Therefore, the JAK-STAT system is well positioned to serve as a central mediator in fibrotic responses and contribute to atrial remodeling.

Although PDGF is secreted by both fibroblasts and cardiomyocytes, PDGF receptors are predominantly expressed in fibroblasts (Supplemental Figure 2B). Thus, PDGF/JAK-STAT system is a potential target for fibroblast-specific treatment. PDGF receptor inhibitors attenuate fibrosis in multiple studies [10, 38, 39] and suppress atrial-selective cardiac fibroblast activation [11]. However, most PDGFR inhibitors are non-selective tyrosine kinase inhibitors, greatly limiting their clinical use. Therefore, the identification of JAK-STAT as an alternative target, and

the development of JAK-STAT inhibitors like S3I-201 may help in providing novel therapeutic approaches for AF-prevention.

Potential limitations

It has been shown that during myocardial fibrosis in salt-sensitive hypertensive rats, PDGFRα acts at early stages, but PDGFRβ function is enhanced throughout the remodeling process [9]. This might explain why we observed up-regulation of PDGFRβ protein in CHF but no changes in PDGFRα (Figure 1F and G), as we analyzed tissue samples from dogs with 2 week-VTP only because of a lack of protein sample availability from earlier time-points.

In this study, we focused on changes in fibroblasts since we were interested in the role of the JAK-STAT system in profibrillatory fibrotic remodeling. We did study the evolution of JAK2 and STAT3 mRNA expression over VTP time in cardiomyocytes from CHF dogs. As shown in Supplemental Figure 5, the only change we saw was an isolated increase in STAT3 expression at 12-hour VTP. However, a detailed exploration of possible JAK-STAT changes in CHF cardiomyocytes would require measurement of protein expression of JAK-STAT components, as well as phosphorylated-JAK/STAT moieties.

Acknowledgments

The authors wish to thank Nathalie L'Heureux and Chantal St-Cyr for expert technical assistance.

Funding

Supported by the Canadian Institutes of Health Research (MGP6957), the Quebec Heart and Stroke Foundation, and the Foundation Leducq (European-North American Atrial Fibrillation Research Alliance, ENAFRA).

Disclosures

None.

References

[1] Corradi D, Callegari S, Maestri R, Benussi S and Alfieri O. Structural remodeling in atrial fibrillation. *Nat Clin Pract Cardiovas Med*. 2008;5:782-96.

[2] Burstein B and Nattel S. Atrial structural remodeling as an antiarrhythmic target. *J Cardiovasc Pharmacol*. 2008;52:4-10.

[3] Burstein B and Nattel S. Atrial fibrosis: mechanisms and clinical relevance in atrial fibrillation. *J Am Coll Cardiol*. 2008;51:802-9.

[4] Pellman J, Lyon RC and Sheikh F. Extracellular matrix remodeling in atrial fibrosis: mechanisms and implications in atrial fibrillation. *J\MolCell Cardiol*. 2010;48:461-7.

[5] Nattel S, Burstein B and Dobrev D. Atrial remodeling and atrial fibrillation: mechanisms and implications. *Circ Arrhythm electrophysiol*. 2008;1:62-73.

[6] Creemers EE and Pinto YM. Molecular mechanisms that control interstitial fibrosis in the pressure-overloaded heart. *Cardiovasc Res*. 2011;89:265-72.

[7] Lin CS and Pan CH. Regulatory mechanisms of atrial fibrotic remodeling in atrial fibrillation. *Cell Mol Life Sci*. 2008;65:1489-508.

[8] Booz GW and Baker KM. Molecular signalling mechanisms controlling growth and function of cardiac fibroblasts. *Cardiovasc Res*. 1995;30:537-43.

[9] Fan B, Ma L, Li Q, Wang L, Zhou J and Wu J. Role of PDGFs/PDGFRs signaling pathway in myocardial fibrosis of DOCA/salt hypertensive rats. *Int J Clin Exp Pathol*. 2014;7:16-27.

[10] Liu C, Zhao W, Meng W, Zhao T, Chen Y, Ahokas RA, Liu H and Sun Y. Platelet-derived growth factor blockade on cardiac remodeling following infarction. *Mol Cell Biochem*. 2014;397:295-304.

[11] Burstein B, Libby E, Calderone A and Nattel S. Differential behaviors of atrial versus ventricular fibroblasts: a potential role for platelet-derived growth factor in atrial-ventricular remodeling differences. *Circulation*. 2008;117:1630-41.

[12] Mulvany MJ. Small artery remodeling and significance in the development of hypertension. *News Physiol Sci*. 2002;17:105-9.

[13] Ogawa A, Firth AL, Smith KA, Maliakal MV and Yuan JX. PDGF enhances store-operated Ca2+ entry by upregulating STIM1/Orai1 via activation of Akt/mTOR in human pulmonary arterial smooth muscle cells. *Am J Physiol Cell Physiol*. 2012;302:C405-11.

[14] Kishore R and Verma SK. Roles of STATs signaling in cardiovascular diseases. *JAKSTAT*. 2012;1:118-24.

[15] Mohri T, Iwakura T, Nakayama H and Fujio Y. JAK-STAT signaling in cardiomyogenesis of cardiac stem cells.*JAKSTAT*.. 2012;1:125-30.

[16] Patel BK, Wang LM, Lee CC, Taylor WG, Pierce JH and LaRochelle WJ. Stat6 and Jak1 are common elements in platelet-derived growth factor and interleukin-4 signal transduction pathways in NIH 3T3 fibroblasts. *J Biol Chem*. 1996;271:22175-82.

[17] Vignais ML, Sadowski HB, Watling D, Rogers NC and Gilman M. Platelet-derived growth factor induces phosphorylation of multiple JAK family kinases and STAT proteins. *Mol CellBiol*. 1996;16:1759-69.

[18] Bowman T, Broome MA, Sinibaldi D, Wharton W, Pledger WJ, Sedivy JM, Irby R, Yeatman T, Courtneidge SA and Jove R. Stat3-mediated Myc expression is required for Src transformation and PDGF-induced mitogenesis. *Proc Natl Acad Sci U S A*. 2001;98:7319-24.

[19] Tsai CT, Lin JL, Lai LP, Lin CS and Huang SK. Membrane translocation of small GTPase Rac1 and activation of STAT1 and STAT3 in pacing-induced sustained atrial fibrillation. *Heart Rhythm*. 2008;5:1285-93.

[20] Chen Y, Wakili R, Xiao J, Wu CT, Luo X, Clauss S, Dawson K, Qi X, Naud P, Shi YF, Tardif JC, Kaab S, Dobrev D and Nattel S. Detailed characterization of microRNA changes in a canine heart failure model: Relationship to arrhythmogenic structural remodeling. *J Mol Cell Cardiol*. 2014;77:113-24.

[21] Dawson K, Wu CT, Qi XY and Nattel S. Congestive heart failure effects on atrial fibroblast phenotype: differences between freshly-isolated and cultured cells. *PloS One*. 2012;7:e52032.

[22] Booz GW, Day JN and Baker KM. Interplay between the cardiac renin angiotensin system and JAK-STAT signaling: role in cardiac hypertrophy, ischemia/reperfusion dysfunction, and heart failure. *J Mol Cellr Cardiol*. 2002;34:1443-53.

[23] Pan J, Fukuda K, Saito M, Matsuzaki J, Kodama H, Sano M, Takahashi T, Kato T and Ogawa S. Mechanical stretch activates the JAK/STAT pathway in rat cardiomyocytes. *Circ Res*. 1999;84:1127-36.

[24] Krishnamurthy P, Rajasingh J, Lambers E, Qin G, Losordo DW and Kishore R. IL-10 inhibits inflammation and attenuates left ventricular remodeling after myocardial infarction via activation of STAT3 and suppression of HuR. *Circ Res*. 2009;104:e9-18.

[25] Marrero MB, Schieffer B, Paxton WG, Heerdt L, Berk BC, Delafontaine P and Bernstein KE. Direct stimulation of Jak/STAT pathway by the angiotensin II AT1 receptor. *Nature*. 1995;375:247-50.

[26] Jacoby JJ, Kalinowski A, Liu MG, Zhang SS, Gao Q, Chai GX, Ji L, Iwamoto Y, Li E, Schneider M, Russell KS and Fu XY. Cardiomyocyte-restricted knockout of STAT3 results in higher sensitivity to inflammation, cardiac fibrosis, and heart failure with advanced age. *Proc Natl Acad Sci U S A* 2003;100:12929-34.

[27] Obana M, Maeda M, Takeda K, Hayama A, Mohri T, Yamashita T, Nakaoka Y, Komuro I, Takeda K, Matsumiya G, Azuma J and Fujio Y. Therapeutic activation of signal transducer and activator of transcription 3 by interleukin-11 ameliorates cardiac fibrosis after myocardial infarction. *Circulation*. 2010;121:684-91.

[28] Honsho S, Nishikawa S, Amano K, Zen K, Adachi Y, Kishita E, Matsui A, Katsume A, Yamaguchi S, Nishikawa K, Isoda K, Riches DW, Matoba S, Okigaki M and Matsubara H. Pressure-mediated hypertrophy and mechanical stretch induces IL-1 release and subsequent IGF-1 generation to maintain compensative hypertrophy by affecting Akt and JNK pathways. *Circ Res*.. 2009;105:1149-58.

[29] Chang L, Yang R, Wang M, Liu J, Wang Y, Zhang H and Li Y. Angiotensin II type-1 receptor-JAK/STAT pathway mediates the induction of visfatin in angiotensin II-induced cardiomyocyte hypertrophy. *AmJ MedScis*. 2012;343:220-6.

[30] Ma Y, Li H, Yue Z, Guo J, Xu S, Xu J, Jia Y, Yu N, Zhang B, Liu S, Liu M, Shao W, Chen S and Liu P. Cryptotanshinone attenuates cardiac fibrosis via downregulation of COX-2, NOX-2, and NOX-4. *J Cardiovasc Pharmacol*. 2014;64:28-37.

[31] Lakner AM, Moore CC, Gulledge AA and Schrum LW. Daily genetic profiling indicates JAK/STAT signaling promotes early hepatic stellate cell transdifferentiation. *World J Gastroenterol*. 2010;16:5047-56.

[32] Tao L, Liu J, Li Z, Dai X and Li S. Role of the JAK-STAT pathway in proliferation and differentiation of human hypertrophic scar fibroblasts induced by connective tissue growth factor. *Mol Med Rep*. 2010;3:941-5.

[33] Tsai CT, Lai LP, Kuo KT, Hwang JJ, Hsieh CS, Hsu KL, Tseng CD, Tseng YZ, Chiang FT and Lin JL. Angiotensin II activates signal transducer and activators of transcription 3 via Rac1 in atrial myocytes and fibroblasts: implication for the therapeutic effect of statin in atrial structural remodeling. *Circulation*. 2008;117:344-55.

[34] Pang M, Ma L, Gong R, Tolbert E, Mao H, Ponnusamy M, Chin YE, Yan H, Dworkin LD and Zhuang S. A novel STAT3 inhibitor, S3I-201, attenuates renal interstitial fibroblast activation and interstitial fibrosis in obstructive nephropathy. *Kidney Int*. 2010;78:257-68.

[35] Mir SA, Chatterjee A, Mitra A, Pathak K, Mahata SK and Sarkar S. Inhibition of signal transducer and activator of transcription 3 (STAT3) attenuates interleukin-6 (IL-6)-induced collagen synthesis and resultant hypertrophy in rat heart. *Biol Chem*. 2012;287:2666-77.

[36] Xue XD, Huang JH and Wang HS. Angiotensin II activates signal transducers and activators of transcription 3 via Rac1 in the atrial tissue in permanent atrial fibrillation patients with rheumatic heart disease. *Cell biochem Biophys*. 2015;71:205-13.

[37] Rawlings JS, Rosler KM and Harrison DA. The JAK/STAT signaling pathway. *J Cell Sci*. 2004;117:1281-3.

[38] Leipner C, Grun K, Muller A, Buchdunger E, Borsi L, Kosmehl H, Berndt A, Janik T, Uecker A, Kiehntopf M and Bohmer FD. Imatinib mesylate attenuates fibrosis in coxsackievirus b3-induced chronic myocarditis. *Cardiovasc Res*. 2008;79:118-26.

[39] Jang SW, Ihm SH, Choo EH, Kim OR, Chang K, Park CS, Kim HY and Seung KB. Imatinib mesylate attenuates myocardial remodeling through inhibition of platelet-derived

growth factor and transforming growth factor activation in a rat model of hypertension. *Hypertension*. 2014;63:1228-34.

Figure Legends

Figure 1. PDGF isoforms and PDGF receptors (PDGFRs) were upregulated in CHF dogs. (A-D) mRNA expression of PDGF A/B/C/D in left atrial and left ventricular fibroblasts during as a function of ventricular tachypacing (VTP) time. Results are mean ±SEM, n=5-12/group, *p<0.05, **p<0.01, ***p<0.001, vs. corresponding control (CTL). (E) Representative immunoblots for PDGFRα and PDGFRβ from atrial and ventricular tissue. (F-G) Band-intensities for PDGFRα and PDGFRβ normalized to GAPDH. Mean ±SEM, **p<0.01, ***p<0.001. One-way ANOVA with Dunnett's tests (A-D) or Bonferroni-corrected t-tests (F and G) were used for statistical analysis. FB, fibroblast; LA, left atrial; LV, left ventricular; CTL, non-paced controls; CTL-A, control atrium; CTL-V, control ventricle; CHF-A, congestive heart failure atrium; CHF-V, congestive heart failure ventricle.

Figure 2. JAK and STAT changes in CHF dogs. (A-B) mRNA expression of JAK1 and JAK2 in left atrial and left ventricular fibroblasts as a function of ventricular tachypacing (VTP) time. Mean ±SEM, n=5-12/group, *p<0.05, **p<0.01, vs. corresponding control (CTL). (C) Representative immunoblots for phosphorylated STAT3 (p-STAT3) and total STAT3 (t-STAT3) from atrial and ventricular tissue. (D-F) Band-intensities for p-STAT3, t-STAT3 (normalized to GAPDH), and phosphorylated-STAT3/t-STAT3 ratio. *p<0.05, **p<0.01, ***p<0.001. One-way ANOVA with Dunnett's tests (A and B) or Bonferroni-corrected t-tests (D-F) were used for statistical analysis. FB, fibroblast; LA, left atrial; LV, left ventricular; CTL, non-paced controls; CTL-A, control atrium; CTL-V, control ventricle; CHF-A, congestive heart failure atrium; CHF-V, congestive heart failure ventricle.

Figure 3. PDGF receptor (PDGFR) changes caused by exposure to PDGF-stimulation of fibroblasts. (A-B) mRNA expression of PDGFRα and PDGFRβ in atrial and ventricular fibroblasts stimulated with PDGF-AB at different concentrations. (C) Representative immunoblots for PDGFRα in left atrial and ventricular fibroblasts stimulated with PDGF-AB. (D) Band-intensities for PDGFRα normalized to GAPDH. Mean ±SEM, n=4-5/group,*p<0.05, **p<0.01, ***p<0.001 vs. corresponding vehicles. One-way ANOVA with Dunnett's tests were used for statistical analysis. LA, left atrial; LV, left ventricular; FB, fibroblast; Veh: vehicle; P, PDGF.

Figure 4. JAK2 and STAT3 response to PDGF-stimulation in fibroblasts. (A-B) mRNA expression of JAK2 and STAT3 in left atrial and ventricular fibroblasts stimulated with PDGF-AB at different concentrations. (C) Representative immunoblots of phosphorylated-STAT3 and total-STAT3 in left atrial and ventricular fibroblasts stimulated with PDGF-AB at concentrations indicated. (D) Band-intensities for p-STAT3/t-STAT3 ratio. Mean ±SEM, n=4-5/group,*p<0.05, **p<0.01, ***p<0.001 vs. corresponding vehicle. One-way ANOVA with Dunnett's tests were used for statistical analysis. LA, left atrial; LV, left ventricular; FB, fibroblast; Veh: vehicle; P, PDGF.

Figure 5. Cell number, collagen-1 and fibronectin-1 secretion in response to PDGF-AB stimulation in fibroblasts. (A) Fibroblast cell-count (cells/culture-dish) after 24-hour incubation with PDGF-AB at indicated concentrations. (B) Representative immunoblots of secreted collagen type I and fibronectin-1 from culture medium of fibroblasts stimulated with PDGF-AB for 24 hours. (C-D) Band-intensities for secreted collagen type I and fibronectin-1(normalized to

cell number). Mean ±SEM, n=3-4/group,*p<0.05, **p<0.01, vs. corresponding vehicle. One-way ANOVA with Dunnett's tests were used for statistical analysis. LA, left atrium; LV, left ventricle; Veh: vehicle; P, PDGF; COL-1, collagen type-I; FN-1, fibronectin-1.

Figure 6. The effects of the STAT3 inhibitor S3I-201 on PDGF-AB action. (A-C) mRNA expression of STAT3, collagen 1α1 and collagen 3α1 in fibroblasts stimulated with PDGF-AB and incubated with S3I-201 at different concentrations. (D) Representative immunoblots of p-STAT3 and t-STAT3 in fibroblasts stimulated with PDGF-AB with or without S3I-201 (20 μM). (E) Quantitative protein expression of p-STAT3/t-STAT3 ratio.(F) Representative immunoblots of secreted collagen-1 from culture-medium of left atrial and ventricular fibroblasts stimulated with PDGF-AB with or without S3I-201 (50 μM). (G) Band-intensities for secreted collagen-1 (normalized to cell number). n=5-8/group. Mean ±SEM, *p<0.05, **p<0.01, ***p<0.001. One-way ANOVA with Dunnett's tests (A-C) or Bonferroni-corrected *t*-tests (E and G) were used for statistical analysis. COL1A1, collagen 1α1; COL-1, collagen type I COL3A1, collagen 3α1; LA, left atrium; LV, left ventricle; Veh, vehicle; P, PDGF; S3I-20/50/100, S3I-201 at 20/50/100μM.

Figure 7. Effects of S3I-201 administration *in vivo* on atrial remodeling in mice with 2-week old myocardial infarction. (A) Representative histological tissue sections (Masson Trichrome staining) of left atria. (B) Quantification of left atrial fibrous tissue content as %-cross-sectional area. (C) P-wave duration at end-study was decreased by S3I-201 versus vehicle-control (MI). (D-E) Systolic (LADs) and diastolic (LADd) left-atrial dimension. Mean ±SEM, *p<0.05, **p<0.01, ***p<0.001 vs. sham; $^{\#}p$<0.05, $^{\#\#}p$<0.01, $^{\#\#\#}p$<0.001 vs. MI. Sham, sham surgery

without ligation; MI, myocardial infarction; MI+S3I, myocardial infarction with S3I-201 treatment. Two-way ANOVA with Bonferroni post-tests was used for statistical analysis.

Figure 8. Schematic illustration of our findings. Congestive heart failure (CHF; VTP-dogs or MI-mice) increased PDGF-JAK-STAT components and atrial fibrosis (red upward arrows); PDGF-stimulation activated JAK-STAT system and altered fibroblast behavior *in vitro* (blue upward arrows); S3I-201 reduced STAT3 expression/activation and collagen deposition, and attenuated atrial fibrosis (Green "⊥" indicates inhibitory effects). Inhibitory effect of S3I-201 on STAT3 activation occurs via inhibition of phosphorylation, dimer formation and nuclear translocation.

Figure 1

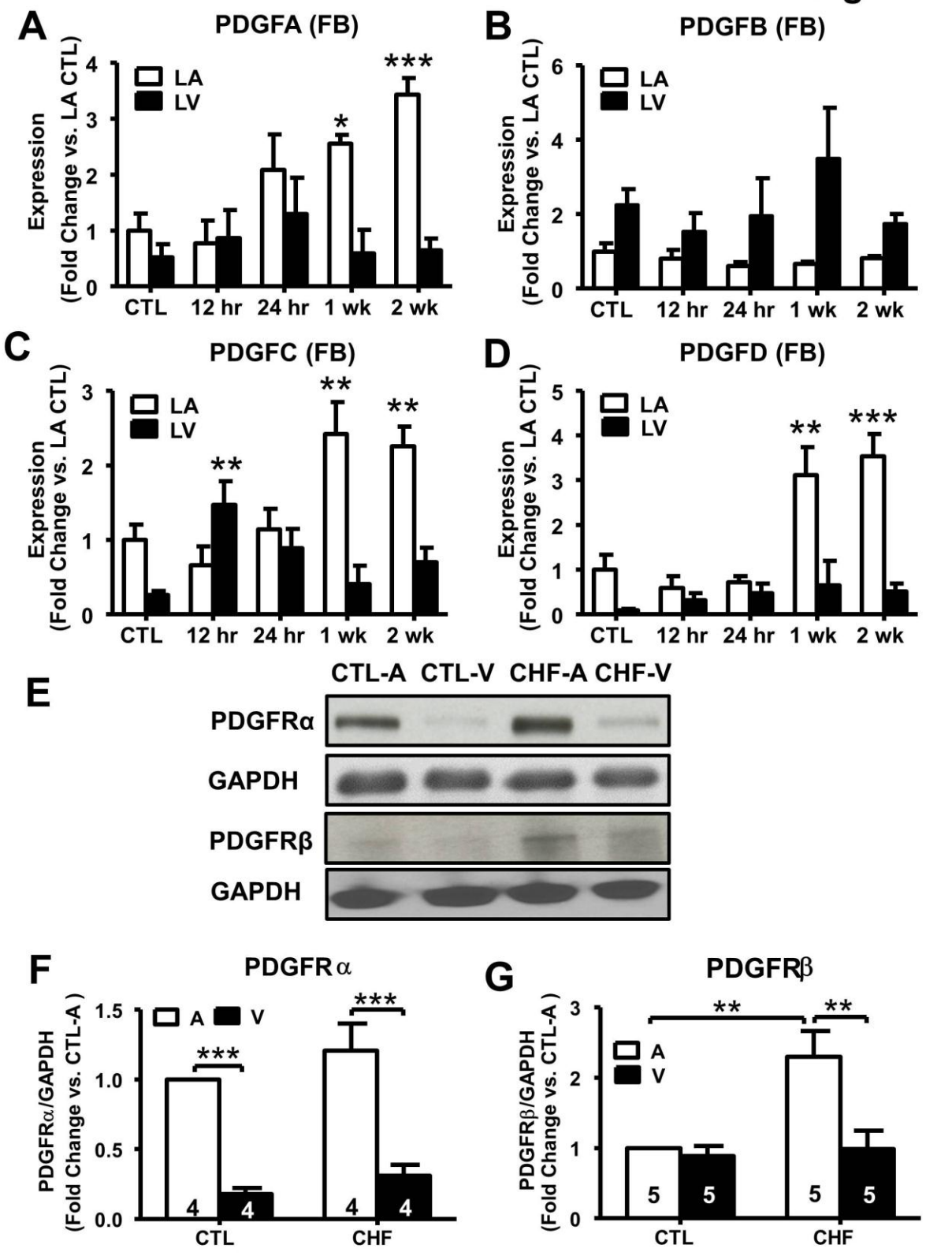
A
PDGFA (FB)
Expression (Fold Change vs. LA CTL)
LA
LV
CTL
12 hr
24 hr
1 wk
2 wk
B
PDGFB (FB)
C
PDGFC (FB)
D
PDGFD (FB)
E
CTL-A CTL-V CHF-A CHF-V
PDGFRα
GAPDH
PDGFRβ
GAPDH
F
PDGFRα
PDGFRα/GAPDH (Fold Change vs. CTL-A)
A
V
CTL
CHF
G
PDGFRβ
PDGFRβ/GAPDH (Fold Change vs. CTL-A)

Figure 2

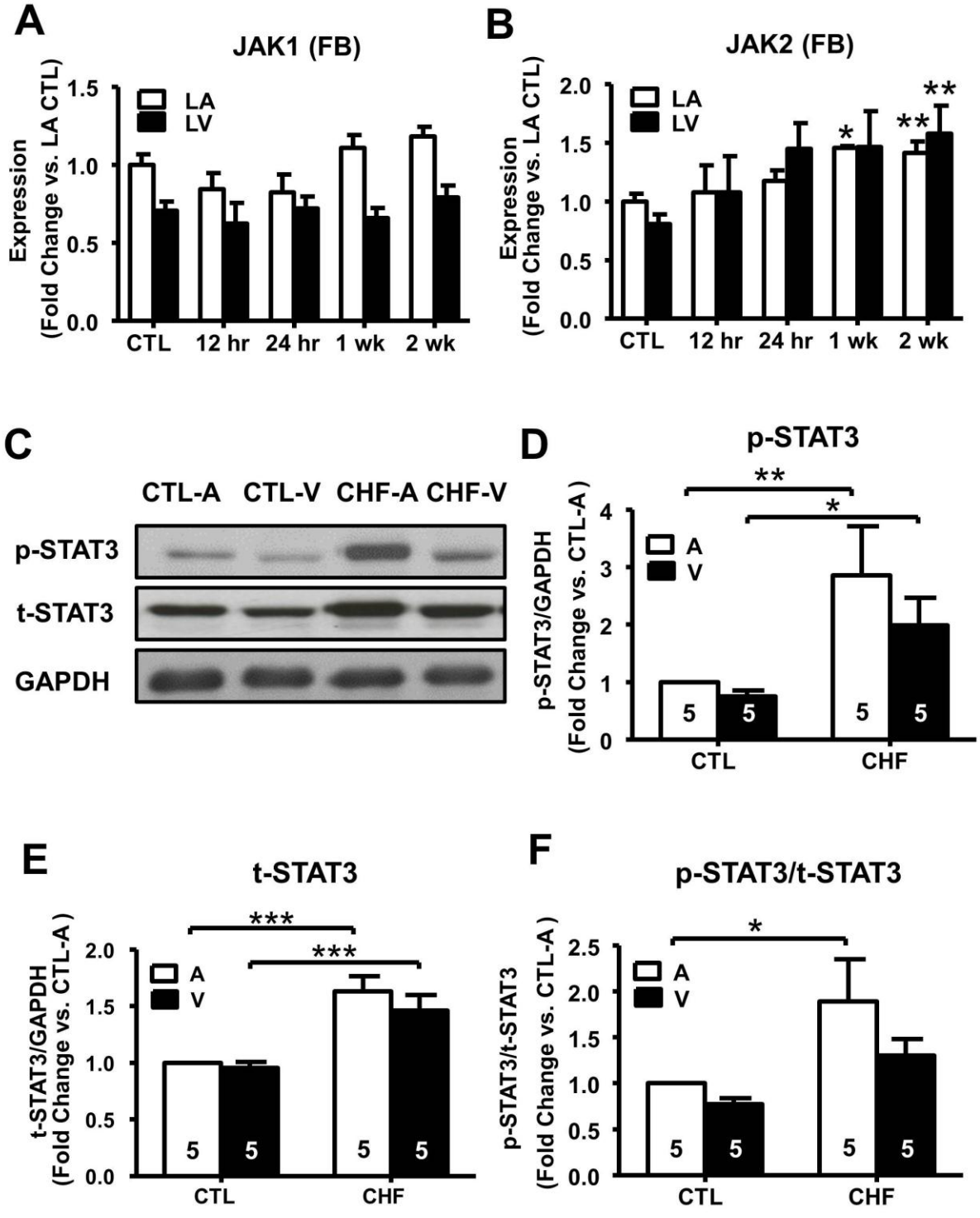
A
JAK1 (FB)
Expression (Fold Change vs. LA CTL)
LA
LV
CTL
12 hr
24 hr
1 wk
2 wk
B
JAK2 (FB)
Expression (Fold Change vs. LA CTL)
LA
LV
*
**
**
CTL
12 hr
24 hr
1 wk
2 wk
C
CTL-A
CTL-V
CHF-A
CHF-V
p-STAT3
t-STAT3
GAPDH
D
p-STAT3
p-STAT3/GAPDH (Fold Change vs. CTL-A)
**
*
A
V
5
5
5
5
CTL
CHF
E
t-STAT3
t-STAT3/GAPDH (Fold Change vs. CTL-A)
***
***
A
V
5
5
5
5
CTL
CHF
F
p-STAT3/t-STAT3
p-STAT3/t-STAT3 (Fold Change vs. CTL-A)
*
A
V
5
5
5
5
CTL
CHF

Figure 3

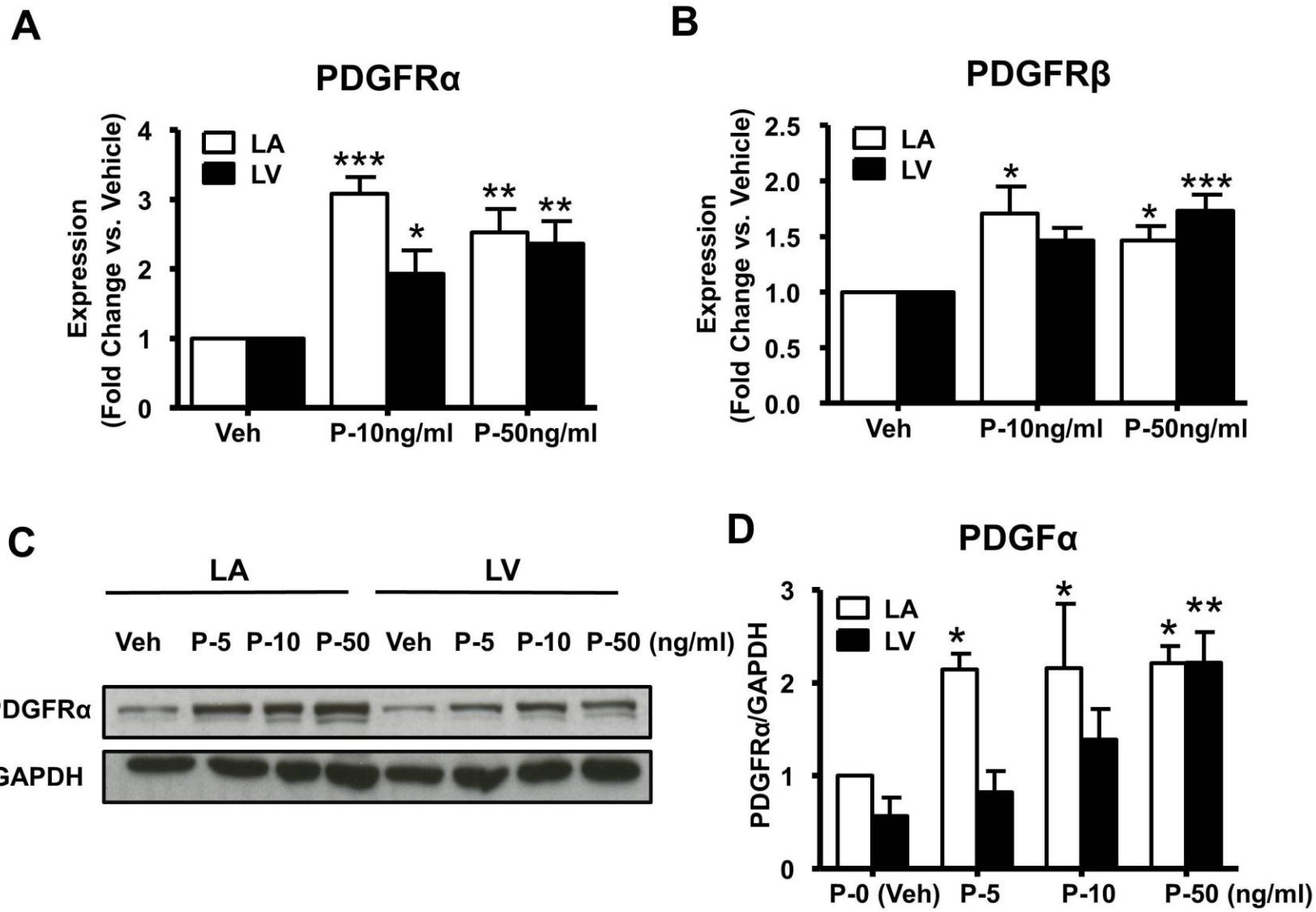
A
PDGFRα
Expression (Fold Change vs. Vehicle)
LA
LV
Veh
P-10ng/ml
P-50ng/ml
B
PDGFRβ
C
LA
LV
Veh P-5 P-10 P-50 Veh P-5 P-10 P-50 (ng/ml)
PDGFRα
GAPDH
D
PDGFα
PDGFRα/GAPDH
P-0 (Veh)
P-5
P-10
P-50 (ng/ml)

Figure 4

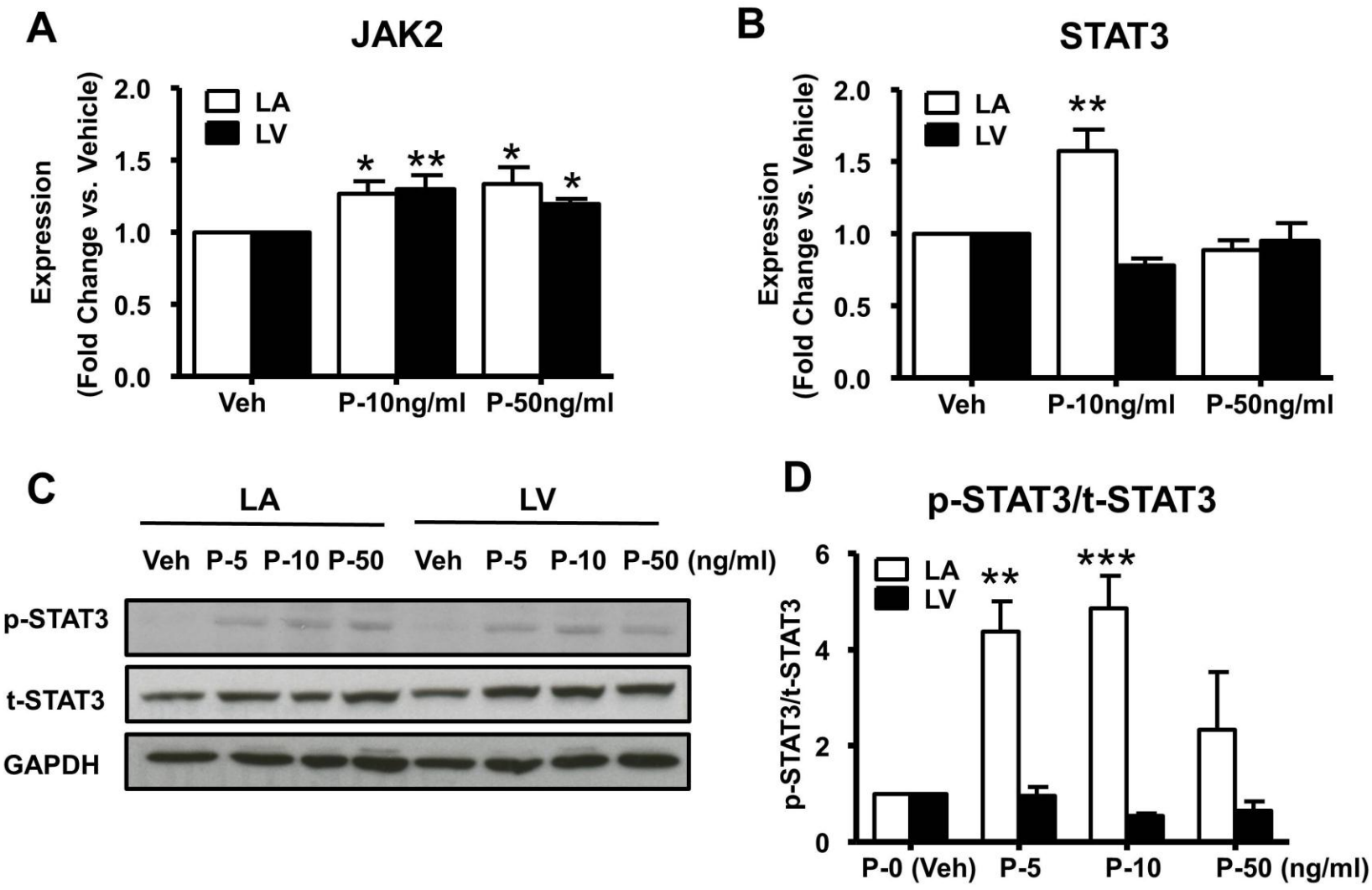
A
JAK2
Expression (Fold Change vs. Vehicle)
2.0
1.5
1.0
0.5
0.0
LA
LV
*
**
*
*
Veh
P-10ng/ml
P-50ng/ml
B
STAT3
Expression (Fold Change vs. Vehicle)
2.0
1.5
1.0
0.5
0.0
LA
LV
**
Veh
P-10ng/ml
P-50ng/ml
C
LA
LV
Veh P-5 P-10 P-50 Veh P-5 P-10 P-50 (ng/ml)
p-STAT3
t-STAT3
GAPDH
D
p-STAT3/t-STAT3
p-STAT3/t-STAT3
6
4
2
0
LA
LV
**
***
P-0 (Veh)
P-5
P-10
P-50 (ng/ml)

Figure 5

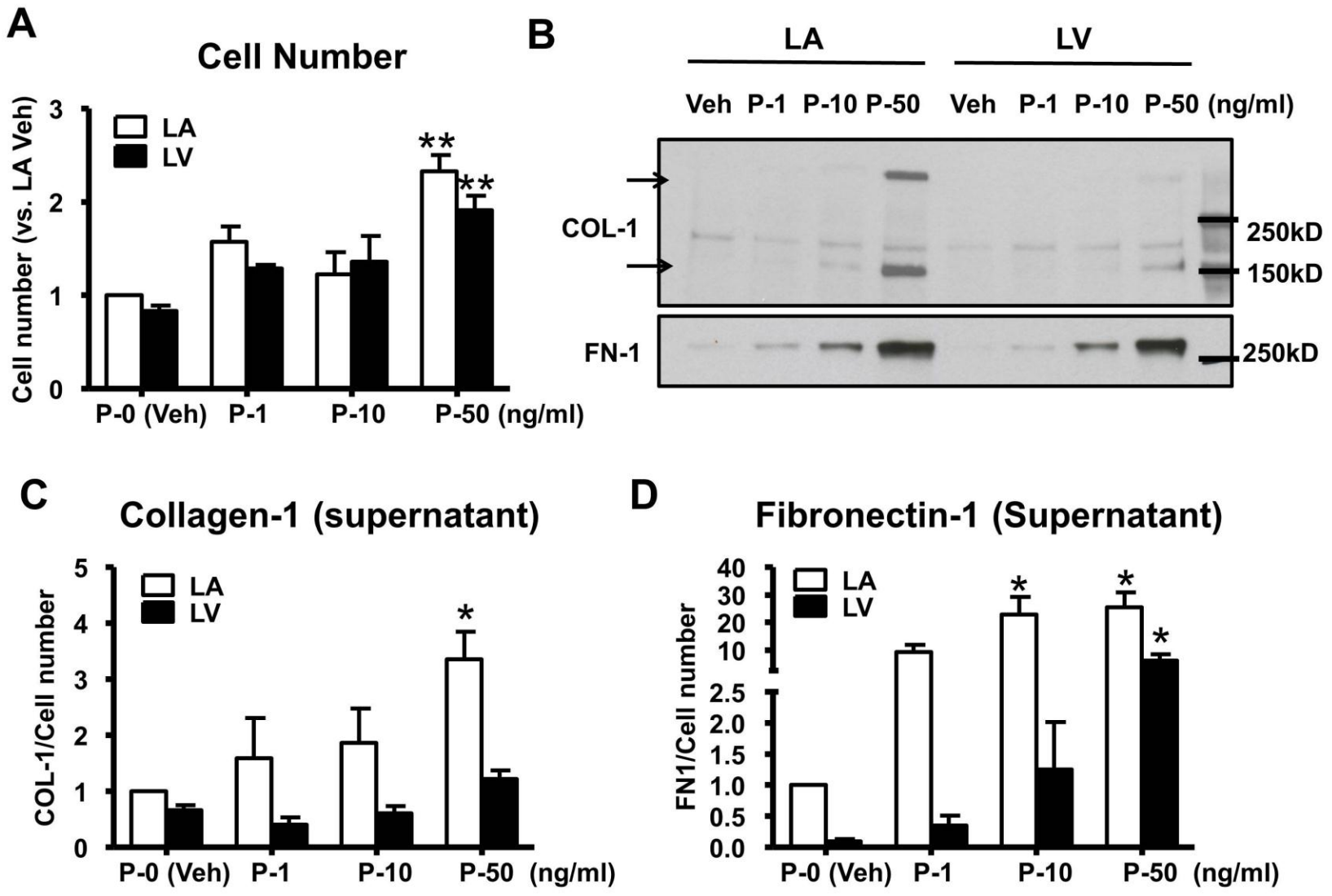
A
Cell Number
Cell number (vs. LA Veh)
LA
LV
**
**
P-0 (Veh)
P-1
P-10
P-50 (ng/ml)
B
LA
LV
Veh P-1 P-10 P-50 Veh P-1 P-10 P-50 (ng/ml)
COL-1
FN-1
250kD
150kD
250kD
C
Collagen-1 (supernatant)
COL-1/Cell number
LA
LV
*
P-0 (Veh)
P-1
P-10
P-50 (ng/ml)
D
Fibronectin-1 (Supernatant)
FN1/Cell number
LA
LV
*
*
*
P-0 (Veh)
P-1
P-10
P-50 (ng/ml)

Figure 6

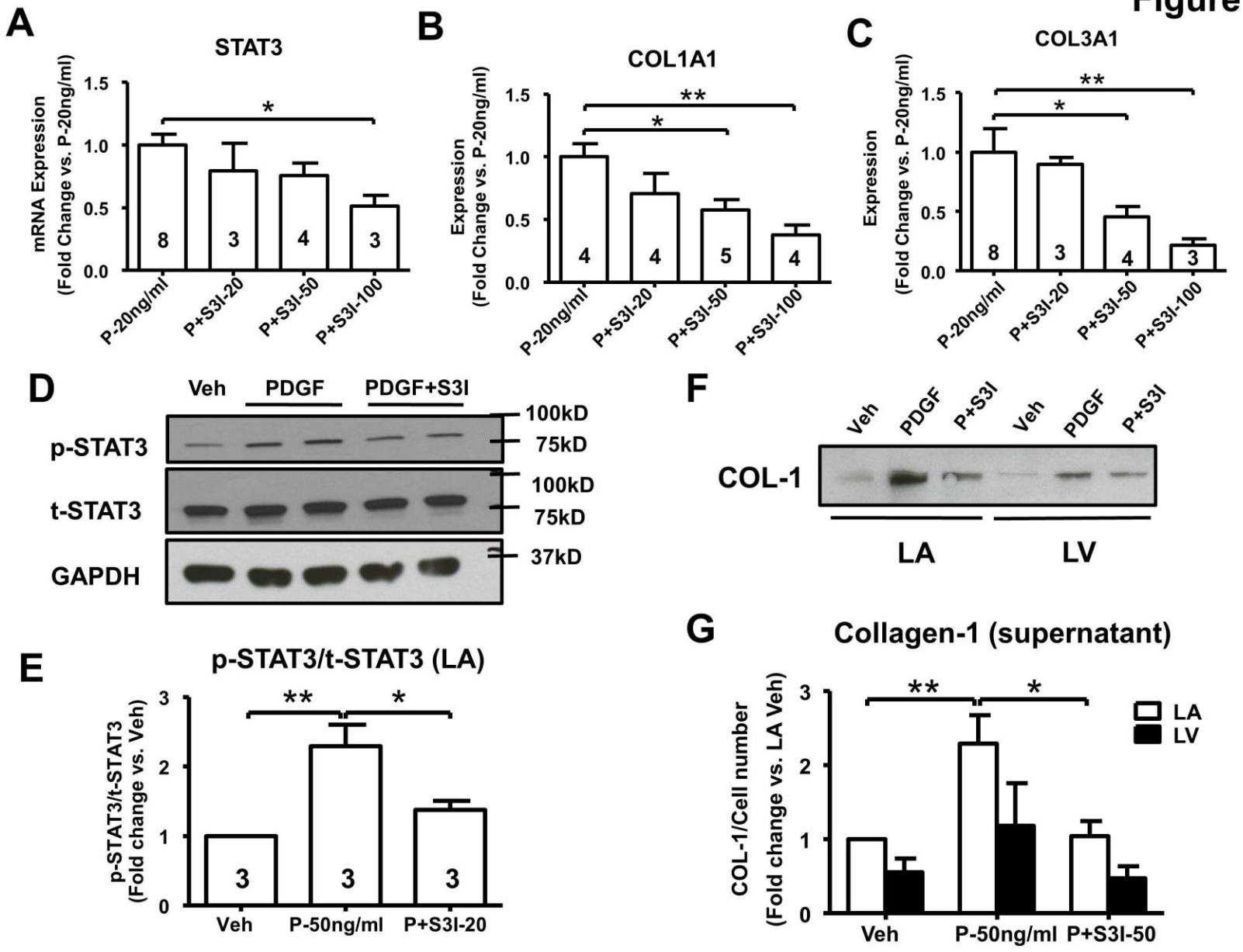
A
STAT3
mRNA Expression
(Fold Change vs. P-20ng/ml)
1.5
1.0
0.5
0.0
*
8
3
4
3
P-20ng/ml
P+S3I-20
P+S3I-50
P+S3I-100
B
COL1A1
Expression
(Fold Change vs. P-20ng/ml)
**
*
4
4
5
4
C
COL3A1
Expression
(Fold Change vs. P-20ng/ml)
**
*
8
3
4
3
D
Veh
PDGF
PDGF+S3I
p-STAT3
t-STAT3
GAPDH
100kD
75kD
100kD
75kD
37kD
F
Veh
PDGF
P+S3I
Veh
PDGF
P+S3I
COL-1
LA
LV
E
p-STAT3/t-STAT3 (LA)
p-STAT3/t-STAT3
(Fold change vs. Veh)
**
*
3
3
3
Veh
P-50ng/ml
P+S3I-20
G
Collagen-1 (supernatant)
COL-1/Cell number
(Fold change vs. LA Veh)
**
*
LA
LV
Veh
P-50ng/ml
P+S3I-50

Figure 7

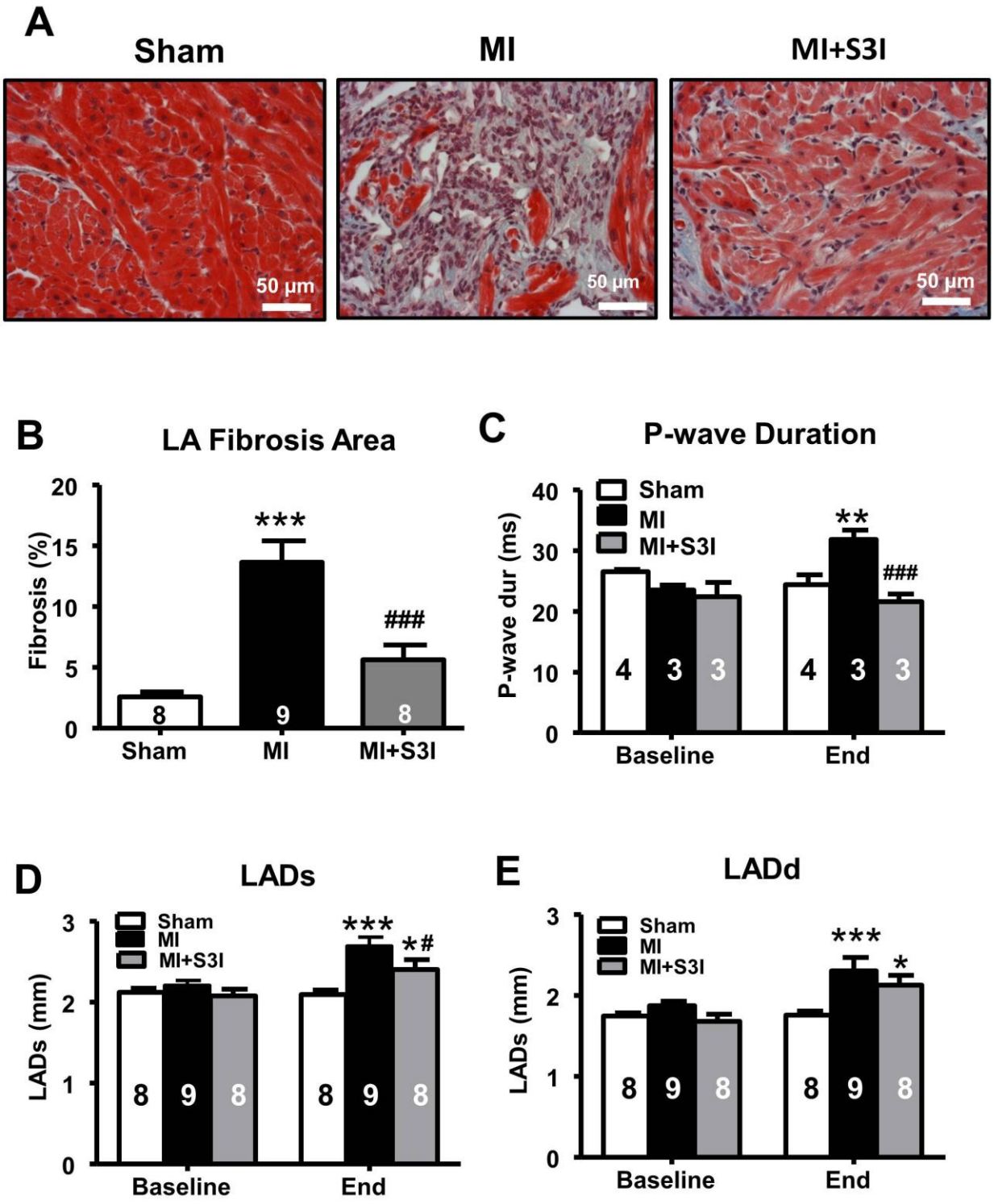
A
Sham
MI
MI+S3I
50 μm
50 μm
50 μm
B
LA Fibrosis Area
Fibrosis (%)
20
15
10
5
0
***
###
8
9
8
Sham
MI
MI+S3I
C
P-wave Duration
P-wave dur (ms)
40
30
20
10
0
Sham
MI
MI+S3I
**
###
4
3
3
4
3
3
Baseline
End
D
LADs
LADs (mm)
3
2
1
0
Sham
MI
MI+S3I
***
*#
8
9
8
8
9
8
Baseline
End
E
LADd
LADs (mm)
3
2
1
0
Sham
MI
MI+S3I
***
*
8
9
8
8
9
8
Baseline
End

Figure 8

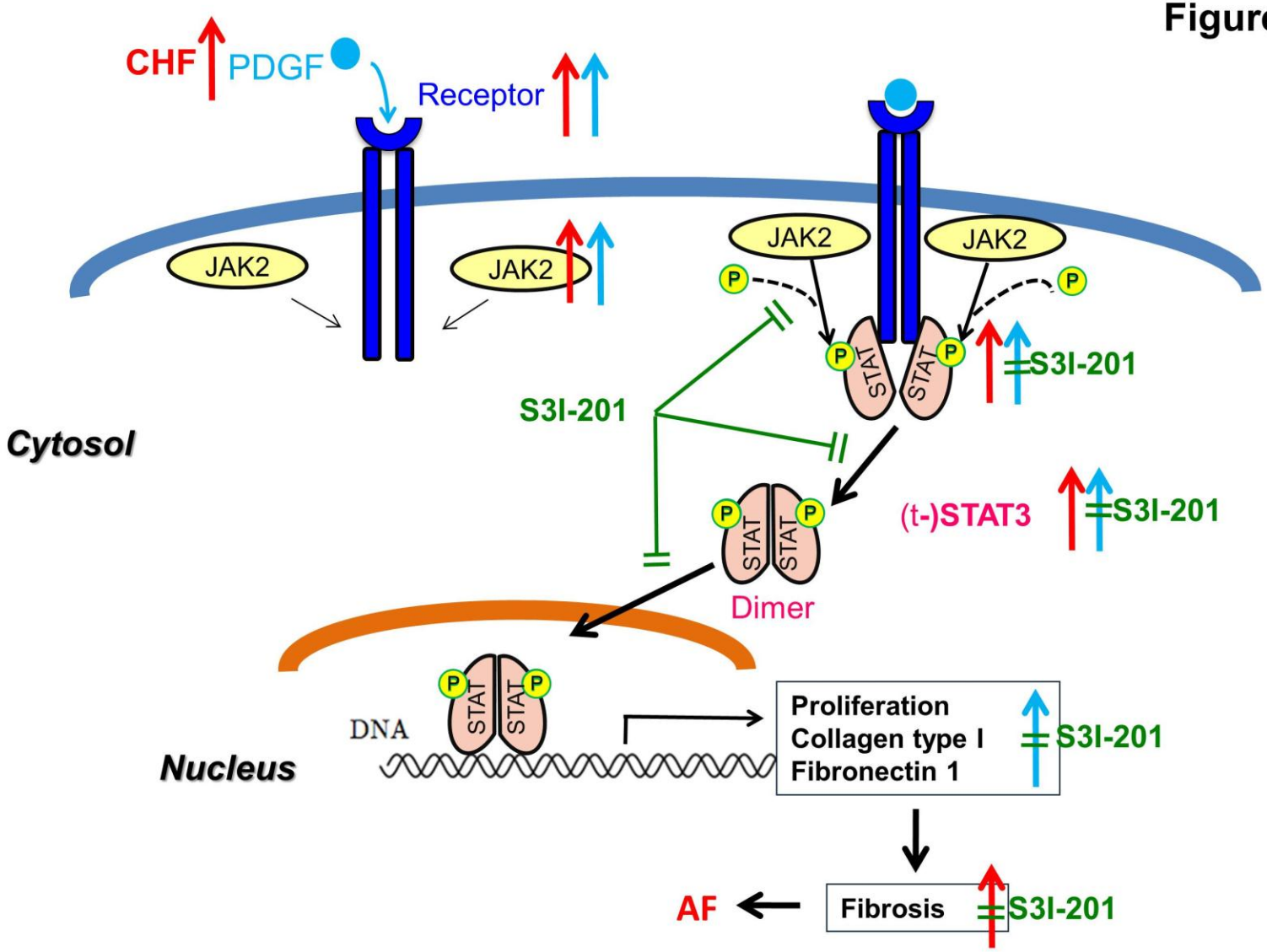
CHF
PDGF
Receptor
JAK2
JAK2
JAK2
JAK2
P
P
P
P
STAT
STAT
STAT
STAT
S3I-201
S3I-201
Cytosol
(t-)STAT3
S3I-201
Dimer
DNA
Nucleus
Proliferation
Collagen type I
Fibronectin 1
S3I-201
AF
Fibrosis
S3I-201

Online-only Data Supplement

Materials and Methods

Surgical Procedures of VTP in dogs and MI in mice

VTP-dogs were anesthetized under diazepam (0.25 mg/kg IV)/ketamine (5.0 mg/kg IV)/halothane (1% to 2% PI) anesthesia, intubated and ventilated. Bipolar pacing leads were fixed to the right-ventricular apex via the left jugular vein, and connected to pacemakers (St. Jude Medical, Minneapolis, MN) implanted subcutaneously in the neck. Following twenty-four hours post-operative recovery time, ventricular-pacing was initiated at 240 bpm. The duration of AF induced by 10 Hz burst pacing was measured repeatedly to measure mean AF-duration as an index of AF-sustainability. The AF-duration for 10 inductions was averaged for each dog.

All experimental mice were fed and housed under a 12:12-hour light/dark cycle at 21 ℃ and 30% humidity. Mice were housed one mouse per cage and had free access to tap water and food. MI mice were anesthetized with 2% isoflurane, intubated, and ventilated after preoperative buprenorphine (0.1 mg/kg S.C.) injection. The thorax was shaved and sterilized with 2% w/v chlorhexidine gluconate in 70% v/v isopropyl alcohol. Body temperature was maintained at 37 ℃ on a heating pad (Harvard Apparatus, Holliston, MA). The beating heart was accessed via a left thoracotomy. Then the left anterior descending coronary artery was ligated with 10-0 silk. Ligation was confirmed by the whitening of a region of the left ventricle, immediately post-ligation. MI mice were compared with sham controls that underwent similar procedures but without left anterior descending ligation. The chest was closed with 5-0 silk and the skin closed with autoclips. The animals were placed in a prone position until the occurrence of spontaneous breathing. Additional doses of ketoprofen (5 mg/kg) and buprenorphine (0.1 mg/kg) were administered subcutaneously immediately after surgery, and 18 hours postoperatively.

Echocardiography

Left ventricular (LV) regional wall motion was scored in LV short axis view at the level of the papillary muscle for the 6 segments viewed in this view as follows: (1) normal, (2) hypo-kinesia, (3) akinesia, (4) dyskinesia, and (5) aneurysmal. Wall motion score index (WMSI) was the mean value of all scores. LV area at end cardiac diastole (LVA_d) and systole (LVA_s) were measured in this view. LV fractional area change was calculated as FAC = (LVA_d-LVA_s) X 100%. Thickness of LV anterior and posterior wall at end cardiac diastole ($LVAW_d$, $LVPW_d$), LV dimension at end cardiac diastole (LVD_d) and systole (LVD_s) were measured by M-mode echocardiography (M-mode) also in this view. LV fractional shortening (FS) and ejection fraction (EF) were obtained by software algorithms within the Vivid 7 system. LV mass was calculated using the formula developed by Liao Y et al, and indexed to body weight (BW) [1]. Left atrial dimension at end cardiac systole (LAD_s) and diastole (LAD_d) were measured by M-mode in parasternal long axis view. The average of 3 consecutive cardiac cycles was used for each measurement, with the operator being blinded to treatment assignment.

In Vivo Electrophysiology

At baseline and 2 weeks post-MI, mice were anaesthetized with 2% isoflurane for electrocardiogram (ECG) recording. Body temperature was maintained at 37℃ with a heating pad. A surface ECG (lead I) was obtained with four 25-gauge subcutaneous electrodes and transmitted to a computer via an analogue-digital converter (IOX v1.585, EMKA Technologies) for monitoring and later analysis with ECG-Auto 2.8.1.18 software (EMKA Technologies). Recordings were filtered between 0.5 and 500 Hz. Measurements were based on averages of a minimum of 10 complexes. Standard criteria were used to measure P-wave duration.

Fibroblast and Cardiomyocyte Isolation

The heart was removed after intra-atrial injection of heparin (10,000 U), immersed in 2 mmol/L Ca^{2+}- containing Tyrode's solution containing (in mM): NaCl 136, KCl 5.4, $MgCl_2$ 1, $CaCl_2$ 2, NaH_2PO_4 0.33, HEPES 5 and dextrose 10, pH 7.35 (NaOH). The left circumflex coronary artery was cannulated and all leaking branches were ligated, followed by perfusion with Ca^{2+}-free Tyrode's solution for 10 minutes. The preparation was then perfused at 10 mL/min with Ca^{2+}-free Tyrode solution containing type II collagenase (0.48 mg/mL, Worthington, OH) and albumin (0.1%, Bioshop Canada Inc. Burlington, ON) for one hour. The harvested cells were collected in DMEM medium and dispersed by gentle trituration with a pipette. Filtration (500-μm nanomesh) was used to remove debris and cells were centrifuged at 800 rpm for 5 minutes to pellet cardiomyocytes. The supernatant was collected and filtered through 20 μm nanomesh and centrifuged at 2,000 rpm for 10 minutes to pellet fibroblasts. Pelleted, freshly isolated fibroblasts and cardiomyocytes were immediately frozen in liquid-N_2 and stored for RNA extraction.

Protein Extraction and Immunoblots

Protein extracts (30 μg) of snap-frozen LA and LV tissue from dogs or cultured fibroblasts were separated by electrophoresis on 12% SDS-PAGE (Bio-Rad) and transferred to PVDF membranes (EMD Millipore, Billerica, MA). For secreted collagen type I, supernatants of medium (30 μl) from cultured fibroblasts were separated by electrophoresis on 8% SDS-PAGE and transferred to nitrocellulose membranes (Bio-Rad). Membranes were blocked and incubated overnight with the primary antibodies and then with secondary antibodies. All of the primary antibodies are listed in Table 1. Secondary antibodies were horseradish peroxidise–conjugated anti-mouse or anti-rabbit (1:10000; Jackson Immuno Research Laboratories). Antibody signals were visualized with

enhanced chemiluminescence (PerkinElmer, Waltham, MA). Data were normalized to GAPDH band intensity from the same samples on the same membranes and/or normalized to cell number (medium supernatant).

Supplemental Table 1. Primary antibodies that were used.

Name (anti-)	**Species**	**Type**	**Dilution**	**Source**
PDGFR-α	Rabbit	Polyclonal	1:2,000	Santa Cruz Biotechnology, Santa Cruz, CA
PDGFRβ	Rabbit	Polyclonal	1:2,000	Santa Cruz Biotechnology
STAT3	Rabbit	Polyclonal	1:2,000	Cell signaling Technology, Danvers, Mass
Phosphorylated - STAT3	Mouse	Monoclonal	1:2,000	Cell signaling Technology
Collagen type I	Rabbit	Polyclonal	1:25,000	MD Biosciences, Zurich Switzerland
GAPDH	Mouse	Monoclonal	1:10,000	Research Diagnostics Inc. RDI, Fitzgerald Industries, NJ

References—Online Supplement

[1]. Liao, Y., et al., *Echocardiographic assessment of LV hypertrophy and function in aortic-banded mice: necropsy validation.* Am J Physiol Heart Circ Physiol, 2002. 282(5): p. H1703-8.

Supplemental Figure Legends

Supplemental Figure 1. Ventricular tachypacing (VTP) dogs developed progressive AF susceptibility and atrial fibrosis. (A) Mean AF duration increased substantially at 1-week and 2-week VTP. (B) Quantification of fibrosis during the course of CHF induced by VTP. (C) Representative histological tissue sections (Masson Trichrome) of left atria (LA) and left ventricles (LV). Area stained with blue color is collagen. Mean ±SEM, n=3-8/group, *p<0.05, **p<0.01, ***p<0.001 vs. corresponding CTL. One-way ANOVA with Dunnett's tests was used for statistical analysis. AF, atrial fibrillation; CTL, non-pacing control.

Supplemental Figure 2. mRNA expression of (A) PDGF isoforms, (B) PDGF receptor (PDGFR) isoforms, and (C) JAK2 and STAT3 in fibroblasts and cardiomyocytes from control dogs. Mean ±SEM, n=4/group. *p<0.05, **p<0.01, ***p<0.001. One-way One-way ANOVA with Bonferroni-corrected *t*-tests was used for statistical analysis. LA, left atrium; LV, left ventricle; FB, fibroblast; CM, cardiomyocyte.

Supplemental Figure 3. mRNA expression of TGFβ1 and TGFβ receptors (TGFβRs) in fibroblasts stimulated with PDGF-AB with or without the addition of S3I-201. (A) TGFβ1 mRNA expression was induced by PDGF-stimulation and the increase was reversed by S3I-201 treatment. (B) TGFβR1 expression was not affected by either PDGF-stimulation or S3I-201 treatment. (C) TGFβR2 mRNA expression was induced by PDGF-stimulation and the increase was reversed by S3I-201 treatment. Mean ±SEM, n=4-10/group. *p<0.05, **p<0.01, ***p<0.001. One-way ANOVA with Bonferroni-corrected *t*-tests was used for statistical

analysis. TGFβR1/2, TGF beta receptor 1/2; Veh, vehicle; P, PDGF; S3I20/50/100, S3I-201 20/50/100 μM.

Supplemental Figure 4. Effects of S3I-201 on LV-remodeling. (A-B) Ratio of heart weight to body weight and LV mass to body weight were increased 2 weeks after myocardial infarction (MI), changes attenuated by S3I-201 treatment. (C-H) LV dilation and LV contractile dysfunction were induced by MI but not improved by S3I-201. Mean±SEM, *p<0.05, **p<0.01, ***p<0.001 vs. sham; $^{\#}p$<0.05, $^{\#\#}p$<0.01 vs. MI. Two-way ANOVA with Bonferroni post-tests was used for statistical analysis. HW, heart weight; BW, body weight; LV, left ventricular; LVDs, left ventricular dimension at end systole; LVDd, left ventricular dimension at end diastole; FS, fractional shortening; EF, ejection fraction; FAC, fractional area change; WMSI, Wall motion score index; Sham, sham surgery without ligation; MI, myocardial infarction; MI+S3I, myocardial infarction with S3I-201 treatment.

Supplemental Figure 5. mRNA expression of (A) JAK2 and (B) STAT3 in left atrial (LA) and left ventricular (LV) cardiomyocytes during the ventricular tachypacing (VTP) time-course. Mean±SEM, n=5-12/group, *p<0.05 vs. corresponding CTL. One-way ANOVA with Dunnett's tests was used for statistical analysis. CM, cardiomyocyte; LA, left atrium; LV, left ventricle; CTL, non-paced controls.

Supplemental Figure 1

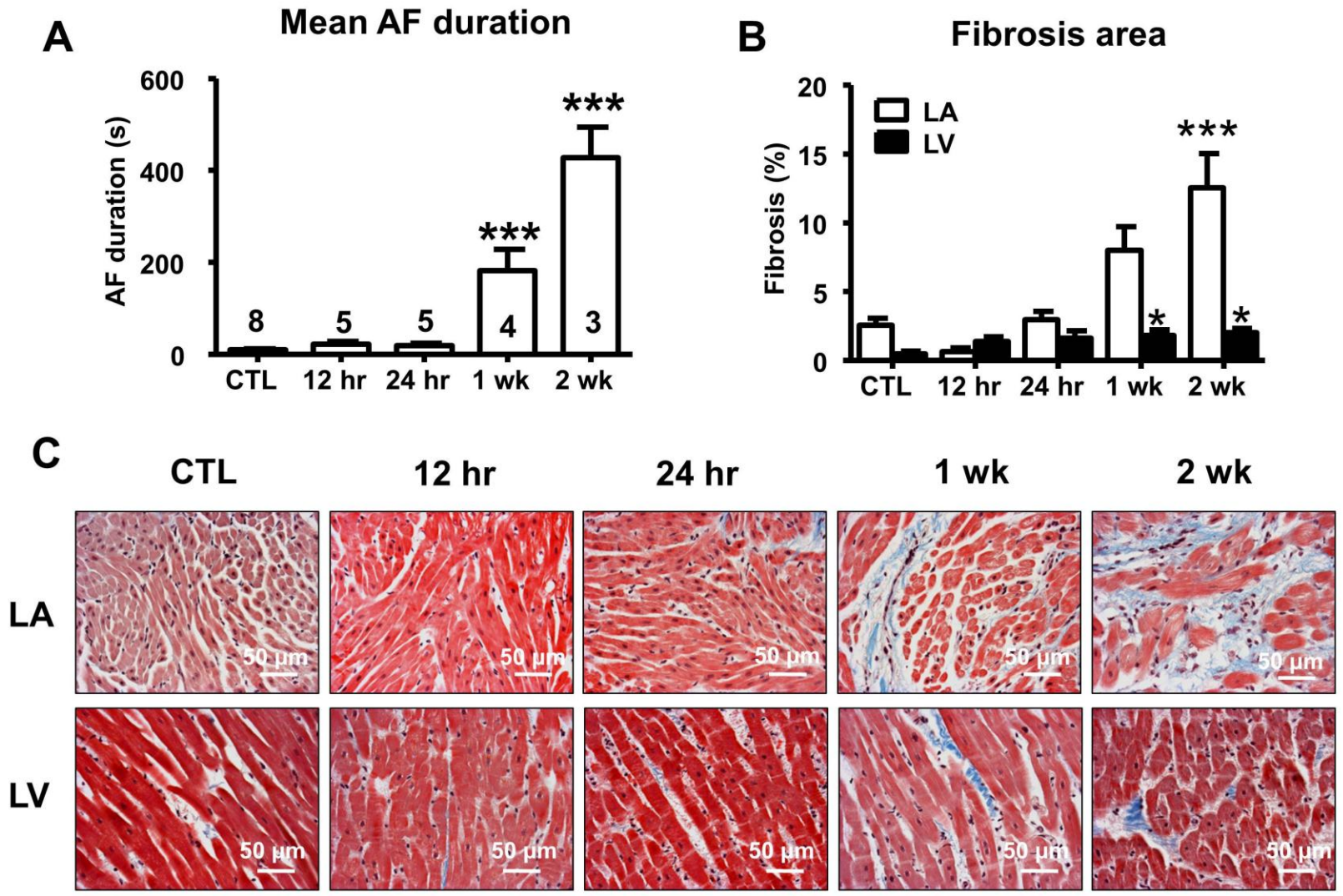

Supplemental Figure 2

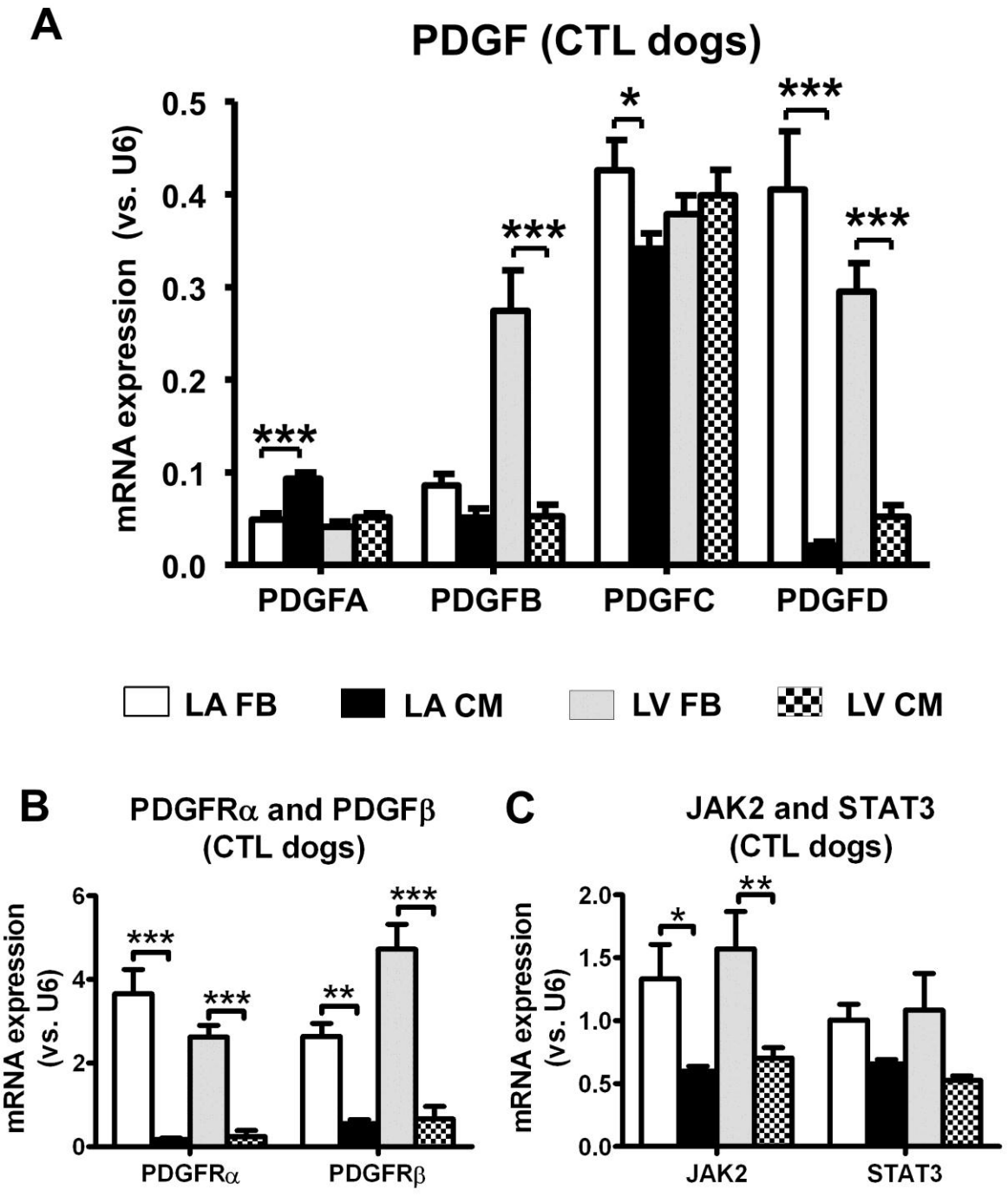

Supplemental Figure 3

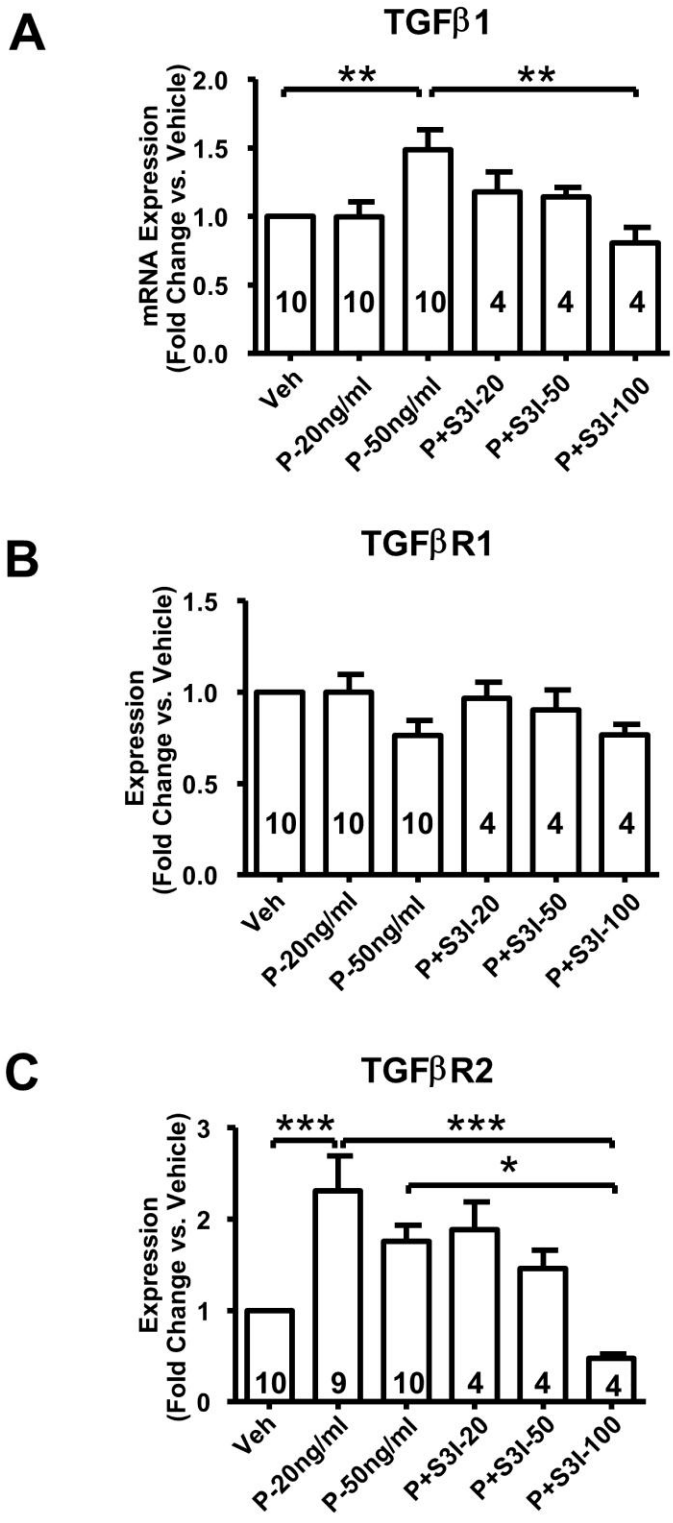

Supplemental Figure 4

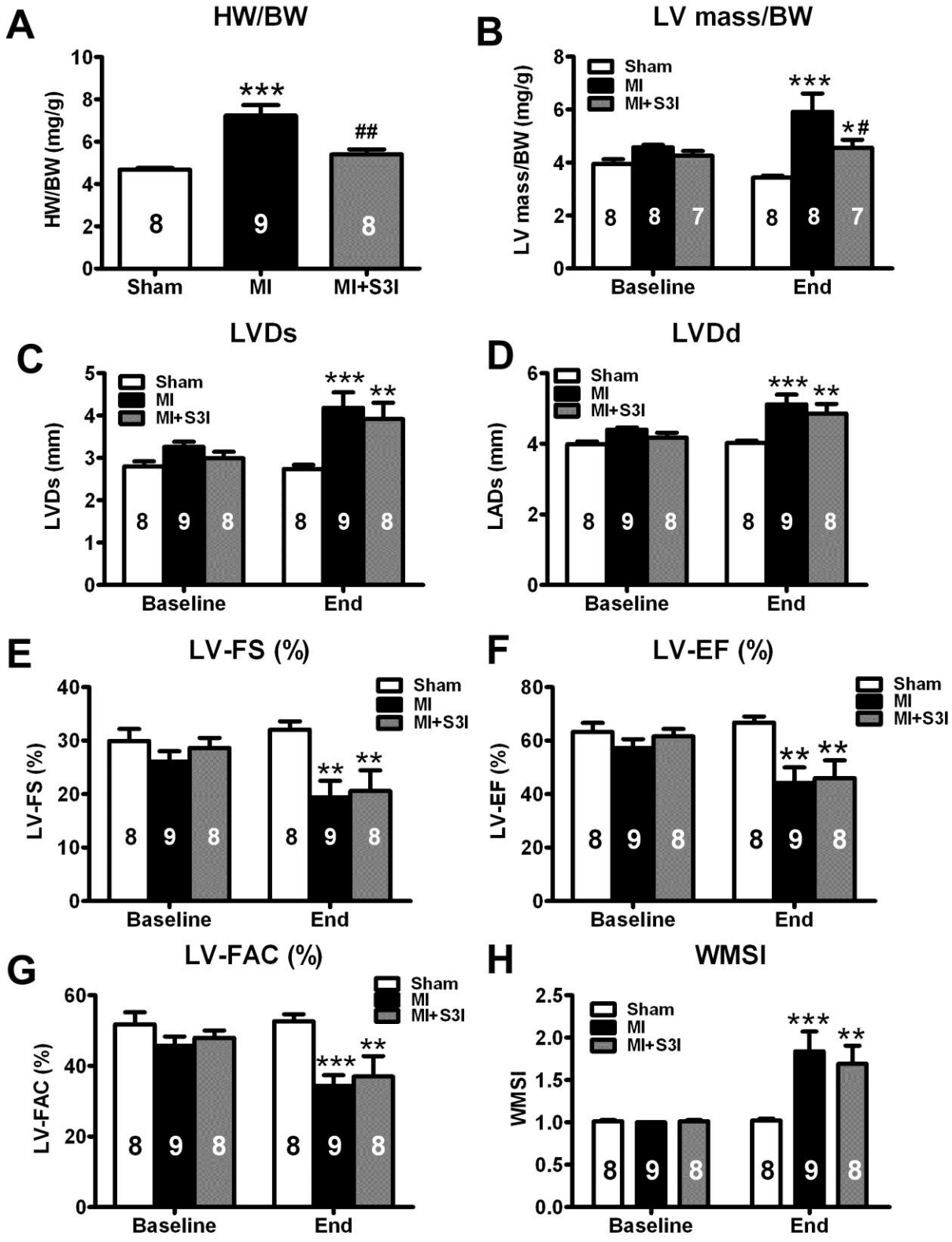

Supplemental Figure 5

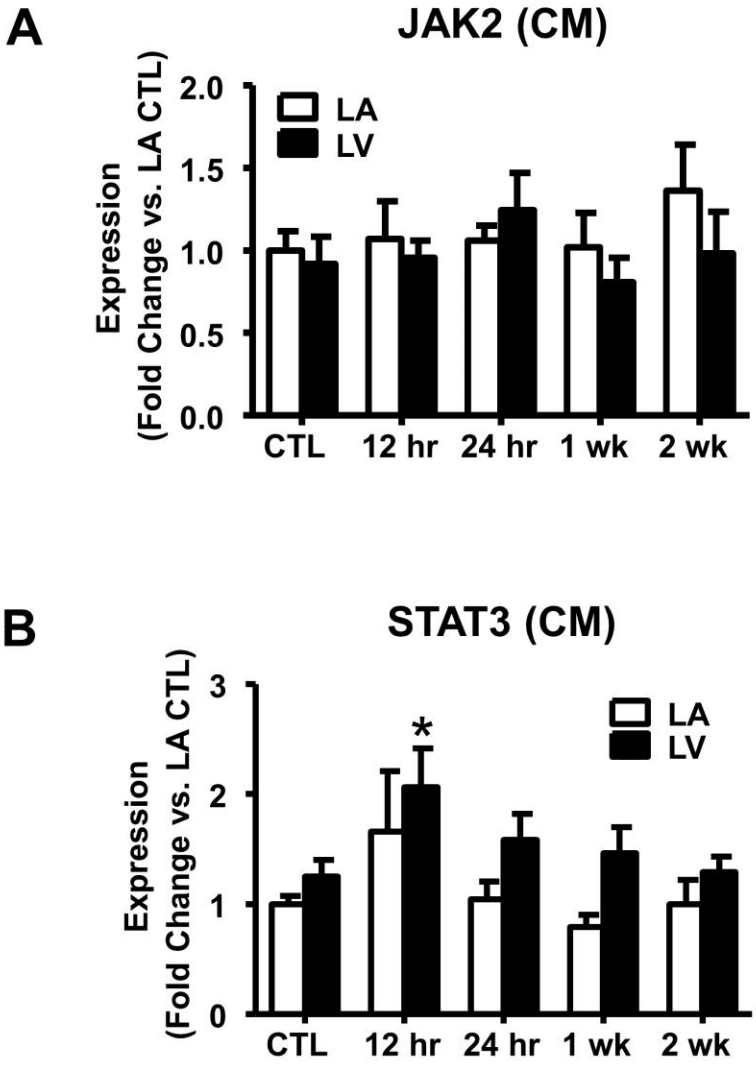

Chapter 3

The characterization of microRNA changes in congestive heart failure

Linking statement

MicroRNAs (miRs) have been studied in cardiac fibrosis but evidence about their role in AF-related atrial fibrotic remodeling is still limited (Section 1.7.2.4). Prior studies from our lab demonstrated potential roles for miR-21, miR-29b and miR-26 in regulating fibroblast behaviour and atrial fibrotic responses. However, despite the fact that multiple miRs have been implicated in atrial fibrosis, no studies have considered a number of important questions: 1) how do the multiple potential miRs that may modify atrial fibrosis change their expression over time in the heart; 2) how do their expression changes compare in different tissues and cellular compartments. I hypothesized that the system-response of miRs is involved in arrhythmogenic fibrotic remodeling. I therefore performed a detailed time-, chamber- and cell-type-specific miRNA analysis in the canine AF-substrate model, aiming to reveal its role in the AF-promoting atrial-selective fibrotic response.

Detailed characterization of microRNA changes in a canine heart failure model: Relationship to arrhythmogenic structural remodeling

Yu Chen, MSc[a,b,]; Reza Wakili, MD[a,c,]; Jiening Xiao, PhD[a], Chia-Tung Wu, MD[a,d]; Xiaobin Luo, PhD[a]; Sebastian Clauss, MD[c]; Kristin Dawson, BSc[a,b]; Xiaoyan Qi, PhD[a]; Patrice Naud, PhD[a]; Yan-Fen Shi, MD[a]; Jean-Claude Tardif, MD[a]; Stefan Kääb, MD[c]; Dobromir Dobrev, MD[e]; Stanley Nattel, MD[a,b,*]

[a]Department of Medicine and Research Center Montreal Heart Institute and Université de Montréal; Montreal, Quebec, Canada;

[b]Department of Pharmacology and Therapeutics McGill University, Montreal, Quebec, Canada;

[c]Ludwig-Maximilians University, Munich; Department of Medicine I, Klinikum Grosshadern;

[d]Chang Gung Memorial Hospital and Chang Gung University Tao-Yuan, Taiwan;

[e]Institute of Pharmacology, Faculty of Medicine, University Duisburg-Essen, Essen, Germany.

Short title: miRNA remodeling in heart failure

Word Count: 5996

*Corresponding author. 5000 Belanger Street East, Montreal, Quebec, Canada, H1T 1C8.

Tel.: (514)-376-3330 ext. 3990. Fax: (514)-376-1355.E-mail: stanley.nattel@icm-mhi.org

Abstract

Background−Heart failure (HF) causes left-atrial (LA) and left-ventricular (LV) remodeling, with particularly-prominent changes in LA that create a substrate for atrial fibrillation (AF). MicroRNAs (miRs) are potential regulators in cardiac remodeling. This study evaluated time-dependent miR expression-changes in LA and LV tissue, fibroblasts and cardiomyocytes in experimental HF.

Methods−HF was induced in dogs by ventricular tachypacing (varying periods, up to 2 weeks). Following screening-microarray, 15 miRs were selected for detailed real-time qPCR assay. Extracellular matrix mRNA-expression was assessed by qPCR.

Results−Tachypacing time-dependently reduced LV ejection-fraction, increased LV-volume and AF-duration, and caused tissue-fibrosis with LA changes greater than LV. Tissue miR-expression significantly changed in LA for 10 miRs; in LV for none. Cell-selective analysis showed significant time-dependent changes in LA-fibroblasts for 10/15 miRs, LV-fibroblasts 8/15, LA-cardiomyocytes in 6/15 and LV-cardiomyocytes 3/15. Cell-expression specificity did not predict cell-specificity of VTP-induced expression-changes, e.g. 4/6 cardiomyocyte-selective miRs changed almost exclusively in fibroblasts (miR-1, miR-208b, miR133a/b). Thirteen miRs directly implicated in fibrosis/extracellular-matrix regulation were prominently changed: 9/13 showed fibroblast-selective alterations and 5/13 LA-selective. Multiple miRs changed in relation to associated extracellular-matrix targets.

Conclusions−Experimental HF causes tissue and cell-type selective, time-dependent changes in cardiac miR-expression. Expression-changes are greater in LA versus LV, and greater in fibroblasts than cardiomyocytes, even for most cardiomyocyte-enriched miRs. This study, the first to examine time, chamber and cell-type selective changes in an experimental model of HF,

suggests that multiple miR-changes underlie the atrial-selective fibrotic response and emphasize the importance of considering cell-specificity of miR expression-changes in cardiac remodeling paradigms.

Keywords: microRNA, heart failure, remodeling, fibrosis

Introduction

Congestive heart failure (CHF) is a leading cause of mortality and morbidity [1], and is associated with important cardiac remodeling [2]. MicroRNAs (miRNAs, miRs) are short, non-coding RNAs that regulate gene-expression by binding to complementary sequences, generally in the 3'-untranslated region, of mRNAs to prevent protein transcription and, in many cases, to destabilize the mRNA. CHF markedly changes cardiac gene-expression profiles at the ventricular [3,4] and atrial [4,5] levels. There is extensive evidence for an important role of miRNAs in CHF-induced cardiac gene-expression remodeling [1,6].

Tissue fibrosis, an important part of the CHF remodeling response, is much more intense at the atrial than ventricular level [7], a difference that is paralleled by discrete gene-change profiles [4]. However, most studies of miRNA changes in CHF-related remodeling have focused on ventricular changes. Those that have examined atrial alterations have not compared them directly to ventricular changes in the same animal.

The targets of miRNAs are many, and their programmatic effects are consistent with the complex gene-expression changes in CHF [1,6]. Furthermore, miRNAs can target and elicit different biological responses in different cell-types [8]. While cardiomyocyte-changes are central to the contractile dysfunction that characterizes CHF, fibroblasts also importantly

contribute to remodeling, notably via altered extracellular-matrix (ECM) protein synthesis, which causes tissue fibrosis, as well as paracrine interactions with cardiomyocytes. A major deficiency in the available literature on miRNA alterations occurring with CHF is that virtually all studies have assayed miRNA-expression changes in whole tissues. It is quite conceivable that the miRNA-responses are cell-type specific, yet no work of which we are aware has systematically examined miRNA changes in different heart-cell compartments.

The objectives of the present study were: 1) to examine the time-dependent changes in miRNA-expression in a well-established dog model of dilated cardiomyopathy; 2) to examine differentially the changes in atria versus ventricles, as well as the cell-selectivity (cardiomyocyte versus fibroblast) of the miRNA-remodeling process; and 3) to relate changes in miRNA expression to those of extracellular-matrix gene targets.

Methods

Animal model

Animal-care procedures followed the guidelines of the Canadian Council on Animal Care and were approved by the Animals Research Ethics Committee of the Montreal Heart Institute. CHF was induced by ventricular tachypacing (VTP, 240 bpm). Sixty-five mongrel dogs were divided into five groups: non-paced controls (n=20), 12 hour VTP (n=10), 24 hour VTP (n=10), 1 week VTP (n=10) and 2 week VTP (n=15). In a first series of dogs, we examined tissue miRNA-expression, with 8 control dogs and 5 dogs each euthanized after 12 hour, 24 hour, 1 week, and 2 week VTP. In a second series, we analyzed cell-type selective changes in 12 control dogs, and 5 each at 12 hours, 24 hours, and 1 week VTP, and 10 dogs at 2 weeks of VTP. VTP dogs were initially anesthetized with acepromazine (0.07 mg/kg i.m.), ketamine (5.3 mg/kg

i.v.), diazepam (0.25 mg/kg, i.v.), and isoflurane (1.5%), intubated and ventilated. Bipolar pacing leads were fixed to the right-ventricular apex via the left jugular vein, and connected to tachypacemakers (St. Jude Medical, Minneapolis, MN) implanted subcutaneously in the neck, with tachypacing started after a 24-hour recovery period.

Echocardiography

Transthoracic echocardiography was performed at baseline and on the last study day prior to euthanasia, with an M3S probe (2.0-4.3 Megaherz) and a Vivid 7 Dimension system (GE Healthcare Ultrasound, Horten, Norway) under sedation with acepromazine (0.07 mg/kg i.m.). M-mode echocardiograms were obtained at the aortic-valve level in the parasternal long-axis view to measure left-atrial (LA) diameters. Left-ventricular (LV) apical 4 and 2 chamber views were recorded. The Simpson biplane method was used to determine LV volumes and ejection fraction (LVEF). The average of three to six cardiac cycles was used for each measurement, with the operator blinded to treatment assignment. The duration of AF induced by 10 Hz burstpacing was measured repeatedly as previously described [2,4,5] to measure mean AF-duration as an index of AF-sustainability. The AF-duration for 10 inductions was averaged for each dog.

Tissue and cell harvesting

On study-days, dogs were anaesthetized with morphine and (2 mg/kg s.c.) and alpha-chloralose (120 mg/kg i.v.) and mechanically ventilated, then euthanized by cardiac excision. Hearts, lungs and adjacent tissues were removed and placed in Tyrode's solution. In the first set of dogs (n=28), right atrial (RA), LA and LV free wall samples were fast-frozen in liquid-N_2 for molecular biology and/or stored in formalin for histology. In the second set of animals (n=37),

the LA and LV were perfused via the left anterior descending coronary artery for cell isolation and collagenase digestion as detailed previously [9,10]. Freshly-isolated fibroblasts were analyzed to avoid the gene-expression changes that occur in culture [10]. After cell-isolation, cell-isolates were snap-frozen in liquid-N_2 and stored at -80°C.

Fibrosis quantification

Fibrosis was quantified blinded to group assignment with Masson's trichrome staining [11]. Microscopic images of Masson's trichrome-stained sections at 400× magnification were digitized (Scion Image Software, Olympus Microscopes, Center Valley, NJ) and analyzed with Sigmascan 4.0 (Jandel Scientific, San Rafael, CA). Fibrotic tissue content was quantified as a percentage of surface area, excluding blood vessels.

RNA extraction and quantification

Total RNA of tissue-samples or freshly isolated cells from each dog was extracted with the mirVana miRNA Isolation Kit (Ambion, Austin, TX) without performing the miRNA enriching step. RNA was quantified by NanoDrop 2000 (Thermo Scientific, Waltham, MA) and diluted to 100 ng/µl. For details about methods for RNA quality control assessment and microarray screening for miR changes, see Online Supplement.

Real-time polymerase chain reaction (PCR)

First-strand cDNA was synthesized from 87.5 ng of total RNA using the Taqman microRNA Reversed Transcription Kit or High Capacity Reverse Transcription Kit (Applied Biosystems, Foster City, CA).PCR-reactions were performedwiththeMx3005P Realtime PCR System

(Agilent Technologies, Santa Clara, CA). Real-time PCR was performed with specific 6-carboxy-fluorescein (FAM)-labeled fluorogenic TaqMan primers, 13 ng (for miRNA) or 10 ng (for ECM-proteins) of cDNA combined with 2×TaqMan Universal PCR Master Mix (Applied Biosystems). Signals were detected in duplicate. The plates were thermal-cycled at 95°C (10 minutes), followed by 40 cycles at 95°C (15 s)/60°C (1 minute). Data were analyzed with MxPro qPCR Software (Agilent). U6 small nuclear RNA (snRNA) was the reference for miRNA-expression. The geometric mean of HPRT and β2-microglobulin mRNA-expression was used as reference for ECM mRNA-expression. All TaqMan probes or primers were purchased from Applied Biosystems.

In silico prediction of potential miRNA targets

MiRNA-targets were predicted by TargetScan v6.2, by searching for the presence of conserved8-merand7-mersites on target mRNAs that match the miRNA seed region. Only mRNA sequences with at least one conserved binding region across human and canine families were chosen as potentially valid targets from mRNA target prediction.

Statistical analysis

Data are mean±SEM. One-way ANOVA was used for multiple-group comparisons, with a post-hoc Dunnett's test to compare differences between individual group and control means. A two-tailed $p<0.05$ represented statistical significance.

Results

Cardiac remodeling

Serial echocardiography revealed LV contractile dysfunction beginning 24 hours after VTP-onset (Figure 1A), accompanied by progressive LV and LA dilation (Figures 1B, 1C). AF duration increased progressively (Figure 1D) and substantial LA fibrosis occurred (Figure 1E, Supplemental Figure 1), consistent with previous reports [11,12]. Significant changes in the expression of alpha smooth-muscle actin (α-SMA), a marker of fibroblast differentiation to myofibroblasts, occurred in LA but not LV fibroblasts (Figure 1F).

Screening microarray results

Of 260 miRNAs probed in dog (Supplemental Table 1), 99 in atrium and 36 in ventricle showed ≥20% deviation in CHF compared to control (Supplemental Table 2). Changes ranged from a 561% increase to a 52% decrease in atrium, and from a 56% increase to a 40% decrease in ventricle. We selected 21 miRNAs for further study, based on the magnitude of change and known abundance in the heart. The expression heat-map for these 21 miRNAs (Supplemental Figure 2) shows chamber-selective alterations, much larger in atrium than ventricle. Based on this heat-map, we performed detailed time, tissue and cell expression analyses for at least one isoform of each miRNA: miR-1, miR-21, miR-26a, miR-26b, miR-29b, miR-30a, miR-133a, miR-133b, miR-146a, miR-146b, miR-208a, miR-208b, miR214, miR-218 and miR-222.

Tissue miRNA-expression

The tissue-expression data for miR-1 are shown in Figure 2A. Expression decreased progressively in the LA, becoming statistically significant within 24 hours, but did not change significantly in LV. MiR-21 increased substantially in LA, with significant changes beginning after 1 week (Figure 2B); once more, LV-expression was unchanged. MiR-26a tended to decrease

in LA, but the changes were not statistically significant, and no consistent trend was observed in LV (Figure 2C). MiR-26b decreased significantly in LA within 12 hours of VTP-onset, and was unchanged in LV (Figure 2D). MiR-29b (Figure 2E), miR-30a (Figure 2F) and miR-133a (Figure 2G) showed rapid (12-24 hours) and sustained decreases in LA, without change in LV. MiR-133b decreased to a lesser extent and later in LA, without changing in LV (Figure 2H). MiR-146a expression did not change in either LA or LV (Figure 3A), but miR-146b increased significantly in LA beginning at 1-week VTP (Figure 3B). By contrast, miR-208a expression decreased rapidly in LA (Figure 3C), whereas miR-208b remained unchanged in both LA and LV (Figure 3D).MiR-214 expression did not change significantly (Figure 3E). LA miR-218 was downregulated rapidly, beginning after 12-hour VTP, and remained suppressed thereafter, without changing in LV (Figure 3F). While miR-222 showed a similar pattern to miR-218, the changes were not statistically significant (Figure 3G). The absolute expression-levels were highest for miR-1 and miR-133 (about 5-10 normalized to U6), intermediate for miR-21, miR26 and miR-30 (about 0.5-2 versus U6), smaller for miR-29b, miR-214 and miR-222 (0.05-0.15) and smallest for miR-146, miR-208 and miR-218 (0.005-0.04).

Cell-type specificity of changes

To follow up on the tissue-changes described above, we prepared an additional series of dogs and analyzed the cell type (fibroblast versus cardiomyocyte) selectivity of changes. We divided miRNAs into fibroblast-enriched and cardiomyocyte-enriched groups based on expression-levels in cells from control dogs (right panels of Figures 4-7).

Cellular miR-21 expression changes in LA (Figure 4A) had a similar time-course to those in tissue: statistically-significant changes were seen at 1 and 2 weeks in fibroblasts and 1 week in

cardiomyocytes. MiR-21 also showed significant increases in both LV-fibroblasts and LV-cardiomyocytes (Figure 4B). At baseline, miR-21 expression in fibroblasts was about 4-fold that in cardiomyocytes (Figure 4C).

In contrast to tissue (Figure 2C), which showed a nonsignificant tendency for decreased miR-26a expression, LA-fibroblasts showed rapid and progressive decreases in miR-26a (Figure 4D), while LA-cardiomyocyte expression remained unaltered; LV expression was not significantly affected by VTP (Figure 4E). Similar to miR-26a, miR-26b decreased rapidly in LA-fibroblasts (Figure4G), without changing significantly in LA-cardiomyocytes or LV cells of either type (Figure 4H). Like miR-26a, miR-26b was expressed selectively in fibroblasts of LA but not LV (Figure 4I).

Cell-type selective analysis of miR-29b showed rapid (within 12 hours) and sustained decreases in LA-fibroblasts (Figure 4J), with nonsignificant variations in LA-cardiomyocytes and no significant alterations in LV (Figure 4K). MiR-218 showed a similar profile to miR-29b: decreased early in LA-fibroblasts (Figure 4M) but nonsigificant changes in LA-cardiomyocytes or LV (Figure 4N).

MiR-146a and miR-146b did not show sustained changes in either cell type or chamber, although miR-146a expression decreased at 24 hours in LA-fibroblasts, and miR-146b increased at 1 week in LV-fibroblasts (Figure 5A, B, D, E).MiR-146b expression increased at 1 week in both LA and LV cardiomyocytes (Figure 5D, E). MiR-214 was upregulated in LA-cardiomyocytes at 1week (Figure 5G) and in LV-fibroblasts from 1 week (Figure 5H). MiR-222 did not show any sustained alterations (Figure 5J, K).

Cardiomyocyte-enriched miRNAs

MiR-1 showed rapid, substantial and statistically-significant changes in fibroblasts from LA (Figure 6A) and LV (Figure 6B). Cardiomyocyte changes were not statistically significant, despite up to >30-fold enrichment in cardiomyocytes (Figure 6C). MiR-30a expression decreased significantly in fibroblasts and cardiomyocytes of both LA (Figure 6D) and LV (Figure 6E), with about 4-fold enrichment in cardiomyocyte expression versus fibroblasts at baseline (Figure 6F).

MiR-133a showed small changes in LA (Figure 6G), with statistically-significant decreases occurring only at the 1-week time-point in cardiomyocytes. In LV, fibroblasts showed rapid and sustained miR-133a expression decreases, with no changes in cardiomyocytes (Figure 6H), despite about 9-fold enrichment in cardiomyocytes versus fibroblasts at baseline (Figure 6I). The changes in miR-133b expression roughly paralleled those for miR-133a: no significant changes in LA (Figure 7A) and fibroblast-restricted changes in LV (Figure 7B), with about 5-fold enrichment of expression in cardiomyocytes versus fibroblasts at baseline (Figure 7C).

As for miR-133, miR-208 changes were noted predominantly in fibroblasts.Rapid reductions in expression were noted in LA miR-208a expression for both fibroblasts and cardiomyocytes (Figure 7D), but fibroblast changes were relatively much larger. No statistically significant changes occurred in LV (Figure 7E). MiR-208b decreased significantly only in fibroblasts (Figures 7G, 7H), with no significant changes in cardiomyocyte-expression.

MiRNA and ECM-related targets

In silico prediction and evaluation of ECM-related target genes

Taken together, our miRNA expression analysis indicates particularly strong changes in LA-fibroblasts, compatible with the important LA-selective fibrotic response seen in this model [4,7,12]. We therefore performed a target scan for fibrosis-related targets of the miRNAs studied.

The principal relevant targets are shown in Supplemental Table 3: 19of the 21miRNAs had one or more targets implicated in ECM remodeling. Many of the targets have been biologically validated in the literature; in addition, we evaluated selected targets for post-transcriptional regulation of ECM genes with dual luciferase reporter assay (for miR-26a, miR-133a and miR-218). MiR-218 overexpression significantly decreased the luciferase-read out for collagen-1α1 (*COL1A1*, Supplemental Figure 4A). Knockdown of miR-218 reversed the effect of miR-218 overexpression. *COL1A1* gene-expression was downregulated by miR-218 overexpression (Supplemental Figure 4B), indicating thatmiR-218 can lead to *COL1A1* mRNA-degradation.The predicted targeting of fibronectin-1 (*FN1*) and fibrillin-1 (*FBN1*) by miR-26a and miR-133a respectively was not supported by the luciferase reporter assay (Supplemental Figures 4C, 4D).

Fibroblast ECM gene expression changes

We analyzed detailed fibroblast expression-profiles for the 9 predicted ECM target-genes shown in bold in Supplemental Table 3. Figure 8 shows the profile of *COL1A1*-expression and its regulating miRNAs. For clarity, statistical significance of changes is shown only for *COL1A1*; for statistical significance of changes in fibroblast-expression for each miRNA see Figures 4-7.*COL1A1*-expression increased substantially in LA-fibroblasts, beginning at 1-week VTP(Figure 8A), consistent with the time course of fibrosis development (Figure 1E). A similar pattern was observed for miR-21, which regulates *COL1A1*indirectly by targeting Sproutyhomolog-1 (*SPRY1*).All the miRNAs directly regulating *COL1A1*decreased early, beginning at 12-hour VTP, consistent with a role in *COL1A1*-upregulation. Among the miRNAs controlling *COL1A1*, miR-29b, miR-133 and miR-218 target *COL1A1*directly; miR-26 and miR-30a regulate *COL1A1*indirectly by targeting transient receptor potential canonical channel type-3

(TRPC3) and connective tissue growth factor (CTGF) [8]. In LV-fibroblasts, a significant increase in *COL1A1*-expression was noted only at 1-week VTP, correspondingly roughly to the miR-21 expression-profile (Figure 8B).

Similar to *COL1A1*, other collagen-family members increased significantly in LA and LV fibroblasts at 1-2 week VTP (Supplemental Figure 5). Their time-course again best-paralleled the changes in miR-21, with changes in other potential regulating miRNAs beginning much earlier in LA and showing much less significant change in LV. Changes in *FN1* and *FBN1*were directionally opposite to those in their regulating miRNAs miR-29b and miR-1 (Supplemental Figure 6A-6D), consistent with miRNA-control. The expression of matrix metalloproteinase-2 (*MMP2*) did not change significantly in LA-fibroblasts (Supplemental Figure 6E), inconsistent with the observed decreases in miR-29b and increases in miR-21, both of which should have upregulated *MMP2*. In LV-fibroblasts, changes in *MMP2* (Supplemental Figure 6F) were consistent with the increases observed in miR-21. The changes in tissue inhibitor of metalloproteinase-3 (*TIMP3*) were also inconsistent with regulation by its targeting miRNAs (Supplemental Figures 6G, 6H)

Discussion

In this study, we analyzed the expression of a variety of miRNAs as a function of time, cardiac chamber and cell-type in a widely used experimental model of dilated cardiomyopathy [13]. We found a complex pattern of changes, which were more marked in LA than LV and in fibroblasts than cardiomyocytes. The time-course and cell-type selectivity of alterations argue against prior notions about the miRNAs that are involved in the cardiac remodeling response, and indicate that

some changes (notably in collagen expression) may result from multiple miRNAs acting in concert.

MiRNAs in heart failure

MiRNAs are accepted to play an important pathogenic role in CHF [1,6,14,15]. The evidence for this association includes miRNA expression-studies in clinical and experimental in vivo models, analyses of the regulatory effects of miRNA knockdown and overexpression in model cell-systems in vitro and the modulation of in vivo phenotypes in genetically-modified animals. MiRNAs that have been implicated include miR-1, miR-21, miR-23, miR-133, miR-199, miR-208 and miR-320 [15]. However, there remain important challenges in knowing the specific role of individual miRNAs in CHF pathophysiology. First, the wide variety of miRNA candidates that have been implicated in similar models begs the question of what role individual miRNAs might play. Presumably, the phenotypic response results from a pattern of miRNA changes occurring in response to the CHF-inducing stressor. The relative contribution and importance of individual components is an important issue that has yet to be addressed. A second concern is the cell-type specificity of changes. Virtually all studies that have examined altered cardiac miRNA expression in cardiac hypertrophy/failure, and made inferences regarding their potential pathophysiological participation, have analyzed miRNA expression in whole tissues without considering the cell-type specificity of expression changes. Examples of investigations examining whole tissue expression, but not specifically expression in cardiomyocytes, fibroblasts or other cell types, include studies in transverse aortic constriction rodent models [16,17],humans with pathological LV hypertrophy [17], mice and humans post-myocardial infarction (MI) [18],

transgenic mouse models of hypertrophic cardiomyopathy [19], and end-stage human dilated cardiomyopathy [20].

Whole-tissue analysis does not reveal the cell subtype(s) in which miRNA expression is altered. The potential limitations of whole-tissue quantification are illustrated by the discrepancies between our results for miRNA expression profiling at the whole-tissue (Figures 2 and 3) and isolated-cell level (Figures 4-7). At the whole-tissue level, statistically-significant changes were seen only in the LA and not in the LV; in contrast, when analyses were performed selectively on cardiomyocytes and fibroblasts, statistically-significant changes were observed in LV-cardiomyocytes for 3 miRNAs (21, 146b, and 30a) and in LV fibroblasts for 8 miRNAs (1, 21, 30a, 133a, 133b, 146b, 124 and 208b). Cell-selective profiling also revealed that fibroblasts show a much stronger miRNA response, with significant changes in 10/15 miRNAs for LA and 8/15 for LV, compared to cardiomyocytes (6/15 and 3/15 respectively). In addition, expression-changes were often quantitatively greater and more persistent over time in fibroblasts compared to cardiomyocytes. These observations suggest that miRNAs are likely to be particularly important in fibroblast-dependent responses (like tissue-fibrosis). Indeed, the fact that only 3miRNAs (miR-21, 146b, and miR-30a) were dysregulated in LV-cardiomyocytes, and these only at 1-week or 2-week VTP, suggests that none of the miRNAs we studied contribute to the LV-remodeling observed at earlier time-points in our model (Figure 1). It is possible that some aspects of cardiomyocyte remodeling previously attributed to miRNA-signaling in cardiomyocytes may actually be secondary to paracrine effects [21] due to release of miRNAs and/or other bioactive products from neighboring fibroblasts remodeled via miRNA-changes.

MiRNAs and chamber-selective fibrosis

Tissue fibrosis is an important component of the cardiac remodeling observed in CHF [22]. The VTP-induced CHF model manifests substantial tissue fibrosis, which is quantitatively greater and faster in onset in LA compared to LV [12]. Our miRNA-analyses are consistent with a role for a variety of miRNAs that have implicated in ECM regulation, including miR-21, miR-26, miR-29, miR-30 and miR-133.Thum provided the first evidence for a role of miR-21 in pathological LV fibrosis [23]. More recently, LA miR-21 upregulation was demonstrated to play an essential role in LA fibrosis and atrial fibrillation (AF) promotion due to MI-induced CHF in rats [24], and is likely the central mediator of Rac1-induced atrial fibrosis and AF [25]. MiR-26 targets the nonselective cation-channel TPRC3, which appears to be an important contributor to regulatory Ca^{2+} entry in cardiac fibroblasts [26]. Mir-26 downregulation in AF disinhibits and enhances TRPC3-channel expression in LA fibroblasts, promoting their proliferation and differentiation, leading to an AF substrate [26]. In addition, our target predictions (Supplemental Table 3) suggest that miR-26 targets ECM genes and ECM regulators like PDGF-receptor alpha and CTGF, known to be important profibrotic factors [4,7,27]. MiR-29 prominently targets collagen and is involved in post-MI fibrosis [18]. Recent work has implicated miR-29 downregulation in atrial collagen regulation associated with VTP-induced CHF [28]. CTGF-targeting by miR-30 and miR-133 also mediates potentially important profibrotic properties [8].

Figure 8 and Supplemental Figures5 and 6 illustrate the ECM-genes validated to be directly or indirectly targeted by the miRNAs we studied. We observed complex, time-dependent changes in these ECM-regulating miRNAs in fibroblasts from VTP-dogs. Rapid downregulation (within 12 hours) of miR26a/b, miR-29b and miR-30a was noted in LA fibroblasts, with delayed upregulation (at 1 week) of miR-21. Based on the magnitude and time-course of changes, miR-21 appears to be particularly important in the ECM-response, consistent with previous

studies of the effect of miR-21 knockdown on fibrotic remodeling [23-25]. Significant upregulation of collagen genes (*COL1A1, COL1A2, COL3A1, COL5A1*) and *FBN1* was not observed until 1-week VTP (Figure 8 and Supplemental Figure 5 and 6), corresponding to the time of miR-21 upregulation. Nevertheless, other miRNAs changed significantly prior to increases in the expression of collagen genes and could also have contributed. *FN1*, a validated target of miR-1 [29], was significantly upregulated in both LA and LV (Supplemental Figures 6C and 6D). Within 12 hours of VTP-onset, decreased expression was seen for miR-1 (in both LA and LV), potentially leading to the changes in *FBN1*. For *FBN1, MMP2* and *TIMP3*, the alterations in gene expression were generally not compatible with direct regulation by the miRNAs studied (Supplemental Figure 6).

The greater miRNA change in atria versus ventricles and fibroblasts versus cardiomyocytes is an interesting and novel observation of unknown mechanism. Previous studies have documented greater changes in terms of gene-expression, tissue-fibrosis, inflammation, neurohormones, mitogen-activated protein kinases and cell-death in LA versus LV [4,12]. Atrial fibroblasts are known to be more responsive than ventricular to a broad range of stimuli [7]. The atrial-selective miRNA response may simply be part of the generally more intense response of the atria in CHF. The fibroblast versus cardiomyocyte differences remain unexplained, but may relate to the important mechanosensitivity of fibroblasts [30] in response to the stretch imposed by CHF, particularly in this model of dilated cardiomyopathy with a high prevalence of mitral regurgitation [2]. Transforming growth-factor β is differentially activated in LA versus LV in CHF [12], and is known to regulate miRNAs like miR-21 and miR-29 [31,32], potentially contributing to the differential responses we observed.

Novelty and potential significance

To the best of our knowledge this is the first study to systematically evaluate time-dependent miRNA remodeling in experimental CHF, while comparing miRNA profiling in LA vs. LV as well as in fibroblasts vs. cardiomyocytes. Our results highlight the fact that miRs are distinctly regulated in different cardiac cell-types and that expression data needed to assess hypotheses about the role of miRNAs must be obtained in purified cell preparations of the relevant type. Surprisingly, the expression of some cardiomyocyte-selective miRNAs generally assumed to be central in adverse ventricular remodeling, like miR-1, miR-133 and miR-208, was not altered in LV-cardiomyocytes, raising questions about their putative roles. Our results argue strongly that if a miRNA is hypothesized to be directly involved in a cardiomyocyte response (e.g. hypertrophy, cell death) the relevant expression-changes must be assessed in cardiomyocytes; if in a fibroblast response (e.g. ECM-regulation, fibrosis) expression must be verified in fibroblasts, because changes in overall tissue-expression do not necessarily reflect alterations in specific cell-types. Baseline differences in cell-type specific expression is not a reliable indicator of cell-type specificity of tissue expression changes: the fibroblast-enriched miRNA miR-21 was significantly dysregulated by VTP in both LA and LV cardiomyocytes; whereas expression of the cardiomyocyte-enriched miRNAs miR-1, miR-133a, miR-133b and miR-208b changed in fibroblasts and not cardiomyocytes.

AF is a clinically important arrhythmia, often associated with CHF, in which atrial fibrosis plays an important pathophysiological role [2,7,33]. Although there is evidence for the involvement of a number of miRNAs in AF-associated atrial fibrosis [24-26,28], here we characterize for the first time the detailed time-course of changes in multiple ECM-regulating miRNAs in atrial fibroblasts from a model that produces clinically-relevant AF-promoting

fibrosis. The results suggest that miR-21 is likely the most important contributor to profibrotic collagen-production, but that a number of other miRNAs may well play an ancillary role. For other ECM-genes, the pattern was largely incompatible with miRNA-regulation and other factors must be involved.

Potential limitations

We used a specific canine model of CHF, which produces a well-characterized cardiomyopathy [8]. Our results cannot be directly extrapolated to other forms of cardiomyopathy or causes of CHF, nor to other species, including man. Further work characterizing cell-specific expression changes in miRNAs in other models and species would be of interest. In addition, we did not continue VTP beyond 2 weeks to drive the dogs to severe/terminal CHF, because of the high associated mortality-rate. Nevertheless, our dogs manifested substantial reductions in LV ejection-fraction, increases in LV and LA dimensions, and LA fibrosis. Cell-culture is often used to multiply and purify fibroblasts prior to analysis; however, it can substantially alter fibroblast phenotype and gene-expression [10]. For this reason, we used a well-characterized acutely-isolated fibroblast preparation [10]; however, this limited the amount of miRNA and mRNA available for study and the number of analyses that were possible. We performed preliminary miRNA microarray analysis (Supplemental Figure 2) in RA tissue (rather than LA) to select miRNAs for further study, and then did further detailed analyses in LA, in order to make optimal use of the limited atrial tissue samples available from each dog. The impression obtained from the microarray experiment comparing RA to LV, that miRNA expression changes in atrium are greater than those in ventricle, was confirmed by the subsequent detailed qPCR studies on LA

and LV tissue (Figures 2 and 3). It would be of interest in future work to compare the time-dependent miRNA changes in cardiomyocytes and fibroblasts isolated from LA versus RA.

We have focused primarily on miRNA regulation of ECM proteins, because of their importance in AF and the predominance of changes in ECM-secreting fibroblasts. However, miRNA-changes could also contribute to arrhythmogenesis by regulating targets like ion-channels and Ca^{2+}-handling in cardiomyocytes [34, 35]. This is an area that merits exploration in future research.

Acknowledgments

The authors wish to thank Nathalie L'Heureux and Chantal St-Cyr for expert technical assistance.

Funding

Supported by the Canadian Institutes of Health Research (MGP6957), the Quebec Heart and Stroke Foundation, and the Foundation Leducq (European-North American Atrial Fibrillation Research Alliance, ENAFRA).

Disclosures

Dr Nattel is listed as inventor on a patent pending belonging to the Montreal Heart Institute/Université de Montréal, entitled "MiR21 as a target in prevention of atrial fibrillation".

References

[1] Oliveira-Carvalho V, Silva MM, Guimarães GV, Bacal F, Bocchi EA. MicroRNAs: new players in heart failure. Mol Biol Rep 2013;40:2663-70.

[2] Li D, Fareh S, Leung TK, Nattel S. Promotion of atrial fibrillation by heart failure in dogs: atrial remodeling of a different sort.Circulation 1999;100:87-95.

[3] Barth AS, Merk S, Arnoldi E, Zwermann L, Kloos P, Gebauer M, et al. Reprogramming of the human atrial transcriptome in permanent atrial fibrillation: expression of a ventricular-like genomic signature. Circ Res 2005;96:1022-9.

[4] Cardin S, Pelletier P, Libby E, Le Bouter S, Xiao L, Kaab S, et al. Marked differences between atrial and ventricular gene-expression remodeling in dogs with experimental heart failure. J Mol Cell Cardiol 2008;45:821-31.

[5] Cardin S, Libby E, Pelletier P, Le Bouter S, Shiroshita-Takeshita A, Le Meur N, et al. Contrasting gene expression profiles in two canine models of atrial fibrillation. Circ Res 2007;100:425-33.

[6] Divakaran V, Mann DL. The emerging role of microRNAs in cardiacremodeling and heartfailure. Circ Res 2008;103:1072-83.

[7] Burstein B, Libby E, Calderone A, Nattel S. Differential behaviors of atrial versus ventricular fibroblasts: a potential role for platelet-derived growth factor in atrial-ventricular remodeling differences. Circulation2008;117:1630-41.

[8] Tijsen AJ, Pinto YM, Creemers EE. Non-cardiomyocyte microRNAs in heart failure. Cardiovasc Res 2012;93:573-82.

[9] Qi XY, Yeh YH, Xiao L, Burstein B, Maguy A, Chartier D, et al. Cellular signaling underlying atrial tachycardia remodeling of L-type calcium current. Circ Res 2008;103:845-54.

[10] Dawson K, Wu CT, Qi XY, Nattel S. Congestive heart failure effects on atrial fibroblast phenotype: differences between freshly-isolated and cultured cells. PLoS One 2012;7:e52032.

[11] Cardin S, Li D, Thorin-Trescases N, Leung TK, Thorin E, Nattel S. Evolution of the atrial fibrillation substrate in experimental congestive heart failure: angiotensin-dependent and -independent pathways. Cardiovasc Res 2003;60:315-25.

[12] Hanna N, Cardin S, Leung TK, Nattel S. Differences in atrial versus ventricular remodeling in dogs with ventricular tachypacing-induced congestive heart failure. Cardiovasc Res 2004;63:236-44.

[13] Shinbane JS, Wood MA, Jensen DN, Ellenbogen KA, Fitzpatrick AP, Scheinman MM. Tachycardia-induced cardiomyopathy: areviewof animal models and clinical studies. J Am Coll Cardiol 1997;29:709-15.

[14] Dorn GW 2nd. MicroRNAsin cardiac disease. Transl Res 2011;157:226-35.

[15] Topkara VK, MannDL. Role of microRNAsin cardiac remodeling andheart failure. Cardiovasc Drugs Ther 2011;25:171-82.

[16] Duisters RF, Tijsen AJ, Schroen B, Leenders JJ, Lentink V, van der Made I, et al. miR-133 and miR-30 regulate connective tissue growth factor: implications for a role of microRNAs in myocardial matrix remodeling. Circ Res 2009;104:170-8.

[17] Zhang ZH, Li J, Liu BR, Luo CF, Dong Q, Zhao LN, et al. MicroRNA-26 was decreased in rat cardiac hypertrophy model and may be a promising therapeutic target. J Cardiovasc Pharmacol 2013;62:312-9.

[18] van Rooij E, Sutherland LB, Thatcher JE, DiMaio JM, Naseem RH, Marshall WS, et al. Dysregulation of microRNAs after myocardial infarction reveals a role of miR-29 in cardiac fibrosis. Proc Natl Acad Sci USA2008;105:13027-32.

[19] BagnallRD, Tsoutsman T, Shephard RE, Ritchie W, Semsarian C.GlobalmicroRNAprofiling of the mouse ventricles during development of severe hypertrophic cardiomyopathy and heart failure. PLoS One 2012;7:e44744.

[20] Thum T, Galuppo P, Wolf C, Fiedler J, Kneitz S, van Laake LW, et al. MicroRNAsin the humanheart: a clue to fetal gene reprogramming in heart failure. Circulation 2007;116:258-67.

[21] Pedrotty DM, Klinger RY, Kirkton RD, Bursac N. Cardiacfibroblastparacrinefactors alter impulse conduction and ion channel expression of neonatal rat cardiomyocytes. Cardiovasc Res 2009;83:688-97.

[22] Spinale FG, Janicki JS, Zile MR. Membrane-associated matrix proteolysis andheart failure. Circ Res 2013;112:195-208.

[23] Thum T, Gross C, Fiedler J, Fischer T, Kissler S, Bussen M, et al. MicroRNA-21 contributes to myocardial disease by stimulating MAP kinase signalling in fibroblasts. Nature 2008;456:980-4.

[24] Cardin S, Guasch E, Luo X, Naud P, Le Quang K, Shi Y, et al. Role for MicroRNA-21 in atrial profibrillatory fibrotic remodeling associated with experimental postinfarction heart failure. Circ Arrhythm Electrophysiol2012;5:1027-35.

[25] Adam O, Löhfelm B, Thum T, Gupta SK, Puhl SL, Schäfers HJ, et al. Role of miR-21in the pathogenesis ofatrialfibrosis. Basic Res Cardiol 2012;107:278.

[26] Harada M, Luo X, Qi XY, Tadevosyan A, Maguy A, Ordog B, et al. Transient receptor potential canonical-3 channel-dependent fibroblast regulation in atrial fibrillation. Circulation 2012;126:2051-64.

[27] Adam O, Lavall D, Theobald K, Hohl M, Grube M, Ameling S, et al. Rac1-induced connective tissue growth factor regulates connexin 43 and N-cadherin expression in atrialfibrillation. J Am Coll Cardiol 2010;55:469-80.

[28] Dawson K, Wakili R, Ordög B, Clauss S, Chen Y, Iwasaki Y, et al. MicroRNA29: a mechanistic contributor and potential biomarker in atrial fibrillation. Circulation 2013;127:1466-75.

[29] Sayed D, Hong C, Chen IY, Lypowy J, Abdellatif M. MicroRNAs play an essential role in the development of cardiac hypertrophy.Circ Res 2007;100:416-24.

[30] Yue L, Xie J, Nattel S. Molecular determinants of cardiac fibroblast electrical function and therapeutic implications for atrial fibrillation. Cardiovasc Res. 2011;89:744-53.

[31] Davis BN, Hilyard AC, Lagna G, Hata A. SMAD proteins control DROSHA-mediated microRNA maturation. Nature. 2008;454:56-61.

[32] Qin W, Chung AC, Huang XR, Meng XM, Hui DS, Yu CM, Sung JJ, Lan HY. TGF-β/Smad3 signaling promotes renal fibrosis by inhibiting miR-29. J Am SocNephrol. 2011;22(8):1462-74.

[33] Burstein B, Nattel S. Atrial fibrosis: mechanisms and clinical relevance in atrial fibrillation. J Am CollCardiol 2008;51:802-9.

[34] Kim GH.MicroRNA regulation of cardiac conduction and arrhythmias.Transl Res. 2013

May;161(5):381-92.

[35] Harada M, Luo X, Murohara T, Yang B, Dobrev D, Nattel S.MicroRNA regulation and cardiac calcium signaling: role in cardiac disease and therapeutic potential.Circ Res. 2014;114(4):689-705.

Figure Legends

Figure 1. Structural and functional remodeling during development of CHF. (A) Left ventricular (LV) ejection fraction (LVEF) decreases within 24 hours of VTP-onset. (B) LV end-diastolic volume (LVEDV) increases progressively. (C) Left atrial (LA) diameters are increased beginning 1 week post VTP-onset. (D) Mean AF-duration increased substantially at 1-week and 2-week VTP. (E) LA fibrosis appears at 1-week VTP. (F) mRNA expression of alpha-smooth muscle actin (α-SMA) in atrial and ventricular fibroblasts (FBs). Values are mean±SEM, n=5/group (A-C), n=5-12/group (D& F), *p<0.05, **p<0.01, ***p<0.005, vs. baseline (for repeated measures) or control-dogs (CTL) for non-paced controls.

Figure 2. Tissue expression of miR-1, miR-21, miR-26 family, miR-29b, miR-30a and miR-133 family during VTP time-course. Values are mean±SEM, n=5-8/group. *p<0.05, **p<0.01, ***p<0.005, vs. corresponding CTL-samples. CTL, non-paced controls; LA, left atrium; LV, left ventricle.

Figure 3. Tissue expression of miR-146 family, miR-208 family, miR-214, miR-218 and miR-222 during VTP time-course. Values are mean±SEM, n=5-8/group. **p<0.01, ***p<0.005, vs. corresponding CTL-samples. CTL, non-paced controls; LA, left atrium; LV, left ventricle.

Figure 4. Cell-type selective expression-profile of fibroblast-enriched miRNAs during VTP time-course. Left atrial (LA) results are at left, left ventricular (LV) in middle and baseline fibroblast/cardiomyocyte expression-values are at right. Top: miR-21; 2nd row: miR-26a; 3rd row: miR-26b; 4th row: miR-29b; Bottom: miR-218. Values are mean±SEM, n=5-12/group. *p<0.05,

**p<0.01, ***p<0.005, vs. corresponding CTL-samples (left and middle panels) or between two cell-types (right panels).FB, fibroblasts; CM, cardiomyocytes; CTL, non-paced controls.

Figure 5. Cell-type selective expression-profile of fibroblast-enriched miRNAs during VTP time-course. Left atrial (LA) results are at left, left ventricular (LV) in middle and baseline fibroblast/cardiomyocyte expression-values are at right. Top: miR-146a; 2nd row: miR-146b; 3rd row: miR-214; Bottom: miR-222. Values are mean±SEM, n=5-12/group. *p<0.05, **p<0.01, ***p<0.005, vs. corresponding CTL-samples (left and middle panels) or between two cell types (right panels).FB, fibroblasts; CM, cardiomyocytes; CTL, non-paced controls.

Figure 6. Cell-type selective expression-profile of cardiomyocyte-enriched miRNAs during VTP time-course. Left-atrial (LA) results are at left, left-ventricular (LV) in middle and baseline fibroblast/cardiomyocyte expression-values are at right. Top: miR-1; Middle: miR-30a; Bottom: miR-133a. Values are mean±SEM, n=5-12/group. *p<0.05, **p<0.01, ***p<0.005, vs. corresponding CTL-samples (left and middle panels) or between two cell-types (right panels).FB, fibroblasts; CM, cardiomyocytes; CTL, non-paced controls.

Figure 7. Cell-type selective expression-profile of cardiomyocyte-enriched miRNAs during VTP time-course. Left atrial (LA) results are at left, left ventricular (LV) in middle and baseline fibroblast/cardiomyocyte expression-values are at right. Top: miR-133b; Middle: miR-208a; Bottom: miR-208b. Values are mean±SEM, n=5-12/group. *p<0.05, **p<0.01, ***p<0.005, vs. corresponding CTL samples (left and middle panels) or between two cell-types (right panels).FB, fibroblasts; CM, cardiomyocytes; CTL, non-paced controls.

Figure 8. Expression of *COL1A1*mRNA and regulating miRNAs in freshly-isolated fibroblasts (FBs) from left atrium (**A**) and left ventricle (**B**) during VTP time-course. The scale for *COL1A1*-expression (solid orange line) is shown at the left; that for miRNA-expression is on the right. MiRNAs shown with solid lines regulate *COL1A1*directly; dashed lines indicate indirect regulation. Values are mean±SEM, n=5-12/group. ***p<0.005, vs. corresponding CTL-samples.*COL1A1*,collagen-1α1; LA, left atrium; LV, left ventricle; FB, fibroblasts; CTL, non-paced controls.

Figure 1

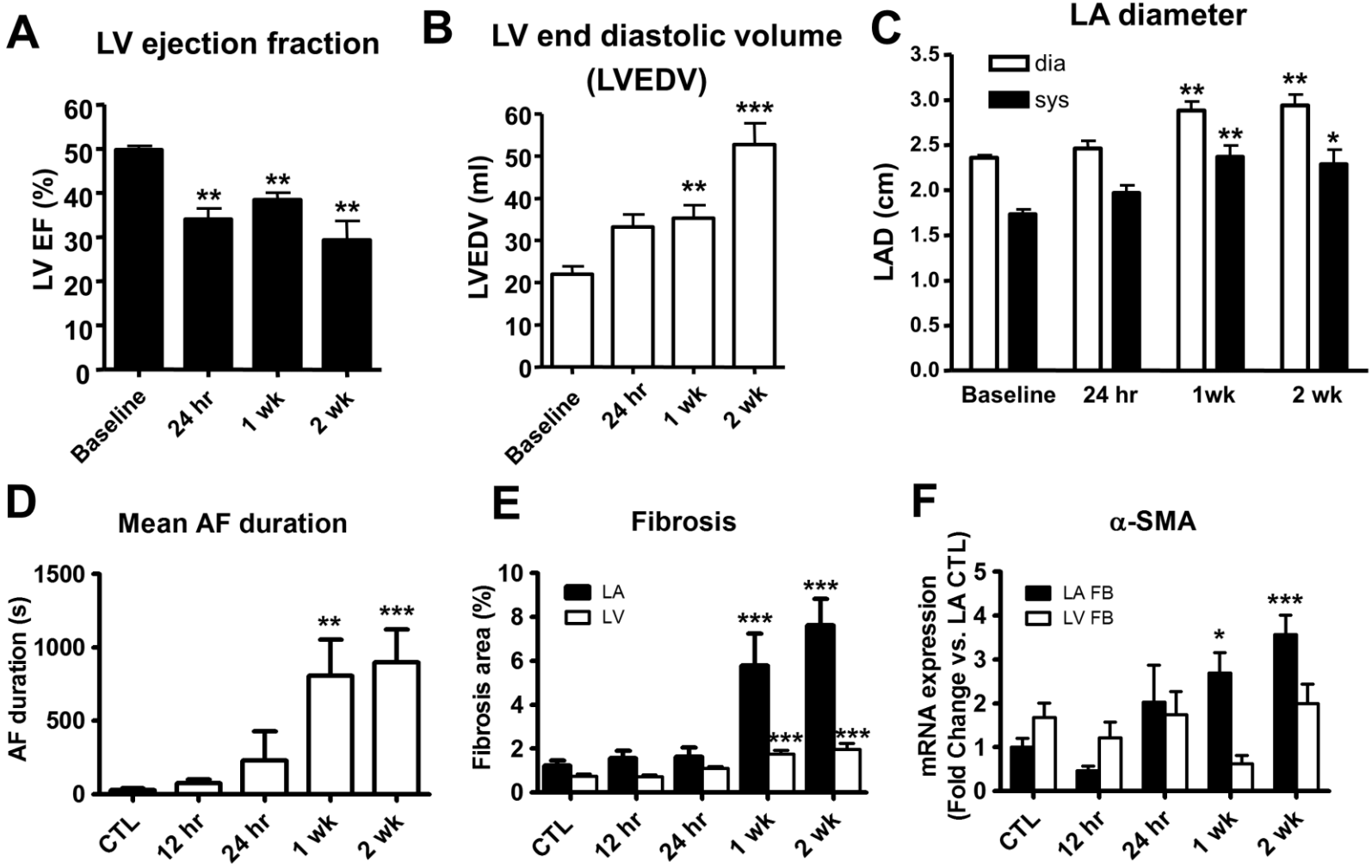
A
LV ejection fraction
LV EF (%)
60
50
40
30
20
10
0
**
**
**
Baseline
24 hr
1 wk
2 wk
B
LV end diastolic volume
(LVEDV)
LVEDV (ml)
60
50
40
30
20
10
0
**
***
Baseline
24 hr
1 wk
2 wk
C
LA diameter
dia
sys
LAD (cm)
3.5
3.0
2.5
2.0
1.5
1.0
0.5
0.0
**
**
**
*
Baseline
24 hr
1wk
2 wk
D
Mean AF duration
AF duration (s)
1500
1000
500
0
**
***
CTL
12 hr
24 hr
1 wk
2 wk
E
Fibrosis
LA
LV
Fibrosis area (%)
10
8
6
4
2
0
***
***
***
***
CTL
12 hr
24 hr
1 wk
2 wk
F
α-SMA
LA FB
LV FB
mRNA expression
(Fold Change vs. LA CTL)
5
4
3
2
1
0
*
***
CTL
12 hr
24 hr
1 wk
2 wk

Figure 2

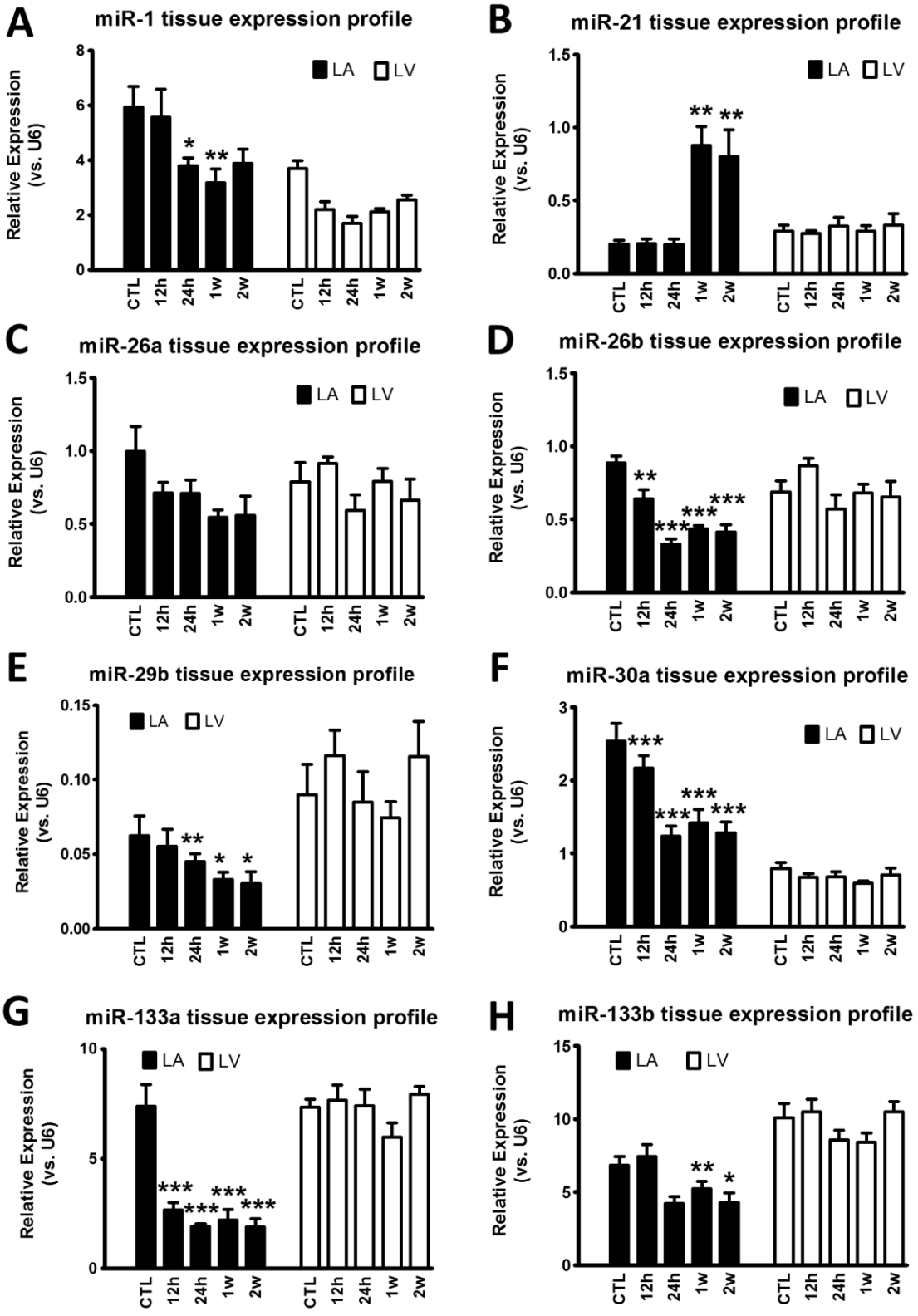
A
miR-1 tissue expression profile
B
miR-21 tissue expression profile
C
miR-26a tissue expression profile
D
miR-26b tissue expression profile
E
miR-29b tissue expression profile
F
miR-30a tissue expression profile
G
miR-133a tissue expression profile
H
miR-133b tissue expression profile
Relative Expression (vs. U6)
LA
LV
CTL
12h
24h
1w
2w

Figure 3

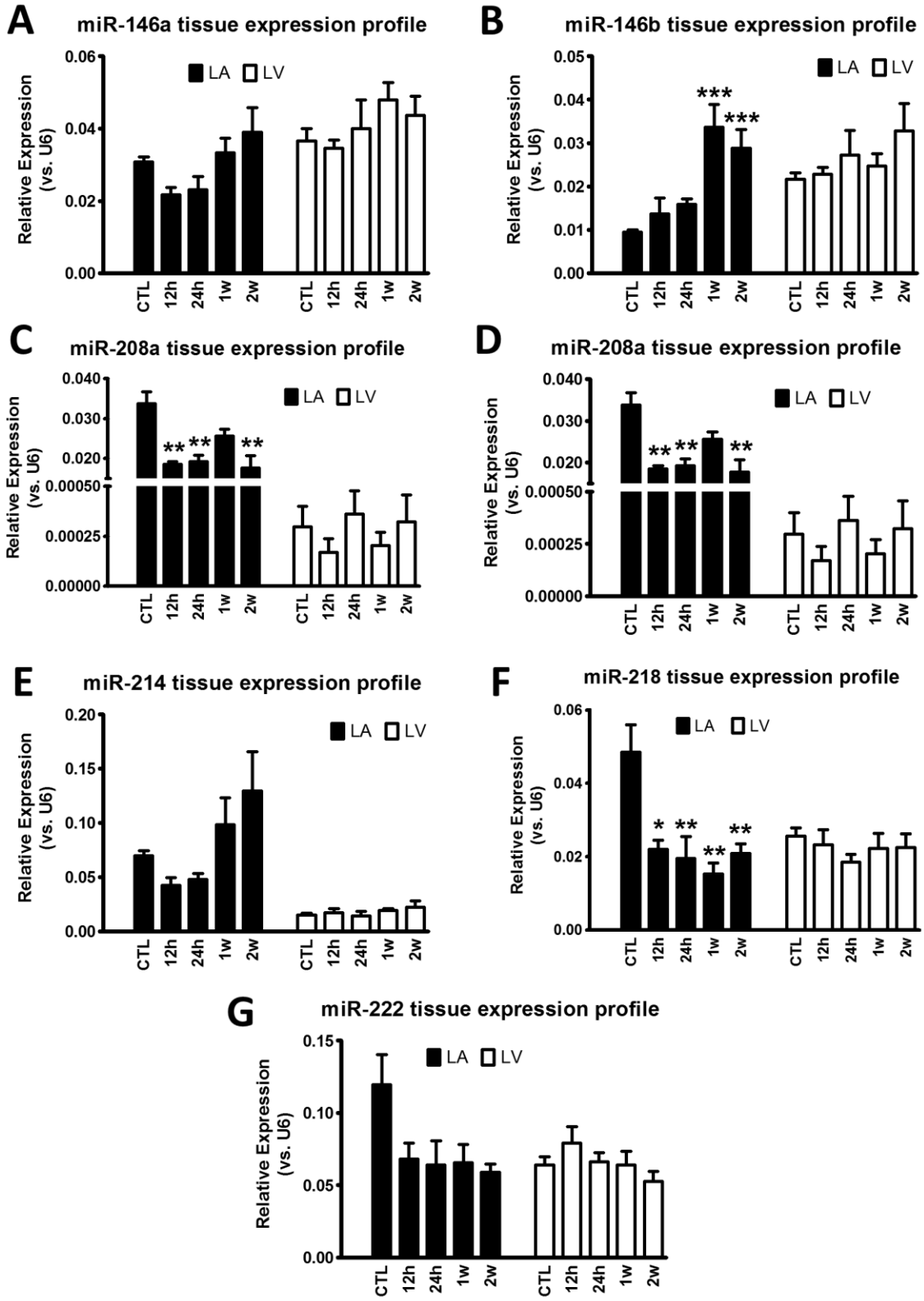
A
miR-146a tissue expression profile
B
miR-146b tissue expression profile
C
miR-208a tissue expression profile
D
miR-208a tissue expression profile
E
miR-214 tissue expression profile
F
miR-218 tissue expression profile
G
miR-222 tissue expression profile
Relative Expression (vs. U6)
LA
LV
CTL
12h
24h
1w
2w

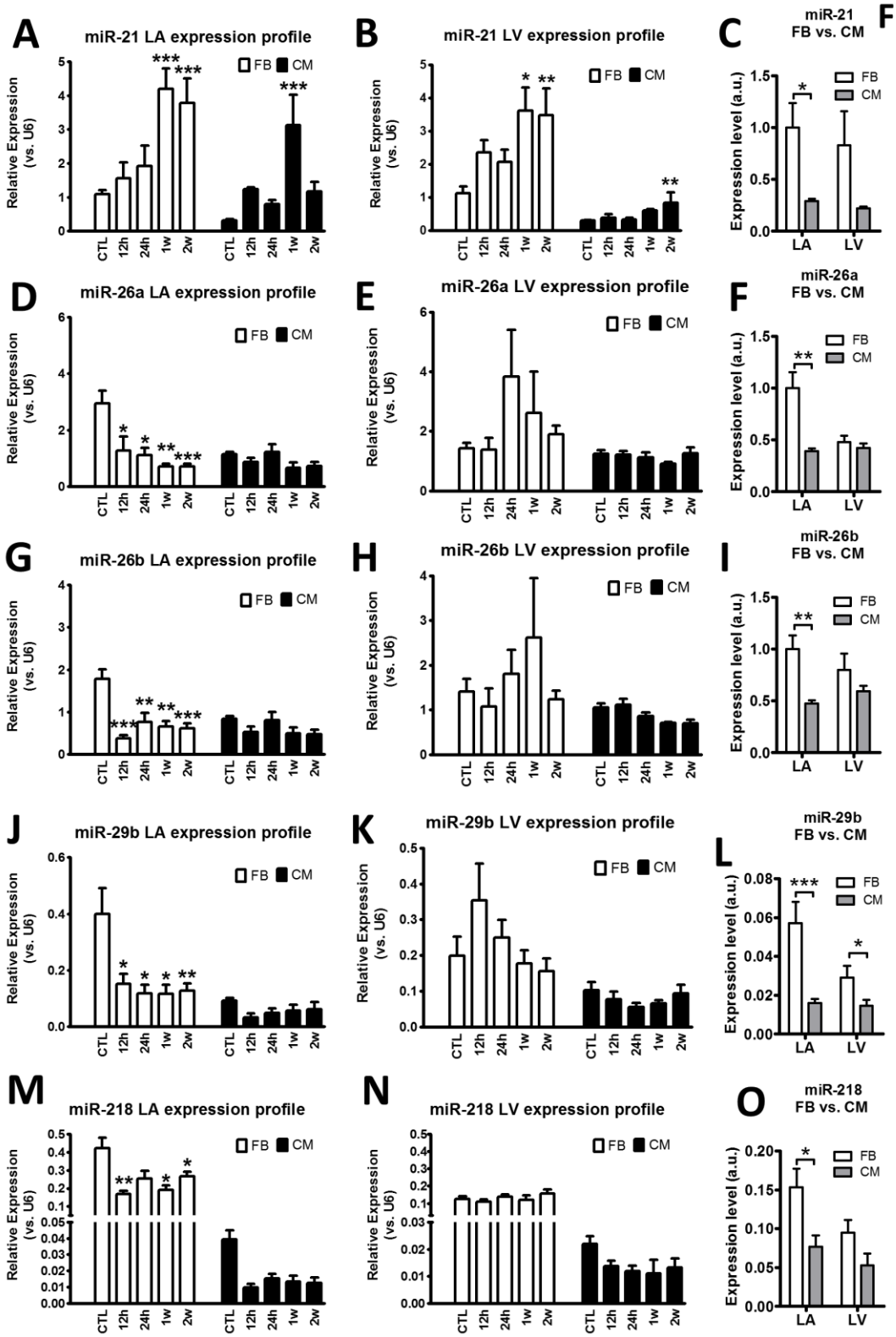
A
miR-21 LA expression profile
B
miR-21 LV expression profile
C
miR-21
FB vs. CM
D
miR-26a LA expression profile
E
miR-26a LV expression profile
F
miR-26a
FB vs. CM
G
miR-26b LA expression profile
H
miR-26b LV expression profile
I
miR-26b
FB vs. CM
J
miR-29b LA expression profile
K
miR-29b LV expression profile
L
miR-29b
FB vs. CM
M
miR-218 LA expression profile
N
miR-218 LV expression profile
O
miR-218
FB vs. CM
Relative Expression (vs. U6)
Expression level (a.u.)
FB
CM
CTL
12h
24h
1w
2w
LA
LV

Figure 4

Figure 5

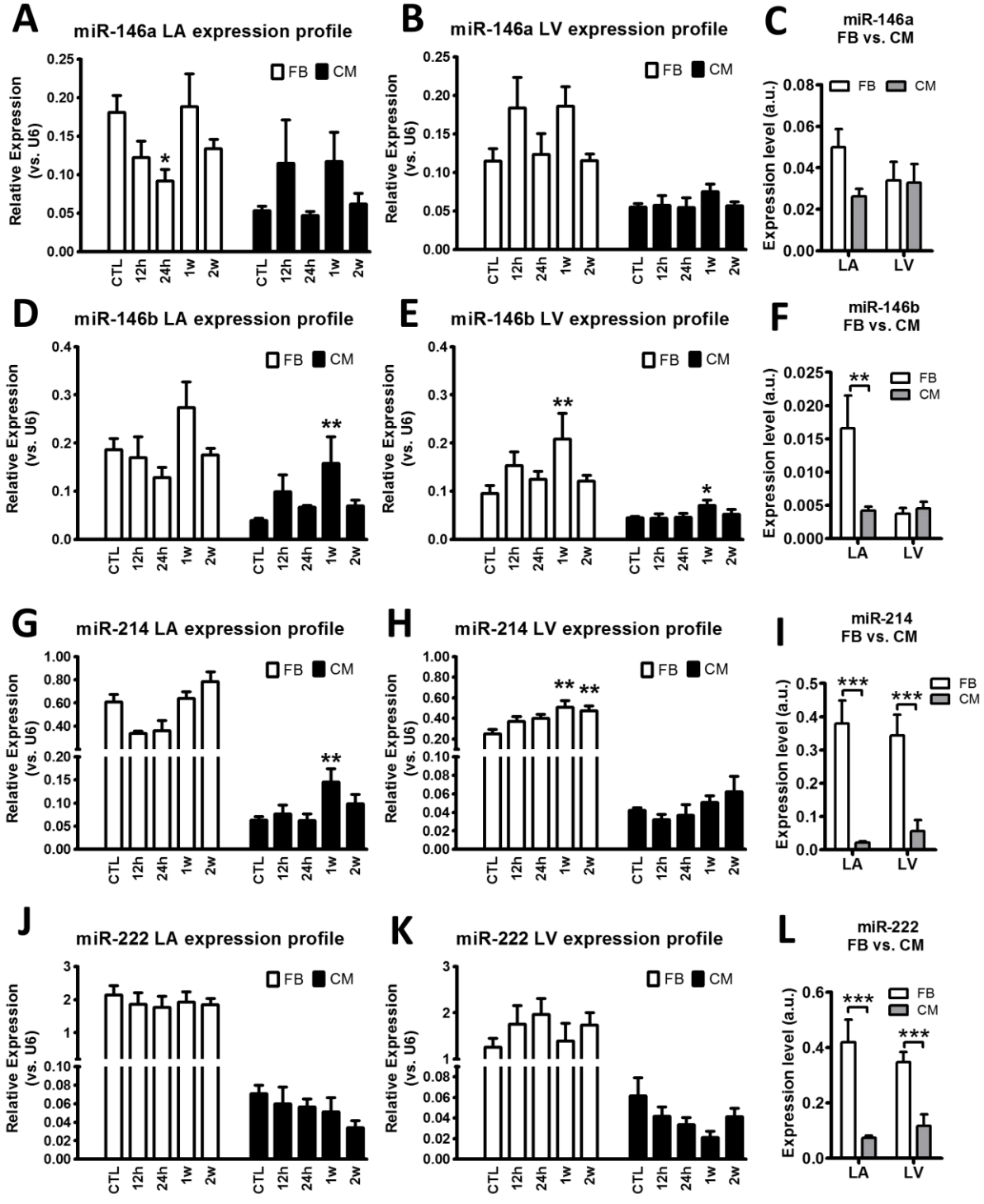
A
miR-146a LA expression profile
B
miR-146a LV expression profile
C
miR-146a
FB vs. CM
D
miR-146b LA expression profile
E
miR-146b LV expression profile
F
miR-146b
FB vs. CM
G
miR-214 LA expression profile
H
miR-214 LV expression profile
I
miR-214
FB vs. CM
J
miR-222 LA expression profile
K
miR-222 LV expression profile
L
miR-222
FB vs. CM
Relative Expression (vs. U6)
Expression level (a.u.)
FB
CM
CTL
12h
24h
1w
2w
LA
LV

Figure 6

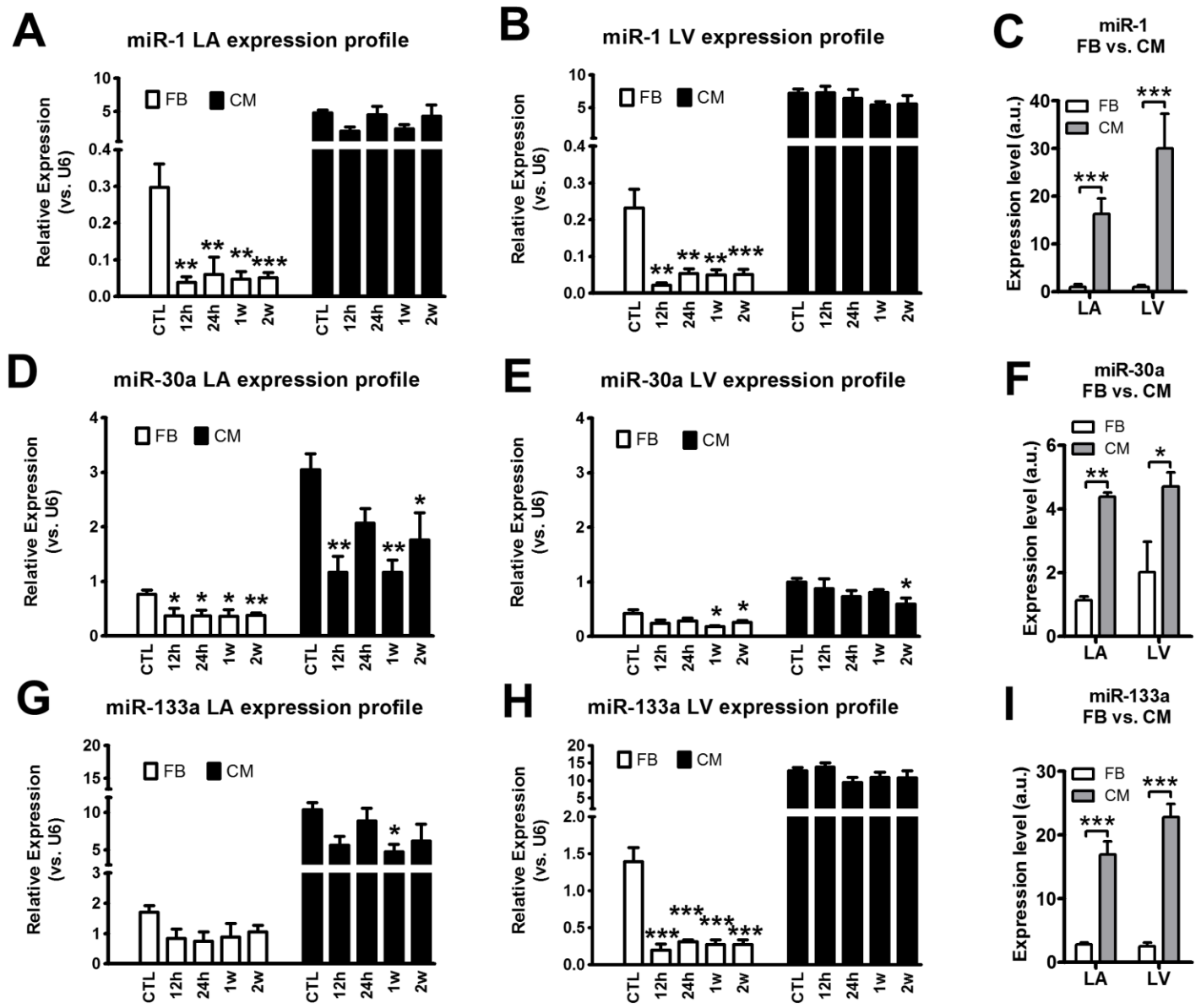
A
miR-1 LA expression profile
B
miR-1 LV expression profile
C
miR-1
FB vs. CM
D
miR-30a LA expression profile
E
miR-30a LV expression profile
F
miR-30a
FB vs. CM
G
miR-133a LA expression profile
H
miR-133a LV expression profile
I
miR-133a
FB vs. CM
Relative Expression (vs. U6)
Expression level (a.u.)
FB
CM
CTL
12h
24h
1w
2w
LA
LV

Figure 7

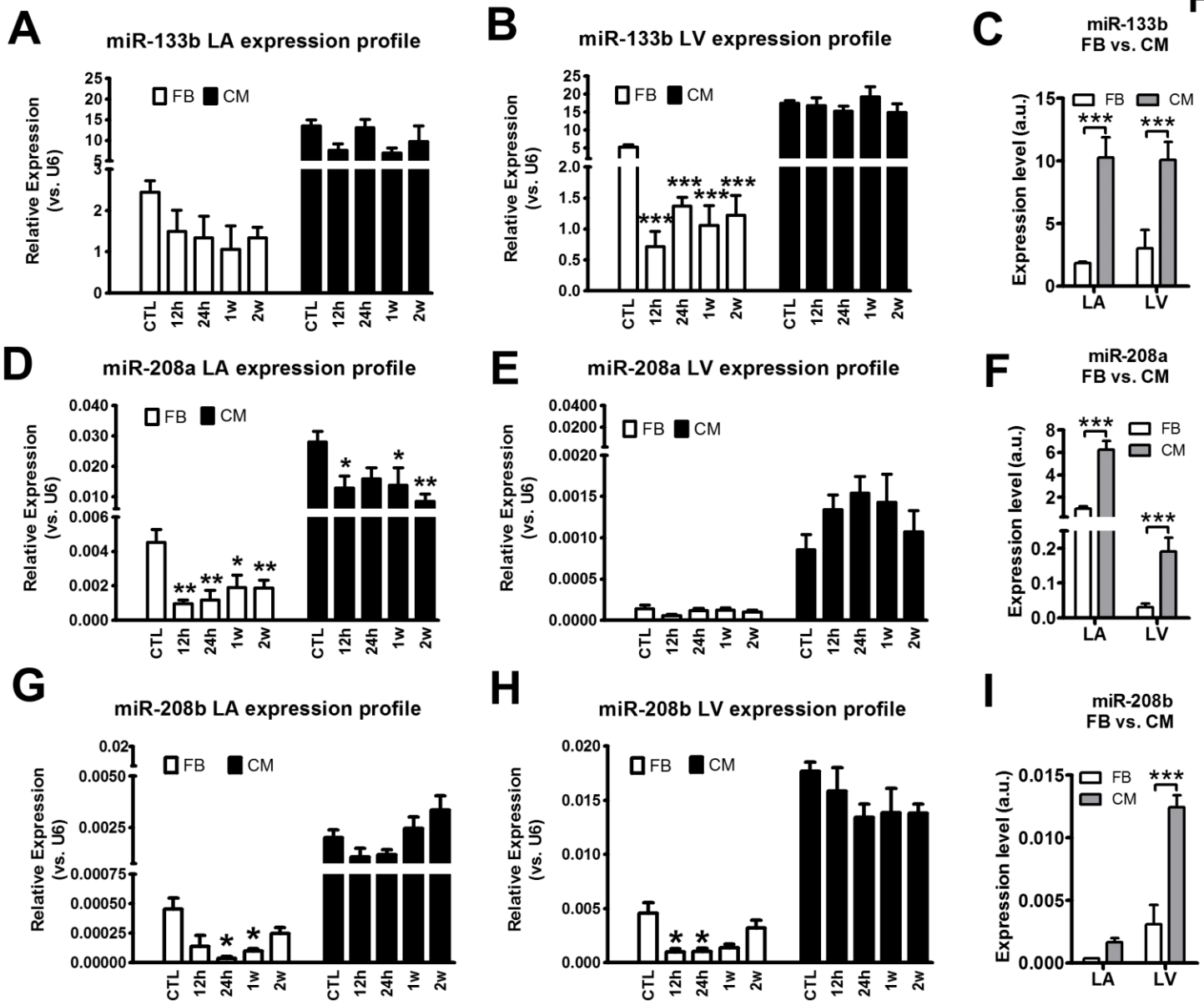
A
miR-133b LA expression profile
Relative Expression (vs. U6)
FB
CM
CTL
12h
24h
1w
2w
B
miR-133b LV expression profile
C
miR-133b FB vs. CM
Expression level (a.u.)
LA
LV
D
miR-208a LA expression profile
E
miR-208a LV expression profile
F
miR-208a FB vs. CM
G
miR-208b LA expression profile
H
miR-208b LV expression profile
I
miR-208b FB vs. CM

Figure 8

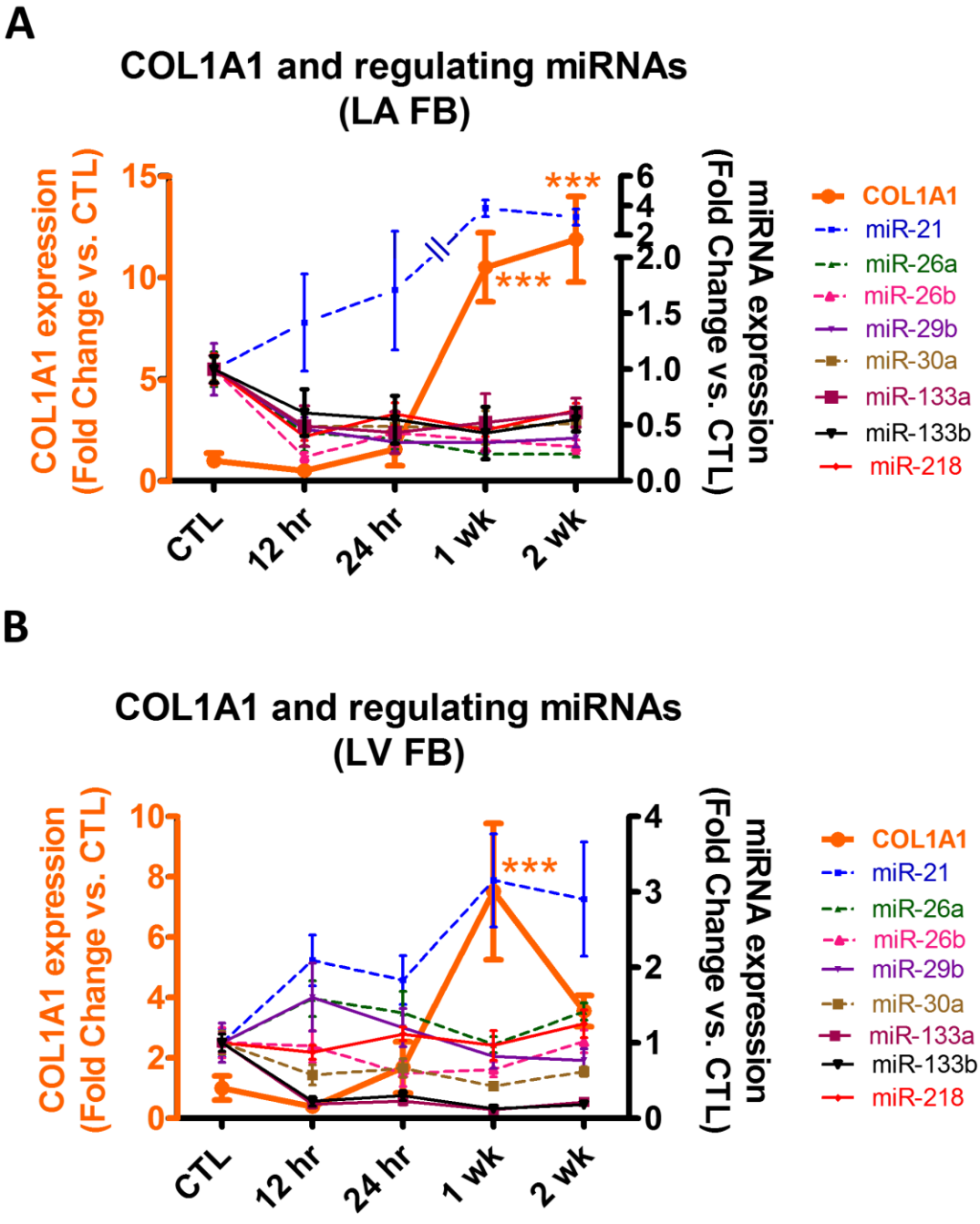
A
COL1A1 and regulating miRNAs
(LA FB)
COL1A1 expression
(Fold Change vs. CTL)
miRNA expression
(Fold Change vs. CTL)
15
10
5
0
6
4
2
2.0
1.5
1.0
0.5
0.0
***
***
CTL
12 hr
24 hr
1 wk
2 wk
COL1A1
miR-21
miR-26a
miR-26b
miR-29b
miR-30a
miR-133a
miR-133b
miR-218
B
COL1A1 and regulating miRNAs
(LV FB)
COL1A1 expression
(Fold Change vs. CTL)
miRNA expression
(Fold Change vs. CTL)
10
8
6
4
2
0
4
3
2
1
0
***
CTL
12 hr
24 hr
1 wk
2 wk
COL1A1
miR-21
miR-26a
miR-26b
miR-29b
miR-30a
miR-133a
miR-133b
miR-218

Supplemental materials

Supplemental Methods

RNA quality control and MicroRNA array profiling

RA and LV tissue-samples were used for microRNA-array profiling. Each chamber included pooled samples from each dog in a set: one set for the control group and one each for the four VTP-time groups. After RNA-extraction, RNA quality was verified via Agilent 2100 Bioanalyzer (Agilent Technologies, Santa Clara, CA) profile. RNAs with an RNA integrity number (RIN) ≥7 were used for miRNA-array analysis. One μg of total RNA from pooled sample and reference was labeled with Hy3™ and Hy5™ fluorescent-label, respectively, using the miRCURY™ LNA Array power labeling kit (Exiqon, Vedbaek, Denmark). The Hy3™-labeled and Hy5™-labeled samples were mixed pair-wise and hybridized to the miRCURY™ LNA array version 11.0 (Exiqon), which contains capture probes targeting all miRNAs for all other species than human, mouse or rat registered in miRBASE version 14.0 (Sanger Institute). Hybridization was performed according to the miRCURY™ LNA array manual with an HS4800 hybridization station (Tecan, Grödig, Austria). After hybridization, the microarray slides were scanned and stored in an ozone free environment (ozone-level below 2.0 ppb) to prevent fluorescent-dye bleaching. Microarray slides were scanned with the Agilent G2565BA Microarray Scanner System (Santa Clara, CA) and image analysis was performed with ImaGene 8.0 software (El Seguno, CA). The quantified signals were background-corrected (Normexp with offset value 10) and normalized with the global Lowess (Locally Weighted Scatterplot Smoothing) regression algorithm.

Cell culture

The HEK293 cell line was purchased from ATCC and cultured in DMEM containing 10% FBS and 1% penicillin/streptomycin. Fibroblasts were freshly isolated from left atria of control dogs and cultured in DMEM containing 5% FBS and 1% penicillin/streptomycin.

Synthesis of miRNAs and anti-miRNA antisense inhibitors

MiR-26a, miR133a and miR-218 were synthesized by Invitrogen, and their respective antisense oligonucleotides, AMO-26a, AMO-133a and AMO-218 were synthesized by Exiqon. Five nucleotides or deoxynucleotides at both ends of the antisense molecules were locked (LNA; the ribose ring is constrained by a methylene bridge between the 2′-O- and the 4′-C atoms). Additionally, a scrambled RNA or AMO was used as a negative control.

Construction of luciferase-miRNA-target site fusion plasmids and luciferase activity assay

To construct reporter vectors bearing miRNA-target sites, we synthesized fragments containing the exact target sites for each miRNA in the 3′-untranslated region (3′-UTR) of their respective target genes (Supplemental Figure 3) synthesized by Invitrogen. These inserts were ligated into SacI and XhoI in pmirGLO Dual-Luciferase miRNA Target Expression Vector(Promega, Madison, WI).For luciferase assay involving miRNA function, HEK293 cells were transfected with the pmirGLO Dual-Luciferase miRNA Target Expression Vector carrying the 3′ UTR of target genes, according to the manufacturer's instructions.

Transfection procedures.

HEK cells were transfected with 10-nMmiRNA and/or 5-nM AMOs, or negative control constructs with Lipofectamine 3000 (Invitrogen), according to the manufacturer's instructions. Cells were used for luciferase assay 24 hours after the transfection. Atrial fibroblasts were

transfected with 100 nM miRNA and/or 50 nM AMOs, or negative control constructs. Fibroblast RNA was collected 24 hours after transfection for further analysis.

Supplemental tables

Supplemental Table1. 260 probes for miRNAs tested in miRCURY™ LNA Array for microRNA profiling (ordered by the numbers of miRNAs)

Probe ID	Anotation	Probe ID	Anotation	Probe ID	Anotation
17748	cfa-let-7a	10946	cfa-miR-141	27536	cfa-miR-190a
17749	cfa-let-7b	49656	cfa-miR-141	32731	cfa-miR-190b
19004	cfa-let-7c	50170	cfa-miR-141	10985	cfa-miR-191
46436	cfa-let-7e	19015	cfa-miR-142	46443	cfa-miR-193a
17752	cfa-let-7f	13177	cfa-miR-143	42962	cfa-miR-193b
19602	cfa-let-7g	29802	cfa-miR-144	10988	cfa-miR-194
50262	cfa-let-7j	42641	cfa-miR-145	13148	cfa-miR-195
10916	cfa-miR-1	10952	cfa-miR-146a	10990	cfa-miR-196a
13485	cfa-miR-10	46713	cfa-miR-146b	42783	cfa-miR-197
50427	cfa-miR-101	17411	cfa-miR-147	10995	cfa-miR-199
10919	cfa-miR-103	10955	cfa-miR-148a	10997	cfa-miR-19a
50005	cfa-miR-103/cfa-miR-107	19585	cfa-miR-148b	10998	cfa-miR-19b
5250	cfa-miR-105a	42810	cfa-miR-149	17427	cfa-miR-200c
48901	cfa-miR-105b	42802	cfa-miR-150	42507	cfa-miR-202
17605	cfa-miR-106a	11260	cfa-miR-151	11004	cfa-miR-203
19582	cfa-miR-106b	17676	cfa-miR-152	11005	cfa-miR-204
10925	cfa-miR-10b	42599	cfa-miR-153	42655	cfa-miR-205
19583	cfa-miR-122	10964	cfa-miR-155	11007	cfa-miR-206
14328	cfa-miR-124	27720	cfa-miR-15a	5730	cfa-miR-208a
10928	cfa-miR-125a	17280	cfa-miR-15b	42555	cfa-miR-208b
30787	cfa-miR-125b	10967	cfa-miR-16	46513	cfa-miR-20a
33596	cfa-miR-126	19588	cfa-miR-17	50240	cfa-miR-20b
42829	cfa-miR-127	42865	cfa-miR-181a	5740	cfa-miR-21
49960	cfa-miR-1271	48944	cfa-miR-181b	42797	cfa-miR-210
33902	cfa-miR-128	42496	cfa-miR-181c	19601	cfa-miR-211
42467	cfa-miR-129	42840	cfa-miR-181d	48987	cfa-miR-212
46219	cfa-miR-1306	10975	cfa-miR-182	11014	cfa-miR-214
42681	cfa-miR-1307	10977	cfa-miR-183	42553	cfa-miR-216a
10138	cfa-miR-130a	49096	cfa-miR-1835	17849	cfa-miR-216b
10936	cfa-miR-130b	49971	cfa-miR-1837	19016	cfa-miR-217
10937	cfa-miR-132	49756	cfa-miR-1838	11018	cfa-miR-218
49449	cfa-miR-133a	49337	cfa-miR-1839	42509	cfa-miR-219
10938	cfa-miR-133a/cfa-miR-133b/cfa-miR-133c	10978	cfa-miR-184	42834	cfa-miR-219*
30755	cfa-miR-133b	49817	cfa-miR-1840	11020	cfa-miR-22
42942	cfa-miR-134	49233	cfa-miR-1841	50421	cfa-miR-220b
46859	cfa-miR-135a-3p	49067	cfa-miR-1842	11022	cfa-miR-221
42839	cfa-miR-135a-5p	49769	cfa-miR-1843	11023	cfa-miR-222
10942	cfa-miR-135b	49191	cfa-miR-1844	11024	cfa-miR-223
10943	cfa-miR-136	42902	cfa-miR-185	42473	cfa-miR-224
50212	cfa-miR-137	18739	cfa-miR-186	49426	cfa-miR-23a
42731	cfa-miR-138a	27539	cfa-miR-187	50375	cfa-miR-23b
49808	cfa-miR-138b	42620	cfa-miR-188	17506	cfa-miR-24
42451	cfa-miR-139	42588	cfa-miR-18a	42682	cfa-miR-25
11201	cfa-miR-140	13141	cfa-miR-18b	11030	cfa-miR-26a

Probe ID	Anotation	Probe ID	Anotation	Probe ID	Anotation
42564	cfa-miR-26b	49336	cfa-miR-369	46406	cfa-miR-500
46483	cfa-miR-27a	42967	cfa-miR-370	46654	cfa-miR-502
46469	cfa-miR-27b	49543	cfa-miR-374a	14288	cfa-miR-503
17940	cfa-miR-28	14302	cfa-miR-374b	28480	cfa-miR-504
11038	cfa-miR-299	11088	cfa-miR-375	17624	cfa-miR-532
11039	cfa-miR-29a	42498	cfa-miR-375	14271	cfa-miR-539
11040	cfa-miR-29b	46484	cfa-miR-376a	14272	cfa-miR-542
11041	cfa-miR-29c	11090	cfa-miR-376b	42470	cfa-miR-543
9634	cfa-miR-301a	11105	cfa-miR-378	29850	cfa-miR-544
13143	cfa-miR-301a	11093	cfa-miR-379	49655	cfa-miR-545
17886	cfa-miR-301b	49979	cfa-miR-380	17272	cfa-miR-551a
50388	cfa-miR-30a	14306	cfa-miR-381	42917	cfa-miR-551b
17565	cfa-miR-30b	46338	cfa-miR-382	42977	cfa-miR-568
42923	cfa-miR-30c	11098	cfa-miR-383	17662	cfa-miR-574
19596	cfa-miR-30d	30973	cfa-miR-384	42567	cfa-miR-590
11224	cfa-miR-30e	50021	cfa-miR-409	17312	cfa-miR-592
11052	cfa-miR-31	11102	cfa-miR-410	30592	cfa-miR-599
11053	cfa-miR-32	17482	cfa-miR-411	17870	cfa-miR-628
27533	cfa-miR-320	17474	cfa-miR-421	42700	cfa-miR-631
42957	cfa-miR-323	27565	cfa-miR-423a	42827	cfa-miR-652
42477	cfa-miR-324	42603	cfa-miR-424	17338	cfa-miR-660
50165	cfa-miR-325	17608	cfa-miR-425	49829	cfa-miR-664
42693	cfa-miR-326	17478	cfa-miR-429	42525	cfa-miR-671
46261	cfa-miR-328	11111	cfa-miR-432	50188	cfa-miR-676
49287	cfa-miR-329a	42853	cfa-miR-433	3980	cfa-miR-7
11061	cfa-miR-329b	11113	cfa-miR-448	29190	cfa-miR-708
42716	cfa-miR-33	11114	cfa-miR-449	28759	cfa-miR-758
42875	cfa-miR-330	17835	cfa-miR-450a	30442	cfa-miR-802
42887	cfa-miR-331	50356	cfa-miR-450b	42808	cfa-miR-874
11065	cfa-miR-335	42866	cfa-miR-451	17850	cfa-miR-875
42592	cfa-miR-338	29379	cfa-miR-452	42940	cfa-miR-876
46521	cfa-miR-33b	42854	cfa-miR-454	4040	cfa-miR-9
29872	cfa-miR-340	13179	cfa-miR-455	42728	cfa-miR-92a
11069	cfa-miR-342	42480	cfa-miR-485	17718	cfa-miR-92b
50390	cfa-miR-345	13183	cfa-miR-487a	30687	cfa-miR-93
42759	cfa-miR-346	14285	cfa-miR-487b	11181	cfa-miR-95
27217	cfa-miR-34a	42703	cfa-miR-490	13147	cfa-miR-96
29153	cfa-miR-34b	49320	cfa-miR-491	11182	cfa-miR-98
32772	cfa-miR-34c	14270	cfa-miR-493	42708	cfa-miR-99a
11234	cfa-miR-350	42540	cfa-miR-494	11184	cfa-miR-99b
14301	cfa-miR-361	42676	cfa-miR-495	46406	
42503	cfa-miR-362	11128	cfa-miR-496	46654	
11077	cfa-miR-363	42847	cfa-miR-497	14288	
11078	cfa-miR-365	14313	cfa-miR-499	28480	

Supplemental Table 2. miRNAs with ≥20% deviation in CHF compared to control from RA and LV tissue (ordered by the maximum change)

A. Atrium

miRNA	Ratio at max. change*	miRNA	Ratio at max. change*	miRNA	Ratio at max. change*
cfa-miR-21	**6.61**	cfa-miR-301a	1.22	**cfa-miR-133b**	**0.68**
cfa-miR-208b	**5.68**	cfa-miR-301a	1.21	**cfa-miR-30b**	**0.68**
cfa-miR-214	2.4	cfa-miR-20a	1.2	cfa-miR-9	0.68
cfa-miR-146b	1.9	cfa-miR-221	1.2	cfa-let-7g	0.67
cfa-miR-502	1.78	cfa-miR-331	1.2	cfa-miR-190a	0.67
cfa-miR-152	1.72	cfa-miR-494	1.2	**cfa-miR-30c**	**0.67**
cfa-miR-199	1.7	cfa-miR-125b	0.83	cfa-miR-144	0.66
cfa-miR-195	1.67	cfa-miR-149	0.83	**cfa-miR-133a/cfa-miR-133b/cfa-miR-133c**	**0.64**
cfa-miR-34a	1.53	cfa-miR-191	0.83	cfa-miR-99a	0.64
cfa-miR-140	1.52	cfa-miR-350	0.82	cfa-miR-223	0.63
cfa-miR-146a	1.52	cfa-miR-450a	0.82	**cfa-miR-29c**	**0.63**
cfa-miR-18b	1.5	cfa-miR-98	0.82	**cfa-miR-30d**	**0.63**
cfa-miR-135a-5p	1.48	cfa-miR-15b	0.81	cfa-miR-338	0.63
cfa-miR-29b	**1.46**	cfa-miR-25	0.81	cfa-miR-499	0.59
cfa-miR-455	1.44	cfa-miR-340	0.81	cfa-miR-10	0.58
cfa-miR-497	1.43	cfa-miR-365	0.81	**cfa-miR-30e**	**0.58**
cfa-miR-500	1.43	cfa-miR-374a	0.81	cfa-miR-101	0.56
cfa-miR-184	1.4	cfa-miR-452	0.81	cfa-miR-142	0.56
cfa-miR-22	1.4	cfa-miR-126	0.8	**cfa-miR-133a**	**0.55**
cfa-miR-106b	1.36	cfa-miR-363	0.8	cfa-miR-10b	0.48
cfa-miR-24	1.36	cfa-miR-27b	0.79	cfa-miR-378	0.48
cfa-miR-503	1.36	cfa-miR-181b	0.78		
cfa-miR-185	1.33	cfa-miR-188	0.78		
cfa-miR-23b	1.33	cfa-miR-652	0.78		
cfa-miR-222	1.32	cfa-miR-151	0.77		
cfa-miR-29a	**1.32**	cfa-miR-181a	0.77		
cfa-miR-491	1.32	**cfa-miR-1**	**0.76**		
cfa-let-7e	1.29	cfa-miR-218	0.76		
cfa-miR-487b	1.29	cfa-miR-660	0.76		
cfa-miR-106a	1.28	**cfa-miR-208a**	**0.74**		
cfa-miR-708	1.28	**cfa-miR-30a**	**0.74**		
cfa-miR-19a	1.27	cfa-miR-130a	0.73		
cfa-miR-23a	1.27	cfa-miR-204	0.72		
cfa-miR-99b	1.26	**cfa-miR-26b**	**0.72**		
cfa-miR-33	1.25	cfa-miR-335	0.71		
cfa-let-7b	1.24	cfa-miR-451	0.71		
cfa-let-7c	1.24	cfa-miR-145	0.7		
cfa-miR-361	1.24	**cfa-miR-26a**	**0.69**		
cfa-miR-27a	1.22	cfa-miR-374b	0.69		

*Values are ratio of expression at the time of maximum change to expression at baseline. MiRNAs in bold were further analyzed by detailed qPCR quantification in tissues and isolated cells. max = maximum.

B. Ventricle

miRNA	Ratio at max. change*	miRNA	Max. Fold change	miRNA	Ratio at max. change*
cfa-miR-21	**1.56**	cfa-miR-193b	1.22	**cfa-miR-29c**	**0.81**
cfa-miR-222	1.56	cfa-miR-199	1.22	**cfa-miR-30d**	**0.81**
cfa-miR-146b	1.54	cfa-miR-24	1.22	cfa-miR-490	0.80
cfa-miR-146a	1.42	cfa-miR-504	1.22	cfa-miR-338	0.79
cfa-miR-652	1.35	**cfa-miR-29a**	**1.21**	cfa-miR-500	0.79
cfa-miR-335	1.34	cfa-miR-101	1.20	cfa-miR-184	0.77
cfa-miR-31	1.30	cfa-miR-221	1.20	cfa-miR-223	0.77
cfa-miR-590	1.30	cfa-miR-25	1.20	cfa-miR-1839	0.73
cfa-miR-708	1.25	cfa-miR-27a	1.20	cfa-miR-204	0.71
cfa-miR-23b	1.24	cfa-miR-99a	0.83	cfa-miR-10	0.67
cfa-miR-150	1.23	cfa-miR-451	0.82	cfa-miR-378	0.64
cfa-miR-152	1.22	cfa-miR-214	0.81	**cfa-miR-208a**	**0.60**

*Values are ratio of expression at the time of maximum change to expression at baseline. MiRNAs indicated in bold were selected for detailed qPCR analysis. Max, maximum.

Supplemental Table 3.miRNAs and predicted targets related to fibrotic response (based on Target Scan *in-silico* prediction on human and dog sequence).

miRNA	**Predicted targets (Validation attempted)***
miR-29a/b/c	**COL1A1, COL1A2, COL3A1,** COL4A1**, COL5A1, FBN1**, **MMP2**, TGFB1, TGFB2, TGFB3, CTGF, PDGFB/C/D, PDGFRB, IGF1, STAT3, SMAD7, NFATC4
miR-26a/b	TRPC3, **COL5A1, (FN1)**, CTGF, PDGFRA, IGF1, SMAD1/4
miR-21	SPRY1, **TIMP3**, PTEN **(MMP2),** SMAD7
miR-1	**FN1**, FBLN2, TGFB3, PDGFA, SMAD4
miR-30a/b/c/d/e	CTGF, PDGFRB, IGF1, CREB1, JAK1
miR-133a/b	**COL1A1, (FBN1)**, TGFB2, TGFBR1, CTGF, FGFR1, JAK2
miR-208a/b	**FBN1**
miR-218	**COL1A1**
miR-214	**TIMP2**
miR-222	**TIMP2, TIMP3**
miR-146a/b	N.A.

*Target genes in blue (without brackets) were validated in the literature or in our study (those in black are predicted but not validated). (Gene targets) in blue with brackets were tested for validation of predicted regulation in the present study, but were not shown by Luciferase assay to be regulated by corresponding miRNA. Underlined targets are genes regulated by the miRNA indicated that leads to indirect ECM gene regulation. Genes in **bold** were quantified by qPCR.

Abbreviations: COL1A1, collagen-1α1; COL1A2, collagen-1α2; COL3A1,collagen-3α1;COL4A1, collagen-4α1; COL5A1, collagen 5α1;CREB, cyclic-AMP response element binding protein; CTGF, connective tissue growth factor; FBLN2, fibulin type-2; FBN1, fibrillin-1; FGFR, fibroblast growth factor receptor; FN1,fibronectin-1;IGF, insulin growth factor; JAK, janus kinase; MMP2, matrix metalloproteinase-2; NFAT, nuclear factor of activated T-cells; PDGF(R)A/B/C/D, platelet-derived growth factor (receptor) type-A/B/C/D;PTEN, phosphatase and tensin homolog; SPRY1,Sproutyhomolog 1; SMAD, mothers against decapentaplegic homolog transcription factor; STAT, signal transducer and activator of transcription; TGFB(R)1/2/3, transforming growth factor beta (receptor)-1/2/3;TIMP2/3, tissue inhibitor of metalloproteinase-2/3; TRPC3,transient receptor potential cation channel, subfamily C, member 3; N.A., not applicable. Please note that while none of the miRNAs regulates MMP2, PTEN (a predicted target of miR-21) is known to negatively regulate MMP2 expression.

Supplemental Figure Legends

Supplemental Figure 1. Representative histological sections (Masson Trichrome staining; shown at 400×magnification) illustrating fibrosis-development in the left atrium (LA, upper panel) and left ventricle (LV, lower panel) at different time-points of ventricular tachypacing (VTP).

Supplemental Figure 2. Heat map of 21 miRNAs in atrial and ventricular tissue-samples. Each row represents a miRNA and each column represents a pooled sample from 5 dogs/group. Non-paced control (CTL) was set as $\log_2$ (change) of 0 (i.e. relative value of 1 versus CTL) and is shown in white. The color scale shown at the bottom indicates the relative expression level of each miRNA at the time-point indicated. Red represents an expression-level above CTL, blue represents expression lower than CTL.

Supplemental Figure 3. Sequences of miRNAs and their antisense molecules used in our study. (A) Alignment of the sequences of miRNAs (upper sequences) with their target sites in the 3'-UTRs of target mRNAs (lower sequences). Complementarity is highlighted in yellow and connected by "|". Weakly complementary binding is shown by ":". (B) Sequences of the negative control miRNA (miR-NC) and negative control miRNA antisense oligodeoxynucleotides (AMO-NC) used for target validation.

Supplemental Figure 4. Validation of miRNA targeting of predicted ECM-genes. (A) Luciferase activity for *COL1A1*-genein HEK293 cells transfected with miR-218 (miR-218 duplex) and/or knockdown (anti-miR218 oligonucleotides, AMO218) probes. (B) *COL1A1* gene-expression in

dog left-atrial fibroblasts transfected with miR-218 duplex/AMO218. (C, D) Luciferase activity in HEK293 cells (C) for fibronectin-1 gene assay for miR-26a regulation or (D) fibrillin-1 gene assay for miR-133a regulation. Values are mean±SEM for each oligonucleotide and numbers in each bar indicate the number of independent experiments (*$p<0.05$, **$p<0.01$vs. cells transfected with negative control oligonucleotides). COL1A1, collagen-1α1; FN1, fibronectin-1; FBN1, fibrillin-1; Lipo, lipofectamine; AMO, anti-miR oligonucleotides.

Supplemental Figure 5. Expression of collagen-1α2, collagen-3α1and collagen-5α1 mRNA and regulating miRNA in freshly isolated fibroblasts (FBs) from left atrium (left panel) and left ventricle (right panel) as a function of VTP time-course. The scale for collagen-family member expression (solid orange line) is shown at the left; that for miRNA-expression is on right. MiRNAs shown with solid lines regulate collagen-family member directly; dashed lines indicate indirect regulation. Values are mean±SEM, n=5-12/group.**$p<0.01$, ***p<0.005, vs. corresponding CTL samples. COL1A2,collagen-1α2; COL3A1, collagen-3α1; COL5A1, collagen-5α1; LA, left atrium; LV, left ventricle; FB, fibroblasts; CTL, non-paced controls.

Supplemental Figure 6. Expression of extracellular matrix (ECM) mRNA and regulating miRNA in freshly isolated fibroblasts (FBs) from left atrium (left panel) and left ventricle (right panel) during VTP time-course. The scale for ECM expression (solid orange line) is shown at the left; that for miRNA-expression is on right. MiRNAs shown with solid lines regulate ECM directly; dashed lines indicate indirect regulation. Values are mean±SEM, n=5-12/group.*$p<0.05$, **$p<0.01$, ***p<0.005, vs. corresponding CTL samples.FBN1, fibrillin-1; FN1,fibronectin-1;

MMP2, matrix metalloproteinase-2; TIMP3, tissue inhibitor of metalloproteinase-3; LA, left atrium; LV, left ventricle; FB, fibroblasts; CTL, non-paced controls.

Supplemental Figure 1

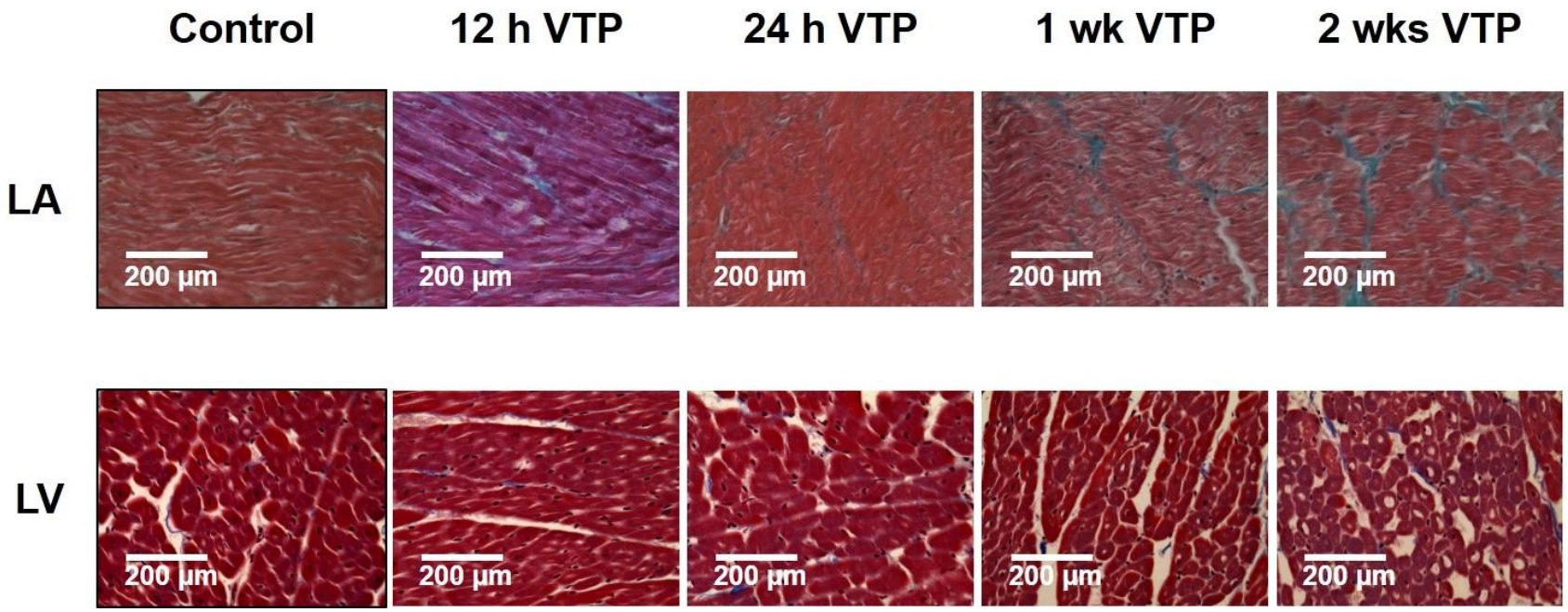

Supplemental Figure 2

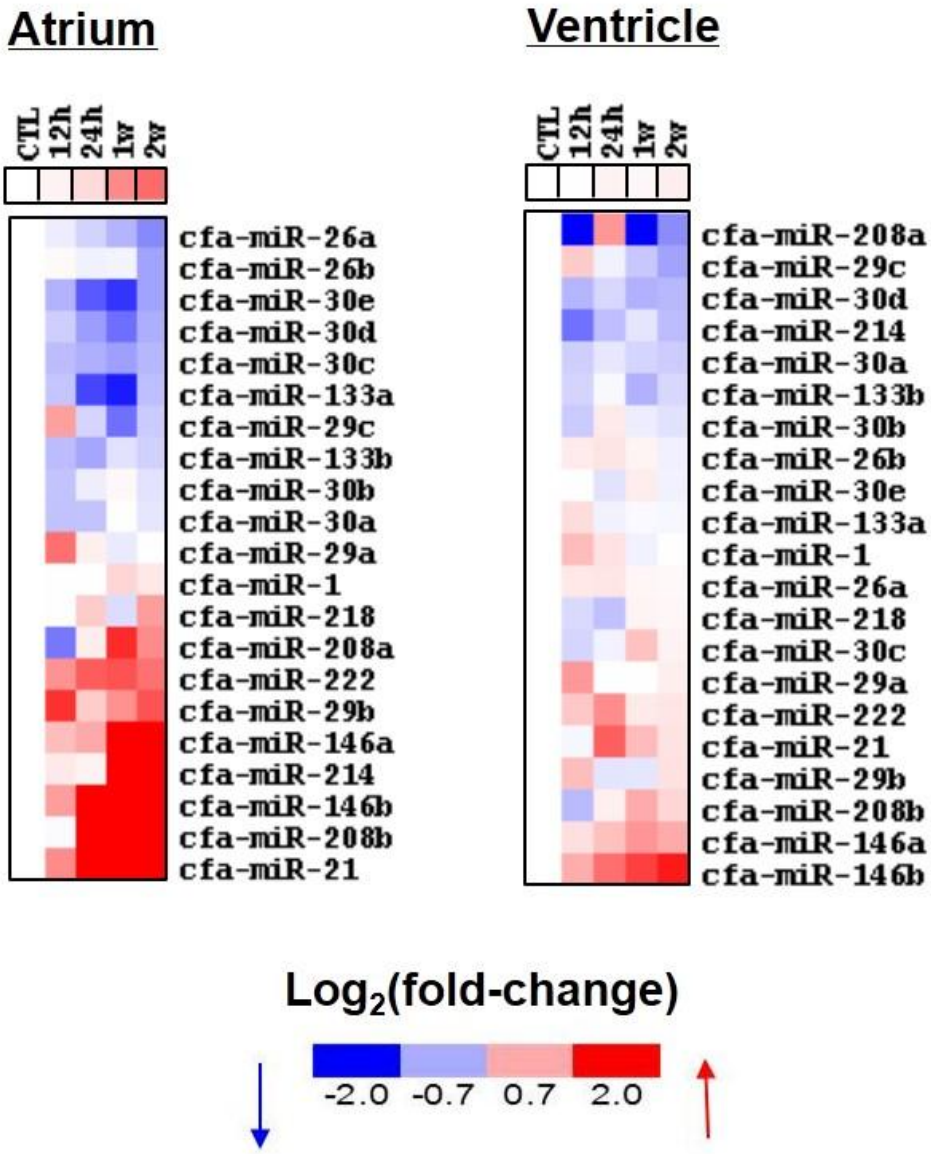

Supplemental Figure 3

A. miR:target mRNA complementarity

```
 3'-UGUACCAAUCUAGUUCGUGUU-5'
    :         |     |||||||
183-GACCAAAAACCAAAAGCACAT-214
```

cfa-miR-218

COL1A1 3'UTR (NM_001003090.1)

```
 3'-UCGGAUAGGACCUAAUGAACUU-5'
    :  ::||   :|   |  |||||||
668-GATTTACATTCCACAACTTGAA-690
```

cfa-miR-26a

FN1 3'UTR (XM_005640741.1)

```
 3'-UGUCGACCAACUUCCCCUGGUU-5'
       |   |||   ::|  |||||||
744-CATGGAGGTCTGGGAGGACCAA-766
```

cfa-miR-133a

FBN1 3'UTR (NM_001287085.1)

B. Negative Control miRNA and AMO miR-NC

miR-NC

5'-UCAAGUAACUUCAACCAGCUGU -3'

5'-AGCUGGUUGAAGUUACUUGAAU -3'

AMO-NC

5'- TCCTAGAAAGAGTAGATCGAT -3'

Supplemental Figure 4

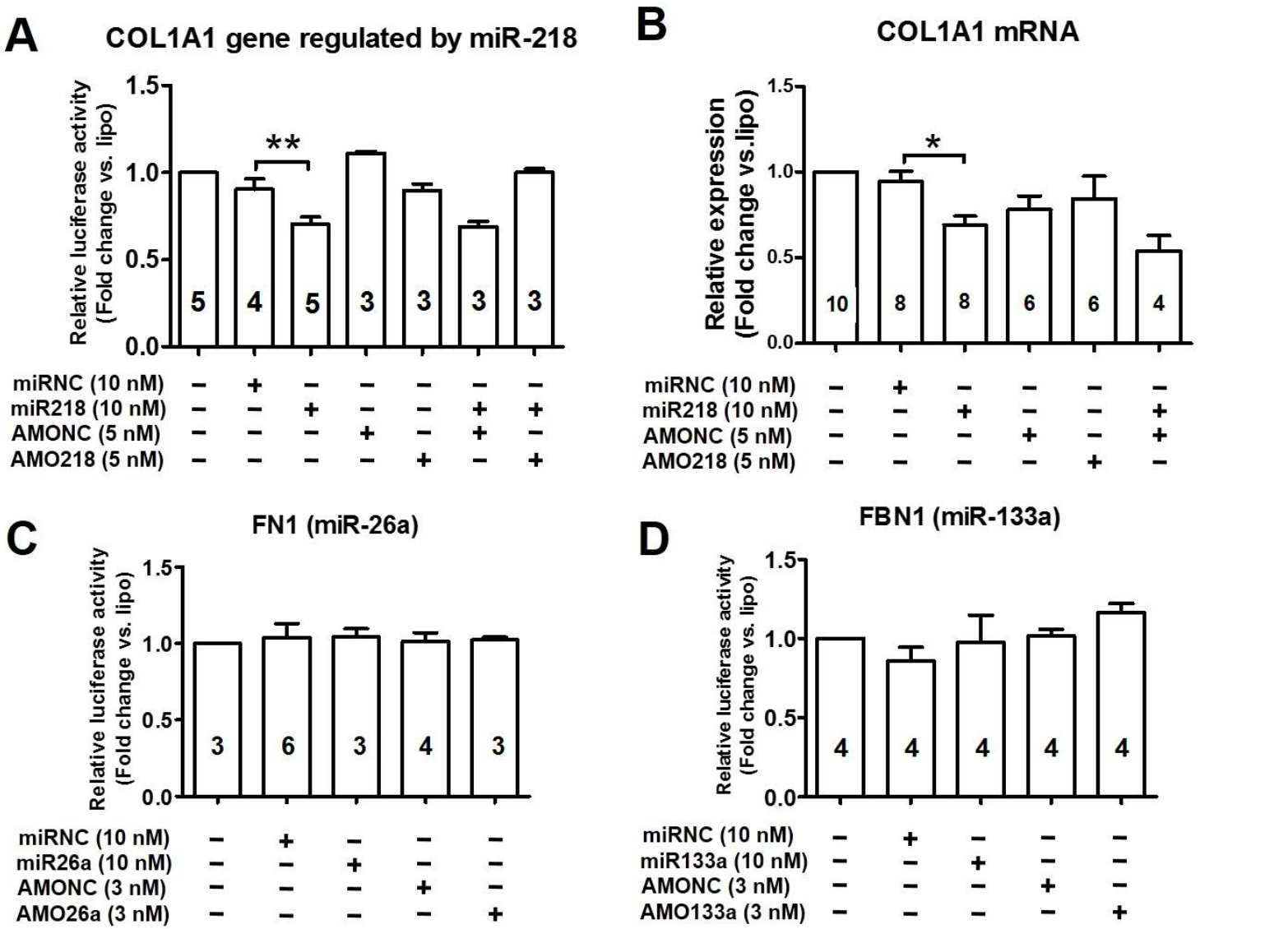

Supplemental Figure 5

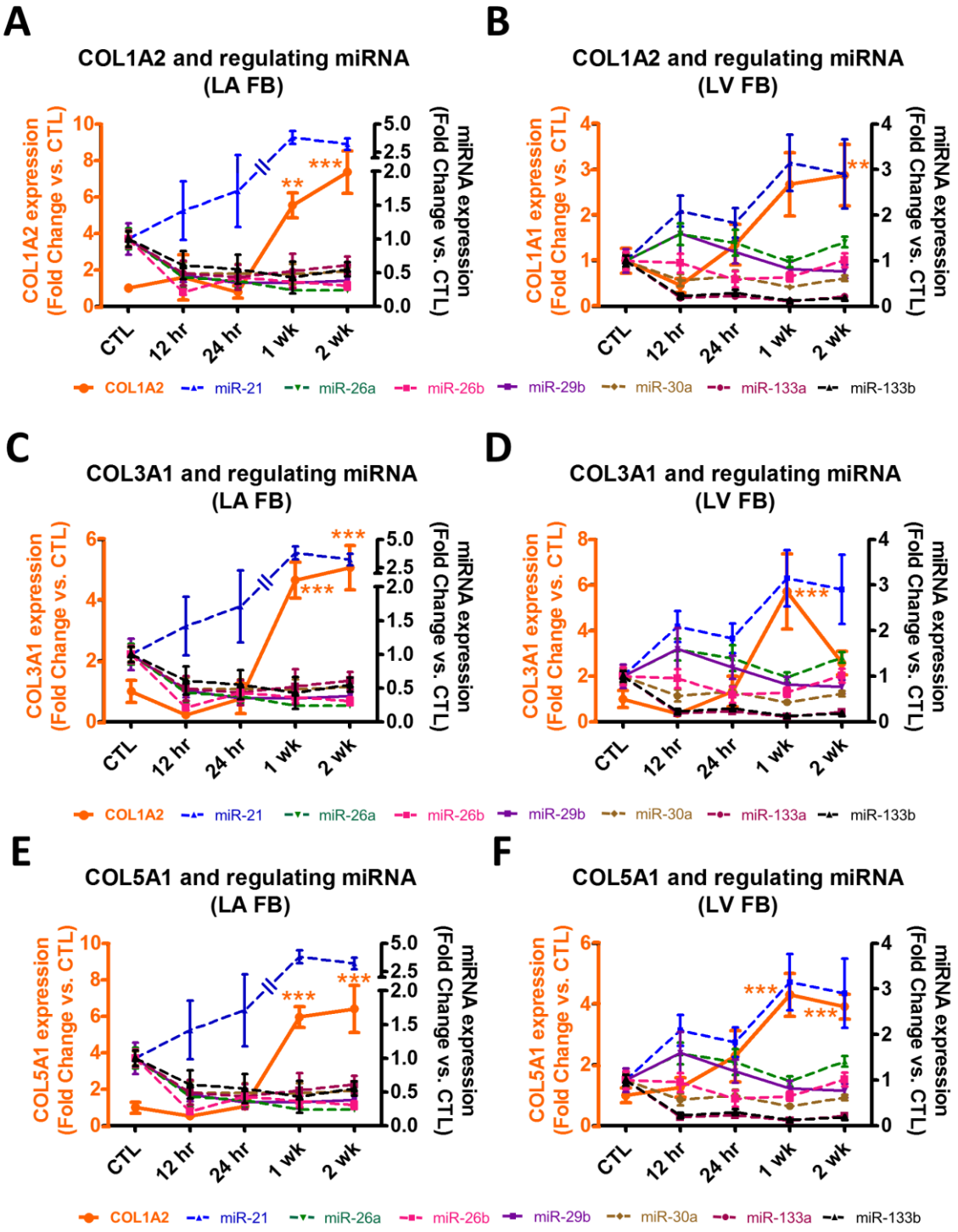

Supplemental Figure 6

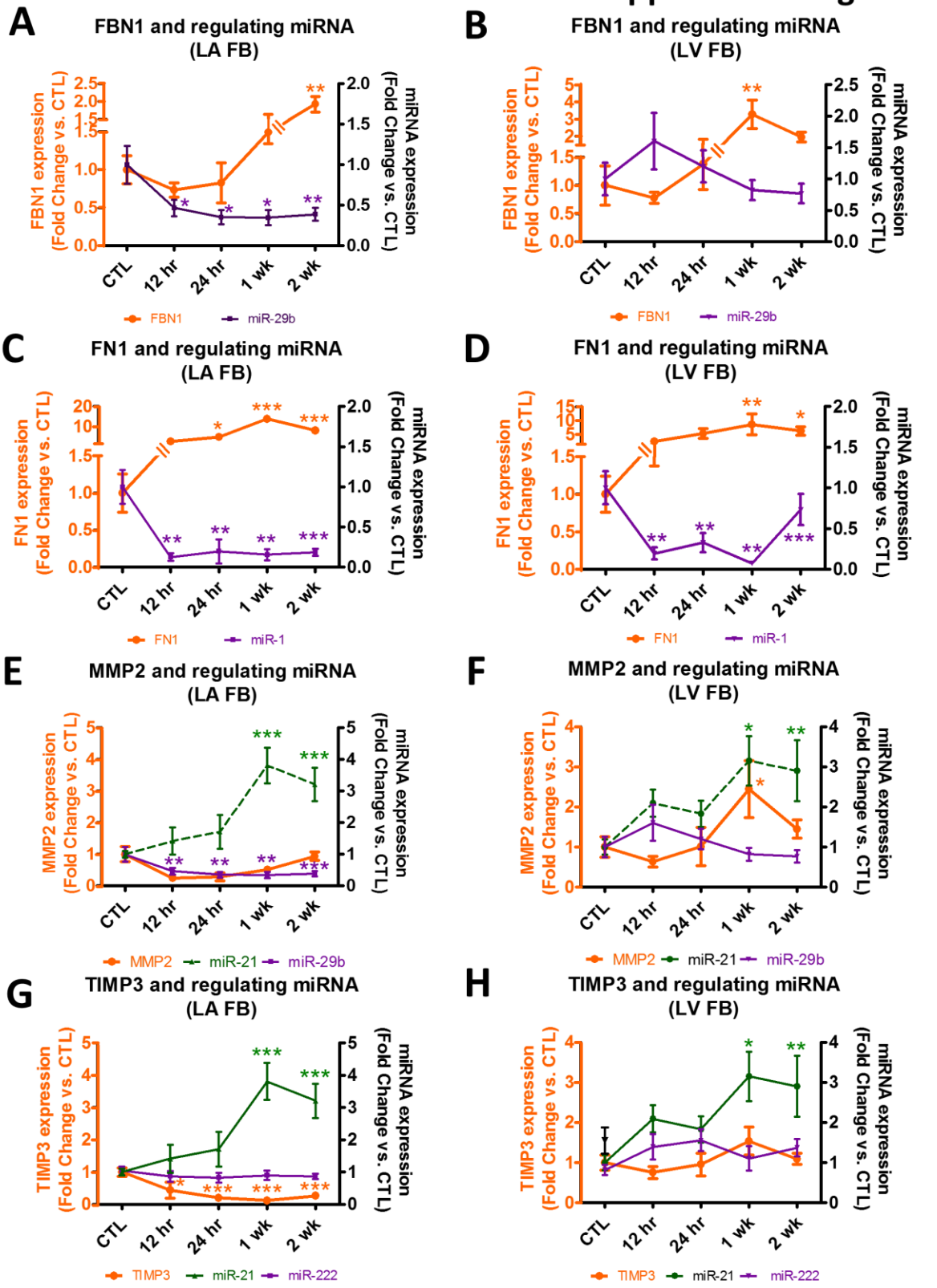

Chapter 4

The role of microRNAs in mediating PDGF effects in heart failure-associated fibrotic response

Linking statement

In Chapter 2, I investigated the role of the JAK-STAT system in HF-associated atrial fibrotic remodeling; In Chapter 3, I assessed miRNA-system changes in the same pathological model (canine HF). While searching the predicted targets of miRs that were altered in HF, I found that certain miRs that change in HF target PDGF/JAK-STAT components, including PDGF, PDGF receptors, JAKs and STATs. I therefore hypothesized that these miRs participate in the HF-related fibrotic response by targeting the JAK-STAT system. In this Chapter, I stimulated cultured fibroblasts with PDGF to mimic the fibrotic effects in HF, attempting to identify the responsive miRs. After validating the binding between potential miRs and the JAK-STAT components, I manipulated miR expression and assessed the resulting changes in target gene expression and ECM production in atrial fibroblasts in order to determine whether miRs may play a crucial part in mediating the PDGF/JAK-STAT effect on atrial tissues.

MicroRNAs mediate PDGF effects by targeting JAK-STAT in heart failure-associated fibrotic response

Yu Chen, MSc[a,b,]; Sirirat Surinkaew, PhD[a]; Jiening Xiao, PhD[a]; Chia-Tung Wu, MD[a,c]; Hai Huang, PhD[a]; YiguoSun, PhD[a]; Dobromir Dobrev, MD[d]; Stanley Nattel, MD[a,b,]

[a]Department of Medicine and Research Center Montreal Heart Institute and Université de Montréal; Montreal, Quebec, Canada;

[b]Department of Pharmacology and Therapeutics McGill University, Montreal, Quebec, Canada;

[c]Chang Gung Memorial Hospital and Chang Gung University Tao-Yuan, Taiwan;

[d]Institute of Pharmacology, Faculty of Medicine, University Duisburg-Essen, Essen, Germany;

Short title: miRNA mediates fibrotic effects by targeting JAK2

*Corresponding author. 5000 Belanger Street East, Montreal, Quebec, Canada, H1T 1C8. Tel.: (514)-376-3330 ext. 3990. Fax: (514)-376-1355.E-mail: stanley.nattel@icm-mhi.org

Abstract

Background: MicroRNAs (miRNAs) are involved in cardiac remodeling, but their role in atrial fibrillation (AF) is poorly understood. I have shown that the PDGF-JAK-STAT system contributes to atrial-selective fibrotic response in experimental heart failure (HF) (Chapter 2), and that multiple miRNAs are implicated in AF-associated atrial fibrosis (Chapter 3). Here, we investigated miRNAs regulation on the JAK-STAT system in AF-related fibrotic response.

Methods: Fibroblasts (FBs) isolated from left atria (LA) and left ventricles (LV) of control (CTL) dogs were treated with PDGF-AB at 10ng/ml and 50ng/ml. miRNA, JAK2 and collagen type I expression was assessed by qPCR. MiRNA targets were validated by luciferase reporter assay. MiRNA mimic or antisense oligonucleotides (AMO) were used for miRNA manipulation. JAK2 and collagen type I proteins were quantified by Western Blot.

Results: PDGF-AB stimulation reduced the expression of miR-1, miR-30a and miR-133a (by ~50%-80%***, ****p*<0.001 versus vehicle) in canine LA FBs. Smaller changes were seen in LV FBs. Luciferase assay confirmed miR-30a and miR-133a targeting of JAK2. Overexpression of miR-133a downregulated JAK2 mRNA (by 30%***) and protein (by 50%, p=0.05) in LA FBs. This effect was abolished by co-transfection with AMO-133a. PDGF-AB stimulation upregulated the protein expression of JAK2 and collagen type I in LA FBs (by ~2-2.5-fold*versus vehicle, **p*<0.05) and these elevations were reversed by miR-133a overexpression (reduced by 49%* and 53%*** versus PDGF stimulation alone).

Conclusions: PDGF-induced disinhibition of JAK2 expression by downregulation of miR-30a and miR-133a may contribute to AF-associated fibrotic responses. MiRNA targeting of the JAK-STAT system regulates LA FB function, appears to be involved in HF-induced LA fibrosis and is a potential therapeutic target for AF prevention.

Introduction

In congestive heart failure (CHF), the myocardium undergoes a number of structural alterations, most notably hypertrophy and interstitial fibrosis. The deposition of extracellular matrix (ECM) protein produced from fibroblasts is the main feature of interstitial fibrosis, which interferes with local conduction and promotes sustained atrial fibrillation (AF) [1]. However, the mechanisms underlying fibrosis are not fully understood. Evidence has been provided that CHF-related fibrosis has important atrial–ventricular differences, and that atrial-selective fibrosis is due to the differential behaviour of atrial versus ventricular fibroblasts [2, 3]. However, mechanisms responsible for this difference remain to be revealed.

Multiple signaling pathways have been shown to induce fibrotic responses. In Chapter 2, we demonstrated that the PDGF/JAK/STAT system plays a role in the atrial-selective fibrotic response. STAT3 is a potential therapeutic target to attenuate atrial fibrosis. The upstream mediators of the JAK-STAT pathway, such as PDGF, PDGF receptor, and JAK2 may also be potential therapeutic targets for atrial fibrosis prevention.

A microRNA (miRNA, miR) is a small interfering non-coding RNA that can negatively regulate mRNA and protein expression. MiRNAs were recently shown to be important regulators of cardiac fibrotic remodeling [4-7]. We have previously shown that alteration of multiple miRNAs change with the development of CHF, with alterations being left atrial (LA)- and fibroblast-selective, and occurring in parallel with ECM gene changes [8]. Some miRNAs have validated ECM targets; for instance, miR-29b regulates the production of multiple collagens, and miR133 targets collagen type I [6, 9, 10]. However, a greater number of miRNAs do not target ECM genes, and instead target the upstream mediators that can influence ECM production, such as Sprouty 1 (SPRY1, a target of miR-21), transforming growth factor-beta1 (TGF-β1, target of

miR-122), connective tissue growth factor (CTGF, target of miR-30a and miR-133a), and transient receptor potential canonical-3 (TRPC3, target of miR-26a) [4, 11-13]. MiRNAs targeting pro-fibrotic or anti-fibrotic factors may have more profound effects than those targeting ECM proteins. Therefore, elucidating the roles of miRNAs in fibrotic signaling is an important goal in understanding the pathology of fibrotic remodeling and may assist in developing anti-fibrotic therapies.

In this study, we sought to relate changes in miRNAs to those in JAK-STAT in CHF-related atrial selective fibrosis, seeking to identify miRNAs involved in mediating PDGF effects in an AF-associated fibrotic response paradigm (CHF).

Materials and Methods

Fibroblast harvesting and culture

Animal-care procedures followed the guidelines of the Canadian Council on Animal Care and were approved by the Animals Research Ethics Committee of the Montreal Heart Institute. Control dogs were anaesthetized with morphine and (2 mg/kg s.c.) and alpha-chloralose (120 mg/kg i.v.) and mechanically ventilated, then euthanized by cardiac excision. Hearts were removed and placed in Tyrode's solution. Left atria (LA) and left ventricles (LV) were perfused via the left anterior descending coronary artery for cell isolation and collagenase digestion as detailed previously [14, 15]. Paired atrial and ventricular cell samples isolated from each dog were plated in 6-well plates in parallel at equal density and cultured in DMEM containing 5% FBS and 1% penicillin/streptomycin. Fibroblasts were allowed to adhere for 2 days, rendered quiescent in serum-free medium for 16 hours, and then stimulated with 10ng/ml or 50ng/ml of

PDGF-AB (Sigma-Aldrich, St. Louis, MO) for 48 hours. Vehicle-treated fibroblasts served as negative control.

RNA extraction and quantitative real-time Polymerase Chain Reaction (PCR) analysis

RNA was isolated with mirVana isolation kits (Ambion/Life Technology, Carlsbad, CA). Real-time quantitative polymerase chain reaction for miRNAs was performed with carboxy-fluorescein (FAM)-labeled fluorogenic TaqMan assay primers (Applied Biosystems, Foster City, CA) and TaqMan Universal Master Mix (Applied Biosystems). Relative quantifications were calculated with the comparative threshold cycle method ($2^{-\Delta Ct}$), with snU6 as an internal standard. Quantitative PCR for JAK2 and procollagen Ia1 was performed with dog-specific TaqMan primers (Applied Biosystems) and relative quantities ($2^{-\Delta Ct}$) calculated with the geometric mean of 2 reference genes (hypoxanthine phosphoribosyl transferase 1 [*HPRT-1*], β2-microglobulin) as internal standards.

***In silico* prediction of potential miRNA targets**

MiRNA-targets were predicted from TargetScan v6.2 and sequence alignment analysis, by searching for the presence of conserved 8-mer and 7-mer sites on target mRNAs that match the miRNA seed region. Only mRNA sequences with at least one conserved binding region across human and canine families were chosen as potentially valid targets from mRNA target prediction.

Construction of luciferase-miRNA-target site fusion plasmids and luciferase activity assay

To construct reporter vectors bearing miRNA-target sites, we synthesized fragments containing the exact target sites for each miRNA in the 3′-untranslated region (3′-UTR) of their respective target genes synthesized by Invitrogen. These inserts were ligated into SacI and XhoI in pmirGLO Dual-Luciferase miRNA Target Expression Vector(Promega, Madison, WI). For luciferase assay involving miRNA function, HEK293 cells were transfected with the pmirGLO Dual-Luciferase miRNA Target Expression Vector carrying the 3′ UTR of target genes, according to the manufacturer's instructions.

Synthesis of miRNAs and anti-miRNA antisense inhibitors

MiR-30a and miR133a were synthesized by Invitrogen. Their antisense oligonucleotides AMO-30a and AMO-133a were synthesized by Exiqon. Five nucleotides or deoxynucleotides at both ends of the antisense molecules were locked (LNA; the ribose ring is constrained by a methylene bridge between the 2′-O- and the 4′-C atoms). Additionally, a scrambled miRNA or AMO was used as a negative control.

Transfection procedures

The HEK293 cell line was purchased from ATCC and cultured in DMEM containing 10% FBS and 1% penicillin/streptomycin. HEK cells were transfected with 10nM miRNA and/or 3 nM AMOs, or negative control constructs with Lipofectamine 3000 (Invitrogen), according to the manufacturer's instructions. Cells were used for luciferase assay 24 hours after the transfection. Atrial fibroblasts were transfected with 100 nM miRNA and/or 50 nM AMOs, or negative control constructs with or without simulation of PDGF-AB (20ng/ml, Sigma). Fibroblasts were

collected 24 hours (mRNA quantification) or 48 hours (protein quantification) after transfection for further analysis.

Protein extraction and immunoblots

Protein extracts (30 μg) of cultured fibroblasts were separated by electrophoresis on 12% SDS-PAGE and transferred to PVDF membranes. For secreted collagen type I, supernatant of medium (30μl) for cultured fibroblasts were separated by electrophoresis on 8% SDS-PAGE and transferred to nitrocellulose membranes. Membranes were blocked and incubated overnight with the primary antibodies mouse anti-JAK2 (1:1000; Abcam), rabbit anti-collagen type I (1:25000, MD Biosciences, Zurich Switzerland), or mouse anti-GAPDH (1:10 000; Research Diagnostics Inc. RDI, Fitzgerald Industries, NJ), and then with secondary antibodies horseradish peroxidise–conjugated anti-mouse or anti-rabbit (1:10000; Jackson ImmunoResearch Laboratories). Antibody signals were visualized with enhanced chemiluminescence (PerkinElmer, Waltham, MA). Data were normalized to GAPDH band intensity from the same samples on the same membranes or normalized to cell number (collagen type I).

Statistical analysis

Data are mean ±SEM. One-way ANOVA was used for multiple-group comparisons, with a post-hoc Dunnett's test to compare differences between individual group and control means. A two-tailed $p<0.05$ represented statistical significance.

Results

MiR-1, miR-30a and miR-133a were down-regulated after PDGF-stimulation

After stimulation with PDGF-AB, the expression level of miR-21, miR-26a, miR-29b, miR-146a or miR-218 did not change in either LA or LV fibroblasts (Figure 1A-E). However, miR-1 expression level was decreased by 70-80% and miR-30a expression decreased by 60% in LA fibroblasts with PDGF-stimulation versus vehicle treatment. The changes in LV fibroblasts were smaller vs. LA changes- miR-1 expression in LV fibroblasts was not significantly altered while miR-30a was decreased by 46%, only at the higher concentration (Figure 1F and 1G). Similarly, miR-133a expression was down-regulated by ~40% at 10 ng/ml of PDGF and by ~80% at 50 ng/ml PDGF in LA fibroblasts, with smaller changes in LV (Figure 1H). Thus, miR-1, miR-30a and miR-133a are responsive to PDGF-stimulation and may participate in the downstream signaling of PDGF.

MiRNAs predicted to target JAK-STAT pathway

In silico prediction showed that multiple miRNAs can target different components of PDGF-JAK/STAT signaling (Figure 2A). In Chapter 3, it was shown that the expression of miR-1, miR-29b, miR-30a and miR-133a were downregulated in atrial fibroblasts from CHF dogs (Figure 2A). MiR-29 is predicted to target PDGFC/D, PDGF receptor β and STAT3. However, miR-29 was not changed after PDGF-stimulation (Figure 1C). Furthermore, miR-29b directly targets multiple extracellular matrix (ECM) genes including collagen-1 and collagen-3 [8, 9]. These findings suggest that the antifibrotic effects of miR-29b (and the profibrotic changes seen with its downregulation) are mediated through targeting ECM protein rather than the PDGF/JAK-STAT system. MiR-1 is predicted to target PDGFA and miR-30 and miR-133, JAK2. The changes in miR-1, miR-30a and miR-133 expression in CHF were inversely correlated with the changes of their putative targets (PDGFA and JAK2 were up-regulated in CHF, Chapter 2). Thus, miR-1,

miR-30 and miR-133 may contribute to the control of atrial fibrotic remodeling in CHF by directly targeting the JAK-STAT system. Sequence alignments between miR-1 and PDGFA, miR-30a and JAK2, miR-133a and JAK2 are shown in Figure 2B. Seven to nine complementary binding sites were found between the 3'-UTR sequences of target genes and the seed sites of these miRNAs. Within these 3 miRNAs, miR-30a and miR-133a share a common target gene (*JAK2*) but bind to different sites, providing the possibility that miR-30a and miR-133a have synergistic effects in regulating JAK-STAT. Hence, we focused on the functional studies of miR-30 and miR-133 in the following sections.

JAK2 is a direct target of miR-30a and miR-133a

Figure 3 shows the results of luciferase reporter assays. The sequences of the synthesized nucleotides are shown in Supplemental Figure 1. MiR-30a mimic reduced the luciferase activity of the construct containing the 3'-UTR sequence of *JAK2* by 30% (Figure 3A) vs. miRNA negative control. Similarly, miR-133a mimic reduced the luciferase activity by 20% (Figure 3B). These findings indicate that miR-30a and miR-133a can directly bind to the 3'UTR of the *JAK2* gene. AMO-30a and AMO-133a tended to increase the luciferase activities but the changes were not significant vs. AMO negative control.

JAK2 expression is regulated by miR-133a

MiR-133a mimic was transfected into atrial fibroblasts for miR-133a-overexpression and AMO-133a was used for miR-133a-knockdown. As shown in Figure 4A, mRNA expression of JAK2 was decreased by 40% (vs. miRNA negative control) after miR-133a-overexpression. This effect was reversed by co-transfection with AMO -133a (Figure 4A, the rightmost column). Similar

changes were seen in protein expression (Figure 4B and 4C): JAK2 protein was reduced by miR-133a mimic ($p=0.05$), and the reduction was attenuated by the addition of AMO-133a (Figure 4C, the rightmost column). These observations suggest that miR-133a regulates both mRNA and protein expression of JAK2 in atrial fibroblasts.

PDGF-AB (20 ng/ml) stimulation increased the protein expression of JAK2 in atrial fibroblasts by 2.5-fold vs. vehicle treatment (Figure 5A and B), consistent with the mRNA elevation of JAK2 after PDGF-stimulation (Chapter 2 Figure 4A). When PDGF-stimulated fibroblasts were transfected with miR-133a, JAK2 expression was attenuated to the level similar to vehicle-treatment. In contrast, when PDGF-stimulated fibroblasts were transfected with AMO-133a, JAK2 expression was upregulated to a higher level vs. PDGF-stimulation only. Similar to the change in JAK2 protein, collagen type I secretion was increased by PDGF-stimulation by ~2-fold vs. vehicle (Figure 5C and 5D). This increase remained upon transfection with miRNA negative control but was reversed by miR-133a overexpression. Taken together, these results suggest that miR-133a suppression may mediate the PDGF regulation of the expression of JAK2 and secreted collagen type I, implicating miR-133a as a potential antifibrotic molecule.

Discussion

In this study, we demonstrated that PDGF-stimulation reduces the expression of miR-1, miR-30a and miR-133a in canine atrial fibroblasts. JAK2 was validated as a direct target of miR-30a and miR-133a. Manipulating miR-133a can regulate JAK2 expression and collagen type I secretion in atrial fibroblasts. Our findings indicate that miR-30a and miR-133a mediate CHF effects by directly targeting the JAK-STAT system. MiR-133a-interference may be a potential therapeutic approach for reversing atrial fibrosis and AF prevention.

MiR-30 and miR-133 in cardiac remodeling and fibrotic signaling

MiR-133 has a critical role in determining cardiomyocyte hypertrophy [16]. MiR-30 and miR-133 have been shown to regulate fibrosis by directly targeting fibrotic regulators. For example, miR-30c and miR-133 regulate ventricular hypertrophy and fibrosis by targeting CTGF in both fibroblasts and cardiomyocytes [12]. MiR-133a reduces Ang-II induced perivascular and interstitial fibrosis by directly targeting collagen 1α1 [10]. Shan et al. showed miR-133 significantly suppressed TGF-β1 expression and contributed to nicotine-induced atrial remodeling and AF [17]. These findings suggest that miR-30 and miR-133 have multiple fibrotic targets and plays a key role in fibrotic response. However, the evidence of a role in AF-related atrial-selective fibrotic remodeling is limited. In this study, we identified a new target of miR-133a, JAK2, which is an important mediator of CHF-induced atrial fibrosis and a potential contributor to AF substrates (Chapter 2). Our results suggest a novel role of miR-30a and miR-133a in atrial fibrotic signaling, inhibiting the expression of PDGF-JAK-STAT components (Supplemental Figure 2). In addition, Liu et al. demonstrated that miR-133a functioned as an inhibitor of cardiomyocyte proliferation by targeting serum response factor (SRF) and cyclin D2 in the murine heart [18]. It is also possible that miR-133 regulates fibroblast proliferation through the same mechanism, which would be of interest for future studies.

MiRNAs in JAK-STAT signaling

Numerous studies have shown the regulatory roles of miRNAs in JAK-STAT signaling. Within these studies, miR-135, miR-216a, and miR-375 were shown to mediate apoptosis and inhibit cancer cell proliferation by targeting JAK2 [19-22]. Some miRNAs were found to be OncomiR (a miRNA that functions as an oncogene) as they target a negative regulator of JAK-STAT signaling

named suppressor of cytokine signaling (SOCS). For instance, miR-155 targets SOCS1, miR-19a targets SOCS3, and miR-9 targets SOCS5. These miRNAs promote the proliferation, migration or angiogenesis of cancer cells [23-25]. Multiple miRNAs were shown to interplay with STAT3 signaling as well [26]. For example, STAT3 induces miR-21 expression, which suppressed the expression of protein inhibitor of activated STAT3 (PIAS3), a negative regulator of STAT3 signaling. Thus STAT3 controls its own function by a positive feedback loop [27, 28]. In contrast, STAT3-mediated upregulation of miR-17-92 cluster could reversely suppress STAT3 expression, forming a negative regulatory loop between miRNAs and the STAT3 signaling; and miR-125b represses the proliferation and migration of osteosarcoma cells through downregulating STAT3 [29]. To date, most studies of the regulatory functions of miRNA on JAK-STAT signaling were on cancer or tumorigenesis. The only evidence available from the heart was that miR-214 regulated cardiomyocyte differentiation by targeting STAT3 [30]. Our study is the first to show the regulatory effects of miR-30a and miR-133a on JAK-STAT system in cardiac fibroblasts. Our findings may lead to further investigations on the roles of miRNAs in JAK-STAT signaling in cardiomyopathy paradigm.

Novelty and potential significance

To the best of our knowledge, this is the first study to provide direct evidence that miR-30a and miR-133a target the *JAK2* gene and modulate JAK2 expression. JAK2 is an important component of the JAK-STAT system that controls cell survival and proliferation. Our findings add to the current knowledge of the mechanisms of cardiac antifibrotic functions of miR-30a and miR-133a. In addition, we demonstrate a negative feed-back loop consisting of PDGF-miR-133a-JAK2, which may contribute to the control of the PDGF-JAK-STAT signaling cascade (Supplemental

Figure 2). Given that miRNAs represent a relatively-recently discovered regulatory molecules, and the JAK-STAT system is important in AF-promoting atrial fibrotic responses, investigating the biological functions of miRNAs and their contribution to fibrotic effects caused by JAK-STAT dysregulation is important to improve our understanding of atrial fibrogenesis and to develop novel miRNA-based therapies for AF prevention.

One important property of miRNAs is that a single miRNA can target hundreds of genes. It has been shown that genes targeted by one miRNA are functionally correlated within one signaling cascade [31]. MiR-30a and miR-133a target multiple levels of fibrotic signaling—from upstream regulatory cytokines (e.g. CTGF and TGF-β) to downstream effectors (e.g. JAK2 and collagen 1α1).

Therapeutic strategies inhibiting JAK-STAT system have been used in clinical such as in the treatment of myelofibrosis. But the side effects of JAK-STAT blockade were usually substantial [32]. Similar to other proliferative factors, JAK-STAT is broadly functional in multiple organs (e.g. liver, lung) and cell types (e.g. cardiomyocytes, fibroblasts). Organ-oriented or cell-targeted delivery may solve a part of this problem, but remains technically challenging. MiRNAs act to fine-tune mRNA or protein expression rather than acting as an all-or-none switch. Also, every miRNA has its own organ- or cell-type-specific expression signatures and a self-controlling metabolism system [33]. MiRNA interference is a promising component of the therapeutic strategy for modulating fibrotic responses, but targeting of multiple miRNAs and/or other targets might be needed.

Potential limitations and future studies

Fibroblast phenotypes may change after cell culture as short as 48 hours [15]. In this study, we cultured fibroblasts for one week before we could get the PDGF-stimulated and/or miRNA-transfected fibroblast samples. Compared to the previous study in which miRNA expression was quantified in freshly isolated fibroblasts (Chapter 2) [8], this study showed that the relative expression level of miR-1, miR-133a, and miR-30a (versus U6) were all decreased after culture (Supplemental Figure 3). For example, the relative expression of miR-30a in freshly isolated atrial fibroblasts was 0.8 (versus U6) while it was 0.025 in cultured fibroblasts; miR-133a was 1.8 in fresh fibroblasts versus 0.005 in the cultured ones. Although we had parallel controls in the culture system, the miRNA alterations observed in fibroblasts may not be directly extrapolated *in vivo*. Hence, the relationship between miRNA changes and *in vivo* PDGF stimulation remains to be explored. And the effects of culturing should be taken into considerations when we conduction functional studies on miRNAs in future.

In addition to miR-30a and miR-133a, miR-1 was also reduced by PDGF-stimulation in fibroblasts (Figure 1). However, the absolute expression levels of miR-1 was very low (0.01% versus U6) in fibroblasts after culture (compared to 0.5% and 2.5% for miR-30a and miR-133a respectively in Supplemental Figure 3). This is the other reason that we did not conduct miR-1-manipulation in cultured fibroblasts. The down-regulation of miR-1 may be due to the co-transcription of miR-1 and miR-133 as they belong to the same bicistronic unit [34]. MiR-30a was also confirmed to target JAK2 but its regulatory effect on JAK2 expression was not studied in this study. As multiple miRNAs may cooperatively target the same mRNA resulting in stimulus- and context-specific miRNA inhibition of protein expression, it is also necessary to investigate the synergistic effects of miR-30a and miR-133a in regulating JAK-STAT expression and their effects on atrial fibrotic remodeling in future.

In the present study, we provided an additional mechanism for miR-30a and miR-133a regulation of collagen secretion in atrial fibroblasts. The observation of collagen reduction after miR-133a overexpression could be attributed to the direct inhibitory effects of miR-133a on collagen 1α1 or CTGF, rather than on JAK2. However, which factor is the prominent regulator, or whether all these miR-133-targets contribute to atrial fibrotic responses and AF pathogenesis, remains to be further explored. Manipulations like CTGF knockout or JAK2 inhibition by pharmacological agents may be interesting in future studies, and may help us to gain a better understanding of the roles of miR-30a and miR-133a in AF-promoting atrial fibrosis.

Acknowledgments

The authors wish to thank Nathalie L'Heureux and Chantal St-Cyr for expert technical assistance.

Funding

Supported by the Canadian Institutes of Health Research (MGP6957), the Quebec Heart and Stroke Foundation, and the Foundation Leducq (European-North American Atrial Fibrillation Research Alliance, ENAFRA).

Disclosures

None.

References

[1] Li D, Fareh S, Leung TK and Nattel S. Promotion of atrial fibrillation by heart failure in dogs: atrial remodeling of a different sort. Circulation, 1999;100:87-95.

[2] Cardin S, Pelletier P, Libby E, Le Bouter S, Xiao L, Kaab S, et al. Marked differences between atrial and ventricular gene-expression remodeling in dogs with experimental heart failure. J Mol Cell Cardiol, 2008;45:821-31.

[3] Burstein B, Libby E, Calderone A and Nattel S. Differential behaviors of atrial versus ventricular fibroblasts: a potential role for platelet-derived growth factor in atrial-ventricular remodeling differences. Circulation, 2008;117:1630-41.

[4] Thum T, Gross C, Fiedler J, Fischer T, Kissler S, Bussen M, et al., MicroRNA-21 contributes to myocardial disease by stimulating MAP kinase signalling in fibroblasts. Nature, 2008;456:980-4.

[5] Bauersachs, J., Regulation of myocardial fibrosis by MicroRNAs. J Cardiovasc Pharmacol, 2010;56:454-9.

[6] van Rooij E, Sutherland LB, Thatcher JE, DiMaio JM, Naseem RH, Marshall WS, et al., Dysregulation of microRNAs after myocardial infarction reveals a role of miR-29 in cardiac fibrosis. Proc Natl Acad Sci U S A, 2008;105:13027-32.

[7] Thum, T., Noncoding RNAs and myocardial fibrosis. Nat Rev Cardiol, 2014;11:655-63.

[8] Chen Y, Wakili R, Xiao J, Wu CT, Luo X, Clauss S, et al., Detailed characterization of microRNA changes in a canine heart failure model: Relationship to arrhythmogenic structural remodeling. J Mol Cell Cardiol, 2014;77:113-24.

[9] Dawson K, Wakili R, Ordog B, Clauss S, Chen Y, Iwasaki Y, et al., MicroRNA29: A Mechanistic Contributor and Potential Biomarker in Atrial Fibrillation. Circulation, 2013;127:1466-75, 1475e1-28.

[10] Castoldi G, Di Gioia CR, Bombardi C, Catalucci D, Corradi B, Gualazzi MG, et al., MiR-133a regulates collagen 1A1: potential role of miR-133a in myocardial fibrosis in angiotensin II-dependent hypertension. J Cell Physiol, 2012;227:850-6.

[11] Beaumont J, Lopez B, Hermida N, Schroen B, San Jose G, Heymans S, et al., microRNA-122 down-regulation may play a role in severe myocardial fibrosis in human aortic stenosis through TGF-beta1 up-regulation. Clin Sci (Lond), 2014;126:497-506.

[12] Duisters RF, Tijsen AJ, Schroen B, Leenders JJ, Lentink V, van der Made I, et al., miR-133 and miR-30 regulate connective tissue growth factor: implications for a role of microRNAs in myocardial matrix remodeling. Circ Res, 2009;104:170-8, 6p following 178.

[13] Harada M, Luo X, Qi XY, Tadevosyan A, Maguy A, Ordog B, et al., Transient receptor potential canonical-3 channel-dependent fibroblast regulation in atrial fibrillation. Circulation, 2012;126:2051-64.

[14] Qi XY, Yeh YH, Xiao L, Burstein B, Maguy A, Chartier D, et al., Cellular signaling underlying atrial tachycardia remodeling of L-type calcium current. Circ Res, 2008;103:845-54.

[15] Dawson K, Wu CT, Qi XY and Nattel S. Congestive heart failure effects on atrial fibroblast phenotype: differences between freshly-isolated and cultured cells. PLoS One, 2012;7:e52032.

[16] Care A, Catalucci D, Felicetti F, Bonci D, Addario A, Gallo P, et al., MicroRNA-133 controls cardiac hypertrophy. Nat Med, 2007;13:613-8.

[17] Shan H, Zhang Y, Lu Y, Zhang Y, Pan Z, Cai B, et al., Downregulation of miR-133 and miR-590 contributes to nicotine-induced atrial remodelling in canines. Cardiovasc Res, 2009;83:465-72.

[18] Liu N, Bezprozvannaya S, Williams AH, Qi X, Richardson JA, Bassel-Duby R and Olson EN. microRNA-133a regulates cardiomyocyte proliferation and suppresses smooth muscle gene expression in the heart. Genes Dev, 2008;22:3242-54.

[19] Wu H, Huang M, Cao P, Wang T, Shu Y and Liu P. MiR-135a targets JAK2 and inhibits gastric cancer cell proliferation. Cancer Biol Ther, 2012;13:281-8.

[20] Navarro A, Diaz T, Martinez A, Gaya A, Pons A, Gel B, et al., Regulation of JAK2 by miR-135a: prognostic impact in classic Hodgkin lymphoma. Blood, 2009;114:2945-51.

[21] Wang S, Chen X and Tang M. MicroRNA-216a inhibits pancreatic cancer by directly targeting Janus kinase 2. Oncol Rep, 2014;32:2824-30.

[22] Ding L, Xu Y, Zhang W, Deng Y, Si M, Du Y, et al., MiR-375 frequently downregulated in gastric cancer inhibits cell proliferation by targeting JAK2. Cell Res, 2010;20:784-93.

[23] Collins AS, McCoy CE, Lloyd AT, O'Farrelly C and Stevenson NJ. miR-19a: an effective regulator of SOCS3 and enhancer of JAK-STAT signalling. PLoS One, 2013;8:e69090.

[24] Jiang S, Zhang HW, Lu MH, He XH, Li Y, Gu H, et al., MicroRNA-155 functions as an OncomiR in breast cancer by targeting the suppressor of cytokine signaling 1 gene. Cancer Res, 2010;70:3119-27.

[25] Zhuang G, Wu X, Jiang Z, Kasman I, Yao J, Guan Y, et al., Tumour-secreted miR-9 promotes endothelial cell migration and angiogenesis by activating the JAK-STAT pathway. EMBO J, 2012;31:3513-23.

[26] Cao Q, Li YY, He WF, Zhang ZZ, Zhou Q, Liu X, et al., Interplay between microRNAs and the STAT3 signaling pathway in human cancers. Physiol Genomics, 2013;45:1206-14.

[27] Loffler D, Brocke-Heidrich K, Pfeifer G, Stocsits C, Hackermuller J, Kretzschmar AK, et al., Interleukin-6 dependent survival of multiple myeloma cells involves the Stat3-mediated induction of microRNA-21 through a highly conserved enhancer. Blood, 2007;110:1330-3.

[28] Xiong Q, Zhong Q, Zhang J, Yang M, Li C, Zheng P, et al., Identification of novel miR-21 target proteins in multiple myeloma cells by quantitative proteomics. J Proteome Res, 2012;11:2078-90.

[29] Liu LH, Li H, Li JP, Zhong H, Zhang HC, Chen J and Xiao T. miR-125b suppresses the proliferation and migration of osteosarcoma cells through down-regulation of STAT3. Biochem Biophys Res Commun, 2011;416:31-8.

[30] Cai B, Li J, Wang J, Luo X, Ai J, Liu Y, et al., microRNA-124 regulates cardiomyocyte differentiation of bone marrow-derived mesenchymal stem cells via targeting STAT3 signaling. Stem Cells, 2012;30:1746-55.

[31] Rayner KJ, Esau CC, Hussain FN, McDaniel AL, Marshall SM, van Gils JM, et al., Inhibition of miR-33a/b in non-human primates raises plasma HDL and lowers VLDL triglycerides. Nature, 2011;478:404-7.

[32] Mascarenhas JO, Cross NC and Mesa RA. The future of JAK inhibition in myelofibrosis and beyond. Blood Rev, 2011;416:31-8.

[33] Chen CY, Chen ST, Fuh CS, Juan Xiong Q, Zhong Q, Zhang J, et al., Coregulation of transcription factors and microRNAs in human transcriptional regulatory network. BMC Bioinformatics, 2011;12 Suppl 1:S41.

[34] Chen JF, Mandel EM, Thomson JM, Wu Q, Callis TE, Hammond SM, et al., The role of microRNA-1 and microRNA-133 in skeletal muscle proliferation and differentiation. Nat Genet, 2006;38:228-33.

Figure Legends

Figure 1. MiRNA expression after PDGF-stimulation in atrial fibroblasts. Values are mean±SEM and presented as fold change relative to vehicle, *p<0.05, **p<0.01, ***p<0.001. Veh, vehicle; 10ng/ml or 50ng/ml, PDGF concentration at 10ng/ml or 50ng/ml; LA, left atrium; LV, left ventricle; FB, fibroblasts.

Figure 2. Putative targets of miRNAs. (A) *In silico* prediction of the putative targets of miRNAs in PDGF-JAK/STAT pathway. Red color indicates the miRNAs/genes up-regulated in CHF; Black color indicates the miRNAs/genes down-regulated in CHF. Black arrows indicate activation effects; Blue arrows indicate "targeting"; (B) Alignment of the sequences of selected miRNAs (lower sequences) with their target sites in the 3'-UTRs of target mRNAs (upper sequences). Complementarity is highlighted in yellow and connected by "|"; "." or ":" connection indicates weaker binding between the nucleotides compared to connection by "|".

Figure 3. MiR-30a and miR-133a directly target JAK2. (A) Luciferase activity for JAK2 gene in HEK293 cells transfected with miR-30a mimic (duplex) or knockdown (anti-miR30a oligonucleotides) probes. (B) Luciferase activity for JAK2 gene in HEK293 cells transfected with miR-133a mimic (duplex) or knockdown (anti-miR133a oligonucleotides) probes. Values are mean±SEM and presented as fold change relative to lipofectamine, ***p<0.005. Lipo, lipofectamine; miR, miRNA; NC, negative control; AMO, antisense oligonucleotides.

Figure 4. JAK2 expression after miR-133a manipulation in atrial fibroblasts. (A) mRNA expression of JAK2 in fibroblasts after miR-133a overexpression, with or without miR-133a-

knockdown. (B-C) Protein expression of JAK2 in fibroblasts with miR-133a overexpression, with or without miR-133a-knockdown. Values are mean ±SEM and presented as fold change relative to lipofectamine, ***p<0.005. Lipo, lipofectamine; miR, miRNA; NC, negative control; AMO, antisense oligonucleotides.

Figure 5. Effects of miR-133a manipulation on atrial fibroblasts with PDGF-stimulation. (A-B) JAK2 protein expression after PDGF-stimulation, with or without miR-133a manipulation. (C-D) Collagen type I (collagen-1) protein expression after PDGF-stimulation, with or without miR-133a manipulation. Values are mean ±SEM and presented as fold change relative to vehicle, *p<0.05, ***p<0.005. Veh, vehicle; miR, miRNA; NC, negative control; AMO, antisense oligonucleotides.

Figure 1

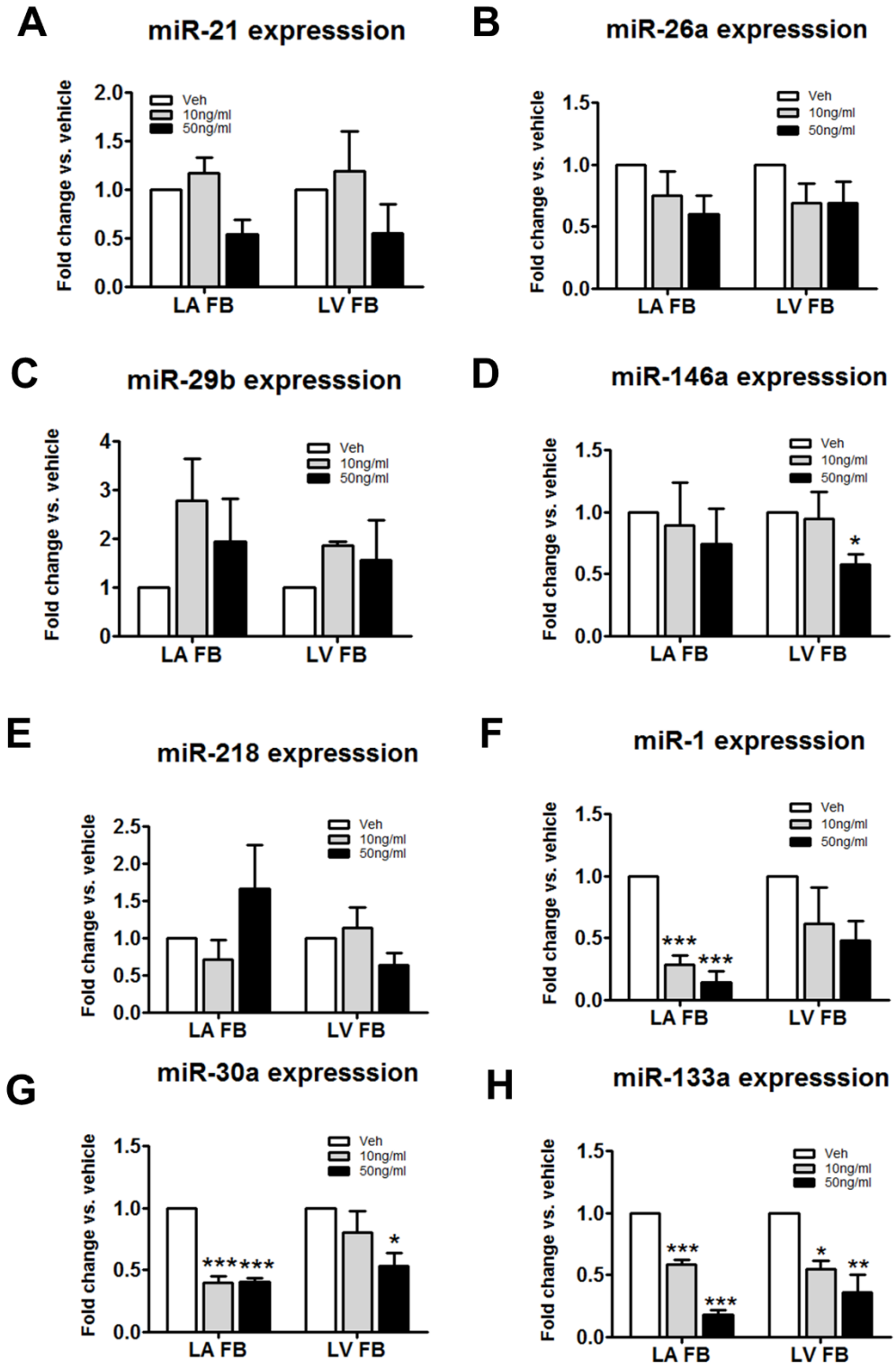
A
miR-21 expresssion
Fold change vs. vehicle
Veh
10ng/ml
50ng/ml
LA FB
LV FB
B
miR-26a expresssion
C
miR-29b expresssion
D
miR-146a expresssion
E
miR-218 expresssion
F
miR-1 expresssion
G
miR-30a expresssion
H
miR-133a expresssion

1

Figure 2

A

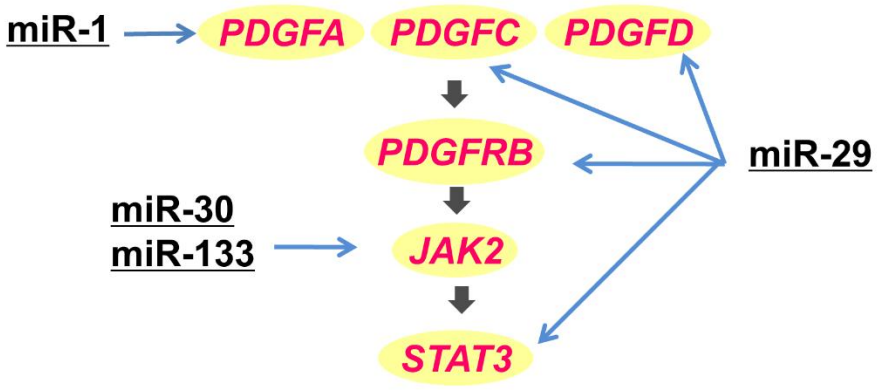

Up-regulated in CHF; Down-regulated in CHF

Activate; Target

B

PDGFA 3'UTR (NM_001190172.1)

```
887-TCTCCGGGACACGGATGTACATGGCGTGTTACATTCCTGA-927
       |.|.            |||:|   |  |  |||||||||:
    3'-AUGU-----------AUGAA--G-A-AAUGUAAGGU-5'
```

cfa-miR-1

JAK2 3'UTR (XM_541301.4)

```
4161-AAGAATACATTTTGAAATGAAACAAGTTTACAAAGATATA-4200
       |.:|.||   |  ||..       |:|||||||
    3'-CGAAGGUC-AGCUCC------UACAAAUGU-5'
```

cfa-miR-30a

JAK2 3'UTR (XM_541301.4)

```
3481-TGGCTGGATGAAGGACACGAACTTCACTCTGAGACCAAAA-3520
       |||||:|||||                  |.||||||
 3'-UGUCGACCAACUUC-----------------CCCUGGUU-5'
```

cfa-miR-133a

Figure 3

A

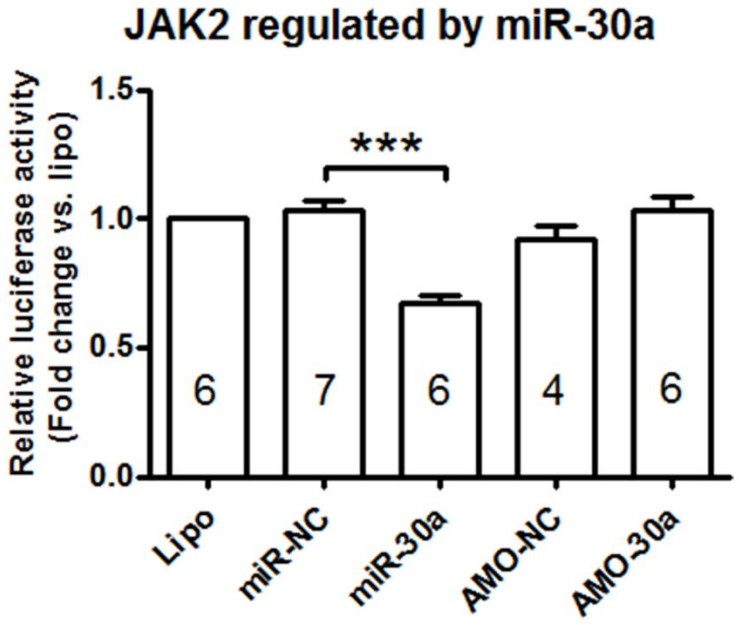
JAK2 regulated by miR-30a
Relative luciferase activity
(Fold change vs. lipo)
1.5
1.0
0.5
0.0
***
6
7
6
4
6
Lipo
miR-NC
miR-30a
AMO-NC
AMO-30a

B

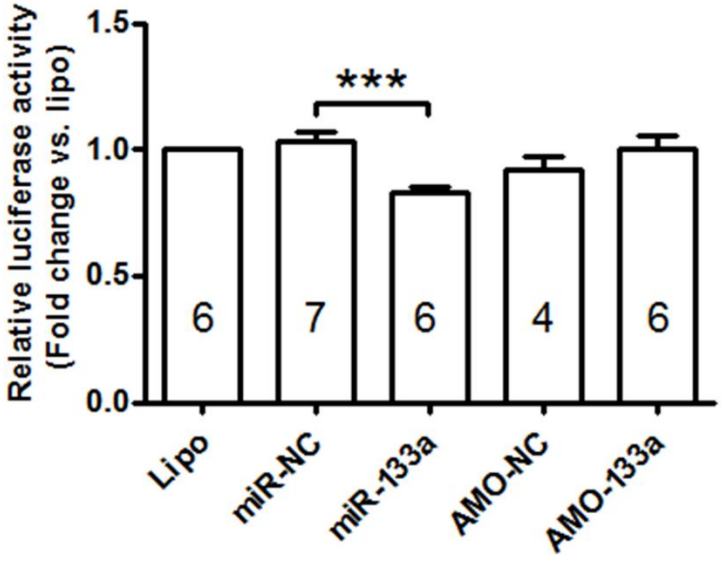
JAK2 regulated by miR-133a
Relative luciferase activity
(Fold change vs. lipo)
1.5
1.0
0.5
0.0
***
6
7
6
4
6
Lipo
miR-NC
miR-133a
AMO-NC
AMO-133a

Figure 4

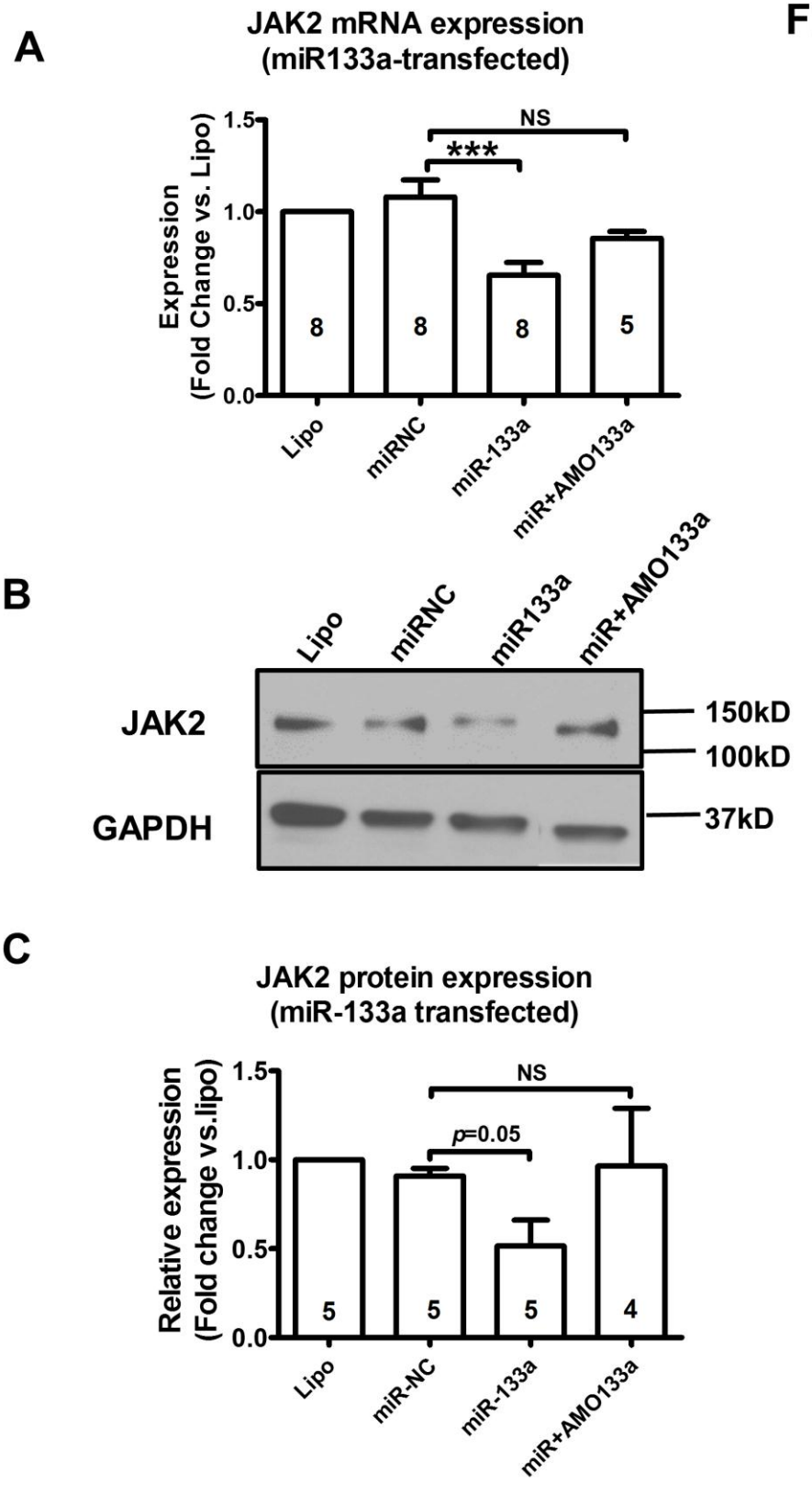
A
JAK2 mRNA expression
(miR133a-transfected)
Expression
(Fold Change vs. Lipo)
1.5
1.0
0.5
0.0
NS
***
8
8
8
5
Lipo
miRNC
miR-133a
miR+AMO133a
B
Lipo
miRNC
miR133a
miR+AMO133a
JAK2
GAPDH
150kD
100kD
37kD
C
JAK2 protein expression
(miR-133a transfected)
Relative expression
(Fold change vs.lipo)
1.5
1.0
0.5
0.0
NS
p=0.05
5
5
5
4
Lipo
miR-NC
miR-133a
miR+AMO133a

Figure 5

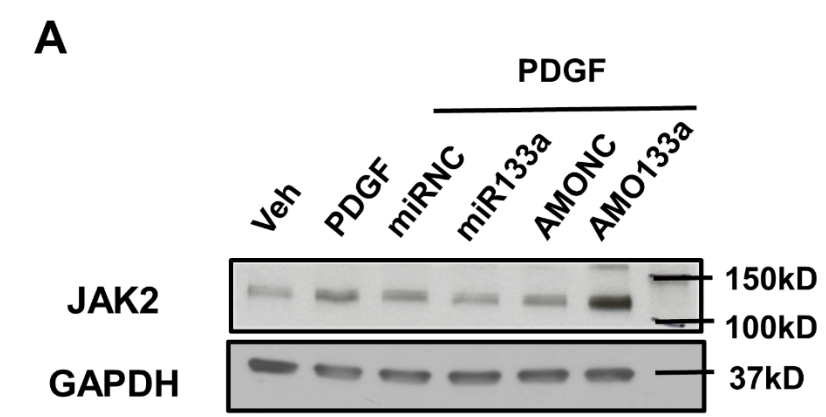
A
PDGF
Veh
PDGF
miRNC
miR133a
AMONC
AMO133a
JAK2
GAPDH
150kD
100kD
37kD

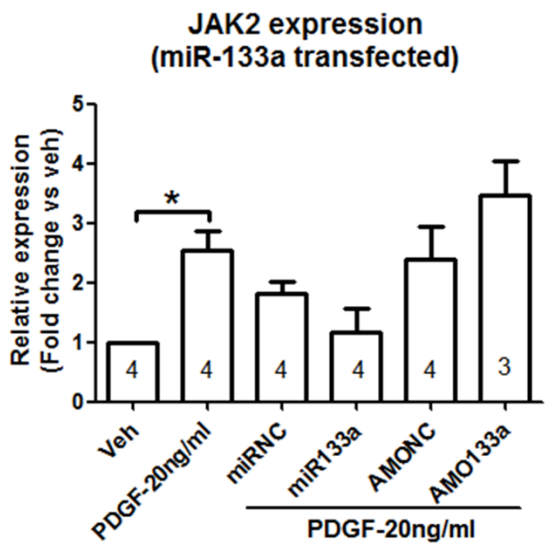
B
JAK2 expression
(miR-133a transfected)
Relative expression
(Fold change vs veh)
0
1
2
3
4
5
*
4
4
4
4
4
3
Veh
PDGF-20ng/ml
miRNC
miR133a
AMONC
AMO133a
PDGF-20ng/ml

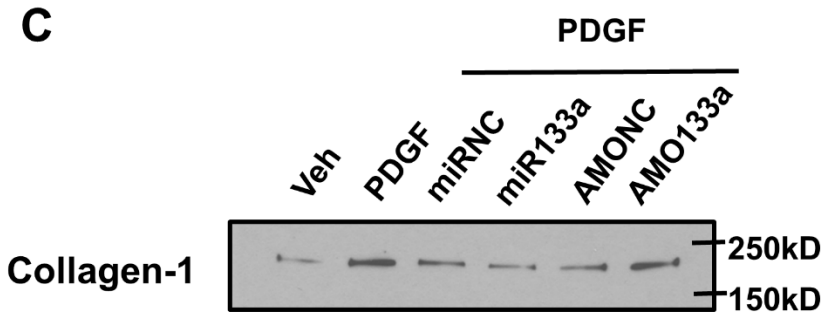
C
PDGF
Veh
PDGF
miRNC
miR133a
AMONC
AMO133a
Collagen-1
250kD
150kD

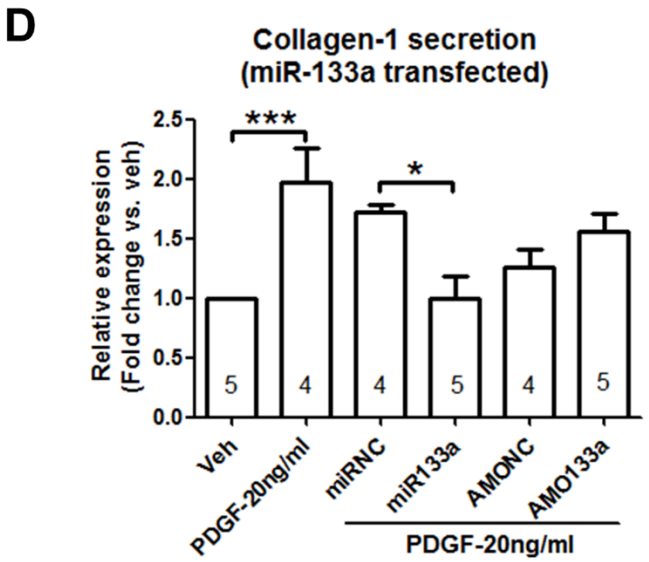
D
Collagen-1 secretion
(miR-133a transfected)
Relative expression
(Fold change vs. veh)
0.0
0.5
1.0
1.5
2.0
2.5
***
*
5
4
4
5
4
5
Veh
PDGF-20ng/ml
miRNC
miR133a
AMONC
AMO133a
PDGF-20ng/ml

Supplemental Figure Legends

Supplemental Figure 1. Sequences of the oligonucleotides used for miRNA manipulation. miR, miRNA; NC, negative control; AMO-NC, miRNA antisense oligonucleotides; "+" indicates the locked sites of the AMO sequence.

Supplemental Figure 2. Schematic illustration of the roles of miR-30a and miR-133a in atrial fibrotic pathways. Black arrows (activation) or "⊥" (inhibition) indicate the known effects from the literature (1); Blue arrows indicate the findings from Chapter 2 (2); Green "⊥" indicate the findings from Chapter 3 (3); Red "⊥" indicate the findings from this study (4). Bold arrows or "⊥" indicate direct effects and dash ones indicates indirect effects. CHF, congestive heart failure; CTGF, connective tissue growth factor; JAK2, Janus kinase 2; PDGF, Platelet derived growth factor; STAT3, signal transducers and activators of transcription 3.

Supplemental Figure 3. Expression of miRNAs in fibroblasts after one week culture. Values are mean±SEM and presented as fold change relative to U6. LA, left atrium; LV, left ventricle.

Supplemental Figure 1

miR-NC
5’- UCAAGUAACUUCAACCAGCUGU -3’
5’- AGCUGGUUGAAGUUACUUGAAU -3’

miR-30a
5’- UGUAAACAUCCUCGACUGGAAG -3’
5’- UCCAGUCGAGGAUGUUUACAGC -3’

miR-133a
5’- UUGGUCCCCUUCAACCAGCUGU -3’
5’- AGCUGGUUGAAGGGGACCAAAU -3’

AMO-NC
5’- T+C+C+T+AGAAAGAGTAGAT+C+G+A+T -3’

AMO-30a
5’- +C+T+T+C+CAGTCGAGGATGT+T+T+A+C+A -3’

AMO-133a
5’- A+C+A+G+CTGGTTGAAGGGGA+C+C+A+A -3’

Supplemental Figure 2

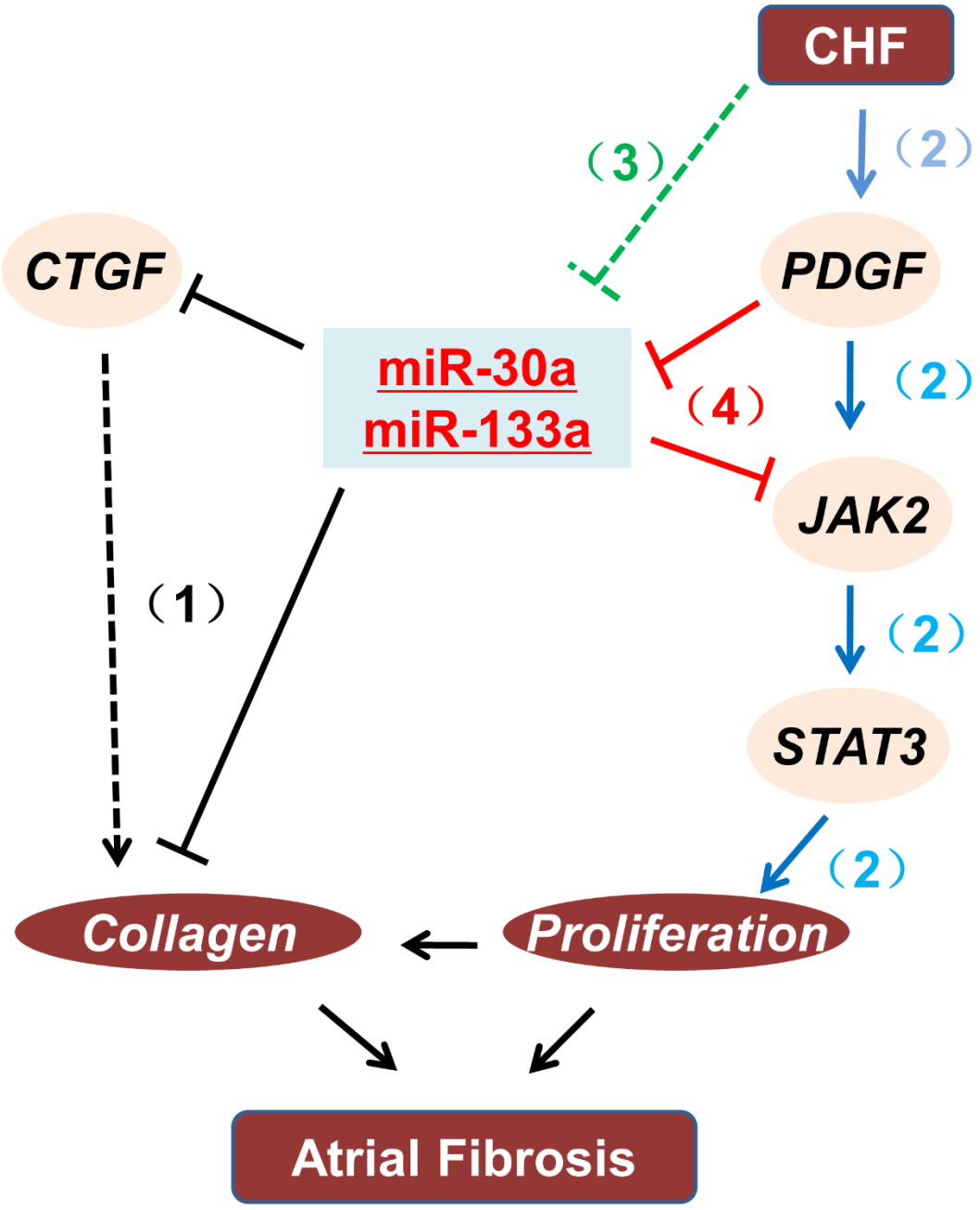

Supplemental Figure 3

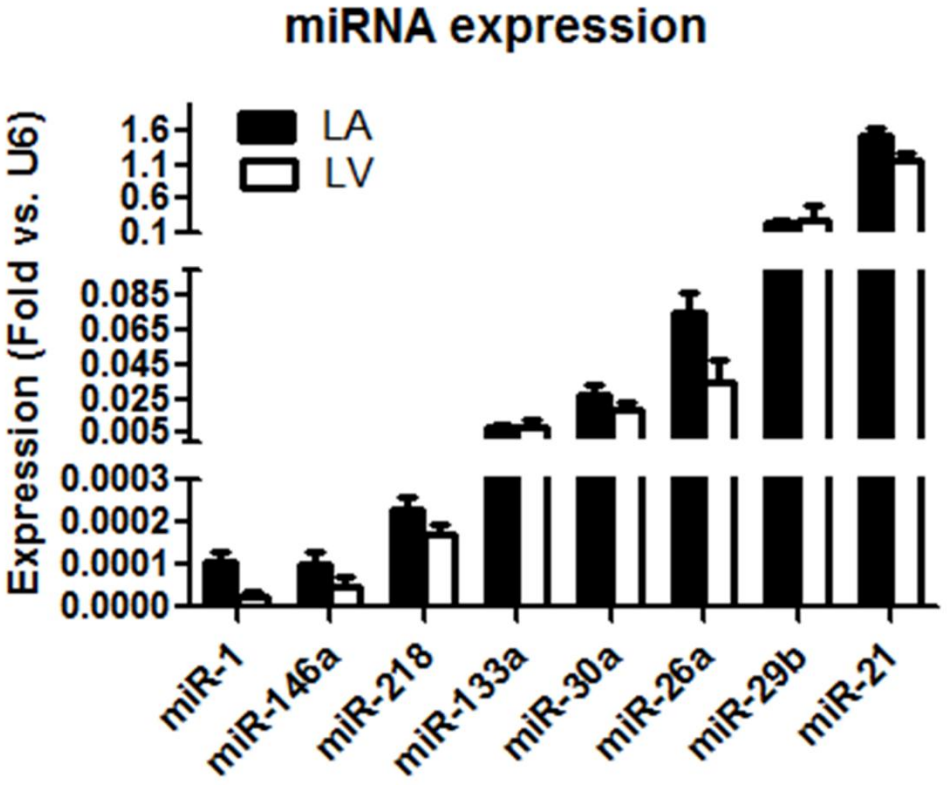

Chapter 5

General Discussion

5.1 **Summary and novel contributions**

The underlying mechanism of atrial-ventricular differential remodeling is important for our understanding of the pathophysiology of AF. A previously published paper from Dr. Nattel's laboratory indicated a potential role for PDGF in the differential response of atrial and ventricular fibroblasts to fibrotic stimuli [1]. However, this paper did not investigate the downstream signaling that was triggered by PDGF and how this regulated atrial-selective fibrosis in the HF paradigm. The first study in this thesis (Chapter 2) addressed these questions and revealed a novel role for the JAK-STAT system in the atrial fibrotic response. In this study, three novel contributions to knowledge arose. First, we showed the activation of PDGF-JAK-STAT components were enhanced in an experimental CHF model and in PDGF-stimulated cultured fibroblasts, revealing JAK-STAT as an active downstream signaling cascade of PDGF that has pathological relevance. Second, we demonstrated that activation of the PDGF-JAK-STAT system in both an in vivo CHF model and in cultured fibroblasts was atrial selective. This finding provides, for the first time, a molecular signaling basis for AF-related atrial-selective remodeling, and explains how PDGF contributes to this process. The third novel contribution of this study was that we identified STAT3 blockade as an effective way to prevent atrial fibrotic remodeling *in vitro* and *in vivo.* STAT3 inhibition by pharmacologic intervention significantly reduced PDGF-promoted ECM enhancement in fibroblasts and attenuated atrial fibrosis post-MI. The effect of STAT3 blockade further confirms that JAK-STAT is an active participant in the PDGF-stimulated fibrotic response in the atria. Treatment with a STAT3 inhibitor improved atrial remodeling, including fibrotic remodeling and electrical conduction in post-MI mice. However, ventricular remodeling was not ameliorated. This is a particularly important finding because thus far there are no specific treatments to prevent atrial fibrosis. STAT inhibition may

be a new therapeutic approach for reversing arrhythmogenic structural remodeling in the atria and for AF prevention.

Although multiple miRNAs are implicated in various AF-associated pathologies (Section 1.7.2.1), the whole picture of the miRNA system response caused by CHF or AF is still lacking. The novel contribution of the second study (Chapter 3) was the detailed cell-type and chamber-specific characterization of miRNA changes with time in a CHF model that has clinical relevance. This study also identified a number of miRNAs as contributors to atrial-selective fibrotic remodeling and AF substrate. The evidence is provided from four aspects: (1) miRNA changes correlated with the time course of atrial fibrosis development; (2) miRNA changes were larger in the atria than the ventricles; (3) fibroblasts were particularly affected compared to cardiomyocytes; and (4) ECM protein changes correlated with those of regulatory miRNAs in fibroblasts. A third distinct contribution of knowledge is that we found that a program of miRNA changes may be more important to a disease condition than a single miRNA change. MiRNAs may work in concert to participate in pro-fibrotic signaling (Section 1.7.1 Figures 7 and 9) by targeting one signaling cascade or common fibrotic genes. The overall miRNA activity often results from the sum of subtle modulations on multiple constituents of the same pathway, rather than from a strong effect on a single regulator. This study also stresses the concept that cellular changes cannot be predicted from tissue data and that cell-type specific miRNA pattern changes must be considered when analyzing miRNA regulation. This is important because most relevant published studies measured miRNA expression in whole tissue samples that may mask changes in specific cell types.

In the second study, we postulated that miRNAs play a role in AF-associated fibrotic remodeling, and we proceeded to correlate changes in regulatory miRNAs to downstream ECM

alterations. However, we did not provide evidence of the direct targeting effects of miRNAs on fibrotic genes. Given the number of miRNAs that changed, this would have been unfeasible. However, we addressed this issue for a specific miRNA signaling system in the third study (Chapter 4). Here, we first demonstrated that three miRNAs, miR-1, miR-30a, and miR-133a are responsive to PDGF stimulation in fibroblasts. Changes in these miRNAs were inversely correlated with the alterations in the PDGF-JAK-STAT system in the canine CHF model, as well as in cultured fibroblasts subjected to PDGF stimulation. Importantly, the alterations in miRNAs and JAK-STAT signaling were both atrial selective, suggesting that miRNAs may serve as a negative regulator of the PDGF-JAK-STAT system. The second novel finding of Study 3 was that we were able to validate JAK2 as a direct target of miR-30a and miR-133a. This will assist future studies in determining novel functions of miR-30a and miR-133a in cardiac remodeling. The third contribution of this study was that we were able to use miR-133a manipulation to modulate JAK2 and collagen type I expression, and fibroblast response subject to PDGF-stimulation. This is an important demonstration as it provides new insight into miRNAs as potential targets for reducing atrial fibrosis and AF prevention. In summary, the main findings of the three studies in this thesis are illustrated in Figure 1.

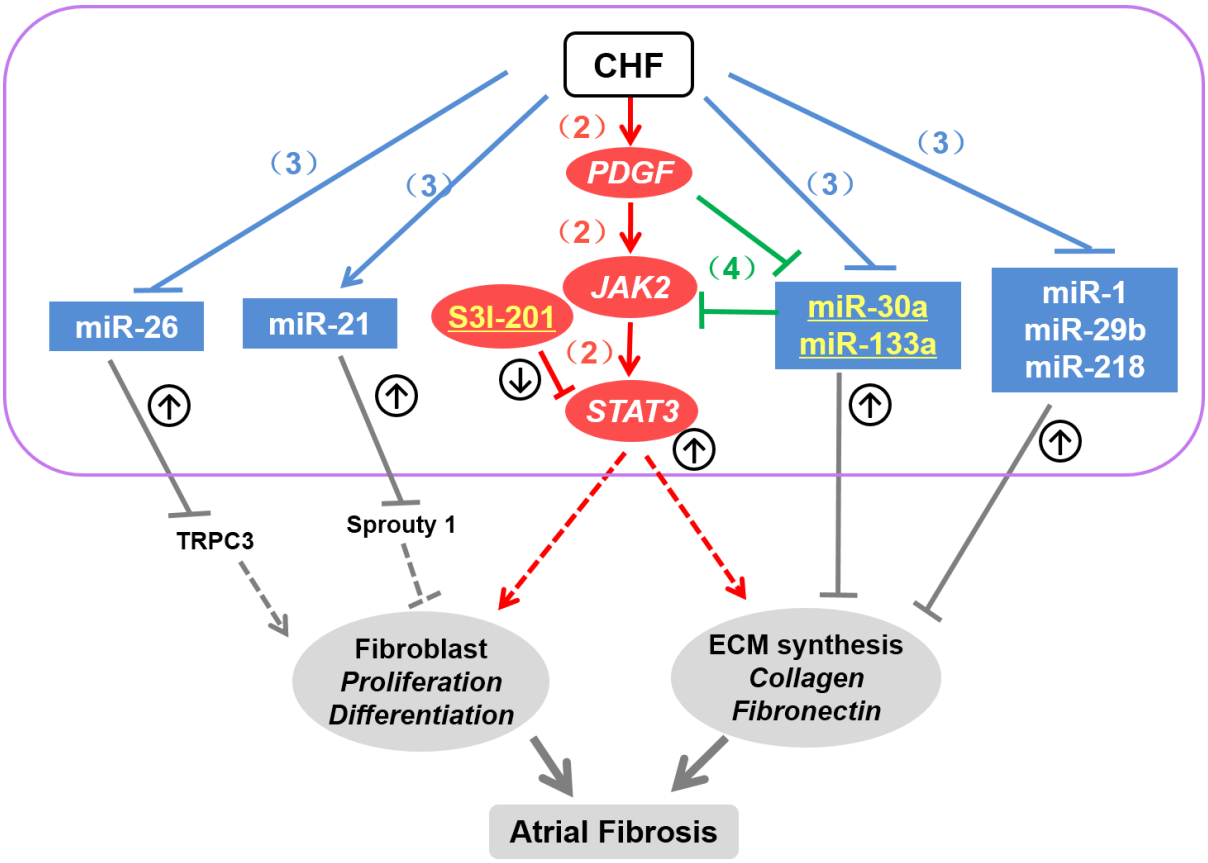

Figure 1. Schematic illustration of the key findings of this thesis.

The upper part in purple frame indicate the molecules or pathways identified in this thesis: The lower part outside of the purple frame are the known functions from the literature (introduced in Section 1.7.2.4). CHF induces activation of PDGF-JAK-STAT system (Chapter 2, red ovals) and alterations of miRNA expressions (Chapter 3, blue rectangles). MiR-30a and miR-133a mediate CHF effect by targeting JAK2 (Chapter 4, green signs). MiRNAs and miR-30a/miR-133a-targeting JAK-STAT system regulate fibroblast behavior and/or ECM synthesis, contributing to the development of atrial fibrosis. MiR-26 inhibit fibroblast proliferation through targeting TRPC3; miR-21 activate regulate fibroblast through targeting sprout 1; miR-30a, miR-133a, miR-1, miR-29b and miR-218 directly target ECM protein synthesis; STAT3 increases both fibroblast proliferation and ECM production, which is evidenced in Chapter 2 (red dash arrows). Yellow color indicate the anti-fibrotic molecules that were used in this thesis. Arrows (without circle) means activation and "⊥" means inhibition. Bold arrow or "⊥" indicate direct effects and dash ones indicate indirect effects. The black upward arrow in circle indicates the net effects of CHF on atrial fibrosis (activation) via mediating different miRNAs and STAT3. The black downward arrow in circle indicates S3I-201 represses atrial fibrosis. CHF, congestive heart failure; ECM, extra-cellular matrix; JAK2, Janus kinase 2; PDGF, Platelet derived growth factor; STAT3, signal transducers and activators of transcription 3; TRPC3, Transient receptor potential canonical 3.

5.2 **Unanswered questions and future directions**

5.2.1 What is the underlying mechanism of atrial vs. ventricular differential remodeling and what is the role of miRNAs?

Previous studies have documented greater changes in terms of gene expression, tissue fibrosis, inflammation, neurohormones, MAPKs, and cell-death in LA vs. LV in dogs with experimental CHF [2, 3]. In Chapter 3, we demonstrated greater alterations in miRNA expression in LA compared with LV. It remains unclear whether miRNAs trigger LA–LV differential remodeling or whether miRNA changes are simply part of a generally more intense response in the atria. Atrial fibroblasts are known to be more responsive than ventricular fibroblasts to a broad range of stimuli, particularly pro-fibrotic stimuli [1]. This may be attributed to higher Ang-II density, or higher STAT3 and PDGF receptor expression in atria vs. ventricles [1, 4, 5]. TGF-β is differentially activated in LA vs. LV in CHF, and is known to regulate miRNAs like miR-21 and miR-29 [3, 6, 7]. In Chapter 2 and Chapter 4, we demonstrated that PDGF expression is higher in LA vs. LV in CHF, and that PDGF stimulation down-regulated the expression of miR-1, miR30a, and miR-133a. Together, this evidence potentially contributes to the differential responses observed in the two chambers. To compare the regulatory roles of secreted factors vs. miRNAs, the first step is to understand the controlling mechanism of miRNA expression. It has been shown that Ang-II induced CTGF and lysyl oxidase (LOX, a secreted protein that enhances collagen crosslinking) expression, and up-regulated miR-21 expression by increasing the expression of Dicer and Drosha [8], which are important enzymes for miRNA generation (Section 1.7.2.2). Downregulation of miR-26a in atrial fibrosis and AF is mediated by nuclear factor of activated T cells (NFAT) [9]. Also, paired-like homeodomain transcription factor 2 (Pitx2), a gene that is strongly associated with AF susceptibility [10], represses SAN

development by altering miRNA expression [11]. The regulatory effects of these miRNA-regulators are possibly predominant in the atria. It would be of interest to compare the expression or functions of these potential regulators (LOX, NFAT, and Pitx2) in atria and ventricles from AF models. Also, it is important to investigate how transcription factors are regulating miRNA expression, which can be studied through protein-DNA promoter binding assays. In addition, some miRNAs are co-transcribed with its host genes during development and pathogenesis, e.g. miR-208 is co-transcribed with the alpha-myosin heavy chain (α-MHC) gene [12]. The relationship between the expression and functions of miRNA and its host genes might provide insights into the regulatory mechanisms of miRNAs.

5.2.2 What are the regulatory mechanisms of STAT3 activity and how is it relevant to AF?

In Chapter 2, we demonstrated that STAT3 is a critical transcription factor that controls fibroblast behavior and atrial fibrotic remodeling. We showed that the activation of STAT3 by PDGF is possibly through JAK2, but we did not provide the direct evidence of how STAT activity is controlled. STAT3 activity is known to be modulated through multiple mechanisms including through Rac1 and JAKs (Section 17.1.6). Three major classes of endogenous inhibitors of STAT3 shave been identified [13-15]. Suppressor of cytokine signaling (SOCS) is a responsive gene and feedback inhibitor of the JAK-STAT pathway. It deactivates JAKs (e.g. SOCS1) and prevents STAT3 dimerization and activation (e.g. SOCS3) [16]. Loss of SOCS3 in the liver promotes fibrosis by enhancing STAT3-mediated TGF-β1 production [17]. However, the role of SOCS in atrial fibrosis has not yet been revealed. Protein inhibitor of activated STAT3 (PIAS3) directly binds to STAT and blocks its activity [18]. PIAS3 expression and STAT3–PIAS3 interaction increase with the progression of liver fibrosis [19]. Pacing induced

atrial myocytes show enhanced STAT3 activity through the formation of a complex of PIAS3 and zinc finger homeobox 3 (ZFHX3, also named ATBF1), a gene variant found in AF patients [20]. However, the detailed mechanism of PIAS3 providing AF substrate remain to be explored. A third negative regulator of STAT3 is protein tyrosine phosphatase non-receptor type 1 (PTPN1, or PTP1B), which can dephosphorylate tyrosine receptor kinases and JAKs [15]. These negative regulators of STAT3 activity have potential roles in mediating AF-associated fibrosis progression. Thus, it is necessary to assess the expression and function of these regulators in CHF or other clinically relevant models of AF. Furthermore, nuclear STAT3 binding capacity and nuclear translocation of STAT3 are increased in a porcine model of AF [21], suggesting that controlling mechanisms of STAT3 translocation and DNA binding are other important aspects that merit further investigation for a better understanding of AF pathology.

5.2.3 Is atrial PDGF/JAK-STAT inhibition an effective and safe approach for AF prevention?

In Chapter 2, we demonstrated that STAT3 inhibition is effective at attenuating atrial fibrosis and improving atrial electrical conduction. Interestingly, we observed a reduction in atrial but not ventricular dilation after S3I-201 treatment. However, we did not measure AF duration after S3I-201 treatment due to the difficulty of inducing AF in mice. It remains to be verified whether STAT3 inhibition can reduce AF susceptibility in a clinically relevant animal model, e.g. VTP in dogs.

The broad range of STAT3 regulated genes control cell survival, cell cycle progression, inflammation, ECM homeostasis and cell-to-cell communication in the heart (Section 1.7.1.6) [22]. Thus, STAT3 inhibition may have significant effects on other cell types, e.g. cardiomyocytes and endothelial cells [22], possibly inducing adverse effects on cardiac function.

In Chapter 2 we focused on the role of JAK-STAT signaling in fibroblasts but we did not assess its role in cardiomyocytes. JAK-STAT was also highly expressed in cardiomyocytes of control dogs (Chapter 2 Supplemental Figure 2). A detailed characterization of JAK-STAT changes in cardiomyocytes during the VTP timecourse is necessary for future studies. No toxic effects of STAT3 inhibition were shown in MI mice of our study, or other animal models of cardiac hypertrophy or tissue fibrosis [23-25]. However, the safety profile of STAT3 inhibition in other animal models of HF or in patients with AF remains to be seen. Also, it is necessary to compare STAT3 blockade to interventions targeting other signaling pathways known to be involved in atrial fibrosis, such as TGFβ-1 and Ang-II pathways. While we demonstrated that STAT3 activation is associated with fibroblast proliferation and increased ECM production, we did not study the mechanism of how STAT3 regulates fibroblast behavior, including ECM production and secretion. We found that TGFβ signaling is one of the strongest contributors (Chapter 2, Supplemental Figure 3) to the downstream signaling of STAT3. We also found that the fibronectin-1 and LOX genes -are predicted to have STAT3-binding sites in their promoters, as indicated by sequence alignment. It would be of interest to study whether STAT3 directly regulates fibronectin-1 and LOX expression and how this contributes to the atrial fibrotic response. Furthermore, STAT3 activates transcription of angiotensinogen via direct binding to its promoter [26]. A STAT response element has been found in the promoter region of L-type calcium channels in mice [27]. Taken together, further work is needed to identify additional STAT-responsive genes for better understanding of the role of STAT3 in atrial fibrogenesis. And this is an important step before we can develop effective STAT3-targeting therapeutic approaches for AF prevention.

5.2.4 How can we target fibrogenesis with better efficacy and safety?

As mentioned in the Introduction, the fibrotic response may have evolved for adaptive and protective purposes, especially during early fibrogenesis [28]. Most pro-fibrotic factors are intrinsically secreted to promote cell growth and survival, and to protect the injured myocardium (Section 1.7.1) [29]. For structural remodeling to be an effective antiarrhythmic strategy, it must target only the maladaptive processes that underlie the dysregulation of ECM balance. Some cytokines may be involved in multiple physiological processes with broad beneficial effects (Section 1.3.3 and 1.7.1). It is important to consider that complete blockade of the signaling cascade might lead to adverse consequences. For example, TGF-β is involved in immunosuppression and tumor suppression [30]. Homozygous TGF-β1 knockout mice die shortly after birth due to hyper-inflammation [31]. Therefore, more specific targets for anti-fibrotic therapy are needed that block pro-fibrotic effects but leave the beneficial effects untouched. However, it is still challenging to distinguish "adaptive" from "maladaptive" fibrotic remodeling, and it varies in different disease conditions. The situation is further complicated by the fact that the dysregulation of fibrotic factors are not only time-dependent, but also tissue- and cell-type–dependent. Adenoassociated viruses (AAV) with cardiac-specific and/or inducible promoters could solve this problem [32]. The promoter of α-myosin heavy chain, the ventricular form of myosin light chain 2, and the cardiac troponin C are considered so far to achieve restricted transgene expression in cardiomyocytes [33]. Fibroblast-specific protein (FSP) 1–Cre-driven gene deletion are suggested for fibroblast-restricted transgene in mice [34, 35], but both of the efficiency and specificity remain questionable [36]. Thus far, none of the available markers of cardiac fibroblasts encompasses the combination of sensitivity and specificity to be considered definitive [37, 38]. Each marker might be utilized in a particular context as the relative

expression may vary with different stages of development or injury. The investigation of specific fibroblast markers merits continued effort, since it will greatly contribute to better understanding this dynamic myocardial cell and to developing fibroblast-targeting therapies for reducing atrial fibrosis.

5.2.5 Targeting miRNAs in AF prevention—which one should we choose?

In Chapter 3, we demonstrated multiple potential miRNAs involved in AF-promoting atrial fibrosis. However, the relative importance of individual miRNAs in AF-pathogenesis remains unknown. Each miRNA has its own expression profile with chamber/cell type-selective and time-dependent signature. The differential changes of miRNAs along the VTP-timecourse indicate that individual miRNA changes likely depend on the underlying pathology and disease stage, suggesting that time-specific treatment may be necessary for miRNA-based therapies. Although we showed a system response of miRNA changes in CHF, it does not necessary mean that we should target all of them to reverse the fibrotic remodeling. Identification of the target genes of the dysregulated miRNAs, and the functional link among these genes is critical before we can develop miRNA-based therapies for AF.

MiR-21 shows the biggest changes in CHF compared to other upregulated miRNAs (Chapter 3 Figure 4A and 4B), and its time-course of changes parallel with ECM changes (Chapter 3 Figure 8). Also it is increased in patients with AF, and anti-miR-21 treatment is sufficient to reduce AF susceptibility in rats [8, 39]. Thus miR-21 may be the most important miRNA in the ECM response. However, our results suggest that the development of atrial fibrosis and AF is a progressive process (Chapter 2 Supplemental Figure 1 and Chapter 3 Figure 1), and it probably takes time for the ECM to deposit in the interstitial space of cardiac tissue.

The alterations of the regulatory miRNAs that target ECM-regulators possibly occur before an increase of atrial fibrosis is observed. Our study (Chapter 3) suggest that miR-1, miR-26a/b, miR-29b and miR-30a and miR-133a/b may be the most relevant miRNAs to AF, as they show the largest and sustained downregulations starting from the early stage (12 hour or 24 hour of VTP) of CHF development. MiR-26 and miR-29b have also been shown to be reduced in AF patients, which is relevant to their anti-fibrotic functions [9, 40]. Thus far, miR-21 and miR-29b are the most intensively studied in cardiac fibrogenesis, and might have the best clinical potential for reversing cardiac fibrotic remodeling. Nevertheless, miR-1, miR-30a and miR-133a/b are important contributors to the AF substrate, but their clinical relevance remains to be revealed. The detailed regulatory mechanisms, the efficacy, specificity, and safety of these miRNAs applied in AF prevention remain to be explored and it will be of great value for a better understanding of AF pathologies.

5.2.6 MiRNAs in the clinic -where should we go?

Given their key function in gene regulation, and their stability, tissue-specific expression pattern and secretion into corresponding bodily fluids, research on miRNA-based therapeutics in cardiovascular disease have been highly appealing over the past few years [41-43]. One important advantage of miRNAs as potential drug targets is that it usually tunes rather than dampens target expression [44], which should be less detrimental to the healthy tissues. Organ- or even cell-type–specific delivery strategies aimed at minimizing off-target effects for miRNA therapies have been developed. For example, cardiac-specific miRNA overexpression can be achieved via cardiotropic AAV-mediated overexpression, which was shown for the treatment of HF and cardiac hypertrophy in *in vivo* studies [45, 46], or AAV-mediated knockdown (miRNA

sponge) which increased fibrosis content in mice [40]. Modification of specific miRNAs by miRNA mimics (overexpression) or antagomir oligonucleotide (AMO, knockdown) has also been evaluated as a therapeutic option in experimental HF and AF models [39, 45, 47]. However, none of these approaches have been tested on patients with AF. Miravirsen (SPC3649) is the only miRNA drug (antagomiR/inhibitor of miR-122) that has entered phase II clinical trials for the treatment of chronic hepatitis C virus infection; thus far, it has demonstrated an excellent safety and efficacy profile [48]. MiRNA-knockdown technologies by anti-miRNA oligos (or AMO) are being developed to improve the stability of delivery methods and specificity of the molecule, and also in avoiding activation of immune responses [49]. Chemical modifications, such as phosphorothioate, 2-O-methylgroup-modifiedoligonucleotides, and locked nucleic acid-modified oligonucleotides are used [49, 50] but remain complex. Further work is clearly needed to improve the modification of anti-miRNA oligos and to assess its clinical value.

In addition to the potential therapeutic role of miRNA in AF, miRNAs have been suggested as a potential biomarker for AF due to their naturally small size and stable properties [51]. MiR-21, miR-29b, miR208a/b, and miR-146a are found to be dysregulated in CHF (Chapter 3), which is consistent with the clinical measurement on AF patients [40, 52, 53]. Liu et al. found that miR-146a, miR-150, miR-19a, and miR-375 were dysregulated in the plasma of AF patients [52]; Nishi et al. demonstrated miR-21, miR-23b, miR-199b, and miR-208b were up-regulated in the right atrial tissue of AF patients [53]; and Dawson et al. showed that miR-29b was reduced in both plasma and atrial tissue of AF patients [40]. Early miRNA changes seen in in the VTP timecourse (e.g. miR-29b and miR-208a were both decreased from 12 hours of VTP in fibroblasts) might be used for early diagnosis or prevention of atrial fibrosis, but their clinical utility has yet to be confirmed. In our studies, we assessed miRNA expression in tissue and cell

preparations, but not in blood samples from CHF dogs. Since blood testing is the fastest, most convenient and least invasive method for diagnostic analysis and comparative studies in the clinical laboratory, further investigation is needed to evaluate the potential of additional miRNAs as biomarkers for AF. Additionally, the exact source, location, and the role in cell-to-cell or tissue-to-tissue communication of circulating miRNAs need to be better defined. Technological advances are required to enable rapid, reliable, and reproducible results for the absolute quantification of circulating miRNA in clinical practice. In summary, it is expected that further investigation of miRNAs as potential therapeutic targets and/or biomarkers may greatly contribute to the development of early diagnostics, monitoring, and treatment for AF and general pathogenic cardiac remodeling.

5.3 **Conclusions**

Given their potential anti-AF benefits, identifying and understanding the regulatory factors and signaling pathways involved in atrial fibrotic remodeling are critically important. In this thesis, we identified the regulatory effects of JAK-STAT system and miRNAs on atrial fibrotic signaling; both mechanisms can be considered as novel regulators, as well as potential therapeutic targets, of AF prevention. We also emphasized the importance of time-, chamber-, and cell-specific studies in cardiac pathophysiology. Data demonstrating atrial-selective fibrotic remodeling mediated by PDGF, JAK-STAT, and miRNAs suggest the presence of respective atrial selective/predominant therapeutic targets, which may be useful for “upstream” AF therapy.

References-General Discussion

1. Burstein, B., et al., *Differential behaviors of atrial versus ventricular fibroblasts: a potential role for platelet-derived growth factor in atrial-ventricular remodeling differences.* Circulation, 2008. **117**(13): p. 1630-41.
2. Cardin, S., et al., *Marked differences between atrial and ventricular gene-expression remodeling in dogs with experimental heart failure.* J Mol Cell Cardiol, 2008. **45**(6): p. 821-31.
3. Hanna, N., et al., *Differences in atrial versus ventricular remodeling in dogs with ventricular tachypacing-induced congestive heart failure.* Cardiovasc Res, 2004. **63**(2): p. 236-44.
4. Tsai, C.T., et al., *Angiotensin II activates signal transducer and activators of transcription 3 via Rac1 in atrial myocytes and fibroblasts: implication for the therapeutic effect of statin in atrial structural remodeling.* Circulation, 2008. **117**(3): p. 344-55.
5. Touyz, R.M., et al., *Cytosolic calcium changes induced by angiotensin II in neonatal rat atrial and ventricular cardiomyocytes are mediated via angiotensin II subtype 1 receptors.* Hypertension, 1996. **27**(5): p. 1090-6.
6. Qin, W., et al., *TGF-beta/Smad3 signaling promotes renal fibrosis by inhibiting miR-29.* J Am Soc Nephrol, 2011. **22**(8): p. 1462-74.
7. Burstein, B. and S. Nattel, *Atrial fibrosis: mechanisms and clinical relevance in atrial fibrillation.* J Am Coll Cardiol, 2008. **51**(8): p. 802-9.
8. Adam, O., et al., *Role of miR-21 in the pathogenesis of atrial fibrosis.* Basic Res Cardiol, 2012. **107**(5): p. 278.
9. Harada, M., et al., *Transient receptor potential canonical-3 channel-dependent fibroblast regulation in atrial fibrillation.* Circulation, 2012. **126**(17): p. 2051-64.
10. Ellinor, P.T., et al., *Meta-analysis identifies six new susceptibility loci for atrial fibrillation.* Nat Genet, 2012. **44**(6): p. 670-5.
11. Wang, J., et al., *Pitx2-microRNA pathway that delimits sinoatrial node development and inhibits predisposition to atrial fibrillation.* Proc Natl Acad Sci U S A, 2014. **111**(25): p. 9181-6.
12. Callis, T.E., et al., *MicroRNA-208a is a regulator of cardiac hypertrophy and conduction in mice.* J Clin Invest, 2009. **119**(9): p. 2772-86.
13. Grote, K., M. Luchtefeld, and B. Schieffer, *JANUS under stress--role of JAK/STAT signaling pathway in vascular diseases.* Vascul Pharmacol, 2005. **43**(5): p. 357-63.
14. Wormald, S. and D.J. Hilton, *Inhibitors of cytokine signal transduction.* J Biol Chem, 2004. **279**(2): p. 821-4.
15. Shuai, K. and B. Liu, *Regulation of JAK-STAT signalling in the immune system.* Nat Rev Immunol, 2003. **3**(11): p. 900-11.
16. Yasukawa, H., et al., *SOCS3: A novel therapeutic target for cardioprotection.* JAKSTAT, 2012. **1**(4): p. 234-40.
17. Ogata, H., et al., *Loss of SOCS3 in the liver promotes fibrosis by enhancing STAT3-mediated TGF-beta1 production.* Oncogene, 2006. **25**(17): p. 2520-30.
18. Yamamoto, T., et al., *Molecular interactions between STAT3 and protein inhibitor of activated STAT3, and androgen receptor.* Biochem Biophys Res Commun, 2003. **306**(2): p. 610-5.
19. Starkel, P., et al., *Role of signal transducer and activator of transcription 3 in liver fibrosis progression in chronic hepatitis C-infected patients.* Lab Invest, 2007. **87**(2): p. 173-81.
20. Jiang, Q., et al., *Down-regulation of ATBF1 activates STAT3 signaling via PIAS3 in pacing-induced HL-1 atrial myocytes.* Biochem Biophys Res Commun, 2014. **449**(3): p. 278-83.
21. Tsai, C.T., et al., *Membrane translocation of small GTPase Rac1 and activation of STAT1 and STAT3 in pacing-induced sustained atrial fibrillation.* Heart Rhythm, 2008. **5**(9): p. 1285-93.

22. Haghikia, A., et al., *STAT3, a key regulator of cell-to-cell communication in the heart.* Cardiovasc Res, 2014. **102**(2): p. 281-9.
23. Pang, M., et al., *A novel STAT3 inhibitor, S3I-201, attenuates renal interstitial fibroblast activation and interstitial fibrosis in obstructive nephropathy.* Kidney Int, 2010. **78**(3): p. 257-68.
24. Zhang, L., et al., *Paclitaxel attenuates renal interstitial fibroblast activation and interstitial fibrosis by inhibiting STAT3 signaling.* Drug Des Devel Ther, 2015. **9**: p. 2139-48.
25. Mir, S.A., et al., *Inhibition of signal transducer and activator of transcription 3 (STAT3) attenuates interleukin-6 (IL-6)-induced collagen synthesis and resultant hypertrophy in rat heart.* J Biol Chem, 2012. **287**(4): p. 2666-77.
26. Mascareno, E., M. Dhar, and M.A. Siddiqui, *Signal transduction and activator of transcription (STAT) protein-dependent activation of angiotensinogen promoter: a cellular signal for hypertrophy in cardiac muscle.* Proc Natl Acad Sci U S A, 1998. **95**(10): p. 5590-4.
27. Liu, L., et al., *Regulation of DHP receptor expression by elements in the 5'-flanking sequence.* Am J Physiol Heart Circ Physiol, 2000. **278**(4): p. H1153-62.
28. Kong, P., P. Christia, and N.G. Frangogiannis, *The pathogenesis of cardiac fibrosis.* Cell Mol Life Sci, 2014. **71**(4): p. 549-74.
29. Baudino, T.A., et al., *Cardiac fibroblasts: friend or foe?* Am J Physiol Heart Circ Physiol, 2006. **291**(3): p. H1015-26.
30. Derynck, R., R.J. Akhurst, and A. Balmain, *TGF-beta signaling in tumor suppression and cancer progression.* Nat Genet, 2001. **29**(2): p. 117-29.
31. Bottinger, E.P., J.J. Letterio, and A.B. Roberts, *Biology of TGF-beta in knockout and transgenic mouse models.* Kidney Int, 1997. **51**(5): p. 1355-60.
32. Zacchigna, S., L. Zentilin, and M. Giacca, *Adeno-associated virus vectors as therapeutic and investigational tools in the cardiovascular system.* Circ Res, 2014. **114**(11): p. 1827-46.
33. Pacak, C.A., et al., *Tissue specific promoters improve specificity of AAV9 mediated transgene expression following intra-vascular gene delivery in neonatal mice.* Genet Vaccines Ther, 2008. **6**: p. 13.
34. Teng, Y., et al., *Deletion of Smad4 in fibroblasts leads to defective chondrocyte maturation and cartilage production in a TGFbeta type II receptor independent manner.* Biochem Biophys Res Commun, 2011. **407**(4): p. 633-9.
35. Inoue, T., et al., *Fibroblast expression of an IkappaB dominant-negative transgene attenuates renal fibrosis.* J Am Soc Nephrol, 2010. **21**(12): p. 2047-52.
36. Kong, P., et al., *Lack of specificity of fibroblast-specific protein 1 in cardiac remodeling and fibrosis.* Am J Physiol Heart Circ Physiol, 2013. **305**(9): p. H1363-72.
37. Lajiness, J.D. and S.J. Conway, *Origin, development, and differentiation of cardiac fibroblasts.* J Mol Cell Cardiol, 2014. **70**: p. 2-8.
38. Krenning, G., E.M. Zeisberg, and R. Kalluri, *The origin of fibroblasts and mechanism of cardiac fibrosis.* J Cell Physiol, 2010. **225**(3): p. 631-7.
39. Cardin, S., et al., *Role for MicroRNA-21 in atrial profibrillatory fibrotic remodeling associated with experimental postinfarction heart failure.* Circ Arrhythm Electrophysiol, 2012. **5**(5): p. 1027-35.
40. Dawson, K., et al., *MicroRNA29: a mechanistic contributor and potential biomarker in atrial fibrillation.* Circulation, 2013. **127**(14): p. 1466-75, 1475e1-28.
41. Duygu, B., L.J. de Windt, and P.A. da Costa Martins, *Targeting microRNAs in heart failure.* Trends Cardiovasc Med, 2015.
42. Nouraee, N. and S.J. Mowla, *miRNA therapeutics in cardiovascular diseases: promises and problems.* Front Genet, 2015. **6**: p. 232.

43. Philippen, L.E., et al., *Antisense MicroRNA Therapeutics in Cardiovascular Disease: Quo Vadis?* Mol Ther, 2015.
44. Bartel, D.P., *MicroRNAs: target recognition and regulatory functions.* Cell, 2009. **136**(2): p. 215-33.
45. Wahlquist, C., et al., *Inhibition of miR-25 improves cardiac contractility in the failing heart.* Nature, 2014. **508**(7497): p. 531-5.
46. Karakikes, I., et al., *Therapeutic cardiac-targeted delivery of miR-1 reverses pressure overload-induced cardiac hypertrophy and attenuates pathological remodeling.* J Am Heart Assoc, 2013. **2**(2): p. e000078.
47. Montgomery, R.L., et al., *Therapeutic inhibition of miR-208a improves cardiac function and survival during heart failure.* Circulation, 2011. **124**(14): p. 1537-47.
48. Janssen, H.L., et al., *Treatment of HCV infection by targeting microRNA.* N Engl J Med, 2013. **368**(18): p. 1685-94.
49. Weiler, J., J. Hunziker, and J. Hall, *Anti-miRNA oligonucleotides (AMOs): ammunition to target miRNAs implicated in human disease?* Gene Ther, 2006. **13**(6): p. 496-502.
50. Lennox, K.A. and M.A. Behlke, *Chemical modification and design of anti-miRNA oligonucleotides.* Gene Ther, 2011. **18**(12): p. 1111-20.
51. Luo, X., B. Yang, and S. Nattel, *MicroRNAs and atrial fibrillation: mechanisms and translational potential.* Nat Rev Cardiol, 2015. **12**(2): p. 80-90.
52. Liu, Z., et al., *The expression levels of plasma micoRNAs in atrial fibrillation patients.* PLoS One, 2012. **7**(9): p. e44906.
53. Nishi, H., et al., *Impact of microRNA expression in human atrial tissue in patients with atrial fibrillation undergoing cardiac surgery.* PLoS One, 2013. **8**(9): p. e73397.